THE UNIVERSITY *of* EDINBURGH

Mammalian cell stress responses during Semliki Forest virus infection

Mhairi C. Ferguson

Thesis submitted for the degree of Doctor of Philosophy

The Roslin Institute, University of Edinburgh

2012

Contents

List of Figures

List of Tables

Declaration

I declare that this thesis has been composed by myself and has not been submitted for any other degree. The work described herein is my own except where otherwise indicated and all work of other authors is duly acknowledged.

Mhairi C. Ferguson
2012

The Roslin Institute
University of Edinburgh
Easterbush
Midlothian
EH25 9RG

Acknowledgements

I would like to thank my supervisors **John Fazakerley** and **Alain Kohl** for their support and guidance throughout my PhD. John has provided a wealth of knowledge from experimental design to presenting at conferences. Even though John has become extremely busy, he has still found time to answer all my questions. Alain has strengthened my work by challenging my experiments and ideas, while also stepping in when needed. During my university honours project, Alain and **Rennos Fragkoudis** introduced me to the fascinating world of arboviruses that led to this PhD, thank you. I would also like to thank **Lesley Bell-Sakyi** for her guidance and for tirelessly reading and correcting my thesis. I owe a huge thank you to **Gerald Barry** for his patience, ideas and encouragement during my PhD. Gerald was always available to explore to my ideas and talk through my experiments and concerns. Finally, thank you to all past and present laboratory members: **Julio Rodriguez**, **Adrian Zagrajek**, **Sabine Weisheit**, **Claudia Rückert**, **Claire Donald**, **Stacey Human**, **Esther Schnettler**, **Ricky Siu** and **Sue Jacobs**. You have all made my time in the Roslin Arbovirus Group a happy and memorable experience.

I would like to thank **Andres Merits**, Institute of Technology, University of Tartu, Estonia for supplying the SFV4 constructs used in this project and for his sequencing advice. The sequencing work would not have been possible without the expertise of **Karen Sherwood**, Roslin Institute, University of Edinburgh. I would also like to thank **Marian Killip**, University of St. Andrews for her advice on establishing the interferon bioassay.

On a personal level, I would have struggled to complete this thesis and overcome my health problems without the love and support of my family **David**, **Maureen**, **Fiona** and **Patricia**. David (Dad) has constantly challenged me by playing ‘devil’s advocate’ and, more recently, has spent hours correcting my thesis. Maureen (Mum) has listened to numerous science stories and given me the encouragement to keep going – you never died of winter yet. Fiona and Patricia have been wonderful and caring big sisters. I would also like to thank **Padraig Looney** for being there whenever I needed him and for being genuinely fascinated by what I do. Finally, I would like to thank my friends for all the entertainment during my PhD.

Abstract

Virus infection of mammalian cells induces several stress mechanisms, including autophagy and type-I interferon (IFN). Autophagy, a cellular homeostatic mechanism in which intracellular materials are sequestered into double-membrane vesicles and targeted to lysosomes for degradation, is also activated in response to virus infection. Most positive single-stranded RNA viruses studied to date utilise autophagy to increase virus replication. IFN is a potent anti-viral mechanism, which can be divided into two parts: (i) induction and secretion of IFN and (ii) IFN signalling and priming of uninfected cells for a rapid response upon infection and induction of an anti-viral state in infected cells. Alphaviruses are medically important RNA viruses. Semliki Forest virus (SFV) provides a well-characterised model for studying alphavirus infection. A number of strains have been identified, which differ in virulence in adult mice. In this thesis three hypotheses were investigated: (i) that SFV infection induces autophagy in cell culture and utilises this response to enhance virus replication, (ii) that the quality, quantity and/or protective efficacy of the IFN response differ between virus strains and between human and murine cells and (iii) that non-structural protein (nsP)-2 and/or nsP3 antagonise the IFN response.

SFV4, SFV L10 and SFV A7(74) infection induced autophagy in Huh7 cells as early as one hour post-infection. Pharmacological induction or inhibition of autophagy had no affect on SFV4 replication, except at a very low multiplicity of infection. NsP3, capsid and dsRNA rarely colocalised with the autophagosome marker LC3. Taken together these results indicate that SFV does not use autophagosomes for replication and autophagy is not important in controlling SFV4 infection at a high MOI, at least in Huh7 cells. However, autophagy may be important in controlling SFV4 spread at a low MOI.

An IFN bioassay was established. In fibroblasts, SFV4, SFV L10 and SFV A7(74) induced relatively little IFN in comparison to that induced by Sendai virus. In human fibroblasts, similar levels of IFN were induced by all three virus strains. In mouse fibroblasts, SFV4 induced more IFN than SFV L10. Treatment of fibroblasts with IFN prior to infection greatly reduced, but did not abolish, the replication and spread of all three strains. Therefore, SFV is sensitive to IFN. Analysis of IFN

signalling demonstrated that all three strains of SFV inhibited STAT1 phosphorylation during infection of fibroblasts. The growth and viability of SFV infected cells varied between human and mouse cells. The complete genetic sequences of SFV L10 and SFV A7(74) were determined using Solexa (Illumina) sequencing and compared to the sequence of SFV4. The sequences of SFV L10 and SFV4 were extremely similar; only seven differences were identified. Multiple amino acid substitutions were identified in SFV A7(74) compared to SFV4, these mostly mapped to nsP3.

To investigate the hypothesis that nsP2 and or nsP3 antagonise the IFN response, two virus mutants were studied: SFV4nsP2RDR and SFV4nsP3Δ50. SFV4nsP2RDR encodes a point mutation in the nuclear localisation signal of nsP2, which largely restricts nsP2 to the cell cytoplasm. SFV4nsP3Δ50 contains a deletion of 50 amino acids in the C-terminus hyperphosphorylated region of nsP3. Neither mutant inhibited STAT1 phosphorylation as efficiently as WT SFV4; SFV4nsP2RDR was particularly poor at inhibiting STAT1 phosphorylation. Both mutants induced more IFN in fibroblasts than SFV4.

In summary, autophagy had a limited affect on SFV replication. In contrast, strains of SFV were highly sensitive to IFN, but antagonised this response through the nsP2 protein inhibiting STAT1 phosphorylation.

Abbreviations

2'-5' A	2'-5'-oligodenylates
3D	Three dimensional
3MA	3-methyladenine
6K	6 kDa protein
APC	Antigen-presenting cell
ATG	Autophagy genes
BC	B cell
BHK-21	Baby Hamster Kidney-21
BSA	Bovine serum albumin
BUNV	Bunyamwera virus
C	Capsid
CARD	Caspase recruitment domain
CBP	CREB-binding protein
CCD	Coil-coiled domain
CHIKV	Chikungunya virus
CIS	SH2-containing proteins
CNS	Central nervous system
CPE	Cytopathic effect
CPV	Cytopathic vacuoles
DAMPs	Danger-associated molecular patterns
DBD	DNA binding domain
DC	Dendritic cell
DENV	Dengue virus
DMEM	Dulbecco’s modified Eagles medium
DMSO	Dimethylsulfoxide
ds	Double-stranded
dsRBM	dsRNA binding motifs
E	Envelope glycoprotein
EEEV	Eastern equine encephalitis virus
eGFP	Enhanced green fluorescent protein
eIF-2a	Eukaryotic translation initiation factor 2a

EMCV	Encephalomyocarditis virus
ER	Endoplasmic reticulum
FACS	Fluorescence-activated cell sorter
FMDV	Foot-and-mouth-disease virus
GMEM	Glasgow's modified Eagles medium
HBV	Hepatitis B virus
HCV	Hepatitis C virus
HeV	Hendra virus
HIV	Human immumodeficiency virus
HMG I (Y)	High mobility group I (Y) proteins
HSP	Heat-shock protein
HSV	Herpes simplex virus
ic	Intracerebral
IFN	Interferon
IFNR	Interferon receptors
IkB	Inhibitor of nuclear factor kappa B
IKK	IKappa kinase
IL	Interleukin
in	intranasal
ip	Intraperitoneal
IRF-3	Interferon regulatory factor-3
ISG	Interferon-stimulated genes
ISGF3	Interferon stimulated gene factor-3
ISRE	Interferon-stimulated response element
JAK	Janus kinase
JEV	Japanese encephalitis virus
L	Linker region
LAMP-2A	lysosome-associated membrane protein type-2A
LC	Langerhans cell
LC3	Microtubule-associated protein light chain-3
LGP2	Laboratory of genetics and physiology 2
mda-5	Melanoma differentiation-associated gene-5

MeV	Measles virus
MHC	Major histocompatibility complex
MHV	Murine hepatitis virus
mTOR	Mammalian target of rapamycin
MYD88	Myeloid differentiation primary response gene 88
NBCS	Newborn calf serum
ND	N-terminus domain
NEMO	NF-$_K$B essential modifier
NF-KB	Nuclear factor kappa B
NiV	Nipah virus
NK cell	Natural killer cell
NKT cell	Natural killer T cell
NLR	Nod-like receptor
NLS	Nuclear localisation signal
nsP	non-structural protein
OAS	2'-5'-oligodenylate synthase
ONNV	O'Nyong-nyong virus
ORF	open-reading frame
PAMPs	Pathogen-associated molecular patterns
PBS	Phosphate buffered saline
pDC	Plasmacytoid dendritic cell
PE	Phosphatidylethanolamine
PFA	Paraformaldehyde
PFU	Plaque forming units
PI3K	Class III phosphatidylinositol 3-phosphate kinase
PIAS	Protein inhibitor of activated STAT
PIV5	Parainfluenza virus 5
PKR	Protein Kinase R
PP2A	Protein phosphatase 2A
PRD	Positive regulatory domains
PRRs	Pattern-recognition receptors
PV	Poliovirus

RIG-I	Retinoic-acid-inducible gene-I
RIP1	Receptor-interacting protein 1
RLR	RIG-I-like receptor
RLuc	*Renilla* luciferase
RNA	ribonucleic acid
RRV	Ross River virus
RVFV	Rift Valley Fever virus
SARS	Severe Acute Respiratory virus
SeV	Sendai virus
SFV	Semliki Forest virus
SH2	Src-homology 2
SHP	SH2 domain-containing protein tyrosine phosphatase
SINV	Sindbis virus
SLRs	Sequestosome 1/p62-like receptors
SOCS	Suppressors of cytokine signalling
ss	single-stranded
STAT	Signal transducers and activators ot transcription
TAD	Transactivator domain
TAE	Tris-acetate-EDTA
TAK1	Transforming growth factor β-activated kinase 1
TANK	TRAF family member-associated NF-$_k$B activator
TBK1	TANK-binding kinase 1
TBP	Tryptose phosphate broth
TC	T cell
TEMED	Tetramethylethylenediamine
TLR	Toll-like receptor
TMV	Tobacco mosaic virus
TRAF	Tumour necrosis factor receptor-associated factor
TRIF	Toll/IL-1R domain-containing adaptor-inducing IFN-β
UPR	Unfolded Protein Response
VEEV	Venezuelan equine encephalitis virus
VRP	Virus replicon particle

VSV	Vesicular stomatitis virus
WEEV	Western equine encephalitis virus
WNV	West Nile virus
WT	Wild-type

Chapter 1: Introduction

Contents

Arthropod-borne viruses (arboviruses) include medically important viruses that mostly belong to four virus families: *Togaviridae*, *Flaviviridae*, *Bunyaviridae* and *Reoviridae*. Alphaviruses are positive single-stranded (ss) ribonucleic acid (RNA) arboviruses of the *Togaviridae* family. Semliki Forest virus (SFV) provides a well-characterised model to study alphavirus infection. In this thesis the interaction of SFV with host cell stress responses, specifically autophagy and the type-I interferon (IFN) response, will be investigated. In chapter 3, the role of autophagy during SFV infection will be explored. In chapter 4, the interaction of different strains of SFV with both the human and mouse type-I IFN system will be analysed. This interaction will be investigated further at the genetic level in chapter 5. In chapter 6, the genetic sequence of three well-characterised strains of SFV will be sequenced and differences between the strains will be identified. Overall, the research presented here will enhance current understanding concerning the relationship between SFV and the host cell stress responses.

1.1 Alphaviruses

Alphaviruses are positive ssRNA arboviruses of the *Togaviridae* family. The *Togaviridae* family consists of two genera: *Alphavirus*, which has 40 members, and *Rubivirus*, which has one member, rubella virus. Alphaviruses are defined as Old World or New World viruses based on their geographical origin of isolation. The New World viruses are located in the Americas and include Venezuelan equine encephalitis virus (VEEV), Western equine encephalitis virus (WEEV) and Eastern equine encephalitis virus (EEEV) (Garmashova *et al.*, 2007b). The Old World viruses are located in Africa and Asia and include SFV, sindbis virus (SINV), chikungunya virus (CHIKV) and O'Nyong-nyong virus (ONNV). Ross River virus (RRV) was isolated in Australia and is considered to be an Old World alphavirus (Garmashova *et al.*, 2007). Alphaviruses have been isolated on every continent of the world, apart from Antarctica (Powers *et al.*, 2001).

The geographical location of alphaviruses is restricted, in part, by their vectors. Alphaviruses cycle between vertebrate hosts and arthropod vectors. Vertebrate hosts are normally small rodents or birds, but large mammals such as humans can be infected. Humans are considered dead-end hosts as the viraemia is

generally too low to enable transmission (Gibbs, 1976). Alphavirus vectors include mosquitoes, ticks and lice in which alphaviruses produce persistent infections with low-level virus production (Weaver *et al.*, 1988;Weaver *et al.*, 1992).

Alphaviruses are responsible for serious epidemics of polyarthralgia and encephalitis in humans, equines, rodents and birds. The Old World and New World viruses have different disease phenotypes: New World viruses generally cause encephalitis, while Old World viruses induce arthralgia, myalgia and a rash. VEEV is epidemic in South and Central America and can cause tens of thousands of cases of febrile disease during an outbreak, as occurred in Columbia, 1995 (Weaver *et al.*, 1992). RRV is endemic in Australia with multiple clinical cases recorded between 1992 and 2003 (Horwood & Bi, 2005). Since 2005, CHIKV has caused thousands of clinical cases of disease in Africa, Asia and, for the first recorded time, Europe. On the Indian Ocean island of La Reunion, near East Africa, 40% of the population developed severe arthralgia during an outbreak of CHIKV between 2005 and 2006 (Enserink, 2007). In India, CHIKV has become a major medical burden with 1,400,000 clinical cases reported in 2006 alone (Pialoux *et al.*, 2007). In 2007, the first cases of febrile disease caused by CHIKV infection were reported in Italy. An individual returning from India (index case) transferred CHIKV to local mosquitoes resulting in an outbreak (Rezza *et al.*, 2007). In 2010, the first confirmed cases of autochthonous CHIKV were reported in southeast France (Grandadam *et al.*, 2011). VEEV is the only alphavirus for which there is a vaccine available (Edelman *et al.*, 1979;Edelman *et al.*, 2003). The continuing threat of CHIKV spread has driven research towards a vaccine (Akahata *et al.*, 2010;Mallilankaraman *et al.*, 2011).

1.1.1 Alphaviruses: genome and replication

The alphavirus genome is positive ssRNA and measures between 11 and 12 kb (11.5 kb for SFV). The genome contains two open reading frames (ORF) that encode nine proteins: the non-structural proteins (nsP) 1-4 are located in the 5’ two-thirds and the structural proteins are located in the 3’ third of the genome (Fig. 1.1). The structural proteins consist of capsid (C), the envelope glycoproteins (E) 1-3 and the 6 kDa (6K) protein (Kaariainen *et al.*, 1987).

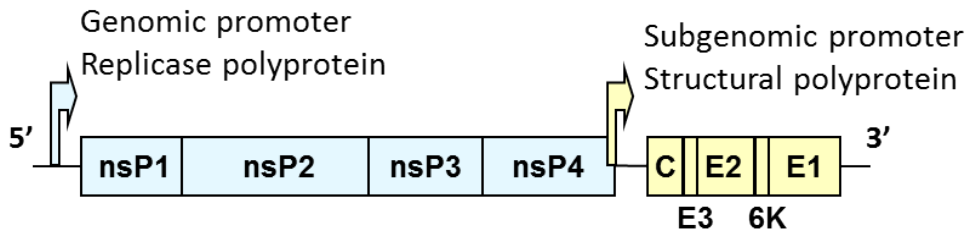

Figure 1.1: Schematic representation of the SFV genome.
Blue boxes correspond to the non-structural proteins (nsP1-4) and yellow boxes correspond to the structural proteins: capsid protein (C), the envelope glycoproteins (E1-3) and the 6 KDa (6K) protein. The arrows represent promoters (reproduced with permission from Fragkoudis (2007).

E2 is located on the surface of alphaviruses in spikes and binds to specific cell surface receptors (Strauss & Strauss, 1994;Smith *et al.*, 1995). Several alphavirus receptors have been identified in both mammalian and mosquito cells (Tsai *et al.*, 2002), although the receptor which binds SFV E2 is unknown. E2 binding induces endocytosis of the alphavirus into clathrin-coated pits (Helenius *et al.*, 1980;Marsh *et al.*, 1983). The pits fuse with endosomes and then lysosomes in the cell cytoplasm (Strous & Govers, 1999). The increasingly acidic pH induces a conformational change in the glycoprotein spike that promotes E1 mediated fusion of the virus envelope with the host membrane. The nucleocapsid enters the cytoplasm, disassembles and the virus genome is released (Helenius *et al.*, 1982;Wahlberg & Garoff, 1992;Fuller *et al.*, 1995).

Alphaviruses replicate in the cytoplasm of cells, as shown in Fig. 1.2. The alphavirus genome has a 5' cap and a 3' polyadenylated tail, which enables it to function like messenger RNA (mRNA) and be directly translated by the cellular replication machinery (Strauss *et al.*, 1983). Translation of the first ORF produces the nsP polyproteins (Takkinen, 1986). Certain alphaviruses, including SINV, encode an opal stop codon (UAG) between nsP3 and nsP4 with read-through occurring at a frequency of 10-20%. As a result, P123 is produced in preference to P1234. In other alphaviruses the opal codon is replaced with an arginine residue and P1234 alone is produced (Strauss *et al.*, 1983;Takkinen, 1986). In most strains of SFV the opal codon is replaced with an arginine, apart from in the strain SFV A7(74) which will be discussed further in 1.1.2.

P1234 is sequentially cleaved by the protease domains of nsP2 (Merits *et al.*, 2001). NsP4 is released first, followed by nsP1 and finally nsP3 that associate to form the replication complex (RC) (Kim *et al.*, 2004). NsP1 and, potentially nsP3, target the RC to modified endosomes, lysosomes and the plasma membrane (Spuul *et al.*, 2007). Alphavirus replication is associated with cytopathic vacuoles (CPV) I and II (Kujala *et al.*, 2001). CPV I contain numerous inward invaginations called spherules, in which the alphavirus genome is replicated. Virus maturation occurs on CPV II membranes (Pathak *et al.*, 1976).

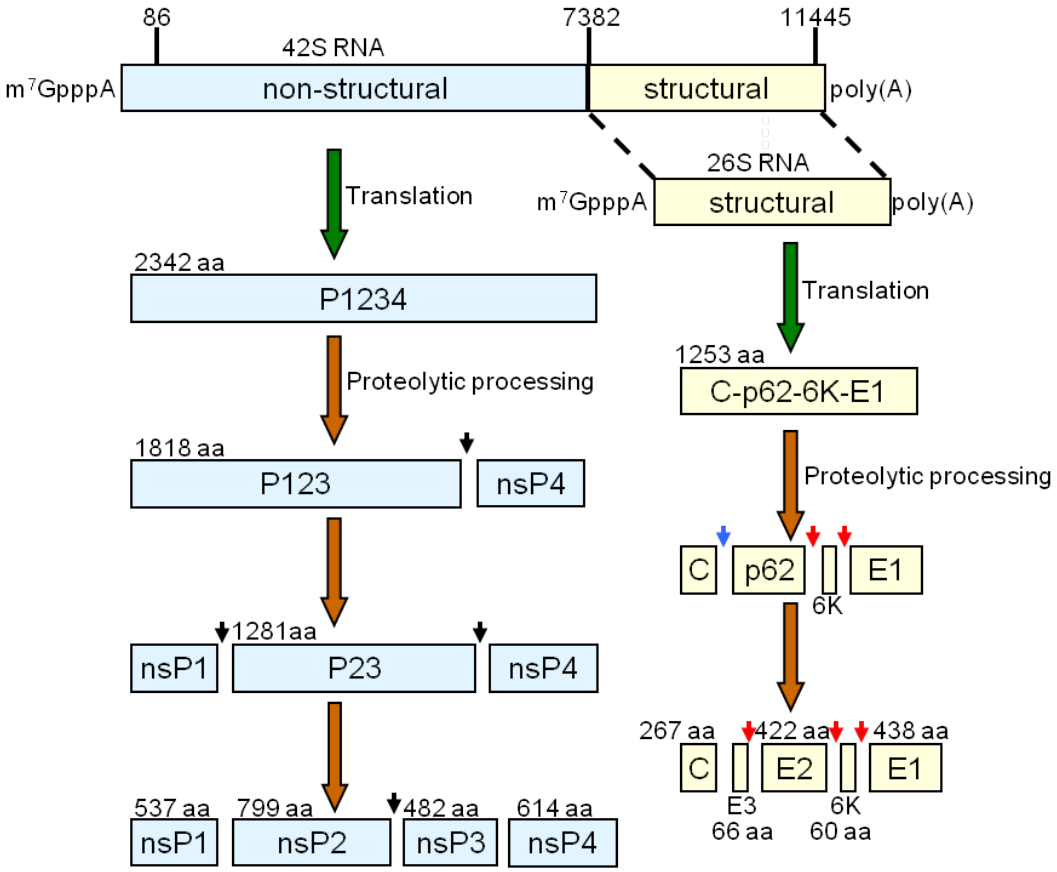

Figure 1.2: Schematic representation of alphavirus replication and polyprotein production.
The non-structural proteins (nsPs) are translated first and sequentially cleaved, which facilitates the replication of the genome. The structural proteins are translated from the sub-genomic RNA. Black, blue and red arrows indicate cleavage sites and amino acid (aa) positions are labelled (reproduced with permission from Fragkoudis, (2007)).

In CPV I, the RC, comprising of P123 and nsP4, transcribes negative-strand RNA from the positive strand RNA genome. The continued processing of P123 to

produce mature nsPs results in the decreased ability of the RC to transcribe negative-strand RNA. Instead, the RC transcribes new genomic RNA by producing full length positive-strand RNA from the 3' end or sub-genomic (sg) RNA from the sg promoter. The sg RNA can be co-translationally and post-translationally processed into the structural proteins (Grimley *et al.*, 1968;Kaariainen *et al.*, 1987;Froshauer *et al.*, 1988;Kujala *et al.*, 2001;Kim *et al.*, 2004).

C has an autoproteolytic function, which facilitates its rapid release from the structural polyprotein leaving p62-6K-E1 (Aliperti & Schlesinger, 1978). Removal of C exposes an N' terminal signal in p62, which directs p62 to the endoplasmic reticulum (ER) (Bonatti *et al.*, 1984). Both E1 and p62 have transmembrane domains that anchor them in the ER membrane (Melancon & Garoff, 1986). The ER and the Golgi apparatus process and modify the proteins by adding carbohydrate chains, fatty acids and side chains. The glycoproteins are transported to the cell membrane and form the alphavirus spikes. E3 associates with the virion spike in some alphaviruses, such as SFV, and in others it remains in the cell cytoplasm. C proteins form a 12 pentamer and 30 hexamer structure, which binds to a packaging signal present in the virus RNA to form the nucleocapsid (Weiss *et al.*, 1989;Geigenmuller-Gnirke *et al.*, 1991). The E2 cytoplasmic domain associates with the nucleocapsid C-terminal domain and drives new virions to bud from the cell membrane (Pathak *et al.*, 1976;Suomalainen *et al.*, 1992;Lopez *et al.*, 1994). The 6K protein is essential for assembly of new virions (McInerney *et al.*, 2004).

1.1.2 Roles of the non-structural proteins

The alphavirus genome encodes four multifunctional nsPs.

NsP1

NsP1 forms part of the RC and, together with nsP3, targets the RC to cellular membranes (Spuul *et al.*, 2007). NsP1 attaches to host membranes via an amphipathic helix and palmitoylation residues (Froshauer *et al.*, 1988;Laakkonen *et al.*, 1996;Kujala *et al.*, 2001). NsP1 also initiates the synthesis of negative-strand RNA from the positive-strand genome (Wang *et al.*, 1991;Shirako *et al.*, 2000).

Finally, NsP1, together with nsP2, caps the newly produced RNA through its RNA triphosphatase, methyl- and guanyl-transferase activity (Vasiljeva *et al.*, 2000).

NsP2

NsP2 contains NTPase, GTPase, ATPase and RNA helicase activity in the N-terminal region (Rikkonen *et al.*, 1994;Rikkonen, 1996;Gomez de *et al.*, 1999). The helicase domain is involved in unwinding and replicating the alphavirus genome. NsP2 is implicated in terminating negative-strand replication and in mediating sg RNA synthesis (Suopanki *et al.*, 1998). NsP2 is cytotoxic to the host cell when expressed alone or in a vector (Garmashova *et al.*, 2006). In Old World alphaviruses, nsP2 is implicated in host protein shutoff (Frolova *et al.*, 2002;Garmashova *et al.*, 2006;Breakwell *et al.*, 2007). The C-terminal region of nsP2 contains papain-like cysteine proteinases, which sequentially cleave the non-structural polypeptide to release the nsPs (Merits *et al.*, 2001). In addition, the C-terminal region contains a nuclear localisation signal (NLS), which consists of a core peptide (A^{645}LPRRRVTWN) (Rikkonen *et al.*, 1992). In cell culture, approximately 50 % of SFV4 nsP2 locates to the nucleus by 5 h post-infection (Rikkonen *et al.*, 1992). The mutation of the second R residue to D results in the mutant virus termed SFV4-RDR, in which nsP2 is largely restricted to the cell cytoplasm (Rikkonen *et al.*, 1992). Inoculation by the intracerebral (*ic*) route of BALB/c mice with SFV4 is fatal, whereas infection with SFV4-RDR is avirulent (Fazakerley *et al.*, 2002). The avirulence of SFV4-RDR has been linked to the type-I interferon (IFN) response (Breakwell *et al.*, 2007), which will be discussed further in 1.4.10.

NsP3

NsP3 contains three domains: the first third of nsP3, termed the macrodomain, is conserved between alphaviruses, rubella virus, hepatitis E virus (HEV) and coronaviruses (Koonin & Dolja, 1993;Neuvonen & Ahola, 2009); the second third is conserved between the alphaviruses, and the final third is hypervariable and varies between alphaviruses both in length and in amino acid sequence (Strauss & Strauss, 1994). The crystal structure of the macrodomain has been generated for both CHIKV and VEEV and contains an adenosine binding pocket (Malet *et al.*, 2009). The hypervariable domain is hyperphosphorylated and has no predicted secondary

structure (Peranen, 1991). NsP3 is implicated in sg 26S and negative-strand RNA synthesis (Hahn *et al.*, 1989;Wang *et al.*, 1994;LaStarza *et al.*, 1994b), cleavage of the polyprotein by nsP2 (de Groot *et al.*, 1990), attaching the RC to membranes (Peranen & Kaariainen, 1991) and determining virus virulence in adult mice. NsP3 attachment to membranes is mediated by host cell Src-homology 3 (SH3) domains of amphiphysin-1 and -2, targeting a region within the hypervariable domain of nsP3 (Neuvonen *et al.*, 2011). In addition, studies have implicated nsP3 as a crucial factor in determining the virulence of different strains of SFV (Tuittila *et al.*, 2000;Vihinen *et al.*, 2001;Tuittila & Hinkkanen, 2003).

NsP4

NsP4 functions as an RNA-dependent RNA polymerase for replication of the alphavirus genome (Keranen & Kaariainen, 1979). NsP4 also has protease activity and contributes to the cleavage of nsP3 from nsP4 during the processing of the nsP polyprotein (Kamer & Argos, 1984;Takkinen *et al.*, 1990).

1.1.2 Semliki Forest virus: strains

SFV is an alphavirus found in sub-Saharan Africa and primarily spread by *Aedes africanus* and *Aedes aegypti* mosquitoes. SFV has been isolated from equines, primates and humans, although the natural host of SFV remains unknown. There are several wild-type (WT) strains of SFV, which can be divided into two groups based on their virulence in adult mice (Bradish *et al.*, 1971). Virulent strains include SFV L10, V13, Prototype and Osterrieth virus (Bradish *et al.*, 1971;Glasgow *et al.*, 1991). Avirulent strains include A8, A7, SFV A7(74), MRS MP 192/7 and V42 (Henderson *et al.*, 1970;Bradish *et al.*, 1971;Deuber & Pavlovic, 2007). All strains of SFV studied to date are virulent in neonatal or suckling mice (Bradish *et al.*, 1971). Following intraperitoneal (*ip*) inoculation in adult mice, SFV replicates in smooth muscles, including the cardiac muscle, and a high plasma viraemia is detected by 24 h post-infection (Pusztai *et al.*, 1971;Amor *et al.*, 1996). SFV is neuroinvasive and enters the brain, probably across cerebral endothelial cells (Pathak & Webb, 1974). SFV infects oligodendrocytes and neurones (Pathak & Webb, 1983;Balluz *et al.*, 1993). A number of strains have been sequenced and cloned, including SFV4 (Garoff

et al., 1980;Takkinen, 1986;Liljestrom & Garoff, 1991;Liljestrom *et al.*, 1991;Glasgow *et al.*, 1994;Santagati *et al.*, 1995;Tarbatt *et al.*, 1997;Santagati *et al.*, 1998;Tuittila *et al.*, 2000). Strains of particular relevance to this project are SFV L10, SFV A7(74) and SFV4.

SFV L10 was isolated from a pool of 130 *Aedes africanus* mosquitoes in the Semliki Forest, Uganda (Smithburn & Haddow, 1944) and passaged eight times by *ic* inoculation in adult mouse brains followed by two passages *ic* in neonatal mouse brains (Bradish *et al.*, 1971). Following *ip* inoculation of adult mice, SFV L10 rapidly disseminates throughout the brain producing a fatal panencephalitis by 4 – 5 days post-infection (Fazakerley *et al.*, 1993). In adult mice infected with SFV L10, a neuronal morphology appears normal while in neonatal mice neuronal cell death is apparent (Fazakerley, 2002). The mechanism by which SFV L10 induces panencephalitis remains unclear.

Prototype virus was isolated from the same mosquito sample as SFV L10 and passaged 4 times by *ic* inoculation in mice. SFV4 is a molecular cDNA clone of Prototype virus (Liljestrom & Garoff, 1991;Liljestrom *et al.*, 1991). SFV L10 and SFV4 have similar replication kinetics in cell culture. SFV4 is virulent in adult mice following *ic* inoculation or intranasal (*in*) inoculation at a high dose. However, unlike SFV L10, *ip* inoculation with SFV4 is avirulent in adult mice, unless administered at a high dose (Glasgow *et al.*, 1991;Fazakerley, 2002). One possible explanation for the difference in virulence between SFV L10 and SFV4 is that a nucleotide substitution occurred during the cloning process which changed the ability of SFV4 to function *in vivo*. SFV4 is a very useful molecular tool, as explained in 1.1.3.

The SFV strain AR2006 was isolated from *Aedes argenteopunctatus* mosquitoes in Mozambique (McIntosh *et al.*, 1961). SFV A7(74) was derived from the AR2006 strain of SFV by passaging seven times by *ic* inoculation in neonatal mice, followed by clonal selection from plaques in monolayers of primary chick embryo cells (Bradish *et al.*, 1971). SFV A7(74), like SFV L10, is virulent in mice under 11 days old and rapidly spreads throughout the brain. However, as mice become older the spread of SFV A7(74) is restricted, at least in the brain, to perivascular foci and the mice survive (Pathak & Webb, 1974;Fleming, 1977;Fazakerley *et al.*, 1993;Oliver *et al.*, 1997;Oliver & Fazakerley, 1998).

Following *ic* inoculation of adult mice, SFV A7(74) is detected in oligodendrocytes and the major white matter tracts of the brain, but infection is avirulent (Fazakerley *et al.*, 2006). The age-related virulence of SFV A7(74) in mice is suggested to be a function of the maturity of central nervous system (CNS) cells. SFV A7(74) can replicate in immature neurones, but is generally non-destructive in mature neurones (Fazakerley, 2002). Possible explanations for the age-related virulence of SFV A7(74) include (i) mature neurones lose their ability to produce smooth membrane vesicles on which SFV replicates and (ii) mature neurones upregulate anti-apoptotic genes and are less prone to SFV A7(74)-induced death (Fazakerley, 2002).

SFV4 and A7 or SFV A7(74) have been sequenced and compared; differences are present in E2, the 5' untranslated region and nsP3 (Santagati *et al.*, 1995;Tarbatt *et al.*, 1997;Santagati *et al.*, 1998;Tuittila *et al.*, 2000;Tuittila & Hinkkanen, 2003). Most differences map to nsP3 (Tuittila *et al.*, 2000). Several studies have demonstrated that nsP3, in part, determines the virulence of SFV4 and SFV A7(74) in adult mice (Tuittila *et al.*, 2000;Tuittila & Hinkkanen, 2003). SFV A7(&4) encodes an opal codon in the C-terminus of nsP3, while SFV4 encodes an arginine residue (Strauss *et al.*, 1983; Takkinen, 1986). Replacement of the opal codon in SFV A7(74) with arginine produces a virulent infection in BALB/c mice, while a reciprocal mutation in SFV4 produces an avirulent infection even at a high dose (Tuittila *et al.*, 2000). Replacing nsP3 in SFV A7(74) with SFV4 nsP3 produces a neurovirulent virus in mice, while a reciprocal change in SFV4 produced an avirulent infection (Tuittila & Hinkkanen, 2003). Substituting individual amino acids in SFV A7(74) nsP3 for those in SFV4 increases neurovirulence (Tuittila & Hinkkanen, 2003). Deletion of 50 amino acids in the hyperphosphorylated region of nsP3 produced a mutant virus named SFV4nsP3Δ50 (Vihinen *et al.*, 2001). SFV4nsP3Δ50 replicates less efficiently *in vitro* and is less virulent *in vivo* than WT SFV4 (Vihinen *et al.*, 2001). The potential interaction of nsP3 with the innate immune response has not been investigated.

1.1.3 Semliki Forest virus: a useful molecular tool

Several strains of SFV have been sequenced and cloned, including the molecular cDNA clone SFV4 (Garoff *et al.*, 1980;Takkinen, 1986;Liljestrom & Garoff,

1991;Liljestrom *et al.*, 1991;Glasgow *et al.*, 1994;Santagati *et al.*, 1995;Tarbatt *et al.*, 1997;Santagati *et al.*, 1998;Tuittila *et al.*, 2000). SFV4 is widely used in research due to the relatively simple manipulation of its genome to include mutations or encode foreign protein(s). Foreign proteins used are Renilla luciferase (*RLuc*) and ZsGreen that enable the indirect measurement of SFV4 replication, as opposed to the traditional plaque assay. In addition, SFV4 can be engineered to encode proteins useful for vaccination (Atkins *et al.*, 1996;Atkins *et al.*, 1999;Lundstrom *et al.*, 2001). Foreign gene(s) can be inserted into various locations in the genome with varying stability and expression (Fig. 1.3).

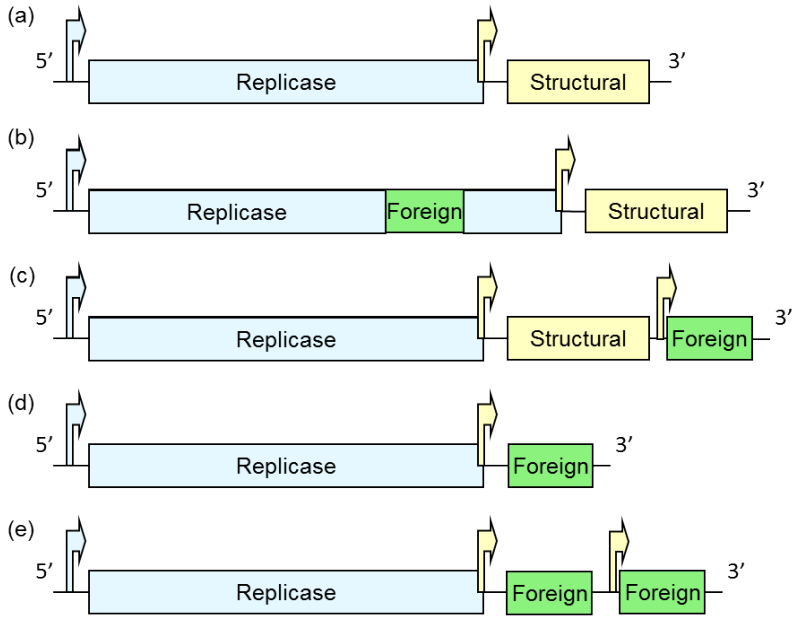

Figure 1.3: Schematic representation of possible insertion positions within the SFV4 genome.
(a) SFV4 genome showing two ORFs: the replicase ORF (blue) and the structural ORF (yellow). (b) SFV4 genome with a foreign gene (green) inserted into the replicase ORF between nsP3 and nsP4. (c) Foreign gene inserted after the structural ORF under the control of a duplicated subgenomic promoter (d) Structural ORF replaced with a foreign gene. (e) Structural ORF replaced with a foreign gene and another foreign gene inserted under the control of a duplicated subgenomic promoter.

Foreign gene(s) can be inserted into the replicase ORF, into the structural ORF or added after or before the structural ORF under the control of a duplicated sg promoter to produce viable viruses expressing foreign genes. For example, SFV4 has been engineered to express enhanced green fluorescent protein (eGFP) fused to nsP3 in a virus called SFV4(3F)eGFP. This enables the visualisation of nsP3 and virus

replication complexes both in cell culture and in the mouse model (Tamberg *et al.*, 2007).

Alternatively, the structural ORF can be replaced with foreign gene(s) producing a virus replicon particle (VRP) (Smerdou & Liljestrom, 1999). VRPs do not encode structural proteins and therefore can only undergo one round of replication. To generate VRPs, the VRP RNA and helper RNA encoding only the structural proteins are supplied in trans (Fig. 1.4). The structural proteins can be supplied in the helper system (all structural proteins) or in the split helper system (the Capsid protein and the envelope glycoproteins are encoded on separate RNA). The split helper system minimises the risk of recombination and production of infectious virus. VRPs are particularly useful for reasons of biosafety when investigating alphaviruses of greater risk to human health, such as CHIKV.

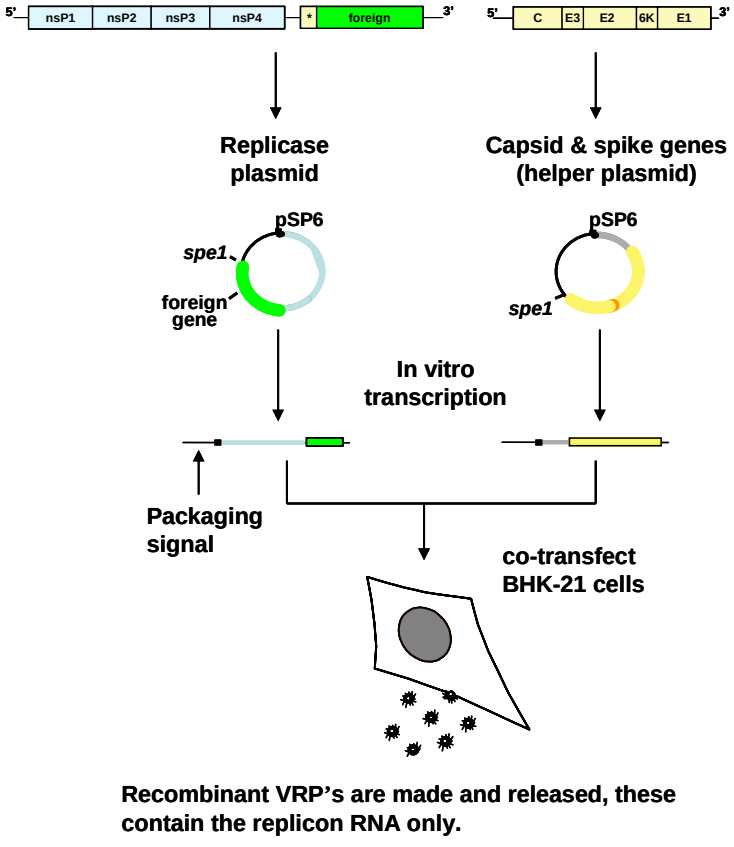

Figure 1.4: Schematic representation of VRP production using the helper system.
The replicon (blue) with the foreign gene insert (green) and the C, 6K and the envelope genes (yellow) in plasmid form are *in vitro* transcribed, electroporated into BHK-21 cells and VRPs are released. In the split helper system, capsid and glycoproteins are encoded on separate plasmids (reproduced by permission of Prof. John Fazakerley, University of Edinburgh).

1.2 The cell stress response: introduction

The cell stress response is a highly conserved process induced by the loss of homeostasis within the cell. The cell stress response functions to restore the cell to its normal state. If the cellular environment cannot be rescued then a cell death pathway is activated, such as apoptosis. The cell stress response was originally identified in *Drosophila* salivary gland cells that undergo morphological changes following temperature change or exposure to chemicals (Ritossa, 1962). At the molecular level, stressed salivary gland cells have a different RNA profile compared to control cells and upregulate heat shock proteins (HSP) (Schlesinger, 1990). HSP, such as hsp70, are chaperones that promote the correct folding of cellular proteins. HSPs have been identified in a diverse range of organisms (Lindquist & Craig, 1988). Since then other cellular pathways have been associated with the cell stress response, including IFN production, the unfolded protein response (UPR) and autophagy. Several cell stress inducers have been identified that can be broadly categorised into chemical and physical inducers, such as ultra-violet (UV) light. More recently, virus infection has been shown to induce the cell stress response. Studies have demonstrated that SFV infection induces type-I IFN production, the UPR and apoptosis (Bradish *et al.*, 1975;Glasgow *et al.*, 1997;Scallan *et al.*, 1997;Barry *et al.*, 2010). The interaction of SFV with type-I IFN and the role of autophagy in SFV infection have not been fully elucidated.

1.3 The cell stress response: autophagy

Autophagy, meaning ‘self-eating’, describes the process in which cytoplasmic materials are degraded by lysosomes. Autophagy can be divided into three types: macroautophagy, microautophagy and chaperone-mediated autophagy. During macroautophagy, hereafter called autophagy, cytoplasmic materials are sequestered into double-membrane vacuoles and degraded by fusion with the lysosomes, described in 1.3.1. In microautophagy, the lysosomal membrane forms invaginations which deliver cytoplasm materials into the lysosome for degradation (Mortimore *et al.*, 1988;Li *et al.*, 2012b). In chaperone-mediated autophagy, proteins are unfolded by chaperone proteins (Dice & Chiang, 1989;Agarraberes *et al.*, 1997); and are

directly transported into lysosomes via the lysosomal-associated membrane (LAMP)-2a transporter for degradation (Cuervo & Dice, 1996;Cuervo & Dice, 2000).

Autophagy is a conserved homeostatic process, which maintains the internal conditions of the cell by removing dysfunctional organelles or by creating a source of amino acids during starvation conditions. In the late 1950s, mitochondria and lysosomal enzymes were detected within membrane-bound compartments in sections from mouse kidneys (Clark, 1957;Novikoff, 1959). Another study observed semi-digested mitochondria and the ER in membrane-bound vacuoles within the hepatocytes of rats (Ashford & Porter, 1962). In 1963, the term autophagy was used to describe double-membrane vacuoles that contain cytoplasmic proteins and organelles in various stages of degradation (De & Wattiaux, 1966). Later, autophagy was identified in yeast (Takeshige *et al.*, 1992) and, since then, autophagy has been observed in plants and other animals, including human cells. Genetic screening of yeast cells has identified over 30 autophagy (Atg) genes and homologues of most of these have been identified in mammals (Tsukada & Ohsumi, 1993;Matsuura *et al.*, 1997;Mizushima *et al.*, 1998b).

Autophagy is implicated in an increasing number of cellular processes both as a homeostatic process and as a defence mechanism against intracellular microbes. As a homeostatic process, autophagy has been linked to cell survival (Kourtis & Tavernarakis, 2009), development (Mizushima & Levine, 2010), aging (Lipinski *et al.*, 2010), cancer (Liang *et al.*, 1999;Qu *et al.*, 2003;Degenhardt *et al.*, 2006), inflammatory disease (Cadwell, 2010;Singh, 2010) and neurodegenerative diseases (Shibata *et al.*, 2006). Multiple studies have implicated autophagy in the innate and adaptive immune responses against diverse intracellular pathogens including bacteria (Gutierrez *et al.*, 2004;Nakagawa *et al.*, 2004;Birmingham *et al.*, 2006), parasites (Andrade *et al.*, 2006;Zhao *et al.*, 2008) and viruses. The role of autophagy in the innate and adaptive immune systems and the link between autophagy and viruses will be further explored below.

1.3.1 Autophagy: mechanism

The autophagy process can be divided into four stages: (i) initiation, (ii) elongation and completion of the autophagosome, (iii) fusion with the lysosome and (iv)

degradation or autophagy flux (Fig. 1.9). Autophagy is a dynamic process that rapidly cycles between these stages based on different stimuli. Our knowledge about autophagy and its mechanism is rapidly expanding, although the precise mechanism and the proteins involved remain to be fully determined. Current understanding of the mechanism is described below.

Initiation

Following induction of autophagy, the isolation membrane (also known as an omegasome or a phagophore) forms in the cell cytoplasm. The source of the isolation membrane remains unknown, although studies strongly suggest the involvement of the ER (Axe *et al.*, 2008;Yla-Anttila *et al.*, 2009;Hayashi-Nishino *et al.*, 2009) potentially in conjunction with the Golgi apparatus (van, V & Reggiori, 2010;Yen *et al.*, 2010), the plasma membrane (Ravikumar *et al.*, 2010) and the mitochondria (Hailey *et al.*, 2010). To date, two pathways are known to stimulate the formation of the isolation membrane: (i) the ULK1 protein kinase pathway, which includes the mammalian target of rapamycin (mTOR) and (ii) the Class III phosphatidylinositol 3-phosphate kinase (PI3K) pathway, which includes Beclin 1.

In the ULK1 protein pathway, mTOR is in a complex with the proteins ULK1, Atg13, FIP200 and Atg101 (Hara *et al.*, 2008;Hosokawa *et al.*, 2009;Jung *et al.*, 2009). Active mTOR prevents autophagy by hyperphosphorylating ULK1 and Atg13 (Hosokawa *et al.*, 2009). mTOR is inhibited by various signals, including genotoxic stress, hypoxia and, potentially, starvation, while growth factors, IL-4 and IL-13 prevent mTOR activation of autophagy. The pharmacological chemical rapamycin induces autophagy by inhibiting mTOR (Chiu *et al.*, 1994;Sabatini *et al.*, 1994). Following the inhibition of mTOR, ULK1, Atg13, FIP200 and Atg101 initiate autophagy, although the mechanism is not fully elucidated.

In the Class III PI3K pathway, Beclin 1 (mammalian homologue of yeast Atg6) is in a complex with the proteins Vps34 and Vps15. Studies have reported other proteins associated with the Class III PI3K complex, which regulate different stages of autophagosome development. Proteins implicated in the Class III PI3K complex include Atg14, Rubicon and UVRAG (Liang *et al.*, 2007;Itakura *et al.*, 2008;Matsunaga *et al.*, 2009;Zhong *et al.*, 2009). Bcl-2 binds Beclin 1 and inhibits the induction of autophagy (Pattingre *et al.*, 2005). The Class III PI3K pathway is

activated by various signals, including starvation and immune signals, and results in the formation of the isolation membrane. The pharmacological chemical 3-methyladenine (3MA) inhibits the class III PI3K pathway and, therefore, prevents autophagy (Seglen & Gordon, 1982).

Other proteins involved in the production of the isolation membrane are double FYVE-containing protein 1 and WD repeat domain phosphoinositide-interacting family proteins (Axe *et al.*, 2008;Polson *et al.*, 2010). However, the exact involvement of these proteins in production of the isolation membrane remains unclear.

Elongation and completion of the autophagosome

The isolation membrane elongates and fuses to form a double-membrane autophagosome surrounding cytoplasmic proteins or organelles. This elongation requires two ubiquitin-like conjugation systems: (i) the Atg5 system and (ii) the microtubule-associated protein light chain 3 (LC3) system. In the Atg5 system, Atg5 covalently conjugates to Atg12 forming Atg5-Atg12, which is facilitated by the E1-like enzyme Atg7 and the E2-like enzyme Atg10. Atg5-Atg12 then non-covalently associates with Atg16L1 (mammalian homologue of Atg16 in yeast) to form Atg5-Atg12-Atg16L1 (Hanada *et al.*, 2007;Fujita *et al.*, 2008). Atg5-Atg12-Atg16L1 locates to the surface of the isolation membrane where it is believed to mediate the expansion and curvature of the developing autophagosome (Mizushima *et al.*, 1998a;Mizushima *et al.*, 1998b;Xie *et al.*, 2008;Xie *et al.*, 2009). On completion of the autophagosome, Atg9 and Atg18 facilitate the removal of Atg5, Atg12 and Atg16L1 from the surface of the autophagosome.

In the LC3 system, LC3-I (mammalian homologue of yeast Atg8) is dispersed throughout the cell cytoplasm until LC3-I is cleaved by the protease Atg4 together with Atg7. Phosphatidylethanoloamine (PE) is then attached to a conserved glycine in the C-terminus of LC3-I by the E2-like enzyme Atg3 to produce LC3-II, which is also known as LC3-PE. LC3-II locates to both the inner and the outer membranes of the autophagosome (Ichimura *et al.*, 2000;Kabeya *et al.*, 2000). Both the double-membrane autophagosome and the presence of LC3-II are considered to be hallmarks of the autophagy process, as described in 1.3.7.

Fusion of the autophagosome with the lysosomes

The final two stages of the autophagy process are the least well understood. The autophagosome targets and fuses with the lysosomes to form the autolysosome. The lysosomal enzymes mediate the degradation of the inner membrane and the contents to produce amino acids. The amino acids can be exported into the cytoplasm and recycled by the cell (Ericsson, 1969;Lee *et al.*, 1989;Lawrence & Brown, 1992). However, the mechanism(s) by which the autophagosome detects and fuses with the lysosomes and the proteins involved remain largely unknown.

Degradation or autophagy flux

After prolonged starvation, mTOR reactivates (Yu *et al.*, 2010), presumably due to release of amino acids from the autolysosome elevating starvation conditions. mTOR induces the production of tubules from the autolysosome, which are termed protolysosomes. The protolysosomes form vesicles that mature into lysosomes and, therefore, prepare the cell for the next round of autophagy (Yu *et al.*, 2010).

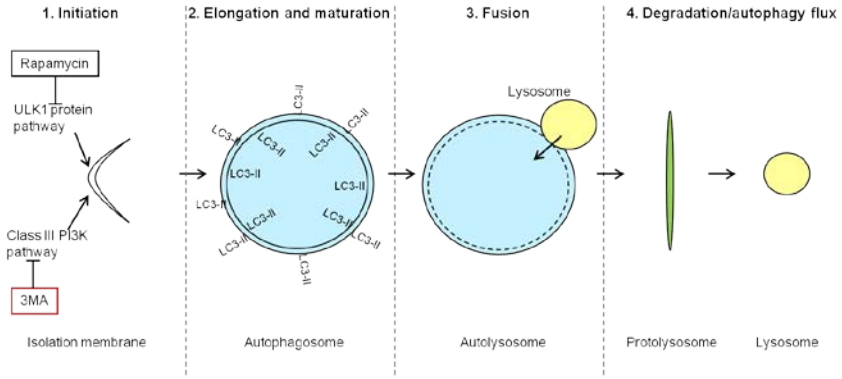

Figure 1.5: Simplified schematic diagram of the autophagy pathway.
Autophagy is a dynamic process that can be divided into four steps. 1) Initiation of the isolation membrane involves the activation of the ULK1 protein pathway, which includes mTOR, and the Class III PI3K pathway, which includes Beclin1. 2) The isolation membrane elongates and fuses to form the double-membrane autophagosome. This process involves Atg5-Atg12 conjugation and LC3-II formation. LC3-II is expressed on the inner and outer membranes of the autophagosome. 3) The autolysome fuses with the lysosome, loses its inner membrane and the lysosomal enzymes enter and degrade the contents. Amino acids are released from the autolysosome, which induces 4) formation of protolysosomes from the autolysome. Protolysosomes mature into lysosomes and the autophagy pathway can be repeated. Rapamycin inhibits mTOR and induces autophagy initiation. 3MA targets the Class III PI3K pathway and inhibits autophagy initiation.

1.3.2 Autophagy and innate immunity

Several studies have linked autophagy to the innate immune response. Studies suggest that autophagy can both regulate and be regulated by the innate immune system. In addition, autophagy is induced during microbial infection by pathogen-associated molecular patterns (PAMPs) binding to their pattern-recognition receptors (PRRs). Furthermore, autophagy can behave as an immune mechanism against invading microbes.

Autophagy regulates the innate immune response

Autophagy can induce the innate immune response by facilitating the activation of PRR. During Sendai virus and vesicular stomatitis virus (VSV) infection of plasmacytoid dendritic cells (pDC), autophagy delivers virus ssRNA to the lumen of endosomal compartments in which toll-like receptor (TLR) 7 is located (Lee *et al.*, 2007). Autophagy can also inhibit the innate immune response, including secretion of type-I IFN (Jounai *et al.*, 2007;Tal & Iwasaki, 2009) and interleukin (IL)-1b and IL-18 (Saitoh *et al.*, 2008). In addition, autophagy can prevent the retinoic-acid-inducible gene-I (RIG-I) signalling pathway through the Atg5-Atg12 conjugate (implicated in elongation of the autophagosome) binding to RIG-I, melanoma differentiation-associated gene-5 (mda-5) and IFN-β promoter stimulator protein 1 (IPS-1) (Jounai *et al.*, 2007).

Studies suggest that autophagy is regulated by cytokines in the innate immune response, including IFN-γ, IL-4, IL-13 (Harris *et al.*, 2007;Subauste *et al.*, 2007), tumour necrosis factor (TNF)-α and nuclear factor kappa B (NF-$_K$B) (Djavaheri-Mergny *et al.*, 2006;Subauste *et al.*, 2007). Taken together, the data suggest that the immune response mediates autophagy, which could provide a mechanism for degrading components of the immune response and prevent their over expression.

Activation of pattern recognition receptors induces autophagy

Several studies suggest that autophagy is induced following detection of PAMPs by their PRRs. In general, these studies have focused on bacterial recognition by TLRs

and nod-like receptors (NLR). TLR4 induces autophagy by binding lipopolysaccharide (LPS) (Yuan *et al.*, 2009), which facilitates the dissociation of Beclin 1 from Bcl-2 and, therefore, the induction of autophagy (Shi & Kehrl, 2010). Nod1 and Nod2 reportedly interact with Atg16L1 and can direct Atg16L1 to the plasma membrane at the site of bacterial entry (Travassos *et al.*, 2010). The role of the TLRs and NLRs in activating autophagy during viral infection remains to be fully elucidated. TLR7 was activated in pDCs following infection with SeV or VSV (Lee *et al.*, 2007). Potentially, TLR3 induces autophagy on detecting double-stranded (ds) RNA and could, therefore, activate autophagy following virus infection (Shi & Kehrl, 2008;Delgado *et al.*, 2008). Similarly, autophagy is activated by RIG-I like receptors (RLR) family detecting dsRNA (Tormo *et al.*, 2009). However, whether the RLRs induces autophagy following virus infection remains to be explored.

Based on autophagy studies, a new class of PRRs has been proposed, termed the Sequestosome 1/p62-like receptors (SLR). The SLRs contain cargo recognition and capture domains and an LC3-interacting domain (Yoshikawa *et al.*, 2009;Zheng *et al.*, 2009;Orvedahl *et al.*, 2010). SLRs include the autophagy adaptor proteins p62 and NBR1, which bind cytoplasmic proteins and transport them to the autophagosomes for degradation. In bacterial studies p62, NDP2 and optineurin have been implicated in the recognition and capturing of the antigens (Zheng *et al.*, 2009;Thurston *et al.*, 2009;Wild *et al.*, 2011). In viral studies, SINV capsid protein immunopreciptated with p62 in HeLa cells and p62 is suggested to transport SINV capsid protein to the autophagosomes for degradation (Orvedahl *et al.*, 2010).

Another potential sensor of virus infection that induces autophagy is protein kinase R (PKR). PKR is required for autophagy induction following Herpes simplex virus type 1 (HSV-1) (Talloczy *et al.*, 2006). Potentially PKR detects dsRNA produced during HSV-1 infection and induces autophagy.

Autophagy as an anti-microbial defence mechanism

Multiple studies have implicated autophagy in the innate immune responses against diverse intracellular pathogens, including bacteria (Gutierrez *et al.*, 2004;Nakagawa *et al.*, 2004;Birmingham *et al.*, 2006), parasites (Andrade *et al.*, 2006;Miller *et al.*,

2008;Zhao *et al.*, 2008) and viruses. The role of autophagy as an antiviral mechanism is discussed in 1.3.4.

1.3.3 Autophagy and adaptive immunity

Autophagy can facilitate major histocompatibility complex (MHC) II antigen presentation by delivering cytosolic proteins to the lumen of the MHC II antigen processing and loading compartments in DCs and B cells (Schmid & Munz, 2007). Autophagy may also support MHC I presentation of viral antigens (English *et al.*, 2009). Furthermore, one study reported that autophagy contributes to the selection of the CD4 T cell repertoire in the thymus and is essential for tolerance (Nedjic *et al.*, 2008). In addition, autophagy may affect the homeostasis of immune cells, including T cells (Pua & He, 2009), B cells (Miller *et al.*, 2008) and Paneth cells in the intestinal epithelium (Cadwell *et al.*, 2008). Finally, studies suggest a role for autophagy in controlling Th1/Th2 polarisation (Djavaheri-Mergny *et al.*, 2006;Harris *et al.*, 2007). In vaccine development studies autophagy enhanced the efficacy of the influenza vaccine (Schmid & Munz, 2007) and the BCG vaccine in the animal model of tuberculosis (Jagannath *et al.*, 2009).

1.3.4 Autophagy as an antiviral mechanism

Several studies in plants, invertebrates and vertebrates have described autophagy as a defence mechanism against both DNA and RNA viruses. In plants, the ATG genes *BECLIN 1*, *ATG7*, *ATG3* and *VPS34* control the replication of tobacco mosaic virus (TMV) and limit cell death induced by the hypersensitive response (Liu *et al.*, 2005). In *Drosophila*, the ATG genes *ATG5*, *ATG8* and *ATG18* protect against VSV infection in both cell culture and *in vivo* (Shelly *et al.*, 2009). In vertebrates, over-expression of Beclin 1 in neurones protects neonatal mice against lethal SINV infection (Liang *et al.*, 1998). Furthermore, in mice lacking Atg5, SINV capsid persisted in the neurones and there was increased neuronal death in contrast to the WT infection (Orvedahl *et al.*, 2010). However, the absence of Atg5 did not affect SINV replication. Taken together, these results suggest that autophagy may function to clear SINV capsid in neurones. In support of this hypothesis, SINV capsid immunoprecipitated with p62, which may, the authors suggest, target capsid to the autophagosomes for degradation (Orvedahl *et al.*, 2010).

In further support of autophagy as an antiviral mechanism, certain viruses have developed mechanisms to inhibit autophagy. HSV-1 protein ICP34.5 binds to Beclin 1 and inhibits autophagy both in cell culture and in mice (Talloczy *et al.*, 2006;Orvedahl *et al.*, 2007). Deletion of the Beclin 1 binding domain in ICP34.5 produces a mutant named HSV-134.5Δ68-87, which is less neurovirulent and more rapidly cleared in mice than WT HSV-1 (Orvedahl *et al.*, 2007;Leib *et al.*, 2009). Interestingly, both HSV-134.5Δ68-87 and the WT HSV-1 have similar replication kinetics *in vitro* and only differ in neurovirulence *in vivo*. Therefore, the role of autophagy may vary in *in vitro* and *in vivo* studies, potentially due to differences between cell types. γ-herpesviruses encode a virus Bcl-2 product that binds to Beclin 1 and inhibits autophagy (Sinha *et al.*, 2008;Ku *et al.*, 2008). Similarly, HIV Nef protein binds Beclin 1, which inhibits autophagy in macrophages (Kyei *et al.*, 2009). Taken together, these results indicate that viruses have evolved mechanism(s) to inhibit autophagy, which is presumably a result of the antiviral role of autophagy.

1.3.5 Autophagy as a proviral mechanism

In most positive ssRNA virus infections studied to date autophagy actually enhances virus replication. Pharmacological induction of autophagy by rapamycin or tamoxifen increases polio virus (PV) replication in HeLa cells, while 3MA had the opposite affect (Jackson *et al.*, 2005). PV replication proteins 2BC and 3A co-localised with GFP-LC3 and the autophagy protein LAMP1 in HEK293 cells (Jackson *et al.*, 2005). This study indicated that PV utilises the autophagosome as a site of replication. Similarly, pharmacological induction of autophagy enhances virus replication in coxsackievirus B3 virus (Wong *et al.*, 2008), foot-and-mouth-disease virus (FMDV) (O'Donnell *et al.*, 2011), DENV (Lee *et al.*, 2008), Japanese encephalitis virus (JEV) (Li *et al.*, 2012a), severe acute respiratory coronavirus (SARS-CoV) (Prentice *et al.*, 2004) and hepatitis C virus (HCV) (Dreux & Chisari, 2009) infections in cell culture.

Recently, autophagy was reported to be a proviral mechanism for CHIKV infection in HEK293 cells (Krejbich-Trotot *et al.*, 2011). This study conflicts with observations made with SINV infection in which autophagy had no affect on SINV replication in mouse embryonic fibroblasts (MEFs) and was suggested to clear SINV

capsid (Orvedahl *et al.*, 2010). Possible explanations for the differences between the role of autophagy in SINV and CHIKV infection include (i) different viruses interact with autophagy differently and/or (ii) the host cell type is fundamental in determining the outcome of autophagy following infection and/or (iii) the different methods used to study autophagy affected the results.

1.3.6 Autophagy as neither an antiviral or a proviral mechanism

Despite the number of studies suggesting that autophagy is a proviral or an antiviral innate mechanism, several studies demonstrate that autophagy has no effect on the replication of certain viruses. Murine hepatitis virus (MHV) had similar replication kinetics in WT MEFs and in MEFs lacking the ATG5 gene (Zhao *et al.*, 2007b). Atg5 is required for elongation and maturation of the autophagosome, as described in 1.3.1. Similarly, induction of autophagy with rapamycin or tamoxifen or inhibition of autophagy with 3MA had no affect on replication of human rhinovirus (HRV2) (Brabec-Zaruba *et al.*, 2007). Furthermore, autophagosomes were not detected on infection with HRV2 (Brabec-Zaruba *et al.*, 2007), unlike in PV (Jackson *et al.*, 2005). Similar titres of SINV were detected in the supernatant of WT MEFs and in MEFs lacking the ATG5 gene (Orvedahl *et al.*, 2010). In a study published during the writing of this thesis, neither the induction of autophagy by rapamycin nor the inhibition of autophagy in Atg5 negative cells had any effect on SFV4 replication (Eng *et al.*, 2012). In conclusion, the role of autophagy appears to depend on the virus and, potentially, the host cell line investigated.

1.3.7 Methods used to study autophagy

The last ten years have witnessed a surge in the number and the quality of assays available to study autophagy. The hallmark of autophagy is the formation of the double-membrane autophagosome. The autophagosome can be detected directly using electron microscope imaging or indirectly using molecular techniques. A frequently used method to indirectly detect autophagosome formation is via LC3. LC3-I is diffused throughout the cytoplasm of healthy cells, while during autophagy phosphatidylethanolamine is conjugated and this forms LC3-II, which locates to the

as autophagosome, as described in 1.3.1. LC3 can be visualised in the cytoplasm by immunostaining or by fluorescently tagging LC3 with GFP and expressing from a plasmid or a transgene in a stable cell line or a mouse model (Kabeya *et al.*, 2000;Mizushima, 2004;Jackson *et al.*, 2005;Ding *et al.*, 2007). The translocation of LC3-II to the autophagosomes produces punctuate staining, which is a recognised feature of autophagy accumulation in cells. Punctate staining can be enumerated manually or, as more recently reported, by FACS analysis (Shvets *et al.*, 2008;Eng *et al.*, 2010). Alternatively, LC3-I and LC3-II, which differ slightly in molecular weight (16 kD and 14 kD respectively), can be detected by Western blot (Kabeya *et al.*, 2000). The techniques mentioned above measure the accumulation of autophagosomes, which could be due to induction of autophagy or downstream inhibition of autophagy. Therefore, these techniques are used in conjunction with other methods to delineate the autophagy response.

More recently, alternative methods of indirectly studying autophagy have been established. Several studies have analysed the interaction of virus proteins with the autophagy proteins p62 or NBR1 by immunostaining and immunoprecipitation (Pankiv *et al.*, 2007;Kirkin *et al.*, 2009). P62 and NBR1 collect cytoplasmic proteins and target them to the autophagosomes for degradation (Pankiv *et al.*, 2007;Kirkin *et al.*, 2009;Zheng *et al.*, 2009;Thurston *et al.*, 2009). Colocalisation and immunoprecipitation of virus proteins with p62 and NBR1 together with the classic LC3 assays to show the accumulation of autophagosomes may indicate that specific virus proteins are transported to the autophagosomes for degradation (Orvedahl *et al.*, 2010).

Autophagy is in a constant state of flux in which autophagosomes are formed and degraded. Autophagy flux can be prevented by inhibiting lysosomal activity, which causes the accumulation of autophagosomes in the cytoplasm. Lysosomal activity can be blocked using chemicals including ammonium chloride, chloroquine or bafilomycin A, or by targeting the lysosomal proteases with E64d or pepstatin A. Following inhibition of the lysosomes, autophagy flux can analysed by (i) observing LC3 punctate staining and degradation visually, by FACS or by Western blot, (ii) transfecting cells with a plasmid expressing mRFP fused to GFP and LC3 (mRFP-GFP-LC3) (Kimura *et al.*, 2007) or (iii) measuring bulk degradation of long-lived

proteins by measuring production of isotope-labelled amino acids (Mizushima *et al.*, 2010). mRFP-GFP-LC3 translocates to the autolysosomes in which GFP is rapidly degraded and RFP is not (Kabeya *et al.*, 2000;Bampton *et al.*, 2005;Kimura *et al.*, 2007). Therefore, it can be visually determined if the autolysomes are functioning. Combinations of the techniques mentioned above are used to study autophagy flux.

A well-documented method to establish the affect of autophagy on virus infection is to modulate autophagy activity. Autophagy can be induced by starvation or pharmacologically, using chemicals such as rapamycin, an inhibitor of mTOR. Autophagy is pharmacologically inhibited by treatment with 3MA, wortmannin or LY294002 (Blommaart *et al.*, 1997;Itakura *et al.*, 2008;Matsunaga *et al.*, 2009). 3MA inhibits the class III PI3K pathway and, therefore, prevents autophagy through this pathway (Seglen & Gordon, 1982). However, chemicals can affect cellular processes other than autophagy. For example, 3MA function is implicated in lysosomal acidification, endocytosis and mitochondrial permeability (Caro *et al.*, 1988;Punnonen *et al.*, 1994;Xue *et al.*, 2002). Therefore, genetic approaches to silence specific genes, including Atg3 (Sou *et al.*, 2008), Atg5 (Mizushima *et al.*, 2001), Beclin 1 (Qu *et al.*, 2003), Atg7 (Komatsu *et al.*, 2005), Atg9a (Saitoh *et al.*, 2009), Atg16L1 (Cadwell *et al.*, 2008), FIP200 (Hara *et al.*, 2008) and Ambra1 (Fimia *et al.*, 2007) have been described both *in vitro* and *in vivo*.

In conclusion, autophagy research is a rapidly developing field and, as such, the techniques reported and reagents available to study autophagy are increasing.

1.4 The cell stress response: interferon

IFNs are a large group of secreted cytokines with roles in antiviral activity, cell growth regulation and immune activation. The antiviral activity of IFN was first discovered in 1957 (Isaacs & Lindenmann, 1957). Since then several different IFNs have been identified that can be divided into type-I, type-II or type-III based on their amino acid sequence, receptor usage and biological activity.

1.4.1 Type-I interferon

Type-I IFN has several members including IFN-α, -β -ω, ε, -τ, -δ and -ζ, which are summarised in Table 1.1. The best characterised of the type-I IFNs are IFN-α and

IFN–β. In humans, IFN-α is encoded by 13 genes which are located on chromosome 9 (Nagata *et al.*, 1980). The mature IFN-α proteins share 75 – 99 % homology (Bekisz *et al.*, 2004). In contrast, only one gene encodes IFN-β in humans; this gene is also is located on chromosome 9 (Roberts *et al.*, 1998). IFN-α and IFN–β are probably the most important innate antiviral defence mechanisms. IFN-α and IFN–β are produced by cells in direct response to virus infection and have both an autocrine and a paracrine function. IFN-α is primarily secreted by leucocytes, such as the pDC (Siegal *et al.*, 1999). IFN-β can be produced by most cells, but is primarily associated with fibroblasts. Both IFN-α and IFN–β bind a common receptor, termed IFNAR, which appears to be ubiquitously expressed. The activated IFNAR induces the IFN-signalling pathway, including the proteins Janus kinase (previously termed just another kinase) (JAK)-1, the signal transducers and activators of transcription (STAT) and interferon response factor (IRF)-9, which causes the transcription of various genes, termed the IFN-stimulated genes (ISG) (described in section 1.4.4). Together the ISG create an antiviral state within the target cell, which is unfavourable for virus replication. The induction and signalling pathways of IFN-α and IFN–β are described in 1.4.3 and 1.4.5.

Other type-I IFNs expressed in humans are IFN-ω, IFN-κ and IFN-ε. IFN-ω was discovered in 1985 and shares 60 – 70 % homology with IFN-α (Capon *et al.*, 1985;Feinstein *et al.*, 1985;Hauptmann & Swetly, 1985). IFN-ω, like IFN-α, binds the IFNAR and is implicated in the antiviral response (Flores *et al.*, 1991). IFN-κ is secreted by keratinocytes and acts through IFNAR to induce the antiviral state in cells (LaFleur *et al.*, 2001). Relatively little is known about IFN-ε, but it is constitutively expressed in mouse placental and ovarian tissues which indicates a role for IFN-ε in pregnancy (Hardy *et al.*, 2004;Krause & Pestka, 2005).

IFN- ζ, IFN-τ and IFN-δ are not expressed by humans. IFN- ζ, also known as limitin, is expressed by mice, shares a 30 % homology with IFN-α and acts through the IFNAR (Oritani *et al.*, 2000;Oritani *et al.*, 2001). IFN- ζ is associated with antiviral activity, but unlike IFN-α, it does not affect the proliferation of normal myeloid or erythroid progenitors (Oritani *et al.*, 2000;Kawamoto *et al.*, 2003). IFN-δ has 140 amino acids and is produced by trophoblasts in the pig. IFN-δ appears to

facilitate pregnancy as opposed to inducing the antiviral state (La *et al.*, 1991;Lefevre *et al.,* 1998). In ruminants IFN-τ is produced by trophoblasts and, like IFN-δ, facilitates pregnancy (Imakawa & Roberts, 1989;Imakawa *et al.,* 1989;Martal *et al.*, 1998). However, IFN-τ is most similar to IFN-ω with 75 % homology (Martal *et al.*, 1998). IFN-τ can act across species and studies suggest a potential application for IFN-τ in human antiviral therapy (Martal *et al.*, 1998).

This thesis focuses on IFN-α and IFN–β and, hereafter, type-I IFN will only refer to IFN-α and IFN-β.

Table 1.1: Summary of type-I interferon members identified to date.

Type	Associated cell type	Example of Species expressing IFN	Receptor	Function	Reference
IFN-α	Leucocytes	Human	IFNAR	Induction of the antiviral state	(Randall & Goodbourn, 2008)
IFN-β	Most cells	Human	IFNAR	Induction of the antiviral state	(Randall & Goodbourn, 2008)
IFN-ω		Human	IFNAR	Induction of the antiviral state	(Capon *et al.*, 1985;Feinstein *et al.*, 1985;Hauptmann & Swetly, 1985;Flores *et al.*, 1991)
IFN-ε		Placental mammals	IFNAR		(Hardy *et al.*, 2004)
IFN-τ	Trophoblasts	Ruminant	IFNAR	Facilitates pregnancy	(Martal *et al.*, 1998)
IFN-δ	Trophoblasts	Pig	IFNAR	Facilitates implantation	(La *et al.*, 1991;Lefevre *et al.*, 1998).
IFN-ζ / limitin		Mouse	IFNAR	Induction of the antiviral state	(Oritani *et al.*, 2000;Kawamoto *et al.*, 2003)
IFN-κ	Keratinocytes	Human		Induction of the antiviral state	(LaFleur *et al.*, 2001)

1.4.2 Type-II interferon

Type-II IFN has one member, IFN-γ, which is encoded on chromosome 12 (Naylor *et al.*, 1983). IFN-γ is structurally unrelated to type-I IFN and binds to a different receptor, named IFNGR. Historically, IFN-γ was believed to be secreted by CD4 Th1 cells, CD8 cytotoxic suppressor cells and natural killer (NK) cells (Bach *et al.*, 1997). However, several studies indicate that B cells, NK T cells and professional antigen-presenting cells (APC) also secrete IFN-γ (Carnaud *et al.*, 1999;Harris *et al.*, 2000;Frucht *et al.*, 2001). IFN-γ is induced following the detection of virus antigens or mitogens on MHC class I and II molecules and cytokines, such as IL-12 and -18 that attract NK cells to the site of infection (Otani *et al.*, 1999;Golab *et al.*,

2000;Fukao *et al.*, 2000;Akira, 2000;Munder *et al.*, 2001). IFN-γ expression is negatively regulated by cytokines, such as IL-12, IL-4 and IL-10 (Schindler *et al.*, 1992;Fukao *et al.*, 2000;Frucht *et al.*, 2001;Hochrein *et al.*, 2001).

IFN-γ signals through the IFNGR and induces the transcription of ISGs that together produce the antiviral state (Huang *et al.*, 1993;Muller *et al.*, 1994). In addition, IFN-γ induces microbiocidal effector functions and regulates cell proliferation and apoptosis in macrophages (Schroder *et al.*, 2004). IFN-γ signalling also increases the quantity and diversity of MHC class I and II complexes on the cell surface, which enhances cytotoxic T cell recognition of antigens and also immunomodulates the $CD4^+$ T cell response (Mach *et al.*, 1996;Boehm *et al.*, 1997;Schroder *et al.*, 2004). Finally, IFN-γ stimulates the trafficking of leucocytes to the site of infection by inducing cytokine production (Schroder *et al.*, 2004).

1.4.2 Type-III interferon

Type-III IFNs were discovered in 2003 and are named IFN-λ1, IFN-λ2 and IFN-λ3 or IL-29, IL-28A and IL-28B (Kotenko *et al.*, 2003;Sheppard *et al.*, 2003). Type-III IFNs share approximately 5 – 18 % homology with type-I IFNs and were originally thought to be members of the type-I IFN group (Sheppard *et al.*, 2003;Kotenko *et al.*, 2003). However, type-III IFNs bind to a novel receptor named IFN-λR1 (also known as IL-28RA), which is composed of the IFN-λR1 and IL-10R2 chains (Kotenko *et al.*, 2003;Sheppard *et al.*, 2003). The IL-10R2 chain is also an essential component of receptors that bind IL-10, IL-22 and IL-26 (Donnelly *et al.*, 2004). Type-I and type-III IFNs bind to different surface receptors, but appear to signal through the same type-I IFN signalling pathway to induce the antiviral state (Kotenko *et al.*, 2003;Dumoutier *et al.*, 2004). Microarray analysis demonstrates that type-I and type-III IFNs induce the expression of similar genes (Doyle *et al.*, 2006;Marcello *et al.*, 2006). Several studies have demonstrated type-III IFN antiviral activity against various virus infections, including encephalomyocarditis virus (EMCV) and VSV (Kotenko *et al.*, 2003;Sheppard *et al.*, 2003;Ank *et al.*, 2006). In inoculation of influenza A virus in mice produces higher levels of type-III IFN than type-I IFN in the lungs, which suggests a role for type-III IFN in the first line of defence against virus infection (Jewell *et al.*, 2010). Type-III IFNs can amplify the antiviral activity

induced by type-I IFN (Biron, 2001;Le & Tough, 2002;Pestka *et al.*, 2004). Similarly, studies indicate that type-I IFN amplifies the production of type-III IFN during influenza or SeV infections (Osterlund *et al.*, 2005;Siren *et al.*, 2005). Type-I and type-III IFNs are co-expressed by virus-infected cells, including SINV, Dengue virus (DENV), EMCV and VSV (Kotenko *et al.*, 2003;Sheppard *et al.*, 2003). In addition to inducing the antiviral state, type-III IFN is implicated in anti-proliferative activity (Maher *et al.*, 2008) and anti-tumour activity (Lasfar *et al.*, 2006;Sato *et al.*, 2006;Numasaki *et al.*, 2007). Furthermore, type-III IFN may serve as a therapeutic reagent for treatment against viruses such as HCV and hepatitis B virus (HBV) (Pagliaccetti & Robek, 2010).

The key difference between type-I and type-III IFN activity is the limited distribution of IFN-λR1. Type-III IFN, unlike type-I IFN, cannot induce STAT phosphorylation in primary fibroblasts, human umbilical vein endothelial cells, murine splenocytes or most leucocytes (Lasfar *et al.*, 2006). Instead, type-III IFN is associated with cells of epithelial origin that express high levels of IFN-λR1 (Lasfar *et al.*, 2006;Sommereyns *et al.*, 2008;Witte *et al.*, 2009). Therefore, type-III IFN may provide a vital first line of defence against viruses entering the body through the skin.

1.4.3 Induction of type-I interferon

Type-I IFN is induced following the detection of PAMPs found on parasites, bacteria and viruses by PRRs. Several PRRs have been identified, such as the TLRs and the RIG-I-like receptors (RLRs), which facilitate the detection of virus at various stages of infection. PRRs detecting viruses can be divided into those located in the endosomes and those in the cytoplasm. Some PRRs are located on the cell surface, but these are generally associated with bacteria or parasite detection. All PRR pathways ultimately induce the transcription factors NF-$_K$B and IFN regulatory factor-3 (IRF-3). NF-$_K$B and IRF-3 together with the transcription factors ATF-2 and c-Jun translocate to the nucleus and form the enhancesome for IFN-β production (Baeuerle & Henkel, 1994;Thanos & Maniatis, 1995;Au *et al.*, 1995). In fibroblasts, IFN-β and mouse IFN-α4 are produced in the first wave of IFN production, while the other IFN-α and IFN-β are secreted in the second wave. SFV is an RNA virus;

therefore this section will mainly focus on the induction of type-I IFN by RNA viruses.

Induction of type-I interferon by pattern recognition receptors located in endosomal compartments

TLR-3, TLR-7 and TLR-9 are located in endosomal compartments and detect phagocytosed material including viruses through the endosomal pathway (Honda *et al.*, 2005). TLR-3 binds dsRNA, which is a replication intermediate produced during virus infection (Alexopoulou *et al.*, 2001;Tabeta *et al.*, 2004;Hewson *et al.*, 2005). TLR-7 detects single-stranded RNA, such as the genome of VSV and influenza virus (Lund *et al.*, 2004). TLR-9 recognises DNA unmethylated at CpG residues (Hemmi *et al.*, 2000;Lund *et al.*, 2004). Other TLRs include TLR-2 and TLR-4, which are generally associated with bacterial infection, but can detect virus infection: TLR-2 binds the haemagglutinin protein of measles virus (MeV) (Bieback *et al.*, 2002) and TLR-4 binds the fusion protein of respiratory syncitial virus (Kurt-Jones *et al.*, 2000).

TLR-3 signals, in a myeloid differentiation primary response gene 88 (MyD88)-independent manner, through Toll/IL-1R domain-containing adaptor-inducing IFN-β (TRIF) (Yamamoto *et al.*, 2003). The induction of type-I IFN by TLR-3 involves TLR-3 binding to dsRNA which causes TLR-3 dimerisation and tyrosine phosphorylation (Sarkar *et al.*, 2003). Dimerised TLR-3 recruits TRIF that activates both IRF-3 and NF-$_K$B (Jiang *et al.*, 2004), shown in Figs 1.5 and 1.6. To induce NF-$_K$B, a protein complex composed of receptor-interacting protein 1 (RIP1) (Meylan *et al.*, 2004;Cusson-Hermance *et al.*, 2005), tumour necrosis factor receptor-associated factor (TRAF) 6 (Sato *et al.*, 2003;Jiang *et al.*, 2004), transforming growth factor β-activated kinase 1 (TAK1) (Deng *et al.*, 2000;Wang *et al.*, 2001) and NF-$_K$B essential modifier (NEMO), which is also known as I_KB kinase complex, (Ea *et al.*, 2006;Li *et al.*, 2006;Wu *et al.*, 2006) is recruited to TRIF. The protein complex associates with IKappa kinase (IKK) α and IKKβ and IKKβ is phosphorylated by TAK1 (Wang *et al.*, 2001). Activated IKKα and IKKβ induce the activation and translocation of NF-$_K$B to the nucleus, as described in 'activation of NF-$_K$B' below.

TLR-3 activation of IRF-3, shown in Fig. 1.6, involves the recruitment of TRAF-3 to TRIF (Hacker *et al.*, 2006;Oganesyan *et al.*, 2006). These proteins then associate with TRAF family member-associated NF-$_k$B activator (TANK) (Li *et al.*, 2002), TANK-binding kinase 1 (TBK-1) (Pomerantz & Baltimore, 1999) and IKKε, which facilitate the activation and translocation of IRF-3 to the nucleus (Fitzgerald *et al.*, 2003;Sharma *et al.*, 2003), described in 'activation of IRF-3' below.

Induction of type-I interferon by pattern recognition receptors located in the cytoplasm

RLRs are located in the cell cytoplasm and include mda-5, RIG-I and a receptor called "laboratory of genetics and physiology 2" (LGP2) (Yoneyama *et al.*, 2004;Rothenfusser *et al.*, 2005;Hornung *et al.*, 2006;Kato *et al.*, 2006). RIG-I and mda-5 are composed of an RNA-binding helicase domain and two caspase recruitment domains (CARDS) (Yoneyama *et al.*, 2004), while LGP2 does not possess CARDs. Several studies have identified RIG-I and mda-5 as essential PRR in detecting RNA viruses, including *Flaviviridae, Paramyxoviridae, Orthomyxoviridae*, and *Rhabdoviridae* (Loo & Gale, Jr., 2011). However, the RNA

form that RIG-I and mda-5 detect remains controversial. Different studies have reported that RIG-I can bind dsRNA, ssRNA, uridine and adenosine-rich regions and/or the 5' triphosphate region on RNA (Yoneyama *et al.*, 2004;Hornung *et al.*, 2006;Pichlmair *et al.*, 2006). The 5' triphosphate group on cellular mRNA is removed by capping or post-translational modification, which may provide a mechanism to differentiate some virus ssRNA from cellular ssRNA (Hornung *et al.*, 2006). One study suggests that the RNA must have an element of dsRNA, perhaps through a hairpin loop, to be detected by RIG-I (Schmidt *et al.*, 2009).

Mda-5 can detect poly(I:C) and, in addition, the positive sense RNA genome of picornaviruses (Kato *et al.*, 2006;Gitlin *et al.*, 2006). A panel of parmyxoviruses were found to bind and antagonise mda-5 through the viral V protein, which indicates the importance of mda-5 as an antiviral protein (Andrejeva *et al.*, 2004). Some viruses are detected by both RIG-I and mda-5, including West Nile virus (WNV) and DENV (Fredericksen *et al.*, 2008;Loo *et al.*, 2008). In SINV infection, mda-5 is associated with virus recognition (Burke *et al.*, 2009). LGP2 was originally associated with the negative regulator of RLR (Rothenfusser *et al.*, 2005). However, one study using LGP2 knock-out mice suggests that LGP2 may actually positively regulate RLR signalling (Venkataraman *et al.*, 2007).

On detecting RNA, RIG-I and mda-5 bind and activate a mitochondrion-associated adaptor protein called IPS-1, also known as CARD adaptor-inducing IFN-*β* (Cardif)/virus-induced signalling adaptor (VISA) and mitochondrial antiviral signalling protein (MAVS) (Kawai *et al.*, 2005;Meylan *et al.*, 2005;Seth *et al.*, 2005;Xu *et al.*, 2005). IPS-1 induces the activation and translocation of NF-$_k$B and IRF-3 to the nucleus through pathways apparently similar to that employed by TLR-3 (Kawai *et al.*, 2005;Meylan *et al.*, 2005;Seth *et al.*, 2005;Xu *et al.*, 2005), see Figs 1.5 and 1.6. To induce NF-$_K$B activation, RIG-I directly interacts with TRAF6 (Xu *et al.*, 2005) in a protein complex with RIP1, NEMO and TAK-1 (Zhao *et al.*, 2007a). The protein complex recruits and activates IKKα and IKKβ which induces NF-$_K$B activation. To induce IRF-3 activation, IPS-1 associates with TRIF, TANK, TBK-1 and IKKε, which facilitates the activation and translocation of IRF-3 to the nucleus.

Another cytoplasmic PRR is PKR, which binds dsRNA via dsRNA binding motifs (dsRBM) located in the N-terminal region of PKR (Clemens *et al.*, 1993).

Binding dsRNA induces autophosphorylation and homodimerisation of PKR, which then activates the transcription factor NF-$_K$B (Kirchhoff *et al.*, 1999;Cheshire *et al.*, 1999).

Activation of NF-kB (Fig. 1.6)

NF-$_K$B is located in an inactive form in the cytoplasm associated with inhibitor of NF-$_K$B (I$_k$B) (Lenardo & Baltimore, 1989;Beg & Baldwin, Jr., 1993). On detection of virus infection, I$_k$B is phosphorylated and undergoes ubiquitination and degradation by proteosomes, which releases NF-$_K$B (Karin & Ben-Neriah, 2000). The NLS on the p65 subunit of NF-$_K$B is exposed, which facilitates the translocation of NF-$_K$B to the nucleus (Ganchi *et al.*, 1993). In the nucleus, NF-$_K$B forms part of the enhanceosome together with the transcription factors IRF-3 and ATF-2/c-jun. ATF-2 and c-Jun are required for optimal induction of IFN-β (Thanos & Maniatis, 1995). ATF-2 and c-Jun are activated through the stress activated mitogen activated kinase (MAP) kinase pathway by dsRNA recognition (Chu *et al.*, 1999;Iordanov *et al.*, 2001;Servant *et al.*, 2002). Active ATF-2 and c-Jun associate to form AP-1, which translocates to the nucleus and forms part of the enhanceosome. The transcription factors NF-$_K$B, IRF-3 and ATF-2/c-Jun associate with specific positive regulatory domains (PRD) of the IFN-β promoter in the enhanceosome. The PRD are located upstream of the IFN-β promoter. PRD I and III associate with IRF-3 and -7, PRD II binds NF-$_K$B and PRD IV associates with ATF-2/c-Jun (Maniatis *et al.*, 1998;Berkowitz *et al.*, 2002;Panne *et al.*, 2004). However, studies suggest that IFN-β secretion can occur without the activation and recruitment of NF-$_K$B and ATF-2/c-Jun to the enhanceosome (Ellis & Goodbourn, 1994;Peters *et al.*, 2002). The enhanceosome is stabilised by association of the high mobility group I (Y) proteins (HMG I (Y)) with PRD II and PRD IV (Yie *et al.*, 1999). However, HMG I (Y) is not required in all models of the enhancesome (Berkowitz *et al.*, 2002;Panne *et al.*, 2004). The enhanceosome recruits CREB-binding protein (CBP)/p300, which promotes the assembly of the basal transcriptional machinery and RNA polymerase to induce IFN-β production (Zhong *et al.*, 1998).

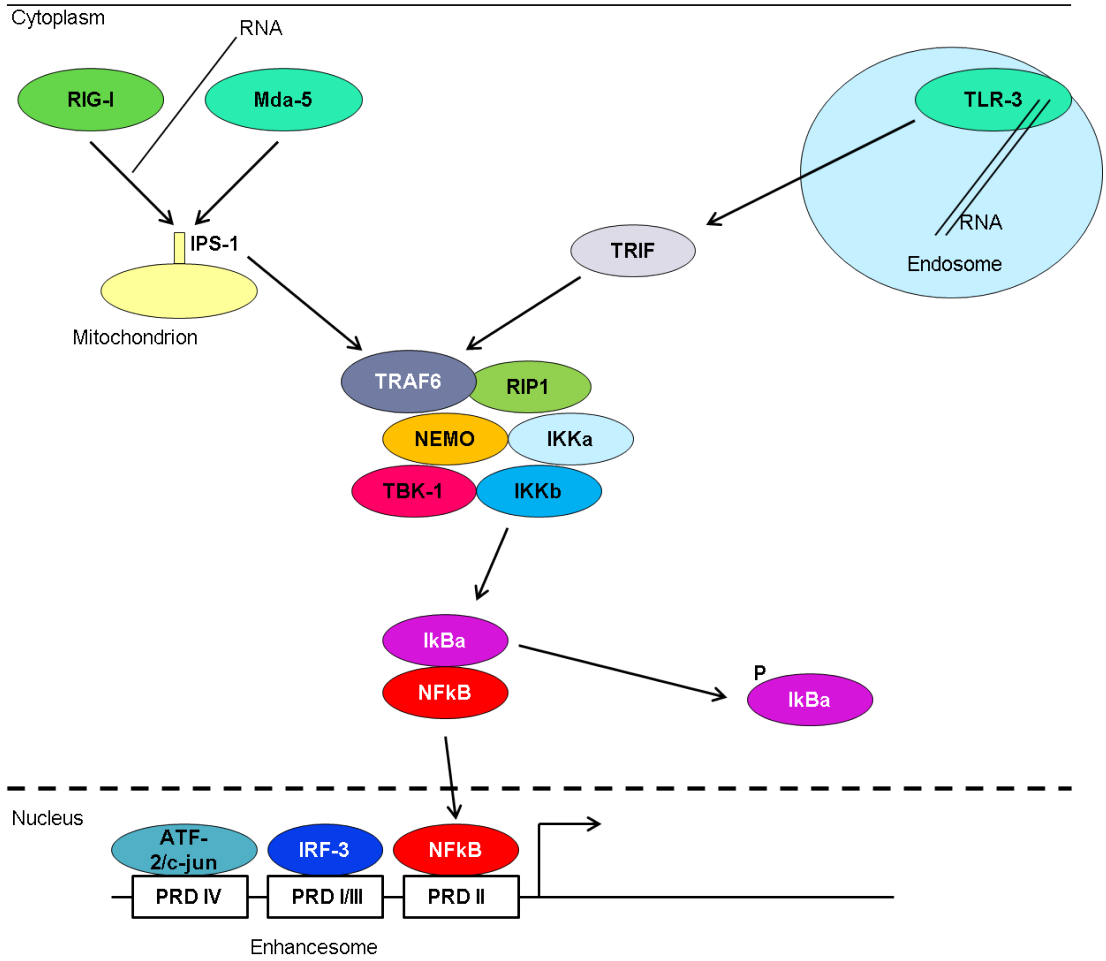

Figure 1.6: Schematic representation of the NF-KB induction pathway. Cytoplasmic PRR RIG-I or mda-5 detect foreign RNA and converge on the adaptor IPS-1/Cardif/VISA/MAVS located on the surface of mitochondria. Active IPS-1 forms a protein complex, which induces the phosphorylation of the inhibitor of NF-$_K$B (IkB) in the cytoplasm. NF-$_K$B is released, translocates to the nucleus, binds PRD II and forms part of the enhancesome together with ATF-2/c-jun and IRF-3. The enhanceosome induces the transcription of IFN-β.

Activation of IRF-3 (Fig. 1.7)

IRF-3 is located in the cellular cytoplasm in an inactive form (Au *et al.*, 1995;Yoneyama *et al.*, 2002). Following PAMP detection, the C-terminus of IRF-3 is phosphorylated which facilitates the dimerisation of two IRF-3 proteins (Au *et al.*, 1995;Lin *et al.*, 1998). The dimerisation of IRF-3 exposes an NLS, which facilitates translocation of IRF-3 into the nucleus (Lin *et al.*, 1998;Dragan *et al.*, 2007;Panne *et al.*, 2007). In the nucleus, IRF-3 binds to PRD I/III to form the enhanceosome together with NF-$_K$B and ATF-2/c-jun, as described in 'activation of NF-$_K$B' above. IRF-3 remains in the nucleus until it is dephosphorylated (Kumar *et al.*, 2000).

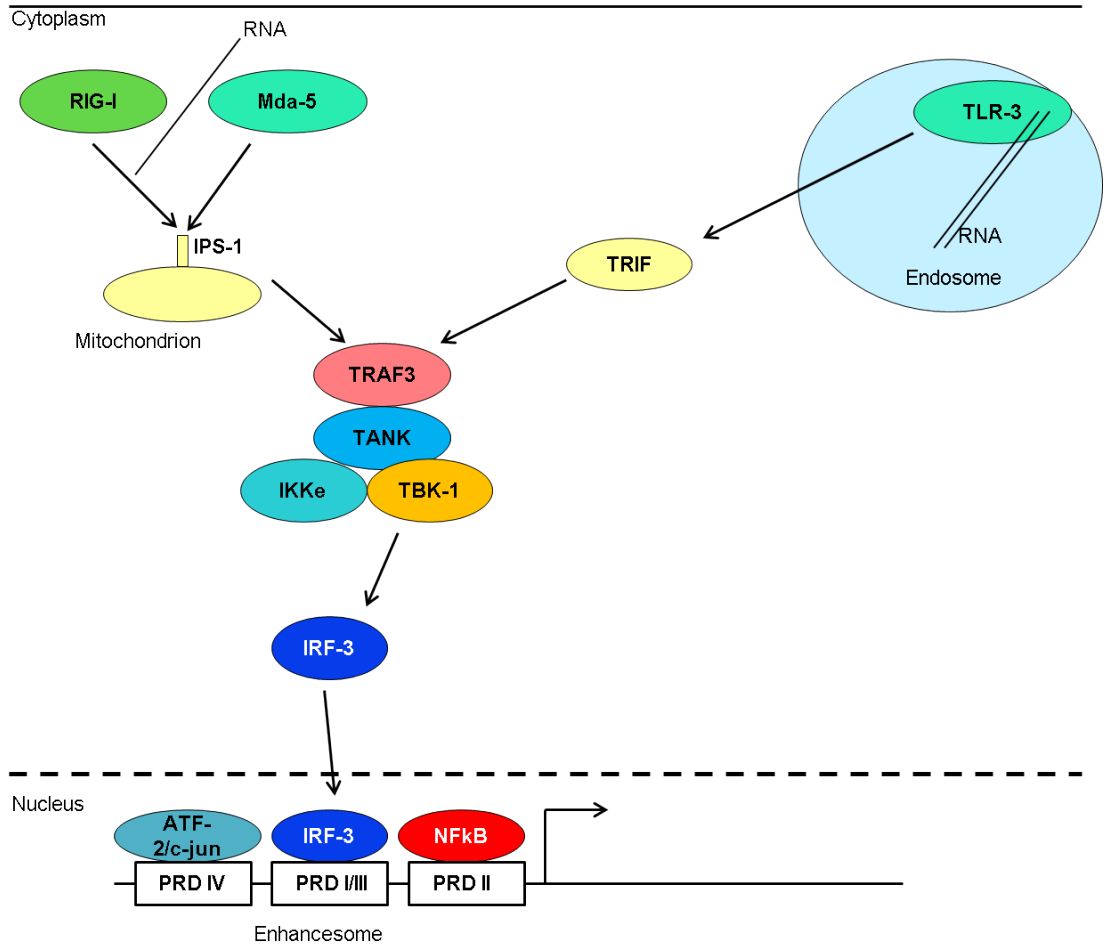

Figure 1.7: Schematic representation of the IRF-3 induction pathway. Cytoplasmic PRR RIG-I or mda-5 detect foreign RNA and converge on the adaptor IPS-1/Cardif/VISA/MAVS located on the surface of mitochondria. Active IPS-1 forms a protein complex, which induces the phosphorylation and dimerisation of IRF-3. IRF-3 translocates to the nucleus, binds PRD I/III and forms part of the IFN-β enhanceosome together with ATF-2/c-jun and NF-$_K$B, which induces the transcription of IFN-β. TLR-3 detects dsRNA in endosomes and activates TRIF, which appears to converge on a similar pathway to IPS-1 to induce IFN-β production.

1.4.4 Interferon regulatory factors and their role in the type-I interferon response

IRFs contain a DNA binding domain at the N-terminus and an IRF-association domain at the C-terminus. In addition to IRF-3, IRF-5, IRF-7 and IRF-9 are implicated in the induction of type-I IFN and the ISGs. As mentioned above, IRF-3 is a transcription factor required for the production of IFN-β and mouse IFN-α4 (Schafer *et al.*, 1998). IRF-5 is induced by TLR-3, TLR-4, TLR-5, TLR-7 and TLR-9

and promotes production of pro-inflammatory genes and several ISGs (Takaoka *et al.*, 2005;Moynagh, 2005). IRF-7 is produced following IFN-β expression and is reported to enhance the production of IFN-α (Marie *et al.*, 1998). IFN-α/β signalling through the type-I IFNAR promotes the formation of the ISGF3, which is composed of IRF-9 and the STAT1-STAT2 complex (see 1.4.5 for details). ISGF3 induces the production of genes with the IFN-stimulated response element (ISRE) within their promoters.

1.4.5 Type-I interferon signalling pathway

Type-I IFN signals through the type-I IFNAR located on the surface of the infected cell and neighbouring cells. Type-I IFN binds IFNAR and activates the JAK/STAT pathway that produces the antiviral state (summarised in Fig. 1.8). IFNAR is heterodimeric and consists of two subunits, IFNAR1 and IFNAR2, which are located in close proximity on the cell surface. The cytoplasmic tail of IFNAR1 associates with tyrosine kinase 2 (Tyk2) and IFNAR2 is bound to JAK-1 and STAT2. STAT2 is weakly associated with STAT1 (Colamonici *et al.*, 1994;Novick *et al.*, 1994;Stancato *et al.*, 1996;Precious *et al.*, 2005;Tang *et al.*, 2007). IFN binding causes the receptor subunits to associate, which promotes the phosphorylation of Tyk2 and JAK-1 (Velazquez *et al.*, 1992;Soh *et al.*, 1994;Gauzzi *et al.*, 1996). Active Tyk2 phosphorylates IFNAR1 at tyrosine 466 (Yan *et al.*, 1996). STAT2 docks, is phosphorylated at tyrosine 690 by Tyk1 and generates a binding site for STAT1 (Fu *et al.*, 1992;Fu, 1992;Schindler *et al.*, 1992). STAT1 docks and is phosphorylated by JAK-1 at tyrosine 701 (Leung *et al.*, 1995). The newly phosphorylated STAT molecules form a stable heterodimer, which exposes a NLS (Banninger & Reich, 2004). The NLS promotes the translocation of the STAT1-STAT2 complex into the nucleus (Improta *et al.*, 1994).

STAT1-STAT2 complexes associate with IRF-9 to form IFN stimulated gene factor 3 (ISGF3) that binds to the ISRE located in the promoters of most ISGs and induces the transcription of the ISGs (Fu *et al.*, 1990;Kessler *et al.*, 1990;Veals *et al.*, 1992). Association of the STAT heterodimer with IRF-9 was thought to occur in the nucleus, but may occur at the plasma membrane (Tang *et al.*, 2007). The C-terminal domain of STAT2 is a strong transcriptional inducer (Qureshi *et al.*, 1995) and

recruits CBP/p300, which is important for transcription (Bhattacharya *et al.*, 1996). IRF-9 binds DNA through its N-terminus and associates with STAT1:STAT2 through its C-terminus (Veals *et al.*, 1993;Horvath *et al.*, 1996).

Alternatives to the traditional type-I IFN signalling model have been suggested. For example, STAT1 homodimers or STAT1-STAT2 heterodimers can induce transcription of ISGs (Decker *et al.*, 1991;Li *et al.*, 1996). The importance of these complexes in infected cells remains unclear.

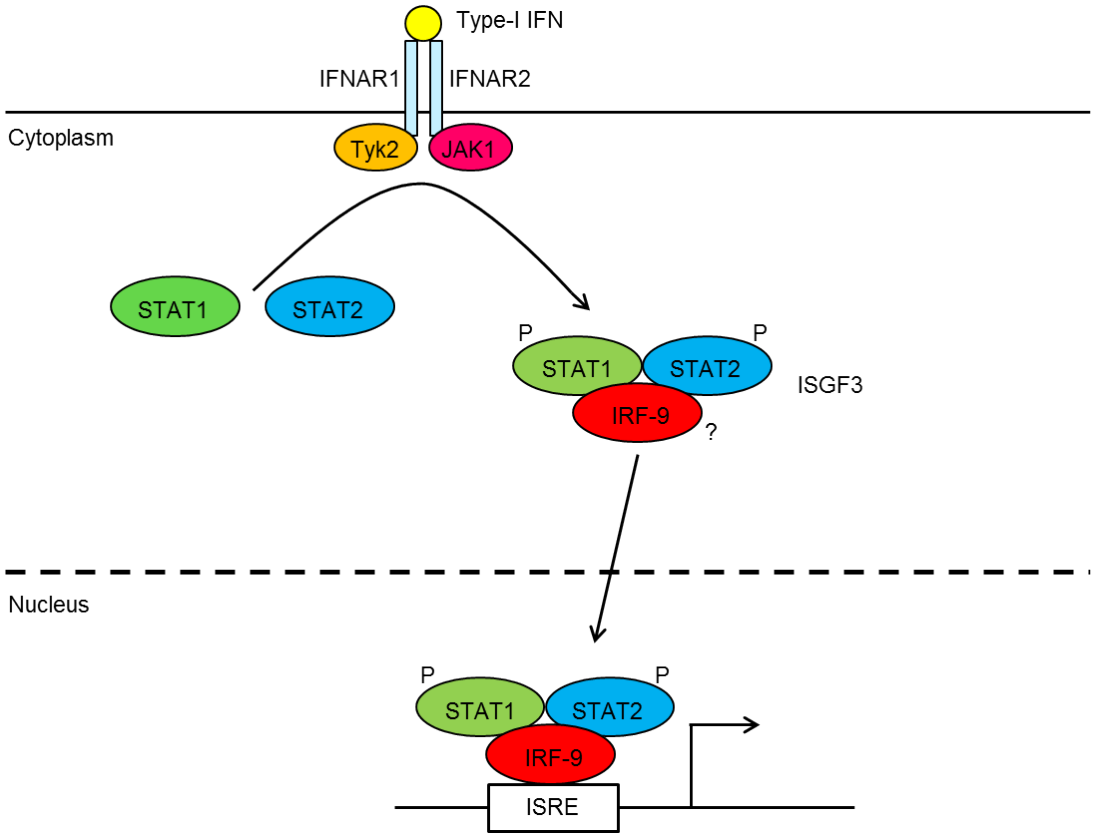

Figure 1.8: Schematic representation of the type-I IFN signalling pathway.
Type-I IFN binds to and induces the dimerisation of IFNAR1 and IFNAR2 in the IFNAR receptor. This activates Tyk2 and JAK-1 (JAK1), which phosphorylate STAT1 and STAT2. STAT1 and STAT2 form a heterodimer, which associates with IRF-9 either in the cytoplasm or the nucleus forming ISGF3. ISGF3 binds to the IFN-stimulated response element (ISRE), which induces the transcription of multiple IFN-stimulated genes.

Signal Transducers and Activators of Transcription (STAT)

The STAT family transmits signals from a receptor to the nucleus and induces the expression of hundreds of genes. The STAT family consists of seven members: 1, 2, 3, 4, 5a, 5b and 6. The seven members share a similar protein structure, but are

associated with different phenotypes within the cell. The STAT protein structure consists of discrete protein domains, as shown in Fig. 1.9. A coiled-coiled domain and a DNA binding domain are located towards the N-terminus. A Src-homology 2 (SH2) domain and a transactivation domain are located towards the C-terminus. The coiled-coiled domain enables protein-protein interactions. The DNA binding domain facilitates STAT association with the IRES in the nucleus. The SH2 domain allows STAT to associate with phosphorylated tyrosines located on receptors, such as active IFNAR, or on other peptides. The transactivation domain facilitates the interaction of STAT with other transcription factors. Downstream of the SH2 domain is a tyrosine residue, which is phosphorylated by IFNAR activation to activate STAT. Following the phophorylation of tyrosine, STAT dimerises and translocates to the nucleus. This general structure and the location of the tyrosine residue vary slightly between the STAT family members.

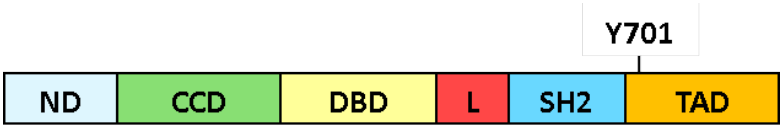

Figure 1.9: Schematic representation of the protein domains in human STAT1.
Schematic representation of the protein domains in STAT1, which is similar in structure to other STAT proteins. N-terminus (ND), coil-coiled domain (CCD), DNA binding domain (DBD), linker region (L), SH2 domain (SH2) and the transactivator domain (TAD) are shown. Y represents the tyrosine domain in STAT1 that is phosphorylated by JAK-1.

STAT1 and STAT2 are strongly associated with the type-I IFN signalling pathway (Fu *et al.*, 1990;Kessler *et al.*, 1990;Veals *et al.*, 1992). STAT1 deficient mice are viable and develop normally, but are very sensitive to virus infection (Durbin *et al.*, 1996;Meraz *et al.*, 1996). Similarly, STAT2 deficient mice are susceptible to virus infection and cells derived from these mice cannot respond to type-I IFN (Park *et al.*, 2000). The role of STAT1 and STAT2 in type-I IFN signalling has been described in 1.4.5. Active STAT1 has been implicated in stimulation of the immune system and establishing the antiviral state, inhibition of cell growth, regulation of cell death, cell differentiation and tumour suppression (Horvath *et al.*, 1996;Bromberg *et al.*, 1996;Huang *et al.*, 2002;Najjar & Fagard,

2010). STAT1 is essential for type-I IFN signalling and, as such, examples of human homozygous and heterozygous STAT1 mutations are very rare. Clinical cases of heterozygous STAT1 mutations have been reported, in which the patients were highly susceptible to mycobacterial infections, but not viral infections (Dupuis *et al.*, 2001). In contrast, two unrelated infants that succumbed to virus infections had homozygous STAT1 mutations (Dupuis *et al.*, 2003).

Initially STAT3 proved difficult to study, as mice lacking STAT3 died early in embryogenesis (Takeda *et al.*, 1998). Since then, studies have demonstrated that STAT3 is activated by type-I IFN signalling (Yang *et al.*, 1996;Pfeffer *et al.*, 1997;Rani *et al.*, 1999). Several studies have also associated STAT3 with experimental tumour models and in primary tumours; over-expression of STAT3 can transform cells (Bromberg *et al.*, 1998;Bromberg & Wang, 2009). STAT3 is emerging as a possible target for cancer immunotherapy (Hwa *et al.*, 2011).

STAT4 are STAT6 are implicated in the adaptive immune response. STAT4 is activated by IL-12 and promotes T helper cell differentiation. In addition, STAT4 is required for immunoglobulin class switching and the production of IgE by B cells in mice (Kaplan *et al.*, 1996;Thierfelder *et al.*, 1996;Alonso *et al.*, 1999). STAT6 is primarily activated by IL-4 and IL-13. Studies have implicated STAT6 in the development of T helper type 2 cells, development of IL-9-secreting T cells, differentiation of $CD8^+$ T cells, immunoglobulin class switching and surface molecule presentation in B cells and in mediating gene expression in macrophages and dendritic cells (Kaplan *et al.*, 1996;Shimoda *et al.*, 1997;Takeda *et al.*, 1997;Dardalhon *et al.*, 2008;Huber *et al.*, 2010;Chang *et al.*, 2010). In addition, STAT6 is essential for establishing allergic inflammation (Kuperman *et al.*, 1998) and in immunity against helminth parasites, including *Schistosoma mansoni* and *Trichinella spiralis* (Kaplan *et al.*, 1996;Finkelman *et al.*, 2004).

STAT5a and STAT5b are activated by a range of cytokines as well as tyrosine kinase receptors. STAT5a and STAT5b share a 92 % homology at the amino acid level and were originally thought to be the same protein (Hwa *et al.*, 2011). Differences between the amino acid sequences in the C-terminal domain clarified that STAT5a and STAT5b are different proteins and they are associated with different phenotypes in mice. In STAT5a deficient mice the mammary glands did not

develop (Liu *et al.*, 1997). In STAT5b deficient mice, reduced levels of insulin-like growth factors were detected and males and females grew less efficiently than WT mice (Udy *et al.*, 1997). Deletion of both STAT5a and STAT5b prevented fertility developing in mice (Teglund *et al.*, 1998). In humans, mutations in STAT5b were described in patients with growth hormone insensitivity syndrome, severe insulin-like growth factor-1 deficiency and postnatal growth retardation (Hwa *et al.*, 2011).

1.4.6 Augmentation of type-I interferon signalling

The IFN response is regulated by several proteins including IRF-7, suppressors of cytokine signalling (SOCS), protein inhibitor of activated STAT (PIAS) proteins, SH2 domain-containing protein tyrosine phosphatase (SHP)-1 proteins, receptor internalisation and proteasomal degradation of signalling adaptor molecules. IRF-7 is induced following activation of the IFN-β promoter, as described in 1.4.5. IRF-7 translocates to the nucleus and induces the production of IFN-α genes, including IFN-α_2, IFN-α_5, IFN-α_6 and IFN-α_8. These IFNs create a varied IFN response (Marie *et al.*, 1998), which is believed to mediate the expression of pro-inflammatory and antiviral genes.

SOCS proteins are expressed following cytokine signalling and regulate over 30 proteins, including the type-I IFN signalling proteins JAK-1 and IFNAR (Naka *et al.*, 1997). Eight SOCS proteins have been indentified to date, SOCS 1 – 7 and cytokine inducible SH2-containing proteins (CIS); of these SOCS1, SOCS2, SOCS3 and CIS are primarily associated with the regulation of the type-I IFN response. SOCS1, SOCS2, CIS and, possibly, SOCS3 bind JAK and IFNAR at different residues. SOCS association with JAK directly blocks type-I IFN signalling, while targeting IFNAR limits the number of STAT1/2 proteins that can bind IFNAR (Endo *et al.*, 1997;Yasukawa *et al.*, 1999;Sasaki *et al.*, 1999;Seki *et al.*, 2003;Fenner *et al.*, 2006).

PIAS proteins directly interact with activated STAT to prevent DNA binding and transcription of the ISG (Chung *et al.*, 1997). PIAS contain five members, which includes PIAS-1 and PIASy. PIAS-1 directly binds STAT1 and prevents DNA binding (Liu *et al.*, 1998). In contrast, PIASy allows STAT1 to bind to DNA, but specifically prevents its transcriptional activity (Liu *et al.*, 2001). SHP-1 directly

interacts with JAK-1 kinases and induces their dephosphorylation (David *et al.*, 1993;ten *et al.*, 2002).

1.4.7 Interferon stimulated genes (ISG)

Hundreds of ISG are upregulated following type-I IFN signalling (Der *et al.*, 1998). ISG products have been implicated in diverse roles, including establishing the antiviral state, antigen presentation, apoptosis, cell stress pathways and membrane trafficking, although many of the ISG are uncharacterised (Stark *et al.*, 1998;Williams, 1999;Sen, 2000;Enninga *et al.*, 2002). Examples of well characterised ISG with antiviral properties will be described here.

PKR is an ISG associated with regulating translation, induction of IFN and cytokines and triggering apoptosis. PKR is constitutively expressed by most cells, although the amount varies with cell type and stage of differentiation (Haines, III *et al.*, 1993). PKR is also upregulated following IFN signalling, which makes it an ISG (Kuhen & Samuel, 1997). PKR is activated by virus-derived dsRNA, cellular RNA and the protein activator of PKR (Clemens *et al.*, 1993). The best characterised inducer of PKR is dsRNA, which is a replication intermediate produced during RNA virus replication. PKR binds dsRNA via the N-terminal domain, which causes homodimerisation and activation. Active PKR inhibits translation by phosphorylating the eukaryotic translation initiation factor 2α (eIF-2α) at serine 51 (Meurs *et al.*, 1992). EIF-2α initiates translation by associating with GTP and Met-tRNA and then transferring Met-tRNA to the 40S ribosomal subunit. GTP is hydrolysed to produce GDP, which promotes the release of eIF-2α bound to GDP from the ribosome. eIF-2B mediates the exchange of GDP for GTP, which enables translation to continue. Following PKR activation, phosphorylated eIF-2α binds eIF-2B and prevents the exchange of GDP for GTP and, therefore, inhibits translation. Active PKR can promote IFN and cytokine production and induce apoptosis by activating the IKK complex, which induces the transcription factor $NF\text{-}_KB$ (Clemens *et al.*, 1993;Henry *et al.*, 1994;Kumar *et al.*, 1994;Lee & Esteban, 1994;Mundschau & Faller, 1995;Gil & Esteban, 2000).

2’-5’-oligoadenylate synthase (OAS) and RNase-L are the ISGs primarily associated with ssRNA degradation (Floyd-Smith *et al.*, 1981). The human genome

encodes three OASs; small OAS1, medium OAS2 and large OAS3 (Justesen *et al.*, 2000). 2'-5' OASs bind dsRNA which induces the polymerisation of ATP and produces 2'-5'oligoadenylates (2'-5' A) (Kerr & Brown, 1978). 2'-5' A binds RNase-L via the N-terminal domain and induce homodimerisation and activation of RNase-L (Hassel *et al.*, 1993). Active RNase-L cleaves specific sequence motifs present in both cellular and viral ssRNAs (Floyd-Smith *et al.*, 1981). RNase-L can degrade 28S ribosomal RNA and, therefore, enhance the inhibition of translation (Iordanov *et al.*, 2000).

1.4.8 Dendritic cells are a source of type-I interferon

Dendritic cells (DC) link the innate immune response to the adaptive immune response. Immature migratory DC circulate in tissues and the blood. On detecting PAMPs via PRRs, DCs are activated and mature, secrete cytokines and migrate to the lymph nodes (LNs) in which they activate the adaptive immune response, including $CD8^+$ cytotoxic T lymphocytes and $CD4^+$ helper T cells. DC can be divided into subsets based on their function, morphology, location in the LNs and cell surface markers. Three important subsets of DCs are the myeloid DC (mDC), the plasmacytoid DC (pDC) and the Langerhans cells (LC). mDC are primarily APCs and activate T cells (Foti *et al.*, 2004), while pDC are believed to be major producers of type-I IFN in response to viruses, including HSV-1, murine cytomegalovirus, influenza virus and VSV (Hemmi *et al.*, 2003;Heil *et al.*, 2004;Krug *et al.*, 2004;Lund *et al.*, 2004). LCs are primarily located in the epidermis of the skin and are associated with detecting pathogens there (Mutyambizi *et al.*, 2009).

pDC, also called IFN producing cells, were first described in humans. In 1958, cells with a similar morphology to plasma cells, but lacking B cell and plasma cell markers were described in the T cell zone of human LNs (Lennert & Remmele, 1958). Later studies reported cells with a plasma cell-like morphology that did not express CD4, CD31, CD36, CD68 or other cell lineage markers (Trinchieri *et al.*, 1978;Muller-Hermelink *et al.*, 1983;Prasthofer *et al.*, 1985). These cells secreted large amounts of type-I IFN in response to infection with virus (Cella *et al.*, 1999;Siegal *et al.*, 1999). In 2001, mouse pDC were identified that express CD11c, Ly-60, B220, but lack the lineage marker CD11b (Asselin-Paturel *et al.*,

2001;Bjorck, 2001;Nakano *et al.*, 2001). Mouse pDC are similar to human pDC in morphology, activation by CpG and secretion of type-I IFN following detection of RNA and DNA viruses (Nakano *et al.*, 2001;Asselin-Paturel *et al.*, 2001;Bjorck, 2001). Mouse pDC secrete type-I IFN and other cytokines following detection of influenza or murine cytomegalovirus (MCMV) via TLR-7 or TLR-9 respectively (Dalod *et al.*, 2002;Krug *et al.*, 2002;Asselin-Paturel *et al.*, 2003;Krug *et al.*, 2004;Diebold *et al.*, 2004). The role of DC during alphavirus infection is poorly understood, as described in 1.4.10.

1.4.9 Inverse interference (Table 1.3).

All viruses studied to date have evolved mechanisms to control the type-I IFN response (Randall & Goodbourn, 2008), which is termed inverse interference. Inverse interference has been detected throughout the type-I IFN pathway and can be divided into (i) global shutoff of cellular transcription and translation, (ii) inhibition of IFN-β production, (iii) inhibition of IFNAR signalling and (iv) inhibition of specific ISG products. These areas will be described below with examples of RNA viruses which employ them.

Global transcription and translation shutoff

Several virus families, such as *Togaviridae*, *Bunyaviridae* and *Picornaviridae*, induce global transcription and translation shutoff within infected cells. This process promotes virus infection by inhibiting the production of type-I IFN and ISGs. However, these cells rapidly die following shutoff of host protein synthesis and, therefore, a persistent infection cannot be established. Global shutoff of host transcription and translation has been observed in infections with the Old World alphaviruses SFV and SINV and the New World alphaviruses VEEV and EEV at 2 to 4 h post-infection (Frolov & Schlesinger, 1994;Kedersha *et al.*, 1999). For Old World viruses, nsP2 is associated with inhibition of the IFN response (Frolova *et al.*, 2002;Garmashova *et al.*, 2006;Breakwell *et al.*, 2007) through mechanisms not yet understood, while in New World viruses capsid is associated with this process (Aguilar *et al.*, 2007;Garmashova *et al.*, 2007a;Garmashova *et al.*, 2007b). The alphavirus sg ORF contains a translational enhancer, which enables the translation of

the structural polyprotein independent of eIF-2α (Frolov & Schlesinger, 1994;Sjoberg *et al.*, 1994;Ventoso *et al.*, 2006). Therefore, the structural proteins are produced later in infection when the host proteins are no longer being produced and are unaffected by the shutoff of host protein synthesis through phosphorylation of eIF2α.

The bunyavirus Bunyamwera virus expresses NSs protein that inhibits cellular RNA polymerase II and, therefore, prevents cellular mRNA transcription (Thomas *et al.*, 2004). Similarly, Rift Valley fever virus (RFVF) expresses NSs protein which inhibits cellular mRNA transcription. However, RVFV NSs protein targets and inhibits the transcription factor $TF_{II}H$ (Billecocq *et al.*, 2004;Le *et al.*, 2004).

The picornaviruses poliovirus (PV) and FMDV express proteases that cleave cellular proteins that are essential for cellular transcription (Etchison *et al.*, 1982;Devaney *et al.*, 1988;Kirchweger *et al.*, 1994;Belsham & Sonenberg, 2000). Finally, the picornavirus EMCV limits the translation of cellular mRNA by disrupting nucleocytoplasmic transportation of mRNA (Porter *et al.*, 2006).

Inhibition of IFN-β induction

Viruses can inhibit the production of IFN-β by (i) limiting and/or hiding dsRNA synthesis, (ii) inhibiting the PRR and/or the PRR signalling pathway (iii) inhibiting IRF-3, (iv) inhibiting NF-$_K$B and/or (v) disrupting the IFN-β promoter. The othomyxoviruses express NS1 that binds RIG-I and limits the induction of IFN-β. In addition, influenza A inhibits IRF-3 activity (Talon *et al.*, 2000;Wang *et al.*, 2000;Mibayashi *et al.*, 2007;Guo *et al.*, 2007;Opitz *et al.*, 2007).

The paramyxoviruses SeV, mumps virus, PIV5 (previously known as simian virus 5, SV5), human parainfluenza virus 2 and Hendra virus (HeV) bind mda-5 via the virus V protein. The C-terminal domain of the V protein binds and inhibits mda-5 and, therefore, prevents PRR signalling (Andrejeva *et al.*, 2004). In contrast, the flavivirus HCV inhibits PRR downstream of RIG-I and mda-5. RIG-I and mda-5 converge and signal through IPS-1. HCV expresses NS3/4A protease that cleaves both IPS-1 and the adaptor protein for TLR-3 and TLR-4 TRIF that prevents IFN-β induction (Foy *et al.*, 2005;Li *et al.*, 2005;Ferreon *et al.*, 2005).

Inoculation of adult mice with alphaviruses drives the production of IFN-β (Klimstra *et al.*, 1999;Ryman *et al.*, 2000;White *et al.*, 2001). However, in cell culture alphaviruses seem to limit the induction of type-I IFN. In MEFs and mouse fibroblast L929 cells, SFV induces less type-I IFN than an SFV derivative with a mutation in nsP2 (Breakwell *et al.*, 2007), while CHIKV, SINV, VEEV and EEEV induced less type-I IFN than a parallel infection with SeV (Burke *et al.*, 2009). To date, a mechanism by which alphaviruses directly inhibit the induction of IFN-β has not been described. However, this apparent inhibition of IFN-β production has been associated with global shutoff of transcription and translation, nsP2, capsid and reduced phosphorylation of STAT1, which are listed with references in table 1.3.

Inhibition of IFNAR signalling

Many viruses antagonise the type-I IFN response by targeting the signalling components, including JAK, STAT and IRF-9 (Randall & Goodbourn, 2008;Najjar & Fagard, 2010). Two recent studies have demonstrated that SINV and CHIKV both limit the phosphorylation of STAT1 in cell culture (Fros *et al.*, 2010;Simmons *et al.*,

2010). For SINV, nsP1 may facilitate this process (Simmons *et al.*, 2010), while for CHIKV nsP2 has been associated with this function (Fros *et al.*, 2010).

The flaviviruses WNV (Guo *et al.*, 2005), JEV (Lin *et al.*, 2004), Langat virus (Best *et al.*, 2005), DENV (Ho *et al.*, 2005) and HCV (Lin *et al.*, 2006) inhibit STAT1 phosphorylation and IFN signalling via NS5 protein disruption of the IFNAR complex. During JEV infection, NS5 limits Tyk2 activation in IFNAR (Lin *et al.*, 2004). During DENV infection, NS5 protein binds and sequesters STAT1 and STAT2 for degradation (Ashour *et al.*, 2009). In addition, DENV protein NS4B inhibits the phosphorylation of STAT1 (Munoz-Jordan *et al.*, 2003). Studies have demonstrated that HCV inhibits the type-I IFN signalling pathway by inducing cellular protein phosphatase 2A (PP2A) and SOCS3 (Heim *et al.*, 1999;Bode *et al.*, 2003;Duong *et al.*, 2004). PP2A is implicated in several cellular processes, including regulation of the JAK/STAT pathway (Zhang *et al.*, 1995). SOCS3 is reported to bind STAT1 and prevent downstream signalling, which is described in 1.4.5.

Several studies have demonstrated that paramyxoviruses reduce the half-life of STAT1 and STAT2 via the virus V protein. However, the mechanism by which the V protein inhibits type-I IFN signalling varies between the different paramyxovirus family members. In PIV5 infection, the V protein facilitates the polyubiquitination of STAT1 and targets it for proteasomal degradation (Young *et al.*, 2000;Andrejeva *et al.*, 2002;Parisien *et al.*, 2002;Ulane & Horvath, 2002). In contrast, Nipah virus (NiV) and MeV sequester STAT1 into high molecular weight complexes in the cytoplasm (Rodriguez *et al.*, 2002;Rodriguez *et al.*, 2003). In NiV infection, the V protein forms a complex with STAT2 (Rodriguez et al., 2002), while MeV V protein forms a high molecular weight complex comprising STAT1, STAT2 and IRF-9 (Palosaari *et al.*, 2003). SeV inhibits type-I IFN signalling by sequestering STAT1 and also disrupting STAT1 phosphorylation (Didcock *et al.*, 1999;Garcin *et al.*, 2002).

The coronavirus SARS-CoV antagonises type-I IFN signalling via the virus protein ORF6. ORF6 prevents the nuclear translocation of STAT1 by binding the nuclear transport protein karyopherin α2 (Frieman *et al.*, 2007).

Inhibition of ISG products

Several studies have demonstrated that viruses can inhibit ISG, including PKR, OAS/RNase L, ISG15 and PML nuclear bodies (Randall & Goodbourn, 2008). Examples of RNA viruses that can inhibit PKR and/or OAS/RNase L will be described here. Latent cytoplasmic PKR binds dsRNA, homodimerises and prevents cellular translation, as described in 1.4.7. OAS/RNase L is activated by binding dsRNA and then cleaves both mRNA and viral RNA at specific sequence motifs, as described in 1.4.7. Influenza expresses NS1 that sequesters dsRNA (Chien *et al.*, 2004) and prevents the activation of PKR (Lu *et al.*, 1995). The genome of HCV contains an IRES structure that competes with dsRNA for binding to PKR (Vyas *et al.*, 2003). In addition, HCV expresses NS5A and E2 proteins that directly bind and inhibit PKR (Taylor *et al.*, 1999;Noguchi *et al.*, 2001;Gimenez-Barcons *et al.*, 2005). In contrast, the PV infection promotes the degradation of PKR (Black *et al.*, 1993). The retrovirus HIV-1 expresses Tat during infection, which binds active PKR and, therefore, prevents PKR binding to eIF2α (McMillan *et al.*, 1995;Brand *et al.*, 1997).

In addition to inhibiting PKR, HCV and HIV-1 can also inhibit the OAS/RNase-L pathway (Martinand *et al.*, 1999;Sumpter, Jr. *et al.*, 2004;Taguchi *et al.*, 2004). One study reports that HCV genomes generally contain very few RNase-L target motifs (Han *et al.*, 2004). HIV-1 induces the expression of the cellular RNase L inhibitor (RLI) (Martinand *et al.*, 1999). Similarly, the paramyxovirus EMCV also induces RLI activity (Martinand *et al.*, 1998).

To date, no studies report the ability of alphaviruses to inhibit PKR or OAS/RNase L activity. This may be due to the limited affect of PKR and OAS/RNase L on alphavirus replication. In mice deficient in PKR, RNase L and the ISG myxovirus resistance-1, SINV only produces a subclinical infection (Ryman *et al.*, 2002). In mice lacking the PKR gene, SFV4 replication increases relative to in WT mice, but the infection remains avirulent (Barry *et al.*, 2009). In dendritic cells OAS/RNase L does not control alphavirus replication (Ryman *et al.*, 2005). However, in HeLa cells OAS3 was implicated in controlling CHIKV replication (Brehin *et al.*, 2009).

Table 1.2: Examples of RNA viruses that inhibit the type-I interferon response.

Role	Virus family	Virus name	Mechanism	Reference
Global shutoff of cellular transcription and translation	*Togaviridae*	SFV, SINV	nsP2 facilitates shutoff	(Frolova *et al.*, 2002;Garmashova *et al.*, 2006;Breakwell *et al.*, 2007).
		VEEV, EEEV	Capsid facilitates shutoff	(Aguilar *et al.*, 2007;Garmashova *et al.*, 2007a).
	Bunyaviridae	BUNV	NSs inhibits cellular RNA polymerase II	(Thomas *et al.*, 2004).
		RVFV	NSs protein inhibits transcription factor $TF_{II}H$	(Billecocq *et al.*, 2004;Le *et al.*, 2004).
	Picornaviridae	PV	Virus protease cleaves cellular proteins essential for transcription	(Etchison *et al.*, 1982); (Clark *et al.*, 1993;Das & Dasgupta, 1993).
		FMDV	Virus protease cleaves eIF4-G and eIF4A	(Devaney *et al.*, 1988;Kirchweger *et al.*, 1994;Belsham & Sonenberg, 2000;Li *et al.*, 2001)
		EMCV	Disrupts nucleocytoplasmic transportation of mRNA	(Porter *et al.*, 2006).
Inhibition of IFN-β induction	*Togaviridae*	SFV, SINV, CHIKV, VEEV, EEEV	Unknown.	(Breakwell *et al.*, 2007;Burke *et al.*, 2009).
	Flaviviridae	HCV	NS3/4A protease cleaves TRIF (adaptor protein for TLR-3 and -4) and IPS-1 (adaptor protein for RIG-I).	(Foy *et al.*, 2005;Ferreon *et al.*, 2005;Li *et al.*, 2005).
	Paramyxoviridae	SeV, mumps virus, PIV5, human parainfluenza virus 2, HeV	V protein binds mda-5 and prevents its activity	(Andrejeva *et al.*, 2004).
	Orthomyxoviridae	Influenza A	NS1 binds RIG-I and IRF-3 and prevents their activity	(Talon *et al.*, 2000;Wang *et al.*, 2000;Mibayashi *et al.*, 2007;Guo *et al.*, 2007;Opitz *et al.*, 2007).
	Coronaviridae	SARS-CoV	Inhibits IRF-3	(Frieman *et al.*, 2007).
Inhibition of type-I IFN	*Togaviridae*	SINV	Limits STAT1 phosphorylation,	(Simmons *et al.*, 2010).

signalling			associated with nsP1	
		CHIKV	Limits STAT1 phosphorylation, associated with nsP2	(Fros *et al.*, 2010).
	Flaviridae	WNV	NS5 limits STAT1 phosphorylation	(Guo *et al.*, 2005)
		JEV	NS5 limits STAT1 phosphorylation	(Lin *et al.*, 2004).
		DENV	NS5 limits STAT1 phosphorylation and sequesters STAT2 for degradation. NS4B also limits STAT1 phosphorylation	(Munoz-Jordan *et al.*, 2003;Ho *et al.*, 2005;Ashour *et al.*, 2009).
		Langat virus	NS5 limits STAT1 phosphorylation	(Best *et al.*, 2005).
		HCV	NS5A protein inhibits the phosphorylation of tyrosine 701 on STAT1. Induces cellular protein phosphatase 2A and SOCS3, which inhibits the JAK/STAT pathway	(Heim *et al.*, 1999;Bode *et al.*, 2003;Duong *et al.*, 2004).
	Paramyxoviridae	PIV5	V protein induces the polyubiquitylation of STAT1 that triggers proteasomal degradation.	(Didcock *et al.*, 1999;Andrejeva *et al.*, 2002;Ulane & Horvath, 2002;Precious *et al.*, 2005).
		SeV	V protein induces the degradation of STAT1	(Didcock *et al.*, 1999;Garcin *et al.*, 2002).
		NiV	V protein sequesters STAT1 and STAT2 into high molecular weight complexes	(Rodriguez *et al.*, 2002).
		HeV	V protein sequesters STAT1 into high molecular weight complexes	(Rodriguez *et al.*, 2003).
		MV	V protein sequesters STAT1, STAT2 and IRF-9 into high molecular weight complexes	(Palosaari *et al.*, 2003).
	Coronaviridae	SARS-CoV	ORF6 by binds the nuclear transport protein karyopherin α2 and prevents the nuclear translocation of STAT1	(Frieman *et al.*, 2007).
Inhibition of ISG: PKR	*Flaviviridae*	HCV	Virus RNA contains an IRES structure that binds PKR. Virus proteins NS5a and E2	(Taylor *et al.*, 1999;Noguchi *et al.*, 2001;Vyas *et al.*,

			directly bind and inhibits PKR	2003;Gimenez-Barcons *et al.*, 2005).
	Picornaviridae	PV	Induces degradation of PKR	(Black *et al.*, 1993)
	Orthomyxoviridae	Influenza	Virus protein NS1 sequesters dsRNA that prevents PKR activation	(Lu *et al.*, 1995;Chien *et al.*, 2004).
	Retroviridae	HIV	Virus protein Tat binds PKR and is a pseudosubstrate for eIF2α	(McMillan *et al.*, 1995;Brand *et al.*, 1997).
OAS/RNase L	*Retroviridae*	HIV-1	Induces the expression of the cellular RNase L inhibitor (RLI)	(Martinand *et al.*, 1999)
	Paramyxoviridae	EMCV	Induces the expression of the cellular RLI	(Martinand *et al.*, 1998)

1.4.10 Semliki Forest virus and the type-I interferon response

Inoculation of Random–Bred Porton mice or inbred A2G, C57 and C3H mice with SFV L10 or SFV A7(74) drives the production of functional IFN; IFN levels increase as the blood viraemia titres increase, peak at 2 to 3 days post-infection and then decrease (Bradish *et al.*, 1975). Type-I IFN is protective against SFV infection in cell culture and in adult mice. Administration of type-I IFN prior to inoculation with SFV (strain not reported) protected mice (strain not reported) from disease, depending on the time of administration and dose of IFN (Finter, 1966). In plaque assays on mouse fibroblast L-cells, addition of anti-IFN antibodies enhanced SFV spread (strain not reported), as demonstrated by an increase in plaque size (Fauconnier, 1969). Similarly, administration of anti-IFN antibodies immediately after inoculation of mice with SFV (strain not reported) enhanced brain viraemia titres and mortality rates (Fauconnier, 1971).

Administration of type-I IFN or poly(I:C) to adult A2G and BALB/c mice prior to inoculation with SFV A7 or SFV L10 reduces virus replication, although SFV L10 remains virulent (Bradish & Titmuss, 1981). In adult mice inoculated first with SFV A7(74) and then with SFV L10 3 h later, SFV L10 was rendered avirulent (Oliver *et al.*, 1997). Similarly, in adult Porton-white mice inoculated with SFV A7 prior to infection with SFV V13, SFV V13 became avirulent (Smillie *et al.*, 1973).

In mice lacking IFN receptors ($IFNAR^{-/-}$) SFV A7(74), SFV4 and SFV4 mutants spread efficiently and are virulent, unlike in WT mice (Muller *et al.*, 1994;Fazakerley *et al.*, 2002;Fragkoudis *et al.*, 2007). Studies using other mutant mouse models demonstrated that the type-I IFN response is essential for controlling the virulence of SFV infection, but the adaptive immune response is required for clearance of SFV from the brain; SFV A7(74) is avirulent and cleared from WT mice, but is virulent in adult $IFNAR^{-/-}$ mice and establishes a persistent infection in adult athymic *nu/nu* mice (Amor *et al.*, 1996;Fragkoudis *et al.*, 2007).

Studies in MEFs and L929 cells demonstrated that SFV4 infection inhibits the induction of type-I IFN; WT SFV4 induces less functional IFN than SFV4 with a mutation in the NLS of nsP2, termed SFV4-RDR (Breakwell *et al.*, 2007). During SFV4 infection, the majority of nsP2 translocates to the nucleus by 5 h post-infection (Rikkonen *et al.*, 1992). In contrast, during SFV4-RDR infection, nsP2 is largely restricted to the cytoplasm (Rikkonen *et al.*, 1992). In mice, SFV4-RDR infection is restricted to foci around the inoculation site, whereas SFV4 spreads throughout the brain (Fazakerley *et al.*, 2002). In contrast, *ic* inoculation of $IFNAR^{-/-}$ mice with SFV4-RDR produces a widespread and fatal infection, similar to SFV4 (Fazakerley *et al.*, 2002). In cell culture, SFV4-RDR replicates less efficiently than SFV4, unless the IFN system is compromised (Rikkonen *et al.*, 1992;Breakwell *et al.*, 2007). In MEFs, SFV4-RDR infection induces more IFN-β transcripts and functional IFN than SFV4 (Breakwell *et al.*, 2007). However, both SFV4 and SFV4-RDR induce shutdown of host protein synthesis and the transcription factors $NF\text{-}_KB$ and IRF-3 both translocate to the cell nucleus (Breakwell *et al.*, 2007). Taken together, these results strongly suggest a role for nsP2 and, in particular, the NLS in controlling the IFN responses. Possible explanations include (i) nsP2 functions in the nucleus to prevent IFN production through an unknown mechanism, (ii) nsP2 interacts with protein(s) in the cytoplasm to inhibit the IFN pathway, which is prevented by mutation of the NLS containing domain and/or (iii) SFV4nsP2RDR replicates less efficiently than SFV4 and, therefore, there are fewer virus proteins to inhibit the IFN pathway.

DCs, particularly the pDCs, produce type-I IFN following virus infection (Cella *et al.*, 1999; Siegal *et al.*, 1999). The interaction of SFV with specific subsets

of DCs during infection is largely unknown. SFV infection induces Langerhan's cells (LC) functional maturation *in vitro* and *in vivo* (Johnston *et al.*, 1996). In adult CD-1, C57BL/6 or BALB/C mice subcutaneously (*sc*) inoculated with SFV, large numbers of mature LC were detected in the LN (MacDonald & Johnston, 2000;Johnston *et al.*, 2000). Other DC studies have focused on VEEV and CHIKV. Studies demonstrate that VEEV can infect human immature DC *in vitro* and induce the secretion of IFN-α, TNF-α and IL-6 *in vitro* (Moran *et al.*, 2005). In mice, pDCs are required for VEEV to enter the LN and, also, for detection of cytokine expression in the sera (Tonkin *et al.*, 2012). The role of DCs and, indeed, macrophages during CHIKV infection is controversial with conflicting data and variation in clinical cases depending on the age of patient and strain of CHIKV (Dupuis-Maguiraga *et al.*, 2012).

In conclusion, these studies suggest that strains of SFV are sensitive to type-I IFN pre-treatment and the antiviral state. The report that SFV L10 is virulent in adult mice despite the production of type-I IFN, while SFV A7(74) is avirulent (Bradish *et al.*, 1975) could indicate that SFV L10 and SFV A7(74) vary in sensitivity to the type-I IFN response. Indeed, one study reported that virulent SFV L10 and avirulent V42 differ in sensitivity to the type-I IFN response; SFV L10 replicates more efficiently in the presence of type-I IFN than SFV V42 (Deuber & Pavlovic, 2007). In addition, it remains unclear (i) which PRR(s) detect SFV infection in cell culture, (ii) if SFV inhibits the type-I IFN response and, if so, (iii) the cellular targets and the virus proteins involved in inhibiting the type-I IFN response and (iv) the role of DCs in secreting type-I IFN during SFV infection *in vivo*.

1.5 Hypotheses and aims

This project has three hypotheses:

1) SFV infection induces autophagy in cell culture and utilises this response to enhance virus replication.
2) The quality, quantity and/or the protective efficacy of the IFN response differ between strains of SFV and between human and murine cells.
3) The replicase proteins nsP2 and/or nsP3 antagonise the IFN response.

Questions to be addressed:

1) **Does SFV induce autophagy and, if so, does this enhance virus replication?**

SINV and CHIKV both induce the accumulation of autophagosomes. In SINV infection autophagy degrades capsid (Orvedahl *et al.*, 2010), while with CHIKV autophagy enhances virus replication (Krejbich-Trotot *et al.*, 2011). At the start of this thesis there were no studies on the role of autophagy in SFV infection.

2) **Do strains of SFV differ in induction of or sensitivity to the type-I IFN response?**

There are several strains of SFV that can be divided into two groups based on their virulence in adult mice; SFV L10 is virulent, while SFV4 and SFV A7(74) are avirulent. One study reports that strains of SFV differ in their sensitivity to type-I IFN and this may dictate virulence in adult mice (Deuber & Pavlovic, 2007). The ability of strains of SFV to induce type-I IFN and their sensitivity to type-I IFN has not been investigated.

3) **Is SFV more sensitive to human IFN than mouse IFN and can SFV evade and/or inhibit the mouse IFN response better than the human IFN response?**

In humans, SFV infection only causes a mild or subclinical disease (Mathiot *et al.*, 1990), while CHIKV is currently causing debilitating disease in millions of humans worldwide (Enserink, 2007). In contrast, in adult mice SFV can induce a fatal panencephalitis (Bradish *et al.*, 1975), while CHIKV is avirulent unless the mice are deficient in the type-I IFN system (Couderc *et al.*, 2008). This data could be explained by SFV inducing more or being more sensitive to human type-I IFN than mouse type-I IFN. Comparison of the interaction of SFV with the mouse and human type-I IFN response has not been investigated.

4) **Do strains of SFV antagonise the type-I IFN response?**

In MEFs and L929 cells, SFV4 induces less functional IFN than SFV4 with a mutation in nsP2, SFV4-RDR (Breakwell *et al.*, 2007). The mechanism(s) by which SFV4 antagonises the type-I IFN response and the role(s) of nsP2 within this has not been delineated.

5) **Do nsP2 and/or nsP3 antagonise the IFN response?**

In MEFs and L929 cells, SFV4 with a mutation in nsP2, SFV4-RDR, induces greater amounts of functional IFN and IFN-β transcripts than WT SFV4 (Breakwell *et al.*, 2007). In cell culture, 50 % of nsP2 translocates to the nucleus by 5 h post-infection during SFV4 infection, while in SFV4-RDR infection nsP2RDR is largely restricted to the cytoplasm (Rikkonen *et al.*, 1992). The mechanism by which nsP2 and nsP2RDR interacts with the IFN response remains unclear. NsP3 is the least well-characterised of the nsPs. NsP3 is a virulence determinant (Tuittila *et al.*, 2000;Tuittila & Hinkkanen, 2003). However, the potential interaction of nsP3 with the IFN response has not been investigated.

6) **Where are the differences in the genetic sequence of SFV L10, SFV A7(74) and SFV4?**

SFV4 was derived from Prototype virus, which is closely related to SFV L10 (Liljestrom *et al.*, 1991). However, SFV L10 is virulent in adult mice, while SFV4 is avirulent unless inoculated *ic*, *in* or at a high dose (Glasgow *et al.*, 1991;Fazakerley, 2002). Previous studies identified several amino acid substitutions between SFV A7(74) and SFV4, which mainly mapped to nsP3 (Tuittila *et al.*, 2000). The genetic sequences for the strains SFV L10 and SFV A7(74) held at the University of Edinburgh have not been determined or compared to SFV4.

Chapter 2 Materials and Methods

Contents

2.1 Cell Lines

All cell lines were maintained in sterile plastic ware (Nunc) at 37^{o}C in a humidified incubator with an atmosphere of 5 % CO_2. Table 2.1 describes the cell lines used in this project.

Baby Hamster Kidney-21 (BHK-21) cells were grown in Glasgow's modified Eagles medium (GMEM, Gibco), supplemented with 10 % (volume/volume (v/v)) newborn calf serum (NBCS, Biosera), 10 % v/v tryptose phosphate broth (TPB, Invitrogen) and penicillin/streptomycin (100 U/ml and 100 μg/ml respectively, Gibco) (10 % NBCS GMEM).

Mouse L929 and NIH 3T3 fibroblast cells were maintained in Dulbeccos modified Eagles medium (DMEM, Gibco), supplemented with 10 % v/v foetal calf serum (FCS, Biosera) and penicillin/streptomycin as above (10 % FCS DMEM).

Human 2fTGH, Hs 633T, Huh7, MRC5 and U4C cells were maintained in DMEM supplemented with FCS and penicillin/streptomycin as above.

Human A549-NPro cells were maintained in DMEM supplemented with 10 % FCS and Puromycin (1 μg/ml, Invivogen).

Table 2.1: Cell lines used in this project

Name	Cell type	Additional information
Hamster		
BHK-21	Fibroblast	IFN incompetent cell line
Mouse		
L929	Fibroblast	IFN competent cell line
NIH 3T3	Fibroblast	IFN competent cell line
Human		
2fTGH	Fibroblast	IFN competent cell line
A549-NPro	Epithelial	IFN incompetent cell line. A549 cells stably expressing the NPro protein of the Bovine viral diarrhoea virus (Pe515strain) with an N-terminal V5 tag (Jackson *et al.*, 2010). NPro targets the transcription factor IRF-3 and prevents it from binding to DNA and instead targets IRF-3 for polyubiquitination and destruction (Hilton *et al.*, 2006). Therefore, A549-NPro cells can respond to IFN, but cannot produce IFN.
Hs 633T	Fibroblast	IFN competent cell line
Huh7	Hepatocyte	IFN competent cell line
MRC5	Fibroblast	IFN competent cell line
U4C	Fibroblast	IFN incompetent cell line. Derivative of 2fTGH that were mutated to express the drug-selectable *gpt* (guanine/hypoxanthine phorphoribosyl tranferase) controlled by an IFN-α/β-inducible promoter. Cells resistant to IFN were selected. These cells, called U4C cells, lacked the JAK1 protein and contained a truncated JAK1 messenger RNA. JAK1 is essential for IFN signalling. Therefore, U4C cells are defective in the IFN response (Muller *et al.*, 1993).

2.1.1 Passaging and counting cell lines

The same procedure was used to passage and count all the cell lines used in this project. When cells were 80% confluent the medium was removed and the monolayer was washed with 5 ml of phosphate buffered saline (PBS). The PBS was replaced with 5 ml of trypsin/EDTA (0.05% trypsin, 0.53 mM EDTA, Gibco) and the cells were incubated at 37^{o}C. When the cells had detached, 5 ml of medium was added to neutralise the trypsin and the cells were pelleted by centrifuging for 5 minutes at 450 x g. The supernatant was discarded and the cell pellet was re-suspended in 10 ml of 10 % media. A 10 μl aliquot of the cell suspension was diluted in 90 μl of PBS and the cells were counted on a haemocytometer. The mean number of cells present in the 10 ml cell suspension was calculated using the following formula:

Mean number of cells in 10 ml = mean number of cells per square of the haemocytometer x 10^6.

The required number of cells were then seeded into a fresh flask with 10 % medium and incubated at 37^{o}C. BHK-21 cells and MRC5 cells were passaged

approximately 30 times after which their growth significantly slowed and they were replaced with fresh stocks from liquid nitrogen stocks (2.1.2). The other cell lines were replaced at passage 60 – 70 with lower passage number cells from liquid nitrogen.

2.1.2 Freezing and resurrecting cell lines

Cells were frozen during the growth phase while still <80 % confluent. The cells were harvested and counted. Cells were centrifuged at 478 x g for 5 minutes and re-suspended in freezing medium (90 % FCS and 10 % dimethylsulfoxide (DMSO)) to produce $5x10^6$ cells per ml, the optimal concentration of cells for freezing. Aliquots of 1 ml of cell suspension were transferred to Nunc cryovials and placed in an isopropanol box at -80^{o}C overnight to gradually freeze the cells. The frozen cells were stored in the vapour phase of a liquid nitrogen refrigerator at below -130^{o}C.

To thaw the cell lines, cryovials were removed from the liquid nitrogen refrigerator and transported to the laboratory on dry ice. The cells were rapidly thawed in a 37^{o}C water bath and 1 ml of pre-warmed 10% media was gradually added to the cryovial. The cell suspension was transferred into a 25 cm^2 flask containing 8 ml of warm 10 % media and then incubated at 37^{o}C. After 24 h the cells were passaged if confluent. Alternatively, the medium was replaced at 24 h with fresh 10 % media to remove all traces of DMSO and the cells were passaged once confluent.

2.2 Viruses and Virus Replicon Particles (VRPs)

Table 2.2 and Fig. 2.1 describe the viruses and virus replicon particles (VRPs) used in this project.

2.2.1 Propagation of wild-type SFV

Strains of WT SFV (SFV L10 and A7(74)) were propagated from the original stocks (Prof. John Fazakerley, The Roslin Institute, University of Edinburgh). BHK-21 cells were seeded into ten 175 cm^2 with 10 % NBCS GMEM. Once confluent, the medium was removed and the BHK-21 cells were infected with virus at a MOI of 0.01 in 5 ml of PBS supplemented with 0.75% bovine serum albumin (BSA, Sigma) (PBSA) for 1

hour at room temperature with constant rocking. Following incubation, the virus suspension was replaced with 20 ml of 10 % NBCS GMEM and the cells were incubated until cyptopathic effect (CPE) was observed, usually after 24 h. The supernatant was collected, centrifuged at 27,200 g for 30 minutes to remove cell debris and stored at -80^{o}C until the virus was purified.

2.2.2 Production of VRPs

VRPs were produced from DNA plasmids, which were kindly provided by Prof. Andres Merits, Institute of Technology, University of Tartu, Estonia. The method used has been previously described (Smerdou & Liljestrom, 1999). Briefly, two plasmids (1 μg each) were linearised with Spe I (New England Biolabs) and *in vitro*-transcribed to produce RNA. One plasmid encoded the SFV4 non-structural proteins and a foreign gene insert and the second plasmid encoded the SFV4 structural proteins. The RNA from both plasmids was electroporated into BHK-21 cells using the BioRad Gene Pulser Xcell electroporator. BHK-21 flasks were trypsinised, the cells counted, and re-suspended in chilled PBS to give a final concentration of 6x10^{6} cells per ml. A 400 μl aliquot of the cell/nucleic acid mix was added to a 0.4 cm electroporation curvette and then pulsed twice using a square wave of 140 volts (V) for 25 mseconds. The cells were carefully transferred into a 175 cm^{2} flask with 20 ml of 10 % NBCS GMEM and incubated at 37^{o}C. The supernatant was collected 24 – 48 h later when CPE was observed, clarified by centrifugation at 27,200 g for 30 minutes and then stored at -80^{o}C.

SFV4 was produced in the same way using a single plasmid that encoded the whole SFV4 genome and, in some cases, a foreign gene insert. This technique produced viable SFV4.

2.2.3 Purification of Viruses and VRPs

The viruses and VRPs were purified from the BHK-21 cell supernatant by ultracentrifugation through a 20 % sucrose cushion. The sucrose cushion contained 20 % (w / v) sucrose (Sigma) and 80 % TNE buffer pH 7.4 (50 mM Tris-HCl pH 7.4, 100 mM NaCl (Sigma) and 0.1 mM EDTA pH 8.0 (Sigma)). The supernatant was poured into an ultracentrifugation tube and 10 ml of the 20 % sucrose cushion was

added below the supernatant using a 10 ml pipette. The supernatant was ultracentrifuged at 82,700 x g for 1.5 h to pellet the virus or VRPs. The supernatant was carefully removed and the pellet was re-suspended in 100 μl of TNE buffer pH 7.4. The re-suspended viruses and VRPs were stored at -80^{o}C.

2.2.4 Restriction Digest of DNA Plasmids

Linearisation of DNA plasmids was carried out using the restriction endonuclease Spe I (New England Biolabs). The plasmid DNA was mixed with the restriction digest mixture, which contained 6 μl of 10x acetylated BSA (New England Biolabs), 6 μl of 10x restriction enzyme buffer (New England Biolabs), 2 μl of Spe I and was made up to 60 μl with nuclease free water. This was incubated at the manufacturer's recommended temperature for 2 – 4 h. The DNA was purified using the High Pure PCR Product Purification Kit (Roche) and the results were checked by agarose gel electrophoresis (2.2.6 and 2.2.7).

2.2.5 In vitro transcription

Spe I linearised plasmid DNA (2.2.4) was transcribed into mRNA using the MegaScript SP6 kit (Ambion). Following the manufacturer's instructions a 20 μl reaction mixture was prepared, which contained 2 μl of ATP, 2 μl of UTP, 2 μl of CTP, 2 μl of GTP (diluted 1 in 5), 2 μl of 10x SP6 reaction buffer, 2 μl of the enzyme polymerase mixture, 2 μl of 10 mM M^{7}G (5')ppp (5') G (cap) (GE Healthcare), 1 μg of linearised plasmid DNA and nuclease free water. The reaction mixture was incubated in a water bath at 37^{o}C for 5 h. The products were checked by agarose gel electrophoresis (2.2.6).

2.2.6 Agarose gel electrophoresis

Agarose (Sigma) was added to Tris-acetate-EDTA (TAE) buffer and heated until the agarose dissolved. The percentage of agarose and the volume of TAE buffer depended on the size of gel and speed of nucleotide movement desired. On cooling, ethidium bromide was added to the agarose mix to give a final concentration of 0.5 μg/ml. The solution was mixed and poured into a plastic frame with a comb. On

solidifying, the gel was moved to a tank, the comb removed and the gel was covered with TAE buffer. Samples were loaded with loading buffer (Promega). A 100 bp or 1000 bp DNA ladder (Promega) was run in lane 1. Gels were normally run at 90 V for 45 minutes. The products were visualised using a UV transilluminator.

2.2.7 DNA purification

DNA was purified from a restriction digest or from an agarose gel using the High Pure PCR Product Purification Kit (Roche) according to the manufacturer's instructions. For the restriction digest, the sample was adjusted to 100 μl using nuclease free water and 500 μl of binding buffer 1 added. For the gel extraction, the DNA band was visualised by placing the gel on a ultra-violet light box, then cutting out the band using a scalpel and dissolving it in 700 μl of binding buffer at 56^{o}C. A High Pure Filter Tube was inserted into a Collection Tube and the digest or the gel mixture was added to this, centrifuged at 6,800 g for 1 minute and the flow-through discarded. The filter was washed with 700 μl of buffer 2, centrifuged at 6,800 g for 1 minute and the flow-through discarded. The wash and centrifugation was repeated with 200 μl of buffer 2. To elute the DNA, the tube was inserted into a fresh eppendorf tube and 50 μl of elution buffer 3 was added for 1 minute at room temperature. The eppendorf tube was centrifuged at 6,800 g for 1 minute and the eluted DNA was stored at -20^{o}C. The concentration of DNA was measured using a NanoDrop Spectrophotometer.

Table 2.2: Viruses and VRPs used in this project

Virus Strain	Backbone	Modification
SFV L10	n/a	Wild type – isolated originally as a naturally occurring strain.
SFV A7(74)	n/a	Wild type – isolated originally as a naturally occurring strain.
SFV4	n/a	Prototype.
SFV4-RDR	SFV4	SFV4 with a point mutation in the nuclear localisation signal of nsP2 (RRR is changed to RDR).
SFV4nsP3Δ50	SFV4	SFV4 with 50 amino acids deleted in the C'-terminus of nsP3 (amino acids between positions 318-369).
SFV4(3H)RLuc	SFV4	The gene encoding *Renilla* luciferase (RLuc) is inserted at the 3' end of the nsP3 gene. RLuc is translated and released during replication of the SFV4 genome. The amount of RLuc produced is used as an indirect measure of virus replication.
SFV4(3F)-ZsGreen	SFV4	The gene encoding ZsGreen is fused to the 3' terminus of the nsP3 gene. During the replication of SFV4(3F)-ZsGreen, nsP3 is produced fused to ZsGreen, which highlights the location of nsP3.
SFV1-d1eGFP VRP	SFV4	SFV1 VRP expressing the enhanced green fluorescent protein (eGFP) under the control of the subgenomic promoter.
Sendai virus (Cantell strain)	n/a	Negative ssRNA virus (*Paramyoxviridae*). Purchased from the American Type Culture Collection.
Encephalomyocarditis virus (EMCV)	n/a	Positive ssRNA virus (*Picornaviridae*).

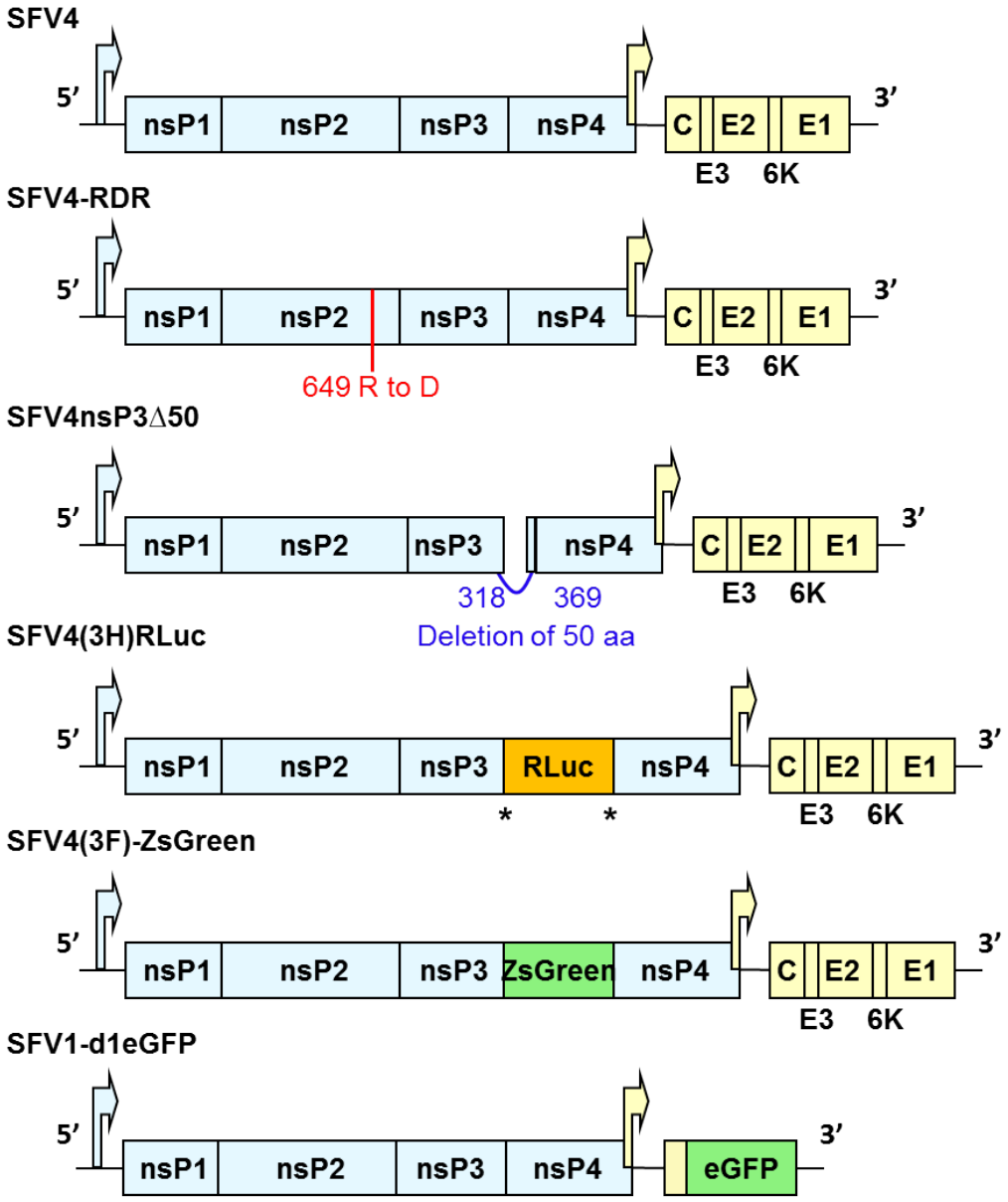

Figure 2.1: Schematic representation of the viruses and VRPs used in this project

Blue boxes correspond to the nsPs 1 – 4 and yellow boxes correspond to the structural proteins: capsid protein (C), the envelope glycoproteins (E1 – 3) and the 6K protein. SFV4-RDR has a point mutation in nsP2 at amino acid position 649, arginine (R) to aspartic acid (D). SFV4nsP3Δ50 has a deletion of 50 amino acids between positions 318 – 369. *RLuc* is inserted into SFV4(3H)RLuc at the 3' end of nsP3 between duplicated nsP2 cleavage sites (*). ZsGreen is inserted into SFV4(3F)-ZsGreen at the 3' terminus of nsP3. SFV1-d1eGFP expresses eGFP under the control of the subgenomic promoter instead of structural proteins.

2.2.8 Infection of cells *in vitro* with virus or VRPs

To infect cells in a 6-well plate, cells were seeded at a concentration of 3x105 per well and incubated overnight. The medium was removed from the wells and the required amount of virus or VRP diluted in 400 μl of PBSA was added. The plates were placed on a rocker at room temperature for 1 hour. After incubation, the virus mixture was replaced with 1 ml of fresh medium and the plates incubated at 37^{o}C. In a 24-well plate, the virus or the VRP was added in 100 μl volumes to each well. In a 96-well plate, the virus or the VRP was added in 30 μl volumes to each well. Time zero in all experiments was considered to be the time at which virus was added to the cells.

2.2.9 Titration of virus by standard plaque assay

Generally, infectious virus was titrated by standard plaque assay in BHK-21 cells. BHK-21 cells were seeded in 6-well plates at a concentration of 3x10^{5} cells per well and incubated overnight. The virus was serially diluted 10-fold in PBSA. The medium was removed from the wells and 400 μl of each dilution was added to two wells of the 6-well plate. The cells were incubated for 1 hour at room temperature with gentle rotation. After incubation, molten agar (4 g of Bacto agar per 100 ml PBS sterilised by autoclave) mixed with GMEM supplemented with 2 % NBCS (2% NBCS GMEM) at a ratio of 10:3 was used to overlay the cells. The cells were incubated for 2-3 days and then fixed by covering the agar with 10 % paraformaldehyde (PFA) (Surgipath) for 1 hour. The PFA and the agar were removed and the monolayer was stained with approximately 1 ml of 0.1% toludine blue. The plates were placed on the rocker for 30 minutes and then rinsed with tap water. Round areas of dead cells unstained by the dye were considered to be plaques. Plaques were counted and the titre of the virus stock determined using the following formula:

Virus titre in plaque forming units (PFU) per ml = average number of plaques in two wells / amount of inoculum x dilution factor

In experiments analysing plaque phenotype the BHK-21 cells were replaced by other cell lines. The rest of the experimental procedure was identical.

2.2.10 Titration of VRPs

The standard plaque assay could not be used to titrate VRPs because VRPs do not produce progeny virus after infection and therefore plaques of dead cells are not formed. Instead, virus infection was visualised by immunostaining. In some cases, the VRP expressed its own marker gene, e.g. ZsGreen and could be visualised directly. BHK-21 cells were seeded on 20 x 20 mm glass coverslips (Menzel Glaser) in 6-well plates at a concentration of $3x10^5$ cells per well and incubated overnight. Next day, a 10-fold serial dilution of the VRP was prepared in PBSA. The medium was removed from the wells and 400 µl of each dilution was added to two wells of the 6-well plate). The cells were incubated for 1 hour at room temperature with gentle rotation. After incubation, the PBSA was replaced by 2 ml of medium and the cells were incubated for 20 h. The cells were fixed with PFA for 1 hour and then immunostained as described in section 2.3.1 or viewed immediately, if cells expressed a marker gene. The coverslips were mounted using Vectashield Aqueous Mounting Medium (Vector Laboratories), dried for 30 minutes at room temperature and the edges of the coverslip sealed with nail varnish. The results were viewed using a Zeiss Axioskop 2 microscope. Fifteen fields were examined for presence of virus, indicated by red fluorescent immunostaining for SFV non-structural protein 3. The average number of infected cells was calculated and this was used to find the titre of the VRP using the following formula:

VRP concentration per ml = Mean number of VRPs x microscope constant / volume of inoculum.

Throughout this project the MOI was calculated based on the titre of the virus or the VRP in BHK-21 cells.

2.3 Immunostaining

2.3.1 Detection of target by immunofluorescence

The antibodies used in this project and the corresponding dilutions are listed in Table 2.3. Cells were seeded on 20 x 20 mm glass coverslips in 6-well plates at a density of $3x10^5$ cells per well overnight. The cells were infected, incubated and fixed using PFA for 1 hour at room temperature as described above in section 2.2.9. The PFA was removed and the cells were washed with PBS (3 x 5 minutes). The PBS was

replaced with 2 ml of PBS with 0.3% Triton-X100 and the cells were placed on the rocker for 20 minutes at room temperature to permeabilise the cell membranes. The cells were washed with PBS (3 x 5 minutes) and covered with 700 µl of Cas-block (Zymed) for 20 minutes at room temperature. The Cas-block was replaced with 700 µl of the primary antibody diluted in Cas-block and incubated for 2 h at room temperature. The cells were washed with PBS (3 x 10 minutes), covered with 700 µl of the secondary antibody diluted in Cas-block and incubated for 1 hour at room temperature. The cells were washed again with PBS (3 x 10 minutes), covered with 700 µl of the tertiary antibody diluted in distilled water and incubated for 45 minutes in darkened conditions. The cells were washed with PBS (3 x 10 minutes), then rinsed with distilled water and mounted using Vectashield Aqueous Mounting Medium. On certain occasions, the Vectamount contained 4', 6-diamidino-2-phenylindole (DapI) that stains DNA. Results were viewed using the Zeiss AxioSkop 2 microscope or a Zeiss AxioObserver D1 microscope with Colibri filters for the visualisation of eGFP, ZsGreen, Alexa Fluor 594 (red) and DapI. For visualisation using confocal microscopy, the cell nuclei were stained using To-Pro-3 (Invitrogen) diluted 1 in 10 with water and incubated for 10 minutes at room temperature. The coverslips were then mounted using Vectashield Aqueous Mounting Medium and the results were viewed using a Zeiss-LSMpascal microscope with lasers suitable for viewing eGFP, ZsGreen, Alexa Fluor 594 (red) and To-Pro-3 (blue).

2.3.2 Detection of target by 3,3'-Diaminobenzide

SIGMA*FAST* 3,3'-Diaminobenzide (Dab) tablets were used to detect peroxidise activity. Immunostaining using Dab was carried out in the same way as immunostaining using fluorescent antibodies. However, the tertiary antibody was replaced with 1 ml of the Dab mix (1 Dab tablet and 1 Urea tablet dissolved in 5 ml of distilled water) and incubated for 5 minutes at room temperature under darkened conditions. Slides were washed with water and mounted using VectaMount Aqueous Mounting Medium. Results were visualised using the Zeiss Axioskop 2 microscope with brightfield settings.

Table 2.3: List of antibodies used for immunostaining

* Reagent kindly provided by Dr. Tero Ahola, University of Helsinki, Finland. **Reagent kindly supplied by Prof. Andres Merits, Institute of Technology, University of Tartu, Estonia.

Target	Source	Host	Isotype	Feature	Dilution	Incubation time
SFV nsP3	Tero Ahola*	Rabbit	Polyclonal	-	1 in 800	2 h
SFV nsP1	Andres Merits**	Rabbit	Polyclonal		1 in 500	2 h
SFV structural proteins	Tero Ahola*	Rabbit	Polyclonal	-	1 in 800	2 h
dsRNA	Scicons	Mouse	Monoclonal IgG1	-	1 in 500	2 h
Rabbit IgG	Vector Labs	Goat	Monoclonal IgG	Biotinylated	1 in 750	1 hour
Mouse IgG		Sheep	Monoclonal IgG	Biotinylated	1 in 750	1 hour
Rabbit IgG	Sigma	Goat	Monoclonal	Peroxidase	1 in 750	1 hour
SA Alexa Fluor 594	Invitrogen	Goat	Monoclonal IgG	Fluorescent	1 in 1200	0.75 hour

2.4 Interferon bioassay

2.4.1 Infection of cells for the interferon bioassay

Cells were seeded in four wells of a 6-well plate at $3x10^5$ cells per well and incubated for 24 h or until 100 % confluent. The supernatant was removed from the wells and the cells were infected with virus at MOI 5 in 400 µl of PBSA. After 1 hour the PBSA was replaced with 1 ml of 2 % FCS DMEM and incubated for 24 h. After incubation, the supernatant from the four wells was combined and centrifuged at 478 g for 5 minutes to remove any cell debris. 2 ml of the supernatant was collected for plaque assay and 2 ml was collected for the IFN bioassay.

2.4.2 Preparation of samples for the interferon bioassay

UV light was used to inactivate virus in the supernatant as follows. The supernatant was divided equally between four wells of a 24-well plate and placed in the Stratalinker 1800 UV cross linker. The plate was placed 5 cm from the UV light bulb with the lid removed and exposed to UV light for 30 minutes. To determine if the virus was inactivated, a plaque assay was subsequently carried out on BHK-21 cells

using an aliquot of the supernatant. The remaining supernatant was stored at -80^{o}C until used.

2.4.3 Mouse interferon bioassay

The mouse IFN bioassay was used to measure the amount of IFN in the supernatant. In a 96-well plate, 2x10^{4} L929 cells were seeded per well in 0.1 ml of 10 % FCS DMEM and incubated for 24 h. In a separate 96-well plate, 2-fold serial dilutions of the supernatant samples were prepared (Fig. 2.2). To each well in column 1, 200 µl of neat sample was added. To each well in column 2 – 12 100 µl of 2 % FCS DMEM was added. A 2-fold serial dilution was created by transferring 100 µl of column 1 to column 2 and repeating this across the plate. All samples were run in duplicate to control for experimental error.

On one plate, a negative control (cells with medium only) was included in three wells of row H and a positive control (cells with challenge virus SFV A7(74)) were also included. A mouse IFN international standard (Stratech Scientific Ltd) was included on one plate to allow quantification of IFN. For the international standard, 90 µl of 2 % FCS DMEM was added to row A. To well A1, 10 µl of the mouse IFN international standard was added giving a final concentration of 100 U/ml. A 10-fold serial dilution was created by adding 10 µl of well A1 to well A2 and repeating this across the plate.

The medium on the L929 cells was replaced with the prepared dilutions and then incubated for a further 24 h. After incubation, the dilutions were removed and replaced with 100 µl of the challenge virus suspension containing SFV A7(74) diluted in 2 % FCS DMEM at MOI 0.1. The negative control wells were replaced with fresh medium instead of the challenge virus suspension.

The cells were incubated until complete CPE was observed in the positive control, which was normally after 48 h. The cells were fixed by adding 100 µl of PFA for 1 hour and stained by removing the PFA and adding 100 µl of 0.1 % toludine blue. The plates were placed on a rocker for 30 minutes and then washed with water. The endpoint was determined as the dilution which protected 50 % of the monolayer.

To determine the amount of IFN within a sample, the endpoint of the IFN standard was determined and the concentration of IFN at this dilution was calculated. This concentration was the amount of IFN required to protect 50 % of the cell monolayer from virus challenge in this experiment. For each dilution series, the concentration of IFN at the endpoint, as determined by the international standard, was multiplied by the dilution factor protecting 50 % of the monolayer to calculate the amount of IFN per ml of the test sample.

2.4.4 Human interferon bioassay

The human IFN bioassay was carried out in the same way as the mouse IFN bioassay with some modifications. The mouse L929 cells were replaced with human A549-NPro cells. These were grown in 10 % FCS DMEM supplemented with Puromycin. A human international IFN standard (NIBSC) was used instead of the mouse standard. The virus challenge suspension contained EMCV at MOI 0.1 in 2 % FCS DMEM instead of SFV A7(74). 100 µl of the suspension was added to each well and the cells were incubated until complete CPE was observed in the positive control, usually after 24 h.

	1	**2**	**3**	**4**	**5**	**6**	**7**	**8**	**9**	**10**	**11**	**12**
A	1	2	4	8	16	32	64	128	256	512	1024	2048
B	1	2	4	8	16	32	64	128	256	512	1024	2048
C	1	2	4	8	16	32	64	128	256	512	1024	2048
D	1	2	4	8	16	32	64	128	256	512	1024	2048
E	1	2	4	8	16	32	64	128	256	512	1024	2048
F	1	2	4	8	16	32	64	128	256	512	1024	2048
G												
H	NC	NC	NC							PC	PC	PC

Figure 2.2: IFN bioassay plate design
The numbers in the wells indicate the reciprocal dilution of the two-fold serial dilution. Samples were run in duplicate such that rows A and B contained the same sample. NC indicates the negative control and PC indicates the positive control, which were included on one plate in each experiment. Where standards were included on a plate, one sample was replaced with the 100 U/ml of the International IFN standard diluted 1 in 10 across the plate.

2.5 Interferon sensitivity assay

The IFN sensitivity assay was used to measure the effect of IFN pre-treatment on SFV replication. In a 96-well plate, $2x10^4$ 2fTGH, Hs 633T, L929 or NIH 3T3 cells

were seeded per well in 0.1 ml of 10 % FCS DMEM and incubated for 24 h. Following incubation, the media was replaced with 10 U/ml of human IFN or mouse IFN in 100 µl of 10% FCS DMEM and incubated for 16 h. Following incubation, the IFN mixture was replaced with virus in 30 µl of PBSA at MOI 5. Three wells were included as a mock infected control and were treated with 30 µl of PBSA. Cells were incubated for 1 hour at 37^{o}C and then 100 µl of 2% FCS DMEM was added to each well. At the desired time post-infection, the cells were analysed for fluorescence or the supernatant was collected for measuring virus titre by plaque assay (2.2.9).

2.6 Western Blot

2.6.1 Sample preparation for sodium dodecyl sulphate – polyacrylamide gel electrophoresis (SDS-PAGE)

The lysis buffer consisted of 20 mM Tris-HCl (pH 8), 137 mM NaCl (Sigma), 10% glycerol (Sigma), 1 % Nonidet-P40 (Fluka) and 2 mM EDTA (Sigma) plus 1X phosphatase inhibitor cocktail (Calbiochem) and 1X Halt Protease Inhibitor Cocktail (Thermo Scientific). Cells in one well of a 6-well plate were lysed by removing the medium from the well, adding 300 µl of lysis buffer and incubating on ice for 20 minutes with continuous rotation. Following incubation, 100 µl of the mixture was collected for measuring protein concentration and 200 µl was collected for SDS-PAGE. The sample for SDS–PAGE was mixed with 200 µl of Laemmli buffer (950 µl of Laemmli buffer (Bio-Rad) mixed with 50 µl of β-mercaptoethanol (Sigma)) and boiled for 10 minutes at 100^{o}C. The samples were stored at -20^{o}C until required.

2.6.2 Measurement of protein concentration

Protein concentration in the lysed samples was measured using the Pierce BCA Protein Assay Kit (Thermo Scientific) according to the manufacturer's instructions. Following the microplate protocol, the working reagent was prepared, which contained 50 parts of reagent A mixed with 1 part of reagent B to give 200 µl per well. The BSA standard was diluted following the manufacturer's instructions. Into wells of a 96-well plate, 25 µl aliquots of the standard or the samples were added in duplicate, 200 µl of the working reagent was added to each well and mixed. The

plate was incubated for 30 minutes at 37^{o}C and protein concentration was measured spectrophotometrically at 750 nm.

2.6.3 SDS-PAGE preparation

A 12 % gel consisted of two parts: a resolving gel and a stacking gel. The resolving gel was made with 30 ml of 40 % acrylamide (Sigma), 25 ml 1.5M Tris-Base pH8.8 (Sigma), 1 ml of 10 % sodium dodecyl sulphate (SDS) (Sigma) and 43 ml of distilled water. Just before use, 10 µl of tetramethylethylenediamine (TEMED, Sigma) and 100 µl of ammonium persulphate (APS, Sigma) were added to 10 ml of the resolving gel solution and it was poured between two glass plates. A space of approximately 2 cm was left at the top of the gel and this was filled with isobutanol (Sigma) to level the gel. The stacking gel was made with 10 ml of 40 % acrylamide, 25 ml of 0.5 M Tris-Base pH 6.8 (Sigma), 1 ml of 10 % SDS and 64 ml of distilled water. Just before use, 5 µl of TEMED and 50 µl APS were added to 5 ml of the stacking gel solution. Once the resolving gel had set, the isobutanol was removed and the stacking gel was added. A 0.75 mm comb was immediately inserted into the stacking gel to create the lanes. The gel was left until solid and then used.

2.6.4 SDS-PAGE and protein transfer

The 12 % gel was placed into an electrophoresis tank and the tank was filled with 1 X running buffer. The 5X running buffer contained 15.1 g of Tris-Base (Sigma), 94 g of glycine (Sigma) dissolved in 900 ml of distilled water and made up to 1000 ml with 10 % SDS. This was diluted to 1X with distilled water for use. The samples in Laemmli buffer (2.6.1) were thawed and aliquots of each sample containing 200 µg of protein were loaded into separate wells. The first well contained 10 µl of Hyperpage Pre-strained Protein Marker (Bioline). The SDS gel was run at 140 V until the blue dye band reached the bottom of the gel. The gel was removed from between the glass plates and the stacking gel was discarded. Hybond ECL nitrocellulose paper (GE Healthcare), extra thick Western blot filter paper (Thermo Scientific) and sponges were soaked in transfer buffer before use. The transfer buffer comprised 3.03 g Tris-Base (Sigma), 14.4 g of glycine (Sigma), 200 ml of methanol (Sigma) and 800 ml of distilled water. The transfer cassette was opened and a sponge

placed on the bottom followed by one piece of filter paper, the gel, the Hybond ECL nitrocellulose paper and another piece of filter paper. The cassette was rolled to remove any air bubbles and a wet sponge was added on top. The cassette was closed and placed into the electrophoresis tank in the orientation that would allow the proteins to transfer from the gel onto the Hybond ECL nitrocellulose paper. An ice pack was added to the tank and the tank was filled with transfer buffer. The electricity was turned on at 30 V for 30 minutes followed by 60 V for 60 minutes. The nitrocellulose paper was removed from the cassette and placed in PBS with 0.1 % Tween-20 (Sigma) (PBS-T), until probed.

2.6.5 Detection of cellular proteins using antibodies (Western blot)

The nitrocellulose paper was probed using the antibodies shown in Table 2.4. The primary antibodies were diluted in blocking buffer (0.3 g blocking powder (GE Healthcare) in 5 ml of PBS-T) and incubated for the time shown in Table 2.4. After incubation, the nitrocellulose paper was washed with PBS-T (3 x 5 minutes), immersed in blocking solution containing the secondary antibody for 1–3 h at room temperature and then re-washed with PBS-T (3 x 5 minutes). To detect the secondary antibody, the ECL Advance Western Blotting Detection Kit (Amersham) or the Pierce Fast Western Blot kit ECL substrate (Thermo Scientific) were used. The ECL kit was used with blots for phosphorylated STAT1 and the Pierce kit was used with blots for total STAT1 or β-actin. To use either kit, the nitrocellulose paper was immersed in 1 ml of reagent 1 or A mixed with 1 ml of reagent 2 or B for 5 minutes. After the incubation the bands were visualised using the G:Box Imaging System.

Table 2.4: List of antibodies used for Western blot

Target	Source	Host	Isotype	Dilution	Incubation time	Temp.
Human STAT1	Cell signaling	Rabbit	Polyclonal	1 in 500	24 h	4°C
Human phosphorylated STAT1	Cell signaling	Rabbit	Polyclonal	1 in 500	24 h	4°C
Human β-actin	Cell signaling	Rabbit	Polyclonal	1 in 750	1 hour	Room temp.
Rabbit IgG	Abcam	Goat	Monoclonal, peroxidase labelled	1 in 1000	1 – 3 h	Room temp.

2.6.6 Quantification of Western blot bands

To quantify protein bands detected by Western blot, ImageJ (http://rsbweb.nih.gov/ij/) was used. ImageJ enabled the quantification of the bands detected relative to β-actin bands.

2.7 Cell viability assay

Cell viability was measured using the Wst-1 assay (Roche), according to the manufacturer's instructions. The Wst-1 assay measures mitochondrial activity by providing formazan dye that the mitochondrial dehydrogenases cleave to produce a product that can be measured spectrophotometrically. 96-well plates were seeded with cells at a density of 9000 cells per well and the experiment carried out. At the termination of the experiment, 10 μl of Wst-1 was added to each well containing 100 μl of media. Plates were incubated for 1 hour and measured the optical density at 450 nm using the Promega GloMax Multi-Detection System.

2.8 Cell transfection

2.8.1 Cell transfection using Lipofectamine 2000

Cells were seeded in 24 or 96-well plates at a concentration of $7x10^4$ or $3x10^5$ cells per well respectively and incubated overnight. In a polystyrene tube, 1 μl of Lipofectamine 2000 (Invitrogen) per well was mixed with 50 μl of Optimem (Invitrogen) and incubated at room temperature for 5 minutes. In a separate tube, the plasmid or RNA to be transfected was mixed with Optimem to give a final volume of

50 μl per well. The total volume of the plasmid/siRNA mix was transferred to the tube containing the Lipofectamine 2000 mix and incubated at room temperature for 20 minutes. During this time, the medium in the wells was replaced with fresh 2 % FCS DMEM (900 μl per well of a 6-well plate and 400 μl per well of a 24-well plate). 100 μl of the Lipofectamine 2000 mix was then added to each well and the plates were incubated. After 5 h, the transfection mix was replaced with fresh medium and the cells were incubated for a further 24 – 48 h.

In certain experiments cells were seeded and transfected simultaneously. Briefly, the Lipofectamine 2000, Optimem and siRNA mix was prepared and incubated for 20 minutes. During the incubation, a 175 cm^2 flask of cells was trypsinised, counted, centrifuged again and re-suspended in medium to produce the desired number of cells for seeding. The cells were seeded into 24-well plates or 6-well plates and 100 μl of the Lipofectamine 2000 mix was added to each well. Cells were incubated for 24 – 48 h.

2.8.2 Dual-Glo Luciferase Assay

The Dual-Glo Luciferase Assay (Promega) was used to measure both firefly and *Renilla* luciferase. The lysis buffer was comprised of passive lysis buffer diluted 1 in 5 with distilled water. The cells to be assayed were lysed by removing the medium in a 24-well plate, adding 100 μl of diluted lysis buffer and placing on a fast rocker until the cells detached. 30 μl from each well was then aliquotted into a white plastic 96-well plate suitable for the Promega GloMax Multi-Detection System. 70 μl per well of luciferase assay reagent was placed in a universal container. To a separate universal container 70 μl per well of stop-glo was added (diluted 1 in 50 in distilled water). An additional 900 μl of both the luciferase reagent and the stop-glo reagent were added to prime the detection system. Firefly and *Renilla* luciferase were measured using the Dual-Luciferase two injector programme in the Promega GloMax Multi-Detection System.

2.9 Polymerase Chain Reaction

2.9.1 RNA extraction

RNA extraction was carried out using the RNeasy Kit (Qiagen) according to the manufacturer's instructions. The cells in 4 wells of a 6-well plate were lysed by removing the medium and adding 600 μl of RLT buffer containing 1 % β-mercaptoethanol. The cell lysate was homogenised by passing it through a 20-gauge needle five times. The lysate was collected, 70 μl of 70 % ethanol was added and the lysate was transferred to an RNeasy spin column. The column was centrifuged at 8,000 g for 15 seconds and the flow-through discarded. 350 μl of buffer RW1 was added to the column, the centrifugation was repeated and the flow-through discarded. 80 μl of DNase I stock in buffer RDD (10 μl and 70 μl respectively) was added to the filter and incubated at room temperature for 15 minutes to remove any residual DNases. The filter was washed with 350 μl of buffer RW1, centrifuged at 8,000 g for 15 seconds and the flow-through discarded. To remove any residual ethanol that would affect purity of the RNA the filter was washed with 500 μl of buffer RPE, centrifuged at 8,000 g for 15 seconds and the flow-through discarded. An additional 200 μl of buffer RPE wash was added, centrifuged at 8,000 g for 2 minutes and the flow-through discarded. RNA was eluted into a 1.5 ml collection tube by adding 30 μl of RNase-free water and centrifuging at 8,000 g for 1 minute. The RNA concentration was measured using a NanoDrop Spectrophotometer. The RNA was then stored at -80^{o}C until use.

2.9.2 Reverse transcription PCR

Reverse transcription PCR converted RNA into cDNA. Five μg of total RNA was combined with 1 μl of 50 μM oligo(dT)$_{15}$ (Promega), 1 μl of 10 mM dNTP Mix (Promega) and made up to 13 μl with RNase-free water. The RNA mix was incubated at 65^{o}C for 5 minutes and placed on ice for 1 minute. The cDNA synthesis mix was prepared with 4 μl of 10X RT buffer (Invitrogen), 1 μl of 0.1 M DTT (Invitrogen), 1 μl of RNasein Ribonuclease Inhibitor (Promega) and 1 μl of SuperScript III (Invitrogen) and 7 μl of this was added to each RNA reaction. The

total RNA was incubated at 50°C for 1 hour, inactivated by heating at 70°C for 15 minutes and stored at -20°C until use.

2.9.3 Polymerase Chain Reaction

Several Polymerase Chain Reaction (PCR) programmes were used in this project. The primer sets and the corresponding annealing temperatures are shown below. The reactions used either Taq polymerase (Promega) or Vent DNA Polymerase (New England Biolabs). The PCR reaction mix for Taq polymerase contained 5 μl of 10X PCR buffer with $MgCl_2$ (Promega), 1 μl of 10 mM dNTP Mix (Promega), 1 μl of the forward primer (50 pM, Sigma), 1 μl of the reverse primer (50 pM, Sigma), nuclease-free water, DNA and 0.4 μl of Taq polymerase. In PCR reactions using Vent DNA Polymerase, the 10X PCR buffer was replaced with Thermo Pol reaction Buffer (New England Biolabs) and the Taq polymerase was replaced with Vent DNA Polymerase (New England Biolabs). The results were checked by agarose gel electrophoresis (2.2.6).

nsP2

The PCR was carried out using Vent DNA Polymerase

95°C 5 minutes, (95°C 1 minute, 56°C 2 minutes, 72°C 4 minutes) x 30, 72°C 8 minutes. The primers used were:

For 5' GAGGCCGAGCTGACTAGAGA; Rev 5' TCATTGAGCAACTCCACAGC

nsP3

The PCR was carried out using Vent DNA Polymerase

95°C 5 minutes, (95°C 1 minute, 56°C 2 minutes, 72°C 4 minutes) x 30, 72°C 8 minutes. The primers used were:

For 5' AGGGTCACTTGGTTGTCACC; Rev 5' TACATCGGGGCTTGAGAATC

β-actin (human)

The PCR was carried out using Taq polymerase.

95°C 5 minutes, (95°C 30 seconds 56°C 20 seconds, 72°C 30 seconds) x 30, 72°C 15 minutes.

For 5' AGAAAATCTGGCACCACACC; Rev 5' AACGGCAGAAGAGAGAACCA

Beclin-1 (human)

The PCR was carried out using Taq polymerase.

95^{o}C 5 minutes, (95^{o}C 30 seconds 56^{o}C 20 seconds, 72^{o}C 30 seconds) x 28, 72^{o}C 15 minutes. The primers used were:

For 5' GAGTGCTAGGAGGGCAACAG; Rev 5' TTTCATATCCGGCCACTCTC

2.10 Autophagy assays

2.10.1 Assay to determine autophagic cells

Cells were seeded on glass coverslips with a 13 mm diameter in 24-well plates at a density of 7x10^{4} cells per well overnight. The cells were transfected with 0.5 μg of GFP-LC3 plasmid (AddGene) per well using Lipofectamine 2000, according to the manufacturer's instructions (Section 2.7.1). LC3 in this plasmid was produced from the gene MAP1LC3B, which is also known as ATG8F, LC3B, MAP1A/1BLC3, MAP1LC3B-a. 24 h later, the cells were treated with chemicals (2.10.2), virus/VRPs or PBSA alone and then fixed with PFA. The coverslips were washed with water, mounted using Vectamount Aqueous Mounting Medium containing DapI and then viewed using the Zeiss Axioskop 2 microscope. Fifteen fields were examined for autophagic cells. An autophagic cell was defined as transfected cells expressing two or more eGFP foci (puncta). The average percentage of autophagic cells in the cell monolayer was calculated using the following formula:

Mean number of autophagic cells (%) = mean number of autophagic cells / total number of transfected cells x 100

2.10.2 Chemical activation or inhibition of autophagy

Cells were seeded in 24-well plates and transfected with the GFP-LC3 plasmid. To induce autophagy, the medium was removed from the wells and replaced with 500 μl of 2 μM of rapamycin (Sigma) diluted in 10% FCS DMEM for 3 h. To inhibit autophagy, the medium was removed from the wells and replaced with 500 μl of 10 mM of 3-methyladenine (Sigma) diluted in 10% FCS DMEM for 3 h.

2.11 DNA transformation and amplification using bacteria

2.11.1 Preparation of agar plates

SURE 2 Supercompetent bacteria cells (Stratagene) or chemically competent *Escherichia coli* strain DH5α cells (Promega) were grown on Luria-Bertani (LB) agar plates or Soya agar plates. LB plates were prepared by mixing 7.5 g agar with 500 ml LB and then autoclaving. Ampicillin or kanamycin was added to give a final concentration of 100 μg/ml and the liquid was poured into 10 cm diameter petri dishes. The antibiotic selected depended on the resistance gene encoded by the plasmid. Soya broth plates were prepared by mixing 15 g soya broth (Oxoid) with 7.5 g agar and 500 ml LB. The soya broth was autoclaved, ampicillin or kanamycin was added (final concentration 50 μg/ml) and the liquid was poured into petri dishes. The plates were stored at -20^{o}C until use.

2.11.2 Bacterial cell transformation

Bacterial cell transformation was carried out using SURE 2 Supercompetent bacteria cells (Stratagene) or chemically competent *Escherichia coli* strain DH5α cells (Promega), according to the manufacturer's instructions. Cells were thawed on ice and 100 μl was added to a fresh tube. The SURE 2 Supercompetent bacteria cells were mixed with 2 μl of β-mercaptoethanol and incubated on ice for 10 minutes with swirling every 2 minutes. After incubation, 1 μl of plasmid DNA (0.1 – 50 ng) was added to the cells and placed on ice for 30 minutes. The cells were then heat-shocked for approximately 30 seconds in a 42^{o}C water bath, then immediately chilled on ice for 2 minutes to induce plasmid uptake. 900 μl of pre-warmed SOC media (Invitrogen) was added to the cells and the suspension was incubated at 37^{o}C with shaking at 225-250 rpm. One hour later, a 50 μl or 100 μl volume of the cell suspension was added to the LB or Soya plates and incubated for 16 h at 37^{o}C. The plates used depended on the plasmid to be amplified. Cells transformed with the plasmid were resistant to the antibiotic and formed colonies on the surface of the agar. These colonies were amplified by Miniprep (2.11.3) or Maxiprep (2.11.4).

2.11.3 Miniprep

DNA plasmids were amplified on a small scale using the QIAprep Miniprep kit (Qiagen), according to the manufacturer's instructions. One colony of transformed cells was selected and added to 5 ml of LB broth supplemented with ampicillin or kanamycin (100 μg/ml). Alternatively, the colony was added to 5 ml of Soya broth supplemented with ampicillin or kanamycin (50 μg/ml). The broths were incubated at 37^{o}C with shaking at 225-250 rpm. After 16 h, the broths were centrifuged at 6,800 g for 5 min at room temperature to pellet the cells. Each pellet was re-suspended in 250 μl of chilled buffer P1, lysed using 250 μl of buffer P2 and neutralised with 350 μl of buffer N3. The cell lysate was centrifuged at 17,900 g for 10 min and the supernatant that contained the DNA was transferred to a QIAprep spin column. The spin column was centrifuged at 17,900 g for 1 minute and the flow-through discarded. The filter was washed by adding 500 μl buffer PB, centrifuging at 17,900 g for 1 minute and discarding the flow-through. The wash was repeated with 750 μl of buffer PE. The filter was dried by centrifuging at 17,900 g for 1 minute. To elute the DNA 50 μl of buffer EB was added to the filter for 1 minute and centrifuged at 17,900 g for 1 minute. The concentration of the DNA was measured using a NanoDrop Spectrophotometer and the DNA was stored at -20^{o}C.

2.11.4 Maxiprep

To amplify large quantities of plasmid DNA, the EndoFree Plasmid Purification kit (Qiagen) was used according to the manufacturer's instructions. One colony of transformed bacteria was selected and added to a 5 ml starter culture containing LB broth with 100 μg/ml ampicillin or kanamycin. Alternatively, the colony was added to a 5 ml starter culture containing Soya broth with 50 μg/ml ampicillin or kanamycin. The broth was incubated at 37^{o}C for 6-8 h with shaking at 225-250 rpm. After incubation, 100 μl of starter culture was added to a 2 L conical flask containing 200 ml of LB or Soya broth supplemented with ampicillin or kanamycin. The antibiotics were added to the LB to give a final concentration of 100 μg/ml and to soya broth to give a final concentration of 50 μg/ml. The broth was incubated for 16

h at 37^{o}C with shaking at 225 – 250 rpm. After incubation, the cells were pelleted by centrifuging at 6,000 g for 15 min at 4^{o}C. The pellet was re-suspended in 10 ml of chilled buffer P1 and lysed by adding 10 ml of buffer P2 for 5 min at room temperature. The buffer was neutralised by adding 10 ml of chilled buffer P3 and the lysate was poured into the QIAfilter Maxi Cartridge. The cartridge was incubated for 10 minutes at room temperature to allow the cell debris to settle at the top of the cartridge and the lysate at the bottom. The lysate was pushed through into a 50 ml centrifuge tube (Falcon), 2.5 ml of buffer ER was added and the lysate was incubated on ice for 30 minutes. During this time the QIAGEN-tip 500 was equilibrated by allowing 10 ml of buffer QBT to flow through. The lysate was poured into the QIAGEN-tip 500 and allowed to flow through. The filter was washed twice with 60 ml of buffer QC and the DNA was then eluted into a fresh 50ml centrifuge tube by adding 15 ml of buffer QN. 10.5 ml of isopropanol was added to precipitate the DNA and the tube was centrifuged at 15,000 g for 10 min. The DNA pellet was washed with 5 ml of 70% ethanol and centrifuged at 15,000 g for 10 min to remove all traces of isopropanol. The ethanol was carefully removed and the pellet was air-dried. 300 µl of endotoxin free buffer TE was added to resuspend the pellet. The concentration of the plasmid DNA was measured using the NanoDrop Spectrophotometer and the DNA was then stored at -20^{o}C

2.12 Statistical analysis

All statistical analysis was carried out using Microsoft Excel or Graphpad Prism. Viral titre, IFN production and autophagy activation were analysed with the non-parametric Mann-Whitney test.

2.13 Sequencing

2.13.1 Standard PCR Sequencing

DNA sequencing was performed using specific primers by DNA Sequencing & Services (MRCPPU, College of Life Sciences, University of Dundee, Scotland, www.dnaseq.co.uk) using Applied Biosystems Big-Dye Ver 3.1 chemistry on an Applied Biosystems model 3730 automated capillary DNA sequencer. The primers used in this project are shown below:

nsP2 set 1

For 5': GAGGCCGAGCTGACTAGAGA

Rev 5': GGTCTCCGCATAACACCACT

nsP2 set 2

For 5': CCGACGAGGAGAACTACGAG

Rev 5': CGTTTTCCACACCAGCCTAT

nsP2 set 3

For 5': CGGAGCACGTGAATGTACTG

Rev 5': TTATCGGCGTATCCGTAAGC

nsP2 set 4

For 5': AGGGTCACTTGGTTGTCACC

Rev 5': TCATTGAGCAACTCCACAGC

nsP3 set 1

For 5': AGGGTCACTTGGTTGTCACC

Rev 5': TCATTGAGCAACTCCACAGC

nsP3 set 2

For 5': CTGTCACTGAGCAGCGTAGC

Rev 5': GTTCTCGAGGTCCACATGGT

nsP3 set 3

For 5': TGCGAGAAGGTTCTCCTGTT

Rev 5': TACATCGGGGCTTGAGAATC

The results were returned as sequence files. These were aligned using the programme APE (http://biologylabs.utah.edu/jorgensen/wayned/ape/) to determine the final sequence.

2.13.2 Solexa (Illumina) sequencing

Solexa (Illumina) sequencing was carried out to determine the complete genome sequence of SFV L10 and SFV A7(74) as follows.

Sample preparation for Solexa (Illumina) sequencing

In 6-well plates, NIH 3T3 cells were seeded at a density of $3x10^5$ cells per well in 10 % FCS DMEM and incubated overnight. The cells were infected with SFV L10 or SFV A7(74) at MOI 10 in 400 μl of PBSA for 1 hour at room temperature. A high MOI was used to ensure that all cells were infected. After incubation, the PBSA was replaced with 2 ml of 2 % FCS DMEM. The plates were incubated for 8 h and then the total RNA was extracted using the RNeasy kit (Qiagen), according to the manufacturer's instructions.

RNA integrity and concentration were measured by the RNA 6000 Nano Assay (Agilent Technologies). 10 μg of RNA was sent to ArkGenomics, Roslin Institute, Edinburgh for Solexa (Illumina) sequencing.

Solexa Genome Analyzer (Illumina) sequencing

Solexa (Illumina) sequencing was carried out by Sarah Smith at ArkGenomics, the Roslin Institute, Edinburgh. Illumina kits were used to make the DNA, according to the manufacturer's instructions and the DNA was run on the Solexa Illumina machine with RTA Software 1.5 and Pipeline Software 1.6 to give 36 reads and to generate raw intensity files. The sequence tag preparation was carried out using the Illumina's Digital Gene Expression Tag Profiling Kit, according to the manufacturer's protocol, to purify cDNA tags. The cDNA tags were sequenced on the Illumina Cluster Station and Genome Analyzer. Image recognition and base calling were performed using the Illumina Pipeline.

Image analysis and De Novo alignment

Image analysis and de novo alignment was carried out by Mark Fell at ArkGenomics, the Roslin Institute, Edinburgh. Briefly, the raw intensity files generated by the Solexa Genome Analyzer were input into 'Firecrest'. This

generated image data in txt form. This data was put into the program 'Bustard' which determined the sequence and quality of the data. The data was then run through the program 'Velvet' to generate high quality contigs. These contigs were run through the programs 'Generation of Recursive Analysis Linked by Dependency' and 'SGA' as further quality controls. The final contigs generated were of high quality and could be analysed with confidence.

Comparative sequence alignment

Comparative sequence alignment was carried out by Dr. Karen Sherwood, Roslin Institute, University of Edinburgh. The contigs were aligned to previously described SFV sequences (reference strains) using 'FASTA'. The reference strains used in this project are listed in Table 2.5. The sequences generated by Solexa (Illumina) sequencing were called ARKL10 (SFV L10) or ARKA774 (SFV A7(74)).

Table 2.5: Reference strains of SFV used in this project

Accession number/code name	Strain of SFV	Source
AY112987; L10-IRE	L10	Logue *et al*, submitted to NCBI in 2002, unpublished
A774-FIN	A7(74)	Supplied by Dr. A. Hinkkanen Turku Immunology Centre, Finland. Strain was used in Tuittila *et al* (2000) and Tuittila & Hinkkanen (2003).
SFV4-EST	SFV4	Provided by Prof. A. Merits, Institute of Technology, University of Tartu, Estonia.

Comparative sequence analysis

Comparative sequence analysis was carried out using Jalview 2.7 (Waterhouse *et al.*, 2009). Evolutionary divergence between sequences at the nucleotide and the amino acid level was determined using MEGA 5 (www.megasoftware.net/megalinux.php).

2.14 Protein structure prediction

Three dimensional (3D) protein structures were predicted using Phyre2 (www.rcsb.org). Phyre2 predicts the secondary structure of an amino acid sequence and generates a 3D model by using homologous crystallised proteins in the online

Protein Data Base as a template (Bennett-Lovsey *et al.*, 2008). The 3D models were formatted using USFC Chimera (www.cgl.ucsf.edu/chimera/).

Chapter 3: Autophagy: an antiviral or proviral response to Semliki Forest virus infection?

Contents

3.1 Introduction

Macroautophagy (autophagy) describes the process in which intracellular materials are sequestered into double-membrane vesicles and targeted to lysosomes for degradation. Several studies have implicated autophagy in the innate and adaptive immune responses against diverse intracellular pathogens (Gutierrez *et al.*, 2004;Nakagawa *et al.*, 2004;Birmingham *et al.*, 2006), (Andrade *et al.*, 2006;Zhao *et al.*, 2008). During virus infection, autophagy is reported to (i) increase virus replication (Jackson *et al.*, 2005), (ii) decrease virus replication (Liu *et al.*, 2005) or (iii) have no affect on virus replication (Zhao *et al.*, 2007b). The role of autophagy during virus infection appears to depend on cell line and virus studied. For alphaviruses, the effect of autophagy on virus replication varies between SINV, CHIKV and SFV. Autophagy functions against SINV infection *in vivo* and *in vitro* (Liang *et al.*, 1998). In contrast, autophagy enhances CHIKV replication in HEK293 cells (Krejbich-Trotot *et al.*, 2011). Until recently, the potential role of autophagy in SFV infection was unknown. However, during the writing of this thesis, a paper was published which demonstrated that SFV4 infection induces the accumulation of autophagosomes in human osteosarcoma cells (HOS) and MEFs and that this has no affect on SFV replication (Eng *et al.*, 2012). The objectives and data presented in this chapter were generated before the Eng *et al* (2012) paper was published.

3.2.1 Objectives

1. Establish an assay to measure the induction of autophagy in cell culture.
2. Determine if SFV activates autophagy and if this differs between strains of SFV.
3. Determine if the pharmacological induction or inhibition of autophagy affects SFV replication in cells.
4. Determine if SFV proteins colocalise with the autophagy machinery.

3.2 Results

3.2.1 Establishment of the autophagy assay to determine the accumulation of autophagosomes in the cell cytoplasm.

In the autophagy assay a plasmid expressing GFP-LC3 is transfected into cells, which enables visualisation of the accumulation of autophagosomes, as described by Jackson *et al*. (2005). To investigate whether SFV4 infection induces autophagosome accumulation in cell culture, the autophagy assay was carried out in Huh7 cells infected with SFV4. The amount of GFP-LC3 plasmid transfected into Huh7 cells was optimised by transfecting cells with 0.5, 2, 4 or 8 μg of GFP-LC3 plasmid and determining the percentage of the cell culture expressing GFP at 24 h post transfection using fluorescence microscopy (2.10.1). Successfully transfected cells expressed GFP and, hereafter, are referred to as transfected cells. A mock-transfected control was included and no fluorescence was detected in this culture (data not shown). The experiment was repeated three times and a representative graph is shown in Fig. 3.1. Transfection using 0.5 – 4 μg of GFP-LC3 plasmid produced fluorescence in ≤25 % of the cell culture (Fig. 3.1). Approximately 13 % more Huh7 cells were transfected using 8 μg of GFP-LC3 plasmid than with other plasmid amounts. However, the cells over expressed GFP which could affect the autophagy studies. Therefore, 0.5 μg of GFP-LC3 plasmid was chosen for further studies.

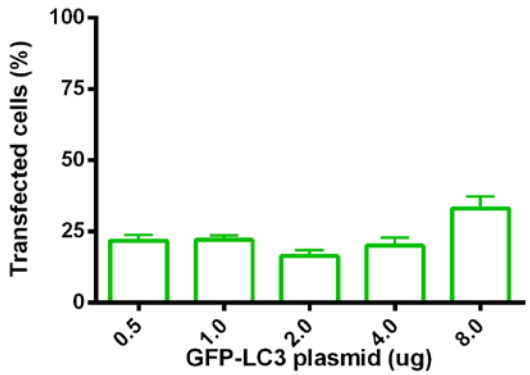

Figure 3.1: Percentage of Huh7 cells expressing GFP following transfection with increasing amounts of GFP-LC3 plasmid.
Huh7 cells were transfected with increasing amounts of GFP-LC3 plasmid. After 24 h, the percentage of cells expressing GFP out of the total cells in a field was calculated. Bars are the mean of 15 microscope fields; error bars are standard deviations of the mean.

To clarify that the GFP-LC3 plasmid could be used to measure autophagosome accumulation, Huh7 cells were transfected with the GFP-LC3 plasmid for 24 h and treated with rapamycin for 3 h. Then the percentage of transfected cells in the culture with ≥2 puncta, as a measure of autophagy, was determined (2.10.1). Rapamycin induces autophagy by inhibiting mTOR. Under normal conditions, mTOR negatively regulates autophagosome formation. Untreated transfected cells were included as a control. To optimise the concentration of rapamycin, Huh7 cells were treated with 2 μM or 4 μM of rapamcyin. Only cells expressing GFP were included in the calculations. Cells treated with rapamycin were markedly different from cells in the untreated control (Fig. 3.2.i). Rapamycin treatment induced the redistribution of GFP-LC3 and, therefore, autophagy in Huh7 cells (Fig. 3.2). Significantly more Huh7 cells were determined to be undergoing autophagy in rapamycin treated cultures compared to the untreated control ($p < 0.05$ using the Mann-Whitney test) (Fig. 3.2.ii). Similar levels of autophagy were observed following treatment with either 2 μM or 4 μM of rapamycin and, therefore, 2 μM of rapamycin was used in further autophagy studies (Fig. 3.2.ii).

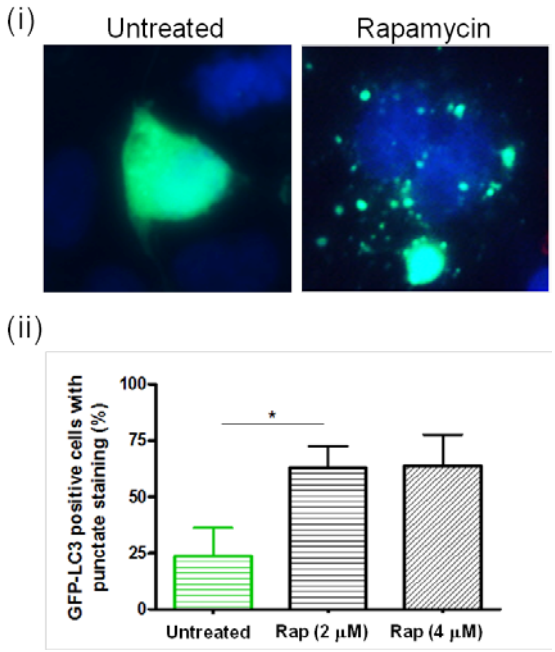

Figure 3.2: Autophagy in Huh7 cells transfected with the GFP-LC3 plasmid and treated with rapamycin.
(i) Huh7 cells were transfected with GFP-LC3 plasmid for 24 h and untreated or treated with 2 μM of rapamcyin for 3 h. Transfected cells with ≥2 GFP puncta were considered to have puncate staining. (ii) Huh7 cells were transfected with GFP-LC3 plasmid for 24 h, mock-treated (green) or treated with 2 μM or 4 μM of rapamycin for 3 h (black) and the percentage of transfected cells undergoing autophagy was calculated out of the total cells in a field. Transfected cells with ≥2 GFP puncta were considered to have punctate staining. Bars are the mean of 15 microscope fields; error bars are standard deviations of the mean. * significant ($p < 0.05$ by the Mann-Whitney test).

Counting the number of puncta per cell as a measure of autophagy has been previously described in alphavirus studies (Krejbich-Trotot *et al.*, 2011; Eng et al., 2012) and was tested in this study. However, the three-dimensional nature of the cell made accurate counting of puncta difficult and the technique was deemed unreliable.

It was therefore decided to establish additional techniques to complement the LC3 assay. A Western blot to detect the two forms of LC3 could not be established. Different methods of protein extraction, increasing antibody incubation times and different developing methods were explored. Several studies use Western blot to determine autophagy induction; possibly user inexperience explains the unsuccessful establishment of the Western blot. An attempt was also made to immunostain Huh7 cells for LC3 or Lamp1. Different methods to permeabilise cell

membranes were explored, various commercial providers of antibodies were tried, different antibody concentrations and incubation times were used, but cultures treated with rapamycin could not be differentiated from the untreated control (results not shown). When these autophagy studies were started, 3 years ago, the reagents available, including antibodies, were limited and probably not fully optimised. Today the autophagy field has expanded and multiple commercial antibodies and reagents are available. Returning to this work and establishing these techniques would enhance future studies.

3.2.2 Does Semliki Forest virus infection induce autophagosome accumulation in Huh7 cells?

The autophagy assay was used to investigate whether SFV infection induces autophagosome accumulation in Huh7 cells (2.10.1). Transfected cells were either mock-infected or infected with SFV4 at MOI 5 for 24 h or treated with rapamycin for 3 h and then the percentage of cells with ≥2 puncta was calculated (2.10.2). In Huh7 cells, SFV4 infection and rapamycin treatment both caused the accumulation of autophagosomes in approximately 50 % more of the monolayer than the mock-infected culture (Fig. 3.3.ii). SFV4 induced autophagosome formation in more cells than rapamycin treatment. In conclusion, by 24 h post-infection SFV4 caused the accumulation of autophagosomes in Huh7 cells.

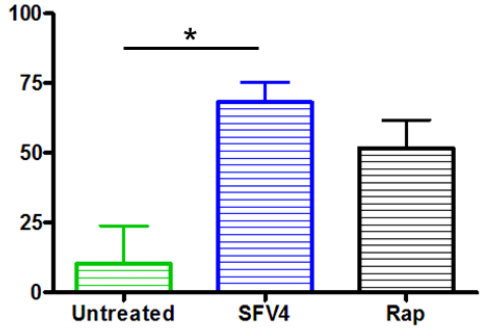

Figure 3.3: Huh7 cells transfected with the GFP-LC3 plasmid and treated with rapamycin.
Huh7 cells were transfected with GFP-LC3 plasmid for 24 h and then mock-treated and mock-infected (green), infected with SFV4 at MOI 5 for 24 h (blue) or treated with 2 μM of rapamycin for 3 h (black). Transfected cells with ≥2 GFP puncta were considered to be undergoing autophagy. The percentage of transfected cells undergoing autophagy was calculated out of the total cells in a field. Bars are the mean of 15 microscope fields; error bars are standard deviations of the mean. * significant ($p < 0.05$ by the Mann-Whitney test).

To use GFP-LC3 expression to measure SFV induction of autophagy, all cells expressing GFP-LC3 must also contain virus. At a high MOI of 5, all cells in the culture should be infected with virus. An experiment was carried out to ensure that Huh7 cells positive for autophagy were also infected with SFV4. The autophagy assay was carried out on Huh7 cells infected with SFV4 at MOI 5 for 24 h and then mock-immunostained or immunostained for nsP3 or structural proteins. After immunostaining, only Huh7 containing ≥2 puncta and also stained positive for SFV nsP3 or the structural proteins were analysed for autophagy. An example of these cells is shown in Fig. 3.4.i. No red fluorescence was detected in the mock-immunostained control (Fig. 3.4.i). Mock-infected cells were included as a control and only GFP was detected (data not shown). The experiment was repeated three times and representative graph is shown in Fig. 3.4.ii. A similar percentage of cells undergoing autophagy was observed in mock-immunostained Huh7 cells and the Huh7 cells positive for nsP3 or the SFV structural proteins. Therefore, Huh7 cells undergoing autophagy were also infected with SFV4. In further autophagy studies, Huh7 cells positive for autophagy in infected cultures were assumed to be infected with virus and immunostaining was not carried out.

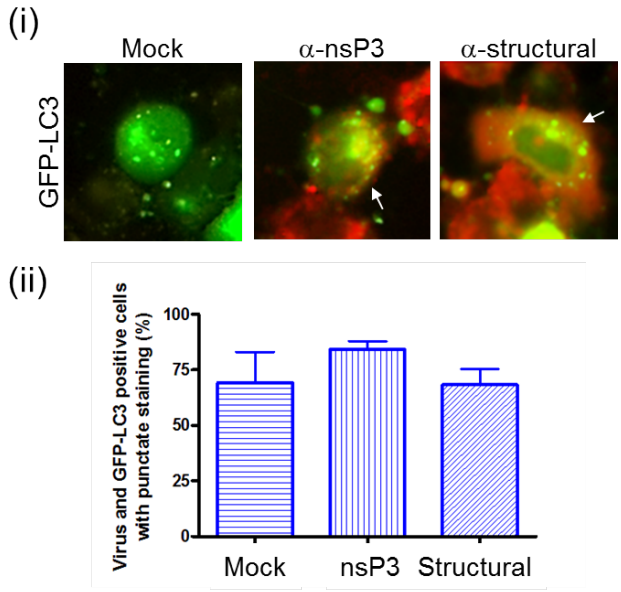

Figure 3.4: Autophagy in Huh7 cells transfected with the GFP-LC3 plasmid and immunostained for nsP3 or structural proteins.
The autophagy assay was carried out on Huh7 cells transfected with GFP-LC3 plasmid for 24 h, infected with SFV4 at MOI 5 for 24 h and then mock immunostained (mock) or immunostained for nsP3 or structural proteins (structural). (i) Merged images. GFP-LC3 is green. NsP3 or structural proteins are red. Arrows indicate cells expressing GFP-LC3 and infected with SFV4. (ii) Cells with ≥2 GFP puncta were considered to have punctate staining. The percentage of transfected cells undergoing autophagy was calculated out of the total cells in a field. Bars are the mean of 15 microscope fields; error bars are standard deviations of the mean.

Accumulation of autophagosomes during SFV4 infection could be due to (i) SFV4 infection inducing autophagy, (ii) SFV4 infection inhibiting autophagy downstream of the autophagosomes, preventing autolysosome formation and autophagy flux resulting in the accumulation of autophagosomes or (iii) SFV4 infection inducing autophagy and also inhibing autophagosome degradation. To investigate the temporal accumulation of autophagosomes in SFV4 infected cultures, the autophagy assay was carried out on transfected Huh7 cells infected with SFV4 at MOI 5 and analysed for induction of autophagy at 3, 6 and 24 h post-infection (2.10.1). Mock-infected Huh7 cells and Huh7 cells treated with rapamycin were included as a controls. The experiment was repeated twice and a representative graph is shown in Fig. 3.5. SFV4 infection induced the accumulation of autophagosomes in significantly more cells than the negative control by 3 h post-infection ($p < 0.05$ by the Mann Whitney test).

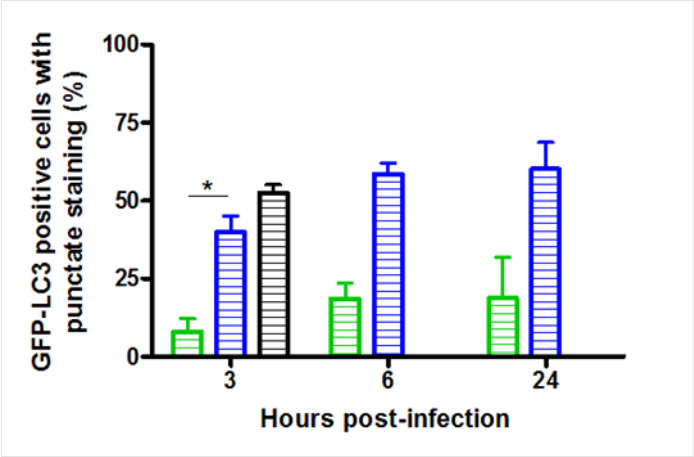

Figure 3.5: Time course of the induction of autophagy in Huh7 cells transfected with GFP-LC3 plasmid and then infected with SFV4.
Huh7 cells were transfected with GFP-LC3 plasmid and then mock-infected (green), or infected with SFV4 at MOI 5 (blue) and analysed for autophagy at 3, 6 and 24 h post-infection. Huh7 cells were treated with 2 μM of rapamycin for 3 h (black). Transfected cells with ≥2 GFP puncta were considered to contain punctate staining. The percentage of transfected cells with punctate staining was calculated out of the total cells in a field. Bars are the mean of 15 microscope fields; error bars are standard deviations of the mean. * significant ($p < 0.05$ by the Mann-Whitney test).

To further investigate this rapid accumulation of autophagosomes, the autophagy assay was carried out on transfected Huh7 cells infected with SFV4 at MOI 5 and at analysed for the induction of autophagy at hourly intervals. Mock-infected Huh7 cells and Huh7 cells treated with rapamycin were included as controls. The experiment was repeated twice and a representative graph is shown in Fig. 3.6. At 1 h post-infection, SFV4 infected cultures had significantly more cells with ≥2 puncta than the mock-infected control ($p < 0.05$ by the Mann-Whitney test). This difference between infected and mock-infected cells was more defined by 3 h post-infection. The percentage of SFV4 infected cells with ≥2 puncta increased over time until 5 - 6 h post-infection when the levels began to plateau. The rapid accumulation of autophagosomes in infected cultures suggests that SFV4 is inducing autophagy, since it is unlikely that SFV4 structural proteins could inhibit autophagosome degradation by 1 hour post-infection. Eng *et al* (2012) demonstrated that SFV4 inhibits autophagosome degradation. SFV4 could both induce autophagy and inhibit autophagosome degradation.

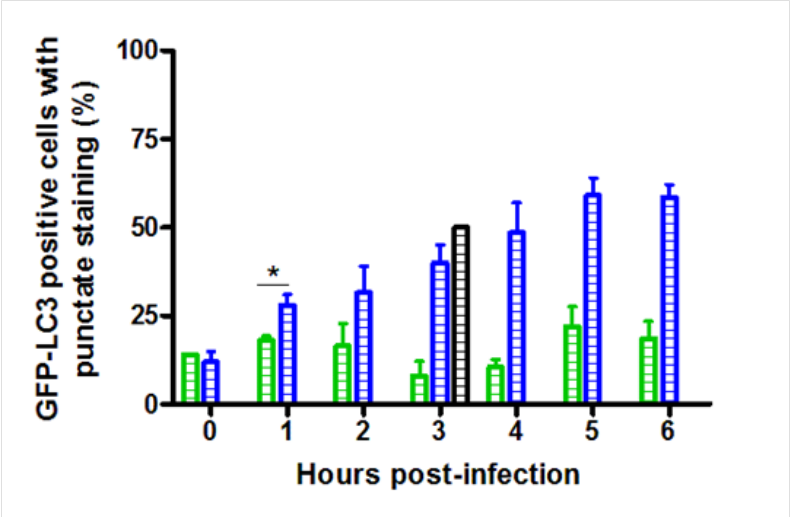

Figure 3.6: Time course of autophagosome accumulation in Huh7 cells transfected with GFP-LC3 plasmid and then infected with SFV4.
Huh7 cells were transfected with GFP-LC3 plasmid and then mock-treated (green) or infected with SFV4 at MOI 5 (blue) and analysed for autophagy at hourly intervals. Huh7 cells were treated with 2 μM of rapamycin for 3 h (black). Transfected cells with ≥2 GFP puncta were considered to contain punctate staining. The percentage of transfected cells with punctate staining was calculated out of the total cells in a field. Bars are the mean of 15 microscope fields; error bars are standard deviations of the mean. * significant ($p < 0.05$ by the Mann-Whitney test).

To investigate whether other strains of SFV cause autophagosome accumulation, the autophagy assay was carried out on transfected Huh7 cells infected with SFV4, SFV L10 or SFV A7(74) at MOI 5 for 24 h and analysed for ≥2 puncta per cell (2.2.8, 2.10.1). Mock-infected cells and rapamycin treated cells were included as controls. The experiment was repeated three times and a representative graph is shown in Fig. 3.7. All three strains of SFV caused the accumulation of autophagosomes in significantly more cells by 24 h post-infection than the mock-infected control. All three strains of SFV induced ≥2 puncta in a similar percentage of the monolayer by 24 h post-infection. The three strains of SFV induced autophagosome accumulation in more cells than the rapamycin control.

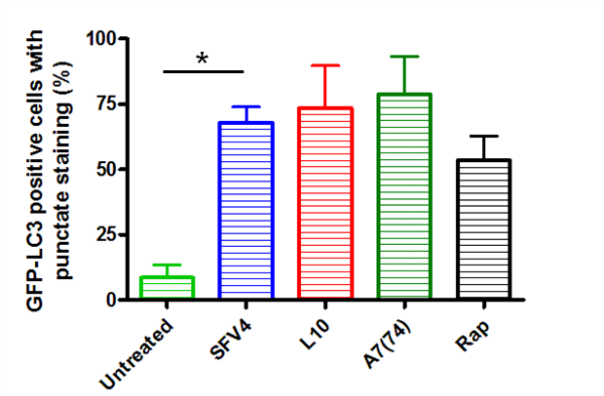

Figure 3.7: Comparison of the induction of autophagy in Huh7 cells transfected with GFP-LC3 plasmid and then infected with SFV4, SFV L10 or SFV A7(74).

Huh7 cells were transfected with GFP-LC3 plasmid and then mock-infected (green; untreated) or infected with SFV4 (blue), SFV L10 (red; L10) or SFV A7(74) (dark green; A7(74)) at MOI 5 for 24 h and analysed. Huh7 cells were treated with 2 μM of rapamycin for 3 h (black; Rap). Transfected cells with ≥2 GFP puncta were considered to be undergoing autophagy. The percentage of transfected cells undergoing autophagy was calculated out of the total cells in a field. Bars are the mean of 15 microscope fields; error bars are standard deviations of the mean. * significant ($p < 0.05$ by the Mann-Whitney test).

3.2.3 Does the pharmacological induction or inhibition of autophagy affect Semliki Forest virus replication?

SFV4 induced autophagy in Huh7 cells by 1 h post-infection (Fig. 3.6). As discussed in the introduction, autophagy can enhance, suppress or have no effect on virus replication. Studies were carried out to investigate the affect of autophagy on SFV replication. As a first study it was decided to investigate the effect of rapamycin treatment on subsequent SFV4 infection. Rapamycin targets mTOR resulting in the induction of autophagy, although that is not rapamycin's only affect on the cell. Huh7 cells were treated with 2 μM of rapamycin for 3 h, infected with SFV4(3H)RLuc at MOI 0.1, 1 and 5 and *RLuc* levels were measured at 2, 3, 4, 5 and 6 h post-infection (2.8.2). Mock-infected cells were included as a control at each time point and the *RLuc* values were subtracted from the infected cell values. Mock-treated infected cells were included as a control at each time point. The experiment was repeated three times and representative graphs are shown in Fig. 3.8. At both MOI 1 and MOI 5, similar *RLuc* levels were detected in infected Huh7 cells with or without rapamycin treatment (Fig. 3.8.ii and iii). However, at a low MOI (0.01) *RLuc* levels were significantly lower following rapamycin treatment at both 5 and 6 h post-

infection. These differences are clearer on a linear scale (Fig. 3.8.i). Since spread in the culture is not an issue at high MOI, this affect at low MOI could indicate that rapamycin pre-treatment is delaying virus release or reducing numbers of infectious virus released. At 5 – 6 h post-infection the second round of virus infection is expected. Overall, the data shows that rapamycin pre-treatment had no detectable affect on virus replication at high (1 or 5) MOI, but delayed virus replication at 5 – 6 h post-infection at low (0.01) MOI.

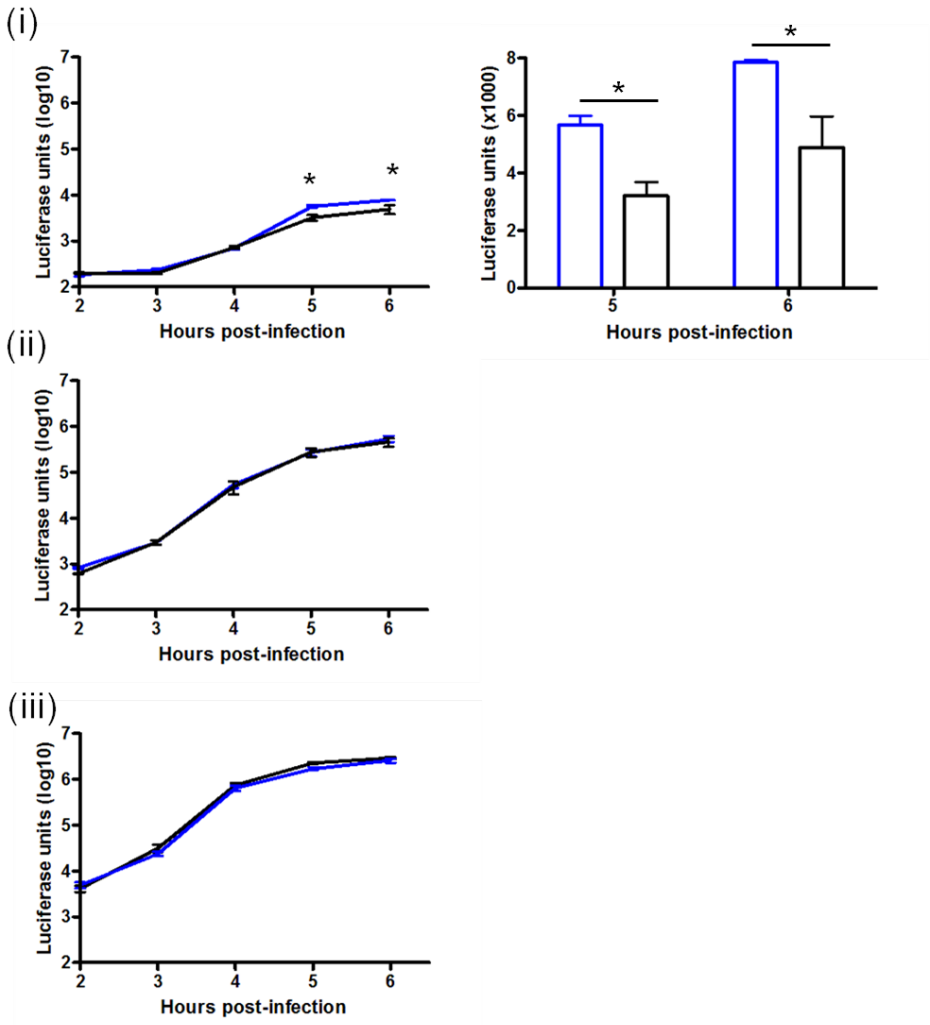

Figure 3.8: The effect of rapamycin pre-treatment on SFV4(3H)RLuc replication in Huh7 cells.

(i) Huh7 cells were treated with 2 μM of rapamycin (black) or mock-treated (blue), infected with SFV4(3H)RLuc at MOI 0.01 and *RLuc* levels were measured at hourly intervals from 2 to 6 h post-infection (right). *RLuc* levels at 5 and 6 h post-infection were plotted on a linear scale (left). Each point or bar represents the mean of three wells; error bars are standard deviations of the mean. The experiment was repeated using MOI 1 (ii) and MOI 5 (iii). * significant ($p < 0.05$ by the Mann-Whitney test).

3MA is a pharmacological inhibitor of the autophagy pathway and its affect on SFV4 replication was investigated using SFV4(3H)RLuc virus. Firstly, to establish whether 3MA treatment inhibits autophagy in Huh7 cells, the autophagy assay was carried out on transfected Huh7 cells, which were mock-treated, treated with 10 mM 3MA and then 2 μM rapamycin or treated with 2 μM rapamycin. The experiment was repeated three times and a representative graph is shown in Fig. 3.9. Rapamycin induced significantly more autophagy in Huh7 cells compared to the mock-treated control ($p < 0.05$ by the Mann Whitney test). However, only background levels of autophagy were detected in Huh7 cells treated with 3MA and then with rapamycin. These results show that 10 mM 3MA inhibited autophagy in Huh7 cells and this concentration of 3MA was used to investigate its effect on SFV4 replication. Several studies have demonstrated that 3MA inhibits autophagy induced by various viruses, including the alphavirus CHIKV (Krejbich-Trotot *et al.*, 2011). It is likely that 3MA inhibits autophagy induced by SFV infection, as with CHIKV. However, this study would have been enhanced by including Huh7 cells treated with 3MA for 3 h and then infected with SFV4 to ensure that the 3MA also inhibits autophagy induced by SFV4.

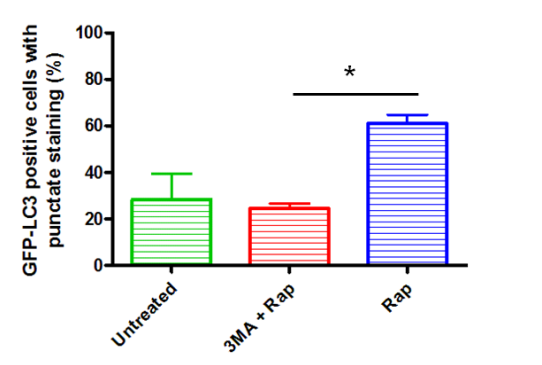

Figure 3.9: 3MA treatment inhibits autophagy in Huh7 cells.
Huh7 cells transfected with GFP-LC3 plasmid were mock-treated (green; untreated), treated with 10 mM of 3MA for 3 h and then challenged with 2 μM of rapamycin for 3 h (red; 3MA + Rap) or treated with 2 μM of rapamycin for 3 h (blue; Rap) and analysed for autophagy. Transfected cells with ≥2 GFP puncta were considered to be undergoing autophagy. The percentage of transfected cells undergoing autophagy was calculated out of the total cells in a field. Bars are the mean of 15 microscope fields; error bars are standard deviations of the mean. * significant ($p < 0.05$ by the Mann-Whitney test).

Huh7 cells were treated with 10 mM 3MA for 3 h, infected with SFV4(3H)RLuc at MOI 0.1 or 5 and *RLuc* levels measured at 2, 3, 4, 5 and 6 h post-infection (2.8.2). Mock-infected cells and mock-treated cells infected with SFV4(3H)RLuc were included as controls at each time point. MOI 1 was not included in these experiments because similar results were observed after infection with MOI 1 and MOI 5 in Fig. 3.8. At MOI 5, similar *RLuc* levels were detected in infected Huh7 cells both with and without 3MA treatment at all time points (Fig. 3.10.ii). At MOI 0.01, *RLuc* levels were significantly higher following 3MA treatment at 4, 5 and 6 h post-infection ($p < 0.05$ using the Mann Whitney test). The 5 and 6 h results are clearer on a linear scale (Fig. 3.10.i). Thus 3MA inhibition of autophagy had no detectable effect on SFV4(3H)RLuc replication at MOI 5. In contrast, at a low MOI (0.01), 3MA treatment produced a significant increase in SFV4(3H)RLuc replication. This result is consistent with the inhibition of replication following rapamycin pre-treatment (Fig. 3.8). Together, these results suggest that autophagy functions against SFV production and spread.

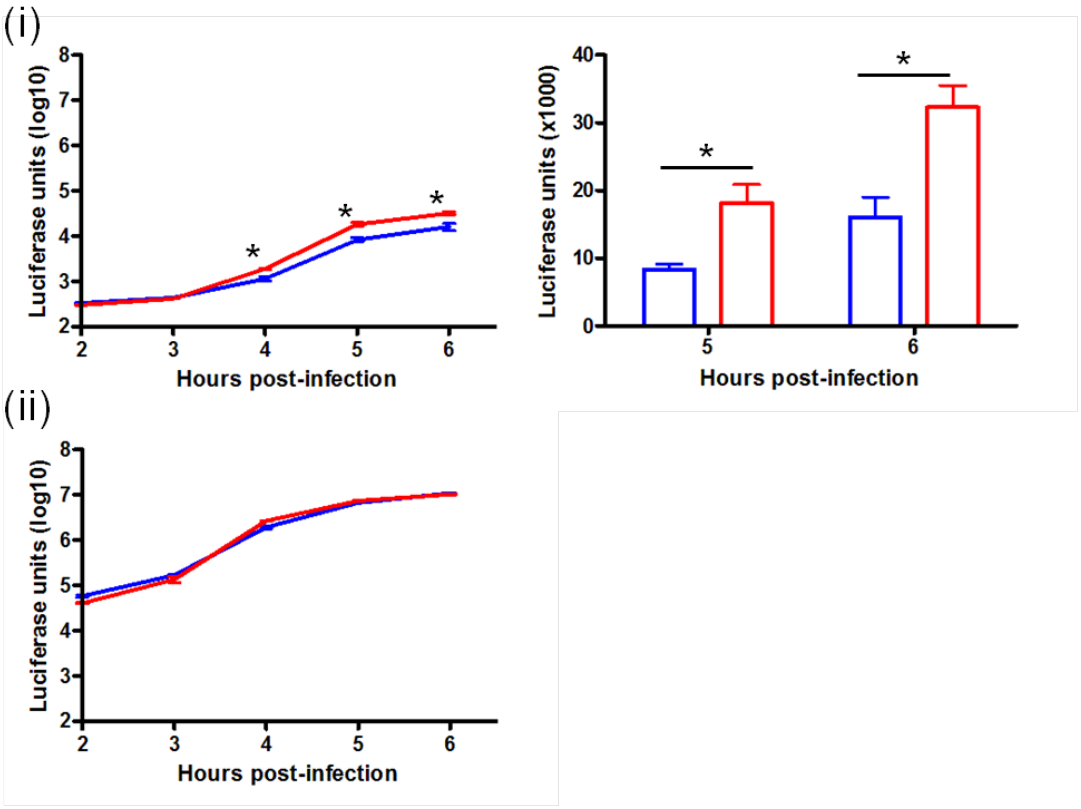

Figure 3.10: The affect of 3MA pre-treatment on SFV4(3H)RLuc replication in Huh7 cells.
(i) Huh7 cells were treated with 10 mM of 3MA (red) or mock-treated (blue), infected with SFV4(3H)RLuc at MOI 0.01 and *RLuc* levels were measured at hourly intervals between 2 to 6 h post-infection (right). *RLuc* levels at 5 and 6 h post-infection were plotted on a linear scale (left). Each point or bar represents the mean of three wells; error bars are standard deviations of the mean. (ii) The experiment was repeated using MOI 5. * significant ($p < 0.05$ by the Mann-Whitney test).

3.2.4 Does GFP-LC3 colocalise with SFV capsid, SFV nsP3 or dsRNA?

Transfected Huh7 cells were infected with SFV4 at MOI 5 and immunostained for capsid, nsP3 or dsRNA at 6 and 24 h post-infection (2.3.1). dsRNA is a replication intermediate produced by viruses during infection. Cells were analysed for colocalisation events using the Zeiss-LSMpascal microscope. Uninfected Huh7 cells were included as a negative control and only GFP was detected (data not shown). At 6 h post-infection, GFP-LC3 colocalised with nsP3, capsid or dsRNA in ≤3 % of 100 cells (Fig. 3.11.i). At 24 h post-infection, the number of colocalisation events between GFP-LC3 and nsP3, capsid or dsRNA increased, but were still extremely rare at ≤5 % of 100 cells (Fig. 3.11.ii and Fig. 3.12). Significantly more nsP3 and

dsRNA colocalised with GFP-LC3 than with capsid (Fig. 3.11.ii). Even in cells where GFP colocalisation had been detected, the majority of the GFP puncta did not colocalise with nsP3, capsid or dsRNA. The results presented here strongly suggest that LC3 and, presumably, the autophagosomes rarely interact with nsP3, capsid or dsRNA.

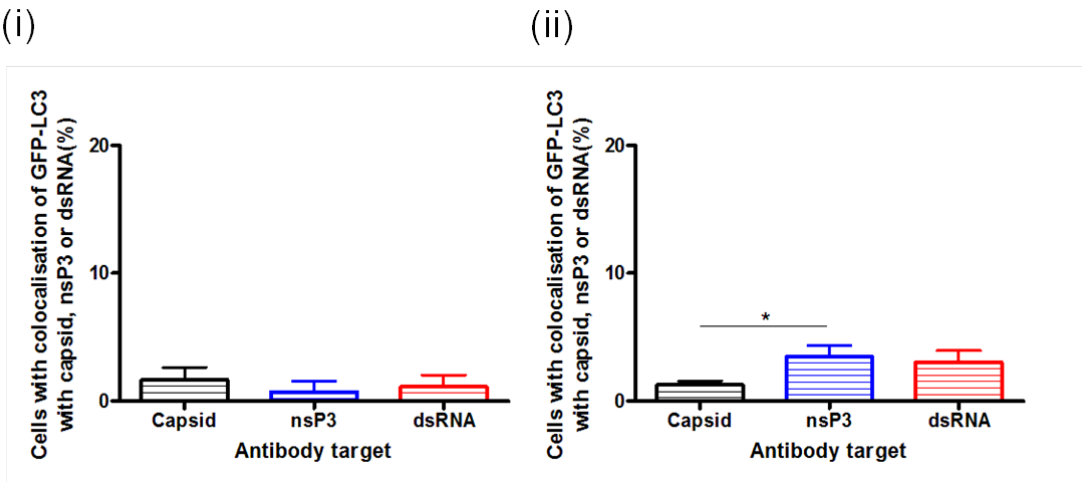

Figure 3.11: GFP-LC3 rarely co-localises with capsid, nsP3 or dsRNA in Huh7 cells infected with SFV4.

Huh7 were transfected with GFP-LC3 plasmid, infected with SFV4 at MOI 5 for (i) 6 h or (ii) 24 h and immunostained for capsid, nsP3 or dsRNA and 100 cells were analysed for colocalisation events. Each bar represents the mean of three experiments; error bars are standard deviations of the mean. * significant ($p < 0.05$ by the Mann-Whitney test).

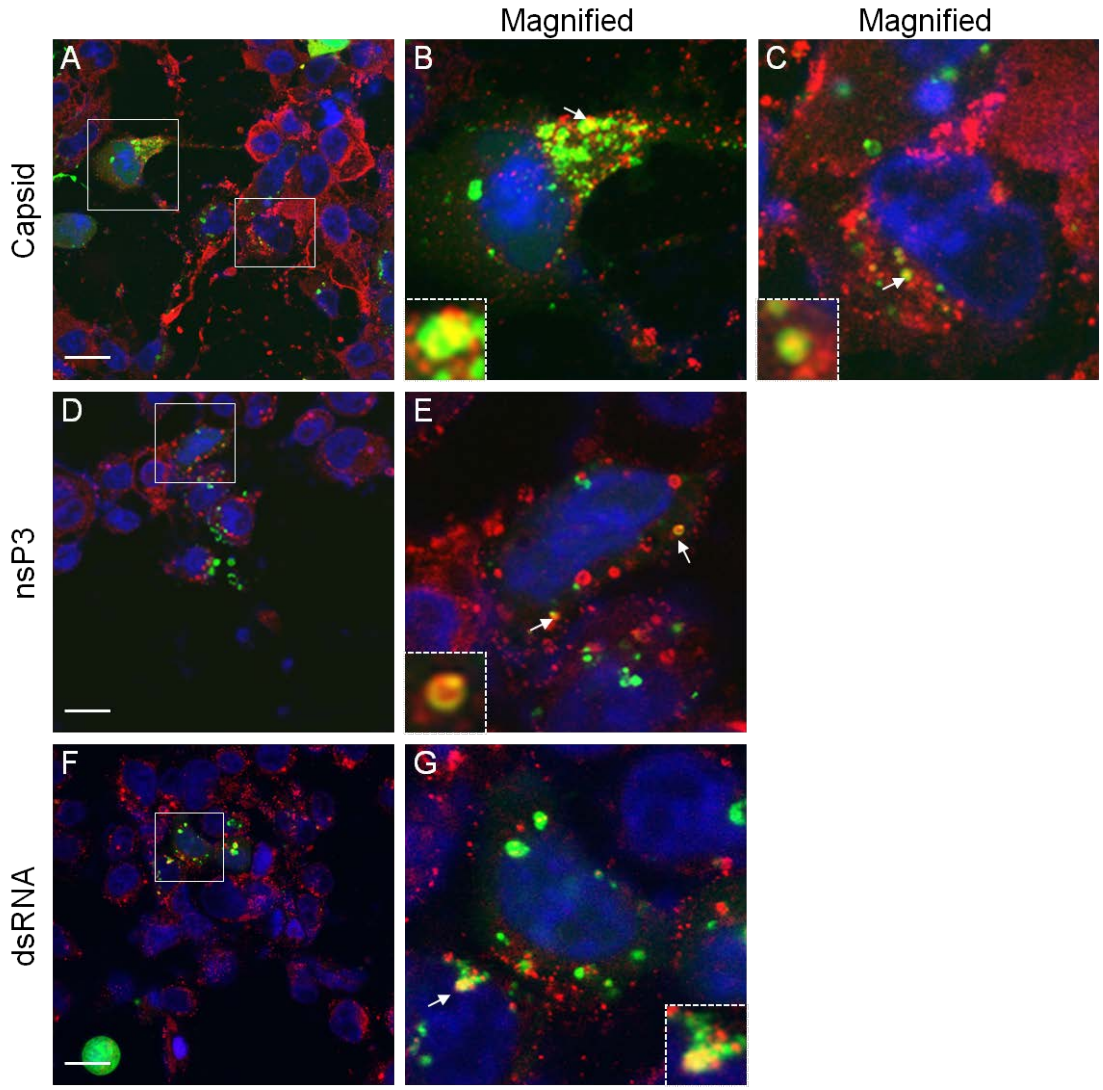

Figure 3.12: Confocal microscopy to determine if GFP-LC3 co-localises with nsP3, capsid or dsRNA in Huh7 cells at 24 h post-infection.
Huh7 cells were transfected with GFP-LC3 plasmid, infected with SFV4 (MOI 5) for 24 h and immunostained for capsid (A, B and C), nsP3 (D and E) or dsRNA (F and G). Each image is one section. Scale bars represent 2 μm. The area within the white boxes was magnified. Arrows indicate possible colocalisation events; white hatched boxes enclose a magnified colocalisation event.

3.2.5 Summary of findings

- SFV4, SFV L10 and SFV A7(74) infection all induced autophagosome accumulation in Huh7 cells by 1 h post-infection.
- At high MOI, pharmacological induction or inhibition of autophagy did not affect SFV4(3H)RLuc replication.
- At low MOI, pharmacological induction of autophagy reduced SFV4(3H)RLuc replication, while pharmacological inhibition increased SFV4(3H)RLuc replication in Huh7 cells.
- GFP-LC3 rarely colocalised with capsid, nsP3 or dsRNA in Huh7 cells at 6 h and 24 h post-infection.

3.3 Discussion

In the results presented in this chapter, SFV4, SFV L10 and SFV A7(74) infection induced the accumulation of autophagosomes in Huh7 cells as early as 1 hour post-infection (Figs 3.6 and 3.7). Accumulation of autophagomes in the cytoplasm of infected cells could be due to (i) SFV infection inducing the formation of autophagosomes, (ii) SFV infection inhibiting the formation and degradation of autolysosomes, which would cause the accumulation of autophagosomes in the cytoplasm or (iii) both induction and inhibition of autophagy. In a paper published during the writing of this thesis, Eng *et al* (2012) reported that SFV4 infection results in the accumulation of autophagosomes at 4 – 8 h post-infection and demonstrated that SFV4 infection inhibits autophagosome degradation in HOS and MEFs. Based on the relatively late detection of autophagosomes, the authors conclude that SFV4 infection inhibits as opposed to induces autophagy. In their study, the authors used a combination of techniques to demonstrate autophagy, including (i) determining the number of cells with GFP-LC3 puncta as a measure of autophagosomes, as in this study, (ii) FACS to measure GFP-LC3 accumulation in cells and (iii) Western blot for LC3-II. In Eng *et al* (2012) GFP-LC3 puncta, autophagosome accumulation was detected by 4 h post-infection; earlier time-points were not analysed. In contrast, by FACS analysis and in the Western blot, autophagy appeared to occur between 4 and 8 h post-infection. Possibly, counting GFP-LC3 is more sensitive than FACS and Western blot and, therefore, autophagosome accumulation could be occurring earlier than 4 h post-infection, as presented in this chapter.

Rapid accumulation of autophagosomes during SFV infection presented in this chapter suggests that SFV activates autophagy. One possible candidate for autophagy induction is dsRNA binding to PRR such as the TLR, NLR and RLR. Studies in bacteria demonstrate that activation of TLR and NLR induces autophagy (Yuan *et al.*, 2009;Travassos *et al.*, 2010). The RLR family can also induce autophagy after binding dsRNA (Tormo *et al.*, 2009). Autophagy can mediate RLR activity through the autophagy conjugate Atg5-Atg12 binding RIG-I, mda-5 and IPS-1 (Jounai *et al.*, 2007). SFV4 enters cells and replicates in the cell cytoplasm on modified endosomes, lysosomes or the plasma membrane. Therefore, the most likely PRRs for inducing autophagy following SFV4 infection are the RLR. The role of

RLRs during SFV infection has not been investigated, but mda-5 was activated during SINV infection of MEFs (Burke *et al.*, 2009). Therefore, it is possible that the RLR, in particular mda-5, rapidly induces autophagy following detection of SFV4 infection. However, Eng *et al* (2012) reported that structural protein production is essential for the induction of autophagy as autophagosome accumulation did not occur in VRP infected cells. This could act through the UPR, which is known to be activated in SFV infection (Barry *et al.*, 2010).

One objective of this chapter was to determine if autophagy had a proviral, antiviral or no affect on SFV replication. Studies have demonstrated autophagy to be an antiviral mechanism against SINV infection both in cell culture and in mice (Liang et al., 1998, Orvedahl et al., 2010). During SINV infection, capsid is reported to colocalise with the autophagosome marker GFP-LC3 in mouse neurones, MEFs and, on occasion, in HeLa cells. Autophagy is essential for the clearance of capsid from mouse neurones and capsid immunoprecipitated with the autophagy protein p62 in HeLa cells (Orvedahl *et al.*, 2010). The authors suggest that p62 selectively targets capsid to the autophagosomes for degradation to clear virus from infected cells (Orvedahl *et al.*, 2010). However, autophagy had no affect on the replication of SINV in MEFs (Orvedahl *et al.*, 2010).

In contrast to SINV, pharmacological inhibition or siRNA inhibition of autophagy decreased CHIKV replication in HEK293 cells (Krejbich-Trotot *et al.*, 2011). Conversely, pharmacological induction of autophagy enhanced CHIKV replication. Taken together, these results suggest that autophagy is proviral in the case of CHIKV infection (Krejbich-Trotot *et al.*, 2011). Autophagy also enhances virus replication in DENV (Lee *et al.*, 2008;Li *et al.*, 2012b), JEV (Li *et al.*, 2012a), PV (Jackson *et al.*, 2005), coxsackievirus B3 virus (Wong *et al.*, 2008), FMDV (O'Donnell *et al.*, 2011), SARS-CoV (Prentice *et al.*, 2004) and HCV (Dreux & Chisari, 2009). Eng *et al* (2012) reported that autophagy had no affect on SFV4 replication in HOS and MEFs and that the autophagy machinery rarely colocalised with either virus replicase or structural proteins. Similarly, in human rhinovirus and coronavirus infections, the absence of gene ATG5 had no affect on virus replication (Brabec-Zaruba *et al.*, 2007;Zhao *et al.*, 2007b).

In the studies presented here, pharmacological induction or inhibition of autophagy did not affect SFV4(3H)RLuc replication at a high MOI (Fig. 3.8 and 3.10). In addition, the autophagosome marker GFP-LC3 rarely colocalised with capsid, nsP3 or dsRNA at either 6 h or 24 h post-infection (Fig. 3.11 and 3.12). However, at low MOI of 0.01, pharmacological induction of autophagy reduced SFV4(3H)RLuc replication in Huh7 cells at 5 and 6 h post-infection, while the pharmacological inhibition of autophagy increased replication at 4, 5 and 6 h post-infection (Fig. 3.8 and 3.10). The data at a high MOI indicate that autophagy is not required for SFV replication or in degrading virus proteins. Since spread in the culture is not an issue at high MOI, the effect at low MOI could indicate that rapamycin pre-treatment is delaying virus release or reducing numbers of infectious virus released, while 3MA enhances this. Indeed, 5 – 6 h post-infection is consistent with the time at which the second round of virus infection is expected. Eng *et al* (2012) only investigated autophagy at MOI 1. Taken together, the studies published by Eng *et al* (2012) confirm the data presented in this chapter.

Possible explanations for the differences between the affect of autophagy on CHIKV, SFV and SINV infection include (i) the viruses interact with the autophagy machinery differently and/or (ii) the affect of autophagy on virus replication varies between cell lines or between species. The observation that autophagy enhances CHIKV replication, while having no affect on SFV4 replication could indicate that CHIKV cannot inhibit autophagosome degradation in contrast to SFV4. It would be interesting to determine if autophagy processes downstream of autophagosome formation occur in CHIKV infected cells.

3.3.1 Final summary

The role of autophagy during SFV infection until recently had not been investigated. Most positive ssRNA viruses studied to date induce autophagy. Autophagy, in general, enhances virus replication, including during CHIKV infection of HEK293 cells. In this chapter, SFV4, SFV L10 and SFV A7(74) induced autophagy in Huh7 cells by 1 hour post-infection. Autophagy had no effect on SFV4 replication at a high MOI of 5. However, at a low MOI of 0.01 the autophagy reduced SFV titres. NsP3, capsid and dsRNA rarely colocalised with the autophagosome marker LC3.

Together, the data suggest that (i) SFV infection causes the accumulation of autophagosomes *in vitro*, (ii) autophagy has no affect on SFV replication at a high MOI and (iii) autophagy reduces SFV titres at a low MOI, presumably by restricting virus spread. Studies recently published by Eng *et al* (2012) largely confirm the data presented here. Investigation into the interaction between SFV and autophagy was not continued in this thesis.

Chapter 4: Interaction of strains of Semliki Forest virus with the interferon response

Contents

4.1 Introduction

There are several strains of SFV which can be divided into two groups based on their virulence in adult mice (Bradish *et al.*, 1971). The most commonly studied strains of SFV include the virulent SFV L10 and the avirulent SFV A7(74) and SFV4. The factors that determine the virulence of the different strains remain unclear. One possibility is differential interaction with the type-I IFN response. Strains of SFV induce the production of IFN both *in vitro* and *in vivo* (Bradish *et al.*, 1975), although direct measurement of IFN induction in cell culture has only been investigated for SFV4 (Breakwell *et al.*, 2007). Several studies have demonstrated that strains of SFV are sensitive to IFN (Finter, 1966). The effect of IFN on SFV infection depends on the virus strain, dose of IFN and the time of administration (Smillie *et al.*, 1973;Bradish & Titmuss, 1981;Deuber & Pavlovic, 2007). More recently, one study reported that strains of SFV vary in their sensitivity to IFN pre-treatment and that this may determine virulence in cell culture (Deuber & Pavlovic, 2007). It is not known if the well-characterised strains of SFV differ in their interaction with IFN and if this determines virulence.

In humans, SFV infection only causes a mild or subclinical disease (Mathiot *et al.*, 1990). In contrast, CHIKV, an alphavirus closely related to SFV, is currently causing debilitating disease in millions of humans worldwide (Enserink, 2007). However, CHIKV is avirulent in mice unless the mice are deficient in the type-I IFN system (Couderc *et al.*, 2008). One explanation for the difference between SFV and CHIKV is that the viruses differ in their sensitivity to human and mouse IFN. It can be hypothesised that CHIKV is more sensitive to mouse IFN than to human IFN and SFV is more sensitive to human IFN than to mouse IFN.

It is clear that the type-I IFN response is essential in controlling SFV infection in mice. It remains to be determined if, (i) strains of SFV interact differently with the type-I IFN system; (ii) sensitivity to type-I IFN is a determinant of virulence; (iii) SFV is more sensitive to human type-I IFN than mouse type-I IFN; (iv) SFV evades and/or inhibits the mouse type-I IFN response better than the human type-I IFN response; (v) SFV and CHIKV differ in their induction and/or sensitivity to human and mouse type-I IFN.

4.1.1 Objectives

1. Determine if virulent (SFV L10) and avirulent (SFV A7(74) and SFV4) strains replicate efficiently in IFN competent human cells and how this compares to replication in IFN competent mouse cells.
2. Determine if IFN affects SFV replication in human and mouse cells.
3. Determine if virulent (SFV L10) and avirulent (SFV A7(74) and SFV4) strains induce different amounts of functional IFN and if this varies between mouse and human cells.
4. Determine if virulent (SFV L10) and avirulent (SFV A7(74) and SFV4) strains differ in their sensitivity to IFN in human and mouse cells.

4.2.1 Comparison of SFV replication in human and mouse cells

To investigate SFV replication in IFN competent human cells, a standard plaque assay was carried out in MRC5, A549 and 2fTGH cells infected with virulent SFV L10 or avirulent SFV A7(74) or SFV4 (2.2.9). All three viruses infected MRC5, A549 and 2fTGH cells, as seen by changes in the monolayer (Fig. 4.1.i). In MRC5 and A549 cells, all three strains formed plaques, which consisted of a mixture of live and dead cells; these were termed “cloudy plaques” (Fig. 4.1.i). These plaques were difficult to detect with the naked eye, but were clearly observed under the microscope (Fig. 4.1.ii). The magnified plaques in Fig. 4.1.ii are representative of plaques produced by SFV L10 and SFV4 infection in MRC5, A549 and 2fTGH cells. Interestingly, in the A549 cells, SFV A7(74) produced larger plaques than either SFV L10 or SFV4. In contrast to the cloudy plaques in MRC5 and A549 cells, in 2fTGH cultures all three viruses produced an unusual response, an agglomeration of cells (Fig. 4.1).

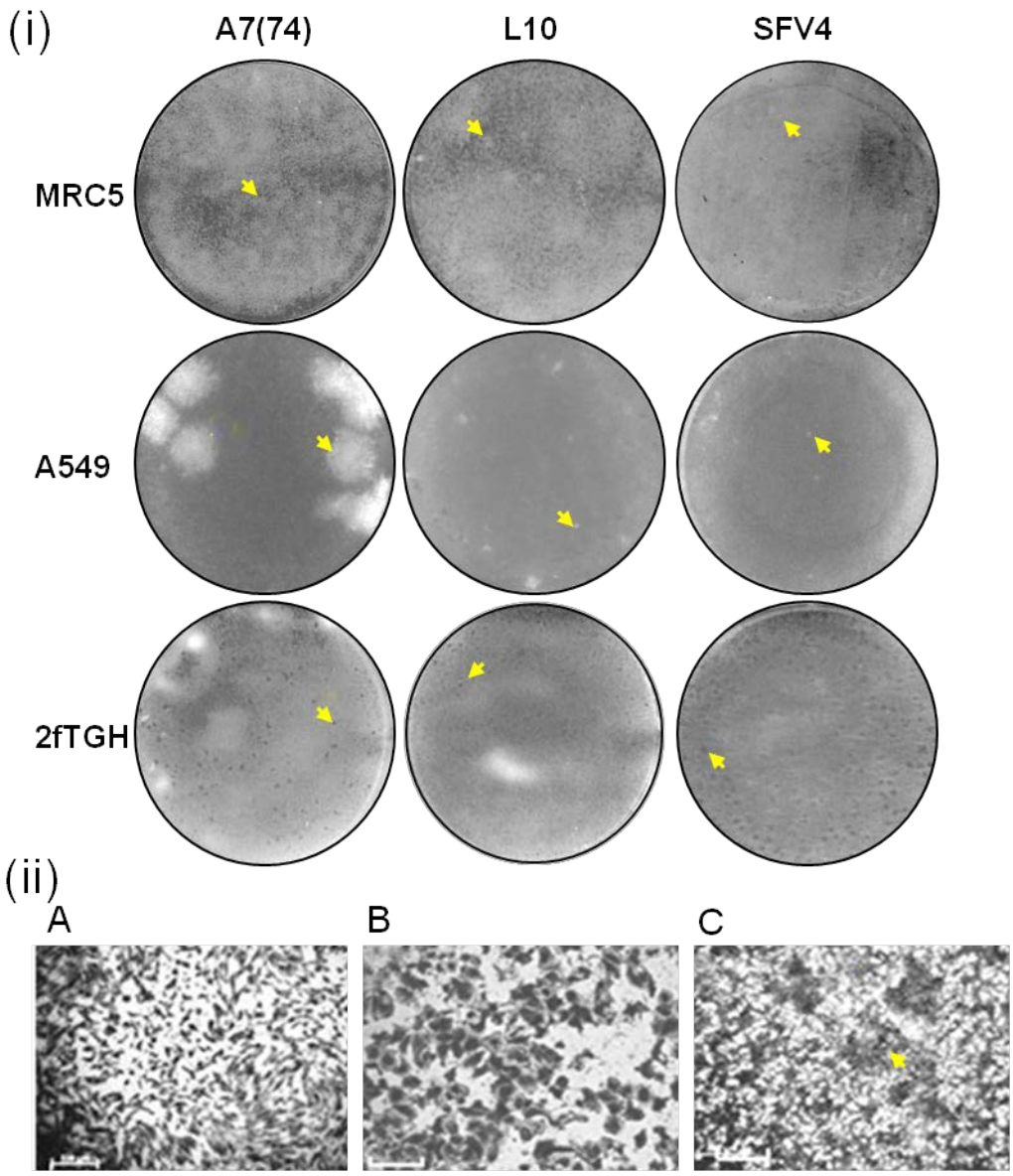

Figure 4.1: Plaque assays of SFV A7(74), L10 and SFV4 in human cell lines.
(i) Plaque assays were carried out in human MRC5, A549 and 2fTGH cell lines infected with SFV A7(74), SFV L10 or SFV4. (ii) Individual plaques from MRC5 (A), A549 (B) or 2fTGH (C) cells infected with SFV A7(74). Bars represent 500 μm. Arrowheads identify one plaque.

To investigate 2fTGH infection in greater detail, a standard plaque assay was carried out on 2fTGH cells infected with one of the three strains, SFV4. To observe the course of infection, cells were immunostained for nsP3 (2.2.9). Mock-infected cells were included as a negative control. No nsP3 was detected in the negative control (Fig. 4.2.C). NsP3 was clearly detected in the distinct cell agglomeration

areas in the infected 2fTGH cell monolayer (Fig. 4.2.A). Under higher magnification, these agglomerations could be seen to be a mixture of infected and uninfected cells (Fig. 4.2.B). Extensive cell death was not detected within these agglomerations (Fig. 4.2.B). In conclusion, SFV4 does infect 2fTGH cells, but does not produce plaques suggesting that virus replication and/or spread is restricted in these cells and that these cells do not readily undergo cell death upon infection. Most studies to date indicate that infection of mammalian cells with various strains of SFV, including SFV L10, A7(74) and SFV4, induce apoptosis (Glasgow *et al.*, 1997;Scallan *et al.*, 1997;Barry *et al.*, 2010).

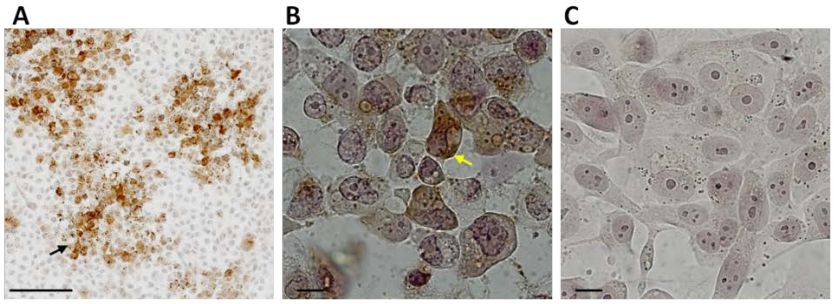

Figure 4.2: SFV4 infection of 2fTGH cells.
Plaque assay in 2fTGH cells infected with SFV4 (A and B) or mock-infected (C). Cells were immunostained for nsP3 (brown cells). The black arrow identifies a group of infected cells. The yellow arrow identifies an infected cell. Bars represent 100 μm (A) or 10 μm (B and C).

To compare SFV replication in human and mouse cells, plaque assays were also carried out in IFN competent mouse L929 cells with the same three strains of SFV (2.2.9). In L929 cells, all three virus strains produced distinct clear plaques (Fig. 4.3), which were markedly different from those seen with human cells (Figs. 4.1 and 4.3). In L929 cells, plaques consisted of dead cells rather than the mixture of live and dead cells as seen with two of the human cell lines MRC5 and A549.

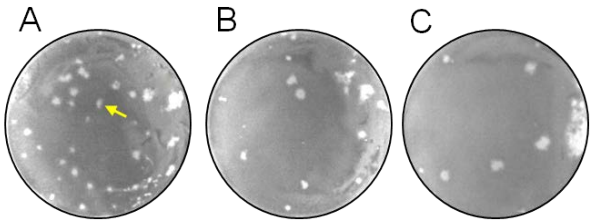

Figure 4.3: SFV A7(74), L10 and SFV4 produce clear plaques in L929 cells.
Plaque assays in L929 cells infected with SFV A7(74) (A), L10 (B) or SFV4 (C). The yellow arrow identifies a single plaque.

To investigate whether the unusual plaques seen with human 2fTGH, MRC5 and A549 cells were due to the IFN response, plaque assays were carried out in human U4C cells. U4C cells, a derivative of 2fTGH, are deficient in JAK1 and cannot respond to IFN (Muller *et al.*, 1993). Infection with all three virus strains produced clear plaques in U4C cells, unlike in 2fTGH, MRC5 or A549 cells (Figs. 4.1 and 4.4). The clear plaques produced by SFV A7(74), L10 and SFV4 on U4C cells were similar to those observed on mouse L929 cells (Figs. 4.3 and 4.4).

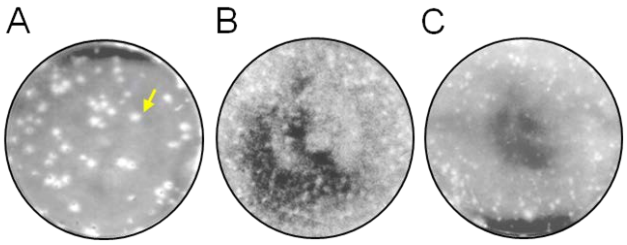

Figure 4.4: SFV A7(74), L10 and SFV4 produce clear plaques in U4C cells.
Plaque assays in U4C cells infected with SFV A7(74) (A), L10 (B) or SFV4 (C). The yellow arrow identifies a single plaque.

The plaques in U4C cells were further analysed by immunostaining for nsP3. Mock-infected cultures were included as a control and no virus was detected (Fig. 4.5.C). Areas of dead cells were clearly identified in the infected U4C monolayer (Fig. 4.5.A). This was completely different to the infected parental 2fTGH cell monolayer (Fig. 4.2.A). NsP3 positive cells were located at the edge of the plaques, consistent with the spread of virus outwards from the initial site of infection. Under higher magnification, unlike with 2fTGH cells, infected U4C cells were clearly undergoing apoptosis (Fig. 4.5.B).

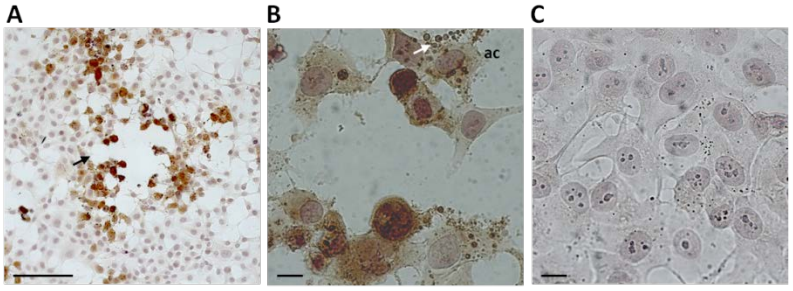

Figure 4.5: SFV4 infection of U4C cells.
Plaque assays on U4C cells infected with SFV4 (A and B) or mock-infected (C). Cells were immunostained for nsP3 (brown cells). The black arrow identifies a plaque. The white arrow identifies apoptotic bodies. ac labels an apoptotic cell. Bars represent 100 μm (A) or 10 μm (B and C).

4.2.2 Does IFN affect SFV replication in human and mouse cells?

An IFN sensitivity assay (2.5) was established to determine if (i) IFN limits SFV4 infection in human cells and (ii) how this compares to the effect of IFN in mouse cells. IFN competent human 2fTGH and mouse L929 cells were treated with 0 (mock-treated control), 1, 10, 100 or 1000 U/ml of IFN-α for 16 h, then infected with SFV4(3H)RLuc at MOI 5 for 24 h and analysed for *RLuc* levels (2.8.2). The IFN-α used was species matched; 2fTGH cells were treated with human IFN-α and L929 cells with mouse IFN-α. The experiment was repeated three times and representative graphs are shown in Fig. 4.6.

In both cell lines, IFN-α pre-treatment reduced *RLuc* levels compared to the mock-treated control (Fig. 4.6). The level of *RLuc* production decreased with increasing concentrations of IFN-α until it plateaued at 100 U/ml of IFN-α. Even at high concentrations of IFN-α, SFV4(3H)RLuc replication was not completely abolished; *RLuc* remained detectable in both human and mouse cultures treated with even 1000 U/ml IFN-α; 100 U/ ml of IFN-α reduced *RLuc* levels by >99 %. These results indicate that SFV is highly, but not completely, sensitive to IFN-α pre-treatment. Based on these results, 10 U/ml of IFN-α was used in all following IFN sensitivity assays.

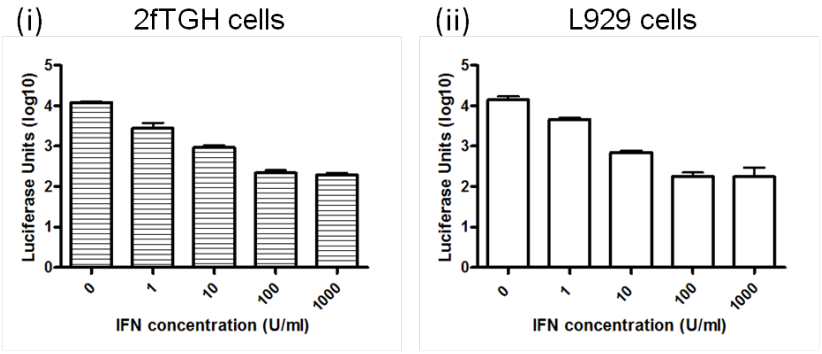

Figure 4.6: Sensitivity of SFV4(3H)RLuc to IFN treatment in 2fTGH and L929 cells.
(i) 2fTGH or (ii) L929 cells were treated with species matched IFN-α for 16 h and then infected with SFV4(3H)RLuc at MOI 5. 24 h post-infection, cultures were assayed for *RLuc* levels. Each bar is the mean of triplicate experiments, error bars are standard deviations of the mean.

In both human and mouse cells, prior treatment of cells with 10 U/ml of IFN-α reduced *RLuc* levels by >90 %, but did not abolish SFV replication (Fig. 4.6). Possible explanations for this residual virus activity include (i) SFV replicates in most IFN treated cells at low levels, (ii) some cells, perhaps related to the cell cycle, are not rendered into the antiviral state by IFN pre-treatment and SFV replicates in these or (iii) in some cells, again perhaps related to cell cycle, SFV is able to disassemble the antiviral state and replicate to high levels. A series of experiments were carried out on 2fTGH and L929 cells to investigate these possibilities.

The mutant virus SFV4(3F)-ZsGreen was used in these experiments, which expresses ZsGreen as a protein fused to nsP3 during replication. This enables the location of nsP3 to be visualised by fluorescence microscopy. First, an experiment was carried out to investigate whether ZsGreen detection during SFV4(3F)-ZsGreen is a sensitive method to detect virus replication. 2fTGH and L929 cells were infected with SFV4(3F)-ZsGreen at MOI 5 for 24 h and then immunostained for dsRNA (2.3.1). Mock-infected negative controls were included. Fluorescence was not detected in the negative control (data not shown). In both 2fTGH and L929 cells, all cells that expressed ZsGreen also stained positive for dsRNA (Fig. 4.7). Similarly, all cells that stained positive for dsRNA expressed ZsGreen. This result indicates that ZsGreen expression is an appropriate tool to detect virus replication.

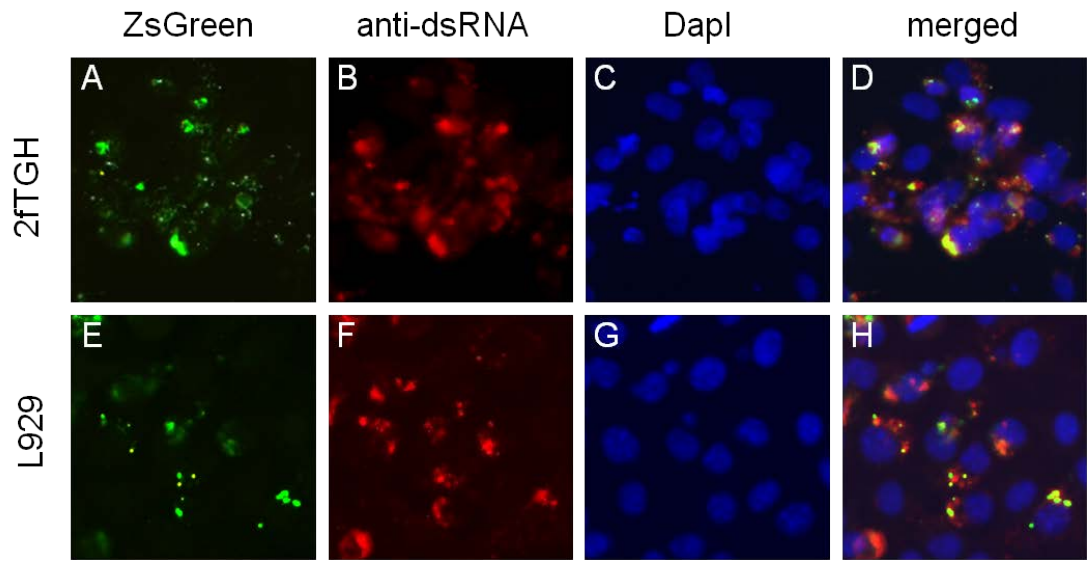

Figure 4.7: All 2fTGH or L929 cells expressing ZsGreen also stained positive for dsRNA
2fTGH and L929 cells were infected with SFV4(3F)-ZsGreen at MOI 5 for 24 h and analysed for ZsGreen fused to virus nsP3 (A), red-stained dsRNA (B), blue-stained nuclei (C) and merged image (D).

Next, the IFN sensitivity assay was carried out on L929 cells infected with SFV4(3F)-ZsGreen or SFV4(3H)RLuc at MOI 30 and analysed by microscopy for ZsGreen expression, cell viability or *RLuc* production at various hours post-infection (Fig. 4.8). In L929 cells, IFN pre-treatment reduced the percentage of the cell monolayer expressing ZsGreen compared to the mock-treated infected control (Figs 4.8.i). At 8 h post-infection, ZsGreen was detected in approximately 5 % of L929 cells pre-treated with IFN. This had not increased by 48 h post-infection (Fig. 4.8.i). In contrast, by 24 h post-infection ZsGreen was detected in approximately 97 % of the L929 cell monolayer in the control (no IFN).

The Wst-1 assay measures mitochondrial dehydrogenase activity. As cells die, mitochondria stop functioning and mitochondrial dehydrogenases lose their activity. Therefore, the Wst-1 assay is a measure of cell viability. A Wst-1 viability assay was carried out on L929 cells pre-treated with IFN and infected with SFV4(3F)-ZsGreen virus at MOI 30 for 0, 8, 12 or 24 h post-infection (2.7). Cultures mock-treated with IFN and infected with SFV4(3F)-ZsGreen and cultures mock-treated with IFN and mock-infected were included controls. Cultures pre-treated with

IFN and infected with SFV4(3F)-ZsGreen increased in viability from 8 h post-infection and had a similar viability to the mock-infected culture (Fig. 4.8.ii).

The IFN sensitivity assay was carried out in L929 cells infected with SFV4(3H)RLuc at MOI 30 and assayed for *RLuc* levels at 2, 4, 6, 8, 10, 12 and 24 h post-infection (2.5). A culture mock-treated and mock-infected was included as a control. In L929 cultures, *RLuc* levels in IFN pre-treated cells were consistently lower at all time points than in the mock-treated cells (Fig. 4.8.iii). *RLuc* was detectable at 2 h post-infection in the mock-treated cells, but was only detectable at 4 h post-infection in IFN pre-treated cells (Fig. 4.8.iii). At 24 h p.i., no *RLuc* was detected in the culture treated with IFN and then infected with SFV4(3H)RLuc, unlike the mock-treated and infected control.

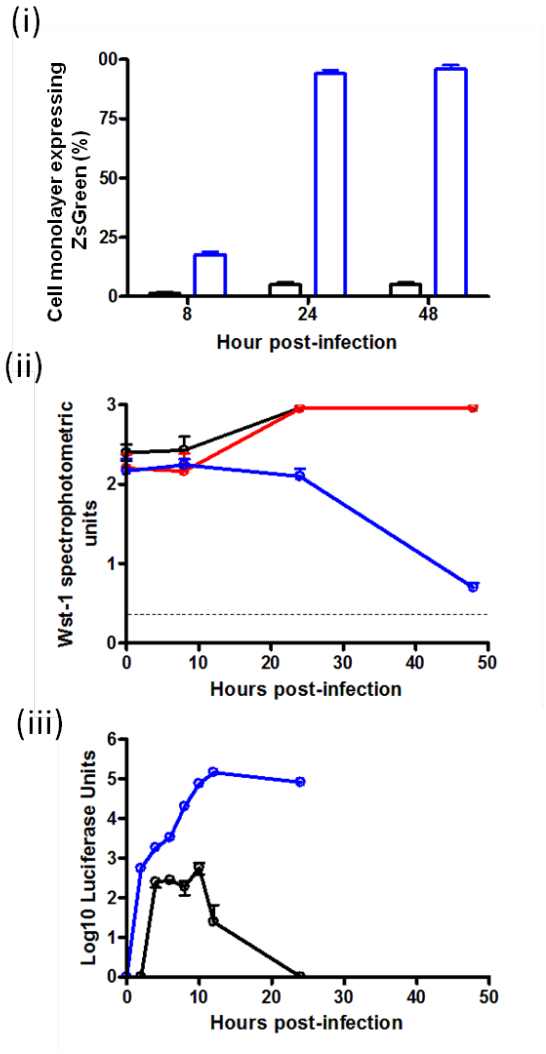

Figure 4.8: Affects of IFN pre-treatment on SFV4(3F)-ZsGreen and SFV4(3H)RLuc replication in L929 cells.

(i) L929 cells were treated with mouse IFN-α (black) or mock-treated (blue) for 16 h and then infected with SFV4(3F)-ZsGreen at MOI 30. At 8, 24 and 48 h post-infection the mean percentage of the cell monolayer expressing ZsGreen in 15 fields was enumerated using fluorescence microscopy. (ii) The experiment was repeated and the Wst-1 cell viability assay was carried out at 0, 8, 24 and 48 h post-infection. Mock-infected cells were included (red). Dotted line represents the background. (iii) L929 cells were treated with mouse IFN-α (black) or mock-treated (blue) for 16 h and then infected with SFV4(3H)RLuc at MOI 30 and assayed for *RLuc* levels at 2 h intervals for 24 h. Luciferase units are given relative to those in a culture mock-treated and mock-infected. Each bar or point are the mean of triplicate experiments, error bars are standard deviations of the mean.

Fig. 4.8.i indicates that SFV only replicated to detectable levels in a small subset of cells; while in Fig. 4.8.iii *RLuc* levels were consistently lower in IFN pre-treated and infected cultures compared to untreated and infected cultures. These

results are consistent with the suggestions described earlier that SFV replicates in IFN pre-treated cells at low levels and at high levels in a few cells either because these cells are somehow different (cell cycle) and are not in an antiviral state or because the virus disassembles the antiviral state.

In Fig. 4.8.iii, there was a delay of 2 h in *RLuc* detection compared to the untreated and mock-infected control. This delay may reflect the time taken for SFV to establish a low level of replication in the small subset of cells not in the antiviral state or, more likely, to successfully dismantle the antiviral state in a few cells. *RLuc* was eliminated from IFN pre-treated cultures by 24 h post-infection, unlike in the untreated and mock-infected control (Fig. 4.8.iii). Most likely this is due to the antiviral state preventing SFV spread and the induction of apoptosis eliminating infected cells. As <5 % of the L929 cell monolayer was detectably infected with SFV in IFN pre-treated cultures, a low level of apoptosis would be masked in these cultures and not visible by Wst-1 assay. Consistent with this explanation, in Fig. 4.8.ii L929 cultures pre-treated with IFN and infected increase in viability, while the mock-treated infected control decreases in viability.

Taken together, the data indicate that (i) SFV4 replication is reduced by pre-treatment of L929 cells with IFN-α; the percentage of cells expressing ZsGreen and the amount of *RLuc* produced were >90 % and >99 % lower respectively than untreated cultures, and (ii) IFN pre-treatment protected L929 cultures from death induced by SFV4(3F)-ZsGreen infection.

The experiments were repeated in human 2fTGH cells. The IFN sensitivity assay was carried on human 2fTGH cultures infected with SFV4(3F)-ZsGreen or SFV4(3H)RLuc again at MOI 30 and analysed for ZsGreen expression, cell viability or *RLuc* production at various hours post-infection (Fig. 4.9). In 2fTGH cells, IFN pre-treatment reduced the percentage of cells expressing ZsGreen compared to the mock-treated control, as observed in the L929 cell cultures (Figs 4.9.i). At 8 h post-infection, ZsGreen was detected in approximately 5 % of the 2fTGH cell monolayer pre-treated with IFN. This had not increased even by 48 h post-infection. In contrast, by 24 h post-infection ZsGreen was detected in approximately 97 % of the 2fTGH cells in the mock-treated control.

A Wst-1 viability assay was carried out on 2fTGH cultures treated with IFN and infected with SFV4(3F)-ZsGreen virus at MOI 30 at 0, 8, 12 and 24 h post-infection (2.7). Cultures mock-treated with IFN and infected with SFV4(3F)-ZsGreen and cells mock-treated with IFN and mock-infected were included as controls. The viability of 2fTGH cultures pre-treated with IFN and then infected with virus was completely different from that of L929 cultures (Figs 4.8.ii and 4.9.ii). In 2fTGH cells, the viability decreased from 8 h post-infection following IFN treatment, which was similar to the untreated infected culture, not the control uninfected culture (Fig. 4.8.ii).

The IFN sensitivity assay was also carried out in 2fTGH cells infected with SFV4(3H)RLuc and *RLuc* levels were measured at 2, 4, 6, 8, 10, 12 and 24 h post-infection (2.5). A culture mock-treated and mock-infected was included as a control. In 2fTGH cells, *RLuc* levels in IFN pre-treated cells were consistently lower at all time points than in the mock-treated and infected cell cultures (Fig. 4.9.iii). *RLuc* was first detected at 2 h post-infection in both treated and mock-treated cells. This is different to the result observed in L929 cells where there was a 2 h delay in first virus detection in IFN pre-treated cells (Figs 4.8.iii and 4.9.iii). Again in contrast to L929 cells, virus replication remained detectable in the IFN pre-treated culture at 24 h post-infection.

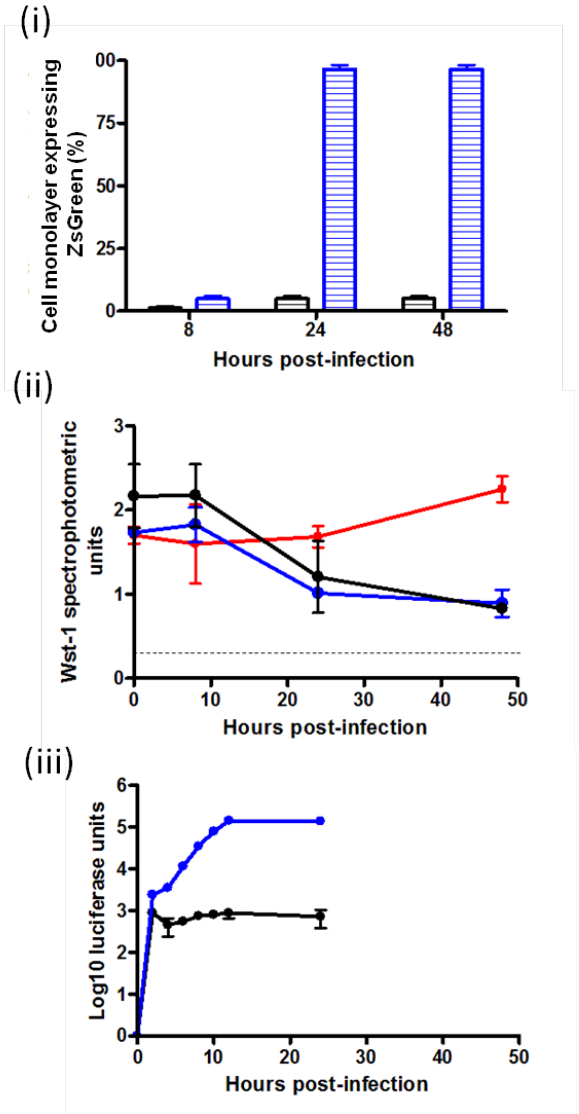

Figure 4.9: Affects of IFN pre-treatment on SFV4(3F)-ZsGreen and SFV4(3H)RLuc replication in 2fTGH cells.

(i) 2fTGH cells were treated with mouse IFN-α (black) or untreated (blue) for 16 h and then infected with SFV4(3F)-ZsGreen at MOI 30. At 8, 24 and 48 h post-infection the mean percentage of the cell monolayer expressing ZsGreen in 15 fields was enumerated using fluorescence microscopy. (ii) The experiment was repeated and the Wst-1 cell viability assay was carried out at 0, 8, 24 and 48 h post-infection. Mock-infected cells were included (red). Dotted line represents the background. (iii) 2fTGH cells were treated with mouse IFN-α (black) or mock-treated (blue) for 16 h and then infected with SFV4(3H)RLuc at MOI 30 and assayed for *RLuc* levels at 2 h intervals for 24 h. Luciferase units are given relative to those in a culture mock-treated and mock-infected. Each bar or point are the mean of triplicate experiments, error bars are standard deviations of the mean.

Taken together, this data indicates that SFV replication is strongly reduced by IFN pre-treatment in both human 2fTGH and mouse L929 cells. However, unlike in

L929 cultures, IFN pre-treatment did not appear to protect the viability of the 2fTGH culture during infection, even though >95 % of the cells in the monolayer were either uninfected or did not have a high enough level of infection for detection. Possible explanations for the loss in 2fTGH culture viability following IFN pre-treatment and SFV infection include, (i) IFN treatment is toxic to 2fTGH cells at this concentration, (ii) the majority of the monolayer was infected with virus, but at low levels which could not be detected by ZsGreen expression and the presence of virus alone or virus and pre-sensitisation by IFN triggered cell death or (iii) the small proportion of 2fTGH cells with a high level of virus replication are secreting a protein (e.g. TNF-α) which induces cell death in neighbouring cells. There is a discrepancy between the viability results and the plaque assay results for 2fTGH cultures (Figs. 4.1 and 4.9).

To investigate if IFN alone is toxic to 2fTGH cells, as has been previously reported (Choi *et al.*, 2003), a Wst-1 assay was carried on 2fTGH cultures treated with IFN for 8, 24 and 48 h. Untreated and mock-infected cultures and untreated cultures infected with SFV4(3F)-ZsGreen at MOI 30 were included as controls. Following IFN treatment, viability of the 2fTGH cultures increased from 8 h post-infection onwards in parallel to the untreated and mock-infected control (Fig. 4.10). In contrast, the viability of the 2fTGH cultures in the virus infected control decreased over 48 h. In conclusion, IFN alone did not reduce the viability of the culture in this experiment.

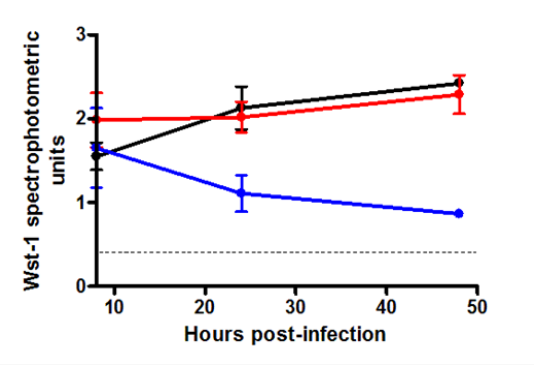

Figure 4.10: IFN does not induce apoptosis in 2fTGH cells.
A Wst-1 assay was carried out on 2fTGH cells treated with 10 U/ml of IFN-α (black), untreated and infected with SFV4(3F)-ZsGreen at MOI 30 (blue) or mock-treated and mock-infected (red) at 8, 24 and 48 h post-infection. Dotted line represents the background. Each point is the mean of triplicate samples, error bars are standard deviations of the mean.

Taken together, these results clearly demonstrate that IFN pre-treatment reduces SFV replication in human 2fTGH and mouse L929 cells. However, the viability of cultures following IFN pre-treatment and SFV infection varies between human 2fTGH and mouse L929 cells.

4.2.3 Establishment of the IFN bioassay

An IFN bioassay was established to measure functional IFN levels. During infection of MEFs SFV4 induces cellular translation shutoff at 2 to 3 h post-infection (Breakwell, 2007). This may affect levels of IFN produced during infection. Functional IFN levels were investigated to measure the IFN response during SFV infection. The bioassay used was based on that previously described by Millers and Anders (2003). In this assay, infectious virus in test samples is neutralised by acid treatment. However, acid treatment is a time consuming process requiring incubation of the supernatant at pH 2 for four days. An alternative method uses UV light to inactivate the virus (Dr. Marian Killip, University of St. Andrews, personal communication). A method to inactivate virus with UV light was established. Efficiency of UV light inactivation depends on the distance of the sample from the UV light source, the surface area, the volume of the sample and the length of exposure. These parameters were examined when the bioassay was established.

IFN bioassay samples were prepared by infecting mouse L929 or human 2fTGH cells with SFV4(3F)-ZsGreen virus at MOI 5 for 24 h (2.4). To optimise the neutralisation of the virus in the sample by UV light, samples were aliquoted in 500 µl volumes into 25 ml universals, eppendorfs, 24-well plates or 6-well plates, exposed to UV light for increasing durations of time, added to BHK-21 cells and compared for virus presence by enumerating green cells by fluorescence microscopy . Mock-infected cultures and infected cultures not exposed to UV light were included as controls. The experiment was repeated three times. A representative result is shown in Fig. 4.11. No virus was detected in the mock-infected control.

Exposure to UV light did not destroy virus infectivity in either 25 ml universals or eppendorfs. Exposure to UV light greatly reduced virus infectivity in 24-well and 6-well plates. Efficacy increased with exposure time. Even after an

exposure time of 120 minutes, on transfer of samples onto a BHK-21 cell monolayer fluorescent virus was detected in the monolayer. This result indicates that at least the replicase section of the genome remained intact for replication. To determine if the virus present in the samples from the 24-well plate could produce a viable infection, a standard plaque assay was carried out on BHK-21 cells treated with the 24-well plate samples after 5, 15, 30 and 60 minutes exposure (2.2.9). No plaques were observed at any time-point (data not shown). Based on these results, the most efficient technique for neutralising virus by UV light was determined to be placing the samples in 24-well plates and exposing them to UV light for ≥30 minutes.

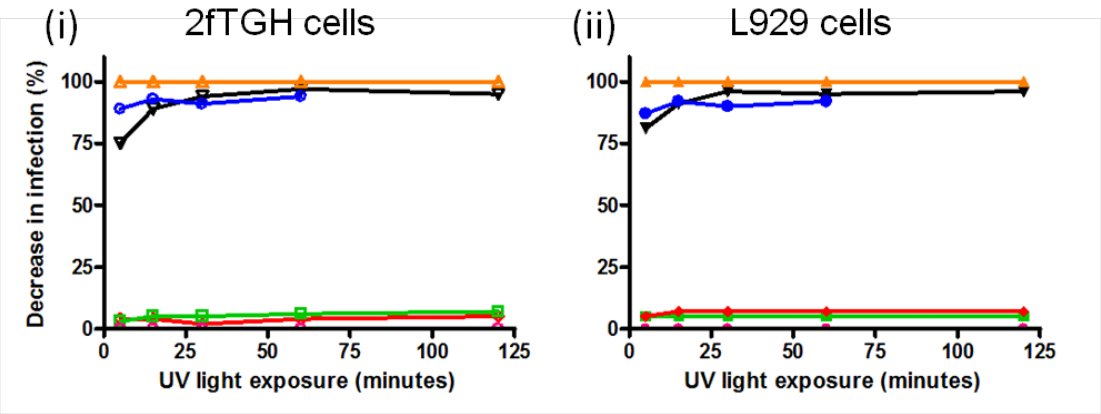

Figure 4.11: UV light inactivation of SFV4(3F)-ZsGreen under different conditions.
(i) 2fTGH or (ii) L929 cells were infected with SFV4(3F)-ZsGreen at MOI 5 for 24 h. The supernatant was divided into 500 µl volumes and added to a 6-well plate (blue), 24-well plate (black), a 25 ml universal (green) or an eppendorf (red) and exposed to UV light in a Stratalinker 1800 for 5, 15, 30 and 60 minutes. Pink, infected supernatant without exposure to UV light. Orange, mock-infected supernatants. The supernatant was then added to BHK-21 cells for 48 h and analysed for ZsGreen positive cells. The decrease in infection was calculated by measuring ZsGreen positive cells in 15 fields and dividing the mean number of cells expressing ZsGreen in mock-treated cultures. Each point represents one experiment. The graph is representative of three experiments.

The efficiency of UV light and acid to neutralise virus was compared by infecting L929 or 2fTGH cells with SFV4(3H)-ZsGreen at MOI 5 for 24 h, exposing the supernatant samples to UV light or acid and then adding samples to BHK-21 cells and analysing the level of infection by fluorescence microscopy. Similar infection levels of BHK-21 cells were observed when cells were exposed to supernatant from L929 or 2fTGH cells inactivated using acid or inactivated by UV

(Fig. 4.12). Therefore, UV light inactivation, which was faster, was selected for future use.

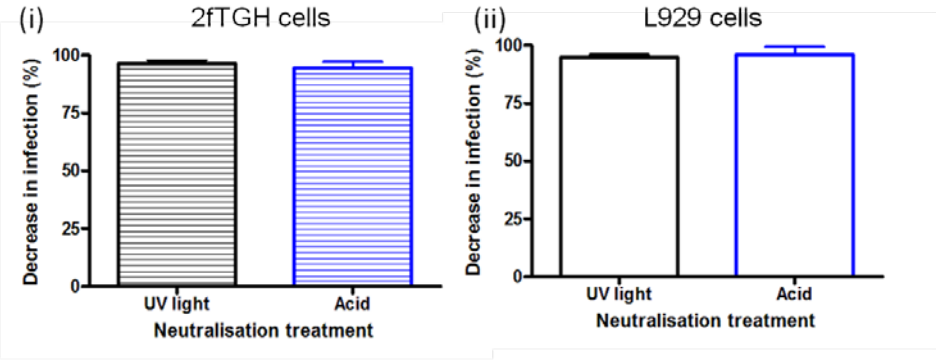

Figure 4.12: Comparison of virus neutralisation using UV light inactivation or acid treatment.
(i) 2fTGH or (ii) L929 cells were infected with SFV4(3F)-ZsGreen at MOI 5 for 24 h, the supernatant was collected, exposed to UV light (30 minutes, Stratalinker 1800) (black) or acid treatment (pH 2, 4 days) (blue) then added to BHK-21 cell monolayers and analysed for ZsGreen expression. The decrease in infection was calculated by measuring the number of ZsGreen positive cells in 15 fields and dividing by the mean number of ZsGreen positive cells in the mock-treated supernatant. Each bar represents the mean of three experiments, error bars are standard deviations of the mean.

To establish the IFN bioassay, samples were prepared from L929 or 2fTGH cells infected with SFV4 or SFV4nsP2RDR at MOI 5 for 24 h and neutalised by UV exposure. SFV4nsP2RDR is a mutant strain of SFV4 with a point mutation in the nuclear localisation signal RRR within nsP2 (Rikkonen *et al.*, 1992). It has been reported that SFV4nsP2RDR induces significantly more functional IFN than SFV4 (Breakwell *et al.*, 2007). Therefore, it was considered that SFV4 and SFV4nsP2RDR would provide the dynamic range of IFN induction needed in the IFN bioassay. The IFN bioassay determines the endpoint of the experiment at which ≥50 % of the cell monolayer is protected by IFN from a challenge virus infection. L929 and A549-NPro cells were used in the bioassay to measure mouse and human IFN respectively; both cell lines respond to IFN. A549-NPro cells cannot produce IFN.

SFV A7(74) was used to challenge L929 cells and EMCV to challenge A549-NPro cells. SFV A7(74) was not used on human cells, due to the hypothesis that SFV is more sensitive to human IFN than to mouse IFN. To determine the amount of challenge virus to use, L929 and A549-NPro cells were pre-treated with samples likely to contain IFN and then infected with different MOIs of challenge virus for 48

h. Monolayers were fixed, stained with toludine blue and analysed for the end-point dilution at which ≥50 % of the cell monolayer is protected. Even at MOI 0.1 of challenge virus, both the L929 and the 2fTGH cell monolayers were completely destroyed if the monolayers were pre-treated with inactivated supernatant from SFV4 infected cells (Fig. 4.13). In contrast, in L929 or 2fTGH cells exposed to supernatant from SFV4nsP2RDR infection, the endpoint dilution increased with decreasing MOI of the challenge virus. The greatest endpoint dilution was at MOI 0.1 (Fig. 4.13). Based on these results, MOI 0.1 was selected for both the SFV A7(74) and the EMCV challenge.

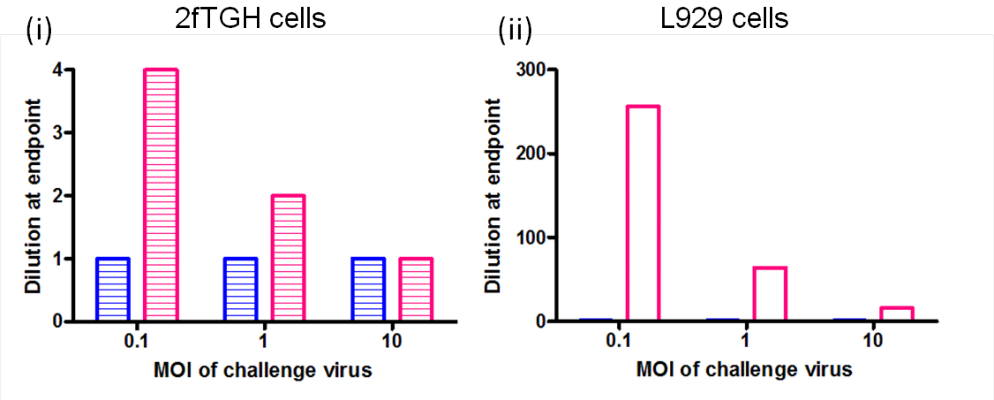

Figure 4.13: IFN bioassay endpoint following challenge with SFV A7(74) at different MOI.
(i) 2fTGH and (ii) L929 cells were overlayed with UV inactivated supernatant from SFV4 (blue) or SFV4nsP2RDR (pink) infection for 24 h. A 2-fold serial dilution was carried out on the supernatant. 2fTGH and L929 cells then challenged was added at MOI 0.1, 1 or 10 and incubated for 48 h. Cells were fixed, stained and analysed for the endpoint. The endpoint is the dilution at which ≥50 % of the cells are protected from challenge virus induced CPE. Each bar is the mean of triplicate results. Values are the reciprocal dilution endpoint. The graph is a representation of three experiments.

A mouse or human International IFN standard was included in all IFN bioassays. The limit of detection for each bioassay was the end-point at which ≥50 % of the monolayer pre-treated with the International IFN standard was protected. The complete IFN bioassay protocol is described in 2.4.

4.2.4 Comparison of IFN production by human and mouse fibroblasts infected with SFV4, SFV L10 or SFV A7(74)

The IFN bioassay was used to compare IFN production by human and mouse fibroblasts infected with SFV4, SFV L10 or SFV A7(74). A similar and high level of infected cells is preferable for comparison of IFN induction. Therefore, the percentage of cell infected was analysed for 2fTGH and L929 cells infected with each of three strains of SFV at MOI 5 by immunostaining for nsP3 at 24 h post-infection (2.3.1). Mock-infected cultures were included as controls. Low levels of non-specific staining were observed in the controls (Figs 4.14.D and H). By 24 h post-infection, all three strains infected approximately 97 % of both cell monolayers (Fig. 4.14).

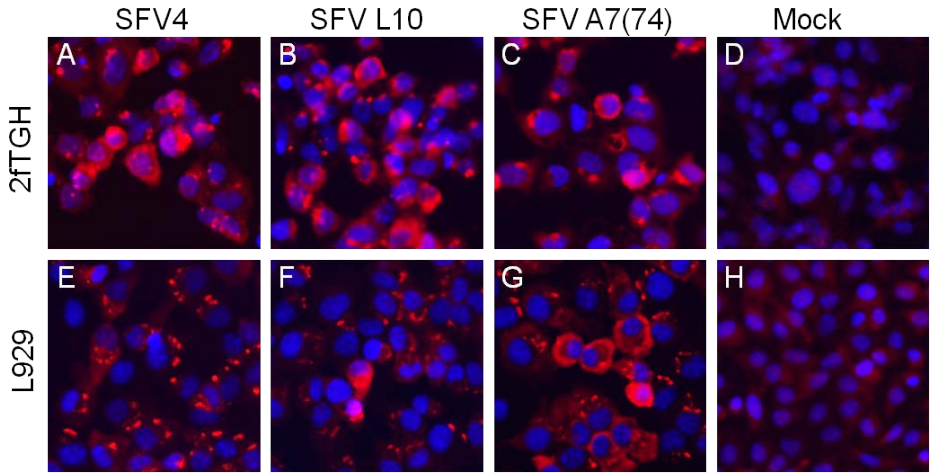

Figure 4.14: Strains of SFV infected most 2fTGH cells and L929 cells by 24 h post-infection.
2fTGH or L929 cells were infected with SFV4 (A & E), SFV L10 (B & F), SFV A7(74) (C & G) (MOI 5) for 24 h or mock-infected (D & H, mock) and immunostained for nsP3. NsP3 is stained red and the nuclei are stained blue.

An IFN bioassay was carried out on UV light inactivated supernatants from 2fTGH and L929 cells infected with SFV L10, SFV A7(74) or SFV4 at MOI 5 for 24 h. In parallel, virus levels in the supernatant were determined by plaque assay (2.2.9). SeV was included to demonstrate the amount of IFN that the cells were capable of producing during a virus infection. SeV (*Paramyxoviridae*) is a negative-strand RNA virus, which is reported to induce high levels of IFN. SeV does not form plaques and, therefore, was not included in the plaque assays. Mock-infected cultures were included as controls. No infectious virus was detected in mock-infected cultures

(data not shown). The experiment was carried out three times and the results were combined.

The titres of infectious virus were similar between SFV L10 and SFV4 in both cell lines (Fig. 4.15.i and ii). SFV A7(74) produced higher titres of infectious virus than SFV4 and SFV L10. This was significant in the L929 cells ($p < 0.05$ by the Mann-Whitney test); SFV A7(74) titres in L929 cells were 0.5 log higher than those for SFV4. In both cell lines, all three strains induced relatively little IFN in comparison to that induced by SeV (Fig. 4.15.iii and iv). Similar levels of IFN were induced by SFV L10, A7(74) and SFV4 in human 2fTGH cells (Fig. 4.15.ii). In contrast, SFV4 induced significantly more IFN than SFV L10 or SFV A7(74) in mouse L929 cells. SFV L10 also induced significantly more IFN than SFV A7(74) in the L929 cells (Fig. 4.15.iv). In L929 cells, infectious virus titres and IFN induction levels were inverse, with SFV A7(74) producing the highest virus tire and inducing the lowest level of IFN.

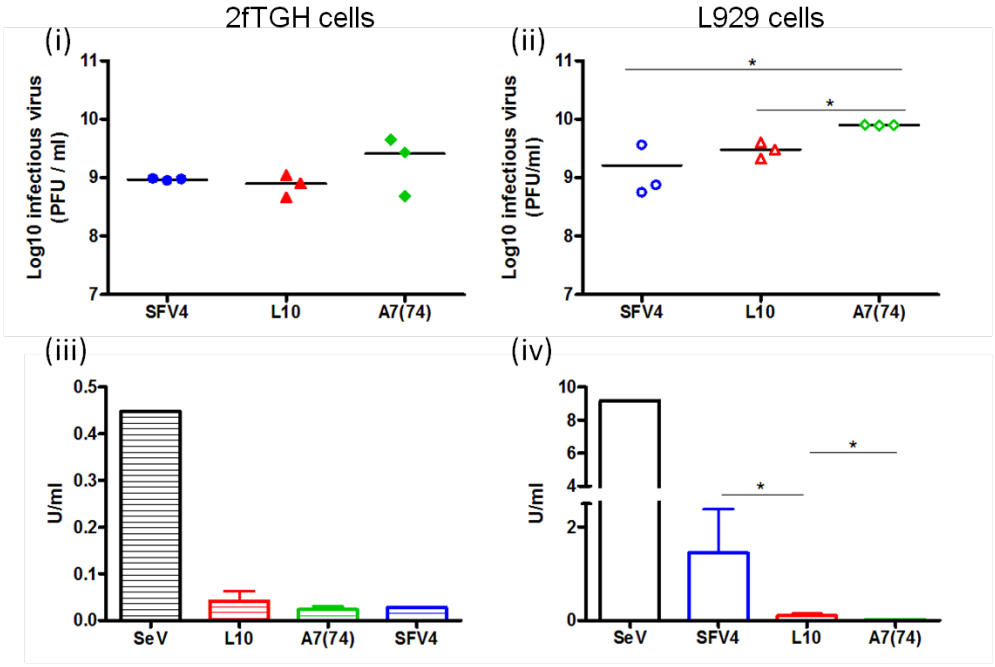

Figure 4.15: Functional IFN induced by SeV , SFV4, SFV L10 or SFV A7(74) infected fibroblasts.
(i) and (iii) 2fTGH or (ii) and (iv) L929 cells were infected with SeV, SFV4, SFV L10 or SFV A7(74) at MOI 5 for 24 h and assayed for infectious virus (i and ii) or functional IFN (iii and iv). Each point represents one experiment. Each bar is the mean of triplicate experiments, error bars are standard deviations of the mean. * = significant difference ($p < 0.05$ Mann-Whitney test).

To determine whether similar results would be observed in different cell lines, the experiment was repeated using human Hs 633T cells and mouse NIH 3T3 cells. No infectious virus was detected in mock-infected cells (data not shown). Similar titres of infectious virus were produced by SFV L10 and SFV4 in both cell lines (Fig. 4.16.i and ii). In both cell lines, significantly higher titres of infectious SFV A7(74) (0.5 log) were detected compared to SFV4. In Hs 633T cells, SFV A7(74) titres were also higher than SFV L10. In contrast, SFV A7(74) and L10 replicated to similar titres in NIH 3T3 cells. Again, all three strains induced considerably lower levels of IFN than SeV in both cell lines (Fig. 4.16.iii and iv). In NIH 3T3 cells, as in L929 cells, SFV4 induced significantly more IFN than SFV L10 ($p < 0.05$ by the Mann-Whitney test).

Taken together with the data presented in Fig. 4.15, it can be concluded that all three strains of SFV tested induced relatively little IFN in human or mouse fibroblasts in comparison to SeV infection. In human fibroblasts, IFN levels were not significantly different between the virus strains, even though SFV A7(74) replicated to higher titres. In mouse L929 cells, virus production (SFV A7(74) > SFV L10 > SFV4) was inversely related to IFN levels (SFV4 > SFV L10 > SFV A7(74)), as might be expected. However, in mouse NIH 3T3 cells, this correlation between virus titres and IFN levels was not observed. In both L929 and NIH 3T3 cells, SFV4 induced significantly more IFN than SFV L10.

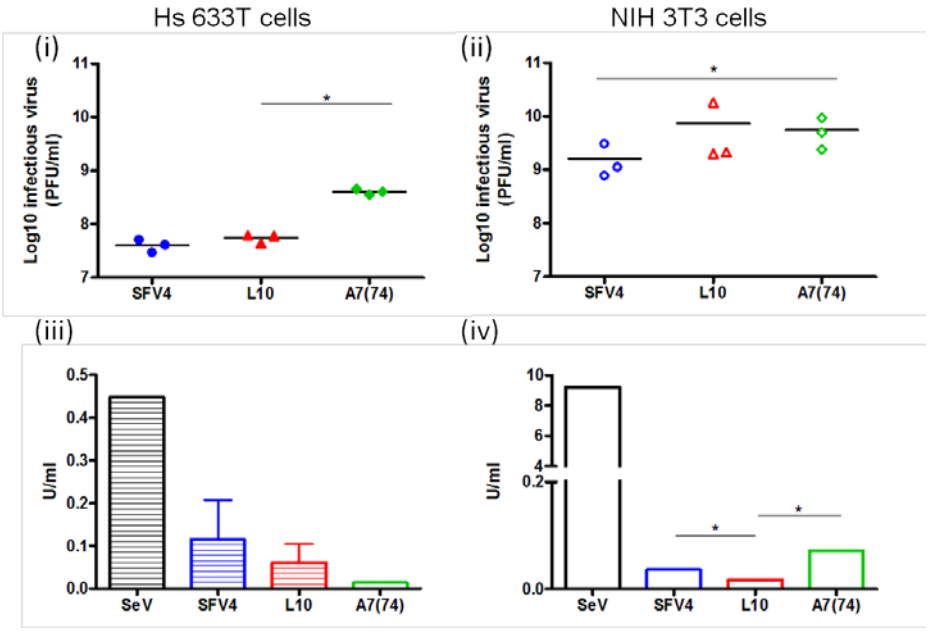

Figure 4.16: Functional IFN induced by SeV, SFV4, SFV L10 or SFV A7(74) infected fibroblasts.
(i) and (iii) Hs 633T cells or (ii) and (iv) NIH 3T3 cells were infected with SeV, SFV4, SFV L10 or SFV A7(74) at MOI 5 for 24 h and then assayed for infectious virus (i and ii) or functional IFN (iii and iv). Each point represents one experiment. Each bar is the mean of triplicate experiments, error bars are standard deviations of the mean. Error bars in (v) are too small to see. * = significant difference (p 0.05 Mann-Whitney test).

4.2.5 Comparison of the sensitivity of SFV L10, A7(74) and SFV4 to human and mouse IFN in fibroblasts

One study reports that SFV strains differ in their sensitivity to the effects of IFN pre-treatment (Deuber & Pavlovic, 2007). To determine if the well characterised SFV L10, A7(74) and SFV4 strains also differ in sensitivity to the affects of IFN, an IFN sensitivity assay was carried out on 2fTGH, Hs 633T, L929 and NIH 3T3 cells infected with the three strains of SFV at MOI 5 for 24 h. Virus titres in the supernatant were measured by plaque assay. The experiment was carried out three times and the results were combined. No infectious virus was detected in mock-infected cells (data not shown). Treatment of mouse or human cells with IFN prior to infection reduced the titres of all three viruses by ≥ 75 % (Fig. 4.17). Taken together, it can be concluded that that these three strains of SFV are highly and equally sensitive to IFN pre-treatment and that this sensitivity does not vary between human and mouse cells.

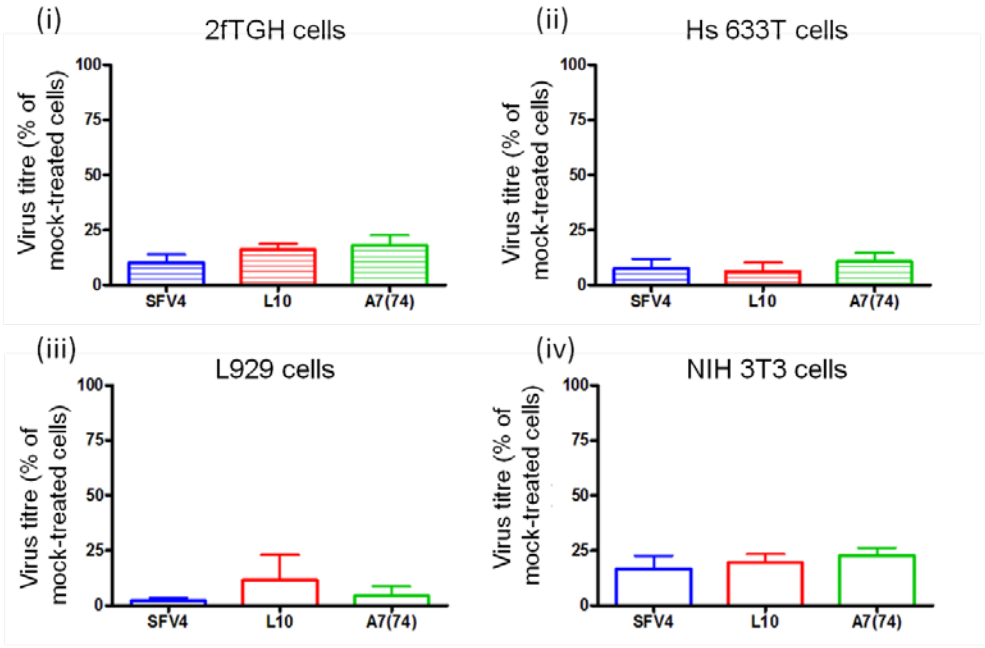

Figure 4.17: SFV4, SFV L10 and SFV A7(74) are equally susceptible to IFN pre-treatment in human and mouse fibroblasts.
(i) 2fTGH cells, (ii) Hs 633T cells, (iii) L929 cells and (iv) NIH 3T3 cells were treated with 10 U/ml of IFN-α or mock-treated for 16 h and then infected with SFV4, SFV L10 or SFV A7(74) at MOI 5. At 24 h post-infection samples were assayed for infectious virus by plaque assay and expressed as a percentage of the mock-treated control. Each bar is the mean of triplicate experiments, error bars are standard deviations of the mean.

4.2.6 Summary of findings

- Plaque phenotype varied between human and mouse cells infected with SFV L10, SFV A7(74) and SFV4.
- Plaque phenotype varied between human cells with an intact IFN system and cells with a defective IFN system infected with SFV L10, SFV A7(74) and SFV4.
- Treatment of cultures with IFN prior to infection with SFV4(3H)RLuc, SFV4(3F)-ZsGreen, SFV L10, SFV A7(74) or SFV4 greatly reduced virus replication.
- SFV L10, SFV A7(74) and SFV4 were equally sensitive to the effects of IFN pre-treatment in both human and mouse cells.
- The viability of cell cultures following IFN treatment and infection was completely different in human cell cultures compared to mouse cell cultures:

human cultures decreased in viability, whereas mouse cultures increased in viability.

- SFV L10, SFV A7(74) and SFV4 infection induced low levels of IFN relative to SeV, in both human and mouse cells.
- In human cells, similar levels of IFN were induced by SFV L10, SFV A7(74) and SFV4 infection.
- In mouse fibroblasts, infection with SFV4 induced more IFN than infection with SFV L10. The results for SFV A7(74) infection were variable.

4.2.7 Conclusions

The results presented in this chapter indicate that SFV plaque phenotype depends on (i) cell species, whether the cells are human or mouse, and (ii), at least in the case of human cells, the presence of an intact IFN system. All three strains of SFV studied were equally sensitive to IFN pre-treatment in mouse and human fibroblasts, although virus replication was not completely abolished. All three strains of SFV induced only small amounts of IFN compared to SeV infection in both mouse and human fibroblasts. In human fibroblasts, the three strains of SFV induced similar amounts of IFN. In mouse fibroblasts, SFV4 induced significantly more IFN than SFV L10. Culture viability varied between human and mouse fibroblasts following IFN pre-treatment and infection.

4.3 Discussion

This chapter examined (i) the interaction of SFV with IFN in human cells compared to mouse cells and (ii) the interaction of different strains of SFV with the IFN system. These will be discussed in turn.

4.3.1 The interaction of SFV with IFN in human cells compared to mouse cells

RNA viruses have been responsible for many recent outbreaks and epidemics in humans and other animals; influenza virus, SARS-CoV, CHIKV, DENV and WNV are examples. The emergence or re-emergence of a virus requires successful infection of a host and in the case of vector-borne disease, a vector. Disease in a new host can be driven by a number of parameters including (i) change in distribution of virus, host or vector, (ii) more efficient virus entry into the host or host tissues or cells and/or (iii) evasion of host cellular innate or adaptive immune responses. In November 2002, SARS-CoV emerged in China and caused severe respiratory disease. Due to rapid international travel, SARS-CoV spread to Canada, Vietnam and Singapore and infected thousands of people. In the case of SARS, the mutation of two amino acids probably enabled it to transfer from Civet cats to humans, replicate efficiently and, presumably, transmit to other humans (Qu *et al.*, 2005). Since 2005, CHIKV has re-emerged throughout Africa, Asia and the Indian Sub-continent. Clinical cases have also occurred in Italy, 2007 and France, 2010 (Rezza *et al.*, 2007;Grandadam *et al.*, 2011). Between 2005 and 2006 CHIKV emerged in the Indian Ocean island of La Reunion and produced 265,000 clinical cases in a population of 770,000 (Enserink, 2007). The original vector of CHIKV was the *Aedes aegypti* mosquito. The mutation of a single amino acid in the glycoprotein E1 enabled CHIKV to efficiently infect *Aedes albopictus* and extend its geographical range (Tsetsarkin *et al.*, 2007). The question remains: why is CHIKV causing human epidemics while the closely related SFV is not? A proposed explanation for the difference between SFV and CHIKV is that SFV cannot evade or control the human IFN system. Conversely, CHIKV may not be able to evade or control the mouse IFN system since it appears to be difficult to infect mice unless they are deficient in IFN responses (Couderc *et al.*, 2008).

In this chapter, the interaction of SFV with the human type-I IFN system was investigated and compared to its interaction with the mouse system. In plaque assays on human cells, SFV infection only produced cloudy plaques or cellular agglomerations (Fig. 4.1). On inspection under the microscope, cell death was not obvious in infected 2fTGH cells. In contrast, clear plaques were observed in mouse L929 cells infected with all three strains of SFV (Fig. 4.3). When the IFN system was compromised in human cells, SFV infection produced clear plaques (Fig. 4.4). Immunostaining studies to investigate numbers of infected cells showed that areas of human cells were infected, but they did not appear to be dying (Fig. 4.2). The data suggests that the plaque phenotype produced by SFV infection depends on the whether the cells are human or mouse and, in the case of human cells, whether the IFN system is intact.

The interaction of SFV with type-I IFN was investigated further in human and mouse fibroblasts. In both human and mouse cells, pre-treatment with IFN reduced SFV replication, although even at high concentrations of IFN-α replication was not completely abolished (Figs 4.6, 4.7, 4.8 and 4.17). Possible explanations for this residual virus activity include (i) SFV replicates in most IFN treated cells at low levels, (ii) some cells, perhaps related to the cell cycle, are not rendered into the antiviral state by IFN pre-treatment and SFV replicates in these or (iii) in some cells, again perhaps related to cell cycle, SFV is able to disassemble the antiviral state and replicate to high levels. In Fig. 4.7.i SFV only replicated to detectable levels in a small subset of cells; while in Fig. 4.7.iii *RLuc* levels were consistently lower in IFN pre-treated and infected cultures compared to untreated and infected cultures. These results are consistent with the suggestions above that SFV replicates in IFN pre-treated cells at low levels (i) and at high levels in a few cells either because these cells are somehow different (cell cycle) and are not in an antiviral state (ii) or because, most likely, the virus disassembles the antiviral state (iii). In Fig. 4.7.iii, there was a delay of 2 h in *RLuc* detection compared to the untreated and mock-infected control. This delay may reflect the time taken for SFV to successfully dismantle the antiviral state in a few cells.

The results in Figs 4.6, 4.7, 4.8 and 4.17 indicate that SFV is sensitive to the IFN-induced antiviral state in both human and mouse fibroblasts. However, the

viability of cultures pre-treated with IFN and then infected with SFV varied between human and mouse cultures. In mouse L929 cultures, viability increased following IFN pre-treatment and infection, as in the mock infected control. This result suggests that IFN pre-treatment protects L929 cultures from SFV induced cell death. In contrast, in 2fTGH cultures pre-treated with IFN and infected with SFV, the viability decreased over time, as in the untreated and infected control. Possible explanations for the loss in 2fTGH culture viability following IFN treatment and SFV infection include that (i) IFN treatment is toxic to 2fTGH cells at this concentration, (ii) the majority of the monolayer was infected with virus at low levels which could not be detected by ZsGreen expression, and IFN pre-treatment sensitised these cells to apoptosis following subsequent virus infection and/or (iii) infected 2fTGH cells secrete a protein which induces cell death in neighbouring cells. Fig. 4.9 indicated that 10 U/ml of IFN-α was not toxic to 2fTGH cell cultures. In support of (iii), Kumar *et al* (1997) reported that the ISG TNF-α can induce 2fTGH cell death TNF-α induction of cell death in 2fTGH or, potentially, other cell lines could prove vital in eliminating SFV infection. Explanations (ii) and (iii) seem most likely and cannot be distinguished by the studies presented here. In conclusion, SFV is sensitive to the antiviral state in both human and mouse fibroblasts.

Treatment of cultures with IFN prior to infection reduced SFV replication by ≥75 % in both human and mouse cells (Fig. 4.17). Therefore increased sensitivity of SFV to human IFN does not appear to be responsible for the avirulence of SFV in humans. The levels of IFN induced during SFV infection were compared in human and mouse cells and here differences were observed (Fig. 4.15 and 4.16). In human cells, SFV L10, SFV A7(74) and SFV4 induced similar low levels of IFN. In contrast in mouse cells, SFV4 induced more IFN than SFV L10. However, all three strains induced extremely little IFN relative to SeV in both human and mouse cells. The SeV used was purchased and may contain defective particles that strongly induce the IFN response in cell culture. In contrast, all three strains of SFV were carefully propagated to limit the production of defective particles. It is likely that poor propagation of SFV would result in defective particles and IFN induction similar to in SeV infection. Potentially, strains of SFV have evolved to inhibit the IFN response

in both human and mouse cells. Given the sensitivity of SFV to IFN pre-treatment, it is unsurprising that SFV may have evolved mechanism(s) to inhibit IFN production.

The data presented here suggests that SFV replicates differently in human and mouse cells. IFN is important in controlling SFV infection and, hence, its production is largely inhibited by SFV. However, based on these results, it is unlikely that IFN induction is responsible for the mild infection of SFV in humans. However, the results presented here do not exclude the possibility that IFN does determine the pathogenesis of CHIKV in mice. It would be interesting to directly compare CHIKV and SFV induction of IFN and sensitivity to the effects of IFN in both human and mouse cells. This was planned to be part of this study, but was not done due to the unavailability of a category 3 laboratory.

4.3.2 The interaction of different strains of SFV with the IFN system

The second focus of this chapter was the influence of IFN in determining the virulence of different strains of SFV. Several strains of SFV have been identified that differ in virulence in adult mice (Bradish *et al.*, 1971). Well-characterised strains include the virulent SFV L10 and the avirulent SFV A7(74) and SFV4. The factor(s) that determine virulence remain unclear. One possible explanation is that the strains have different interactions with the IFN response, which affects IFN induction and/or IFN efficacy and this determines strain virulence. In this chapter, SFV L10, SFV A7(74) and SFV4 strains were compared for IFN induction and sensitivity to the effects of IFN in fibroblasts. Previous studies showed that SFV infection induces IFN production in mice and that IFN controls SFV spread in mice (Bradish *et al.*, 1975;Fragkoudis *et al.*, 2007). One study reports that strains of SFV vary in their sensitivity to IFN pre-treatment in MEFs (Deuber & Pavlovic, 2007). In that study, MEFs were treated with 500 U/ml of IFN-α for 16 h and then infected with the virulent L10 or the previously unreported avirulent SFV V42. At 24 h post-infection, the supernatants were collected and compared for infectious virus titres by plaque assay. SFV V42 had a greater reduction in virus titre than SFV L10 and was suggested, therefore, to be more sensitive to the effects of IFN (Deuber & Pavlovic, 2007). In the similar study carried out in this research project, SFV L10, SFV A7(74)

and SFV4 were equally sensitive to the effects of IFN pre-treatment (Fig. 4.17). This was observed in four different fibroblast cell lines, both human and mouse. This result is consistent with a small study by Bradish and Titmuss (1981) that demonstrated a similar reduction in the replication of SFV L10 and SFV A7(74) following IFN treatment of mice. Possible explanations for the difference found by Deuber and Pavlovic (2007) include (i) SFV replicates differently in primary cells (MEFs) compared to continuous cell lines (L929 cells and others), (ii) high concentrations of IFN are required to detect differences in the strains and/or (iii) V42 is an unusual strain that behaves differently to the other strains of SFV.

Induction of IFN by SFV L10, SFV A7(74) and SFV4 varied between human and mouse cells (Figs 4.15 and 4.16). In human fibroblasts, similar levels of IFN were induced by all three strains (Figs 4.15.iii and 4.16.iii). This suggests that there is no difference between the strains in inducing and/or inhibiting and/or evading the IFN response in human fibroblasts. In contrast, in two lines of mouse fibroblasts, SFV4 induced significantly more IFN than SFV L10 (Figs 4.15.iv and 4.16.iv) and in one cell line more than SFV A7(74). All three strains infected >90 % of the cell monolayer (Fig. 4.14). One possible explanation is that SFV4 is less efficient at inhibiting and/or evading the mouse IFN response than SFV L10 or SFV A7(74) and, therefore, greater levels of IFN are induced. This would also explain why SFV4 is less virulent after *ip* inoculation in the mouse than SFV L10. It would be interesting to compare the IFN levels in mice infected with SFV4 and SFV L10 to confirm this observation.

Interestingly, the levels of IFN induced by SFV infection were extremely low compared to SeV infection (Figs 4.15 and 4.16). This data supports a study showing that CHIKV, SINV, VEEV and EEEV induce low levels of IFN compared to SeV in MEFs (Burke *et al.*, 2009). The ability of alphaviruses to inhibit the IFN response is surprising considering that SFV infection induces a detectable IFN response in mice (Bradish *et al.*, 1975;Fragkoudis *et al.*, 2007). One possible explanation for an observed IFN response in infected mice is that another cell line, such as the pDC, produces IFN and not the fibroblasts. pDCs are potent producers of IFN during virus infection in mice (Cella *et al.*, 1999;Barchet *et al.*, 2002;Dalod *et al.*, 2002). It would be interesting to test this hypothesis in mice deficient in pDCs, as was done with

VEEV VRP (Tonkin *et al.*, 2012). An alternative explanation is that during infection of mice SFV undergoes multiple rounds of replication and defective particles are produced. Defective particles can induce the IFN response, as suggested for SeV infection of cell cultures in the experiments presented here. This hypothesis would explain the levels of IFN detected in mice infected with SFV.

Possible explanations for difference in IFN production by strains of SFV and SeV include (i) strains of SFV inhibit the IFN response more efficiently than SeV infection or (ii) SeV induces the IFN response more efficiently than SFV infection. Studies using SFV and SINV demonstrate that the nuclear transcription factors NF-$_k$B and IRF-3 translocate to the nucleus after infection (Breakwell *et al.*, 2007;Burke *et al.*, 2009). NF-$_k$B and IRF-3 induce transcription of the IFN genes. Therefore, any IFN inhibition is likely to be downstream of the transcription of IFN. Recent studies demonstrate that CHIKV and SINV inhibit the phosphorylation of STAT1 (Fros *et al.*, 2010;Simmons *et al.*, 2010). STAT1 is required for IFN signalling in cells. SFV may also inhibit STAT1 phosphorylation.

4.3.3 Final Summary

CHIKV is currently epidemic throughout the tropics, while the closely related SFV is not. A proposed explanation for the difference between SFV and CHIKV is that SFV cannot evade or control the human IFN system, while CHIKV can. In the data presented here, SFV did not produce typical plaques on human cells and this was related to an intact IFN response. Strains of SFV induced extremely little IFN in both human and mouse cells compared to SeV infection. Furthermore, strains of SFV were extremely sensitive to the effects of IFN pre-treatment in both human and mouse cells. Therefore, IFN is important in controlling SFV infection, but IFN does not appear to be the determining factor in the avirulence of SFV in humans.

Studies in the literature have proposed that the virulence of strains of SFV is determined by the IFN response. However, in the data presented here three strains of SFV, which have a different virulence in adult mice, induced, in general, similar amounts of IFN. Furthermore, the three strains of SFV were equally sensitive to the effects of IFN pre-treatment. Therefore, the IFN response does not appear to determine SFV strain virulence. Interestingly, the three strains induced extremely

little IFN in fibroblasts relative to SeV infection. That SFV may antagonise the IFN response will be explored in the next chapter.

Chapter 5: Genetic determinants of the interaction of Semliki Forest virus with the type-I Interferon pathway

Contents

5.1 Introduction

The results presented in the previous chapter showed that three strains of SFV induced only low levels of IFN, at least relative to SeV infection, in human and mouse fibroblasts (Figs 4.15 and 4.16). SFV encodes nine proteins: the replicase proteins nsPs 1-4 in the 5' two thirds of the genome and the structural proteins (capsid protein, the envelope glycoproteins and 6K) in the 3' third. NsP2 has been implicated in antagonising the IFN system (Fazakerley *et al.*, 2002; Breakwell *et al.*, 2007), although the mechanism remains unclear. NsP3 has been demonstrated to be a virulence determinant (Tarbatt *et al.*, 1997; Tuittila *et al.*, 2000). The potential interaction of nsP3 with the IFN system has not been investigated. In this chapter, nsP2 and nsP3 (1.1.2) and their interaction with the IFN response will be investigated using the mutant viruses SFV4-RDR (Rikkonen *et al.*, 1992) and SFV4nsP3Δ50 (Vihinen *et al.*, 2001)). SFV4-RDR and SFV4nsP3Δ50 are described in section 1.1.2 and 1.1.3 and a schematic representation is shown in Fig 2.1. In addition, a mechanism by which SFV antagonises the IFN system will be proposed.

5.1.2 Objectives

1. Determine if SFV4-RDR or SFV4nsP3Δ50 infections induce more IFN than SFV4 in mouse and human cells.
2. Determine if SFV4-RDR or SFV4nsP3Δ50 are more sensitive to the effect of IFN than SFV4 in mouse and human cells.
3. Determine if strains of SFV inhibit the phosphorylation of STAT1 and, if so, does this differ between SFV4 and SFV4-RDR or SFV4nsP3Δ50 infection in mouse and human cells.

5.2 Results

5.2.1 Comparison of IFN production by fibroblasts infected with SFV4, SFV4-RDR or SFV4nsP3Δ50

To confirm that nsP2 is involved in inhibiting the IFN system and to investigate whether the C-terminal hyperphosphorylated region of nsP3 also affects the IFN system, two mutants were analysed: SFV4-RDR and SFV4nsP3Δ50 (Table 2.2). Firstly, to ensure that SFV4-RDR and SFV4nsP3Δ50 had the correct mutation, NIH 3T3 cells were infected with SFV4, SFV4-RDR or SFV4nsP3Δ50 at MOI 10 for 6 h, the RNA was extracted and converted into cDNA, the sequence encoding nsP2 or nsP3 were amplified by PCR and the product was sent to Dundee Sequencing Services for sequencing (2.13.1). The sequence of each virus was as expected.

To study the effect of IFN induction, a high level of infection is preferable. To determine the level of infection, 2fTGH or L929 cells were infected with SFV4, SFV4-RDR or SFV4nsP3Δ50 at MOI 5 for 24 h and immunostained for virus nsP1 (2.3.1). In Fig. 4.14 cells infected with SFV were immunostained for nsP3. In the present experiment nsP1 was selected instead because the deletion in SFV4nsP3Δ50 could affect the binding affinity of the anti-nsP3 antibody. 2fTGH and L929 cells were used as representative human and mouse cell lines. Low levels of background fluorescence were observed in the negative control (Fig. 5.1). In SFV4 and SFV4-RDR infection, nsP1 was detected in over 90 % of the cells in both cell lines (Fig. 5.1). In contrast, in SFV4nsP3Δ50 infection, nsP1 was only detected in 50 - 70 % of cells in either cell line (Fig. 5.1). Even at MOI 30, the percentage of cells infected with SFV4nsP3Δ50 did not increase (data not shown). Given the nature of the deletion in SFV4nsP3Δ50 it is unlikely that SFV4nsP3Δ50 entered fewer cells than SFV4. It is more likely that this deletion in nsP3 affects the ability of the virus to replicate to detectable levels in some cells in the culture, perhaps related to cell cycle.

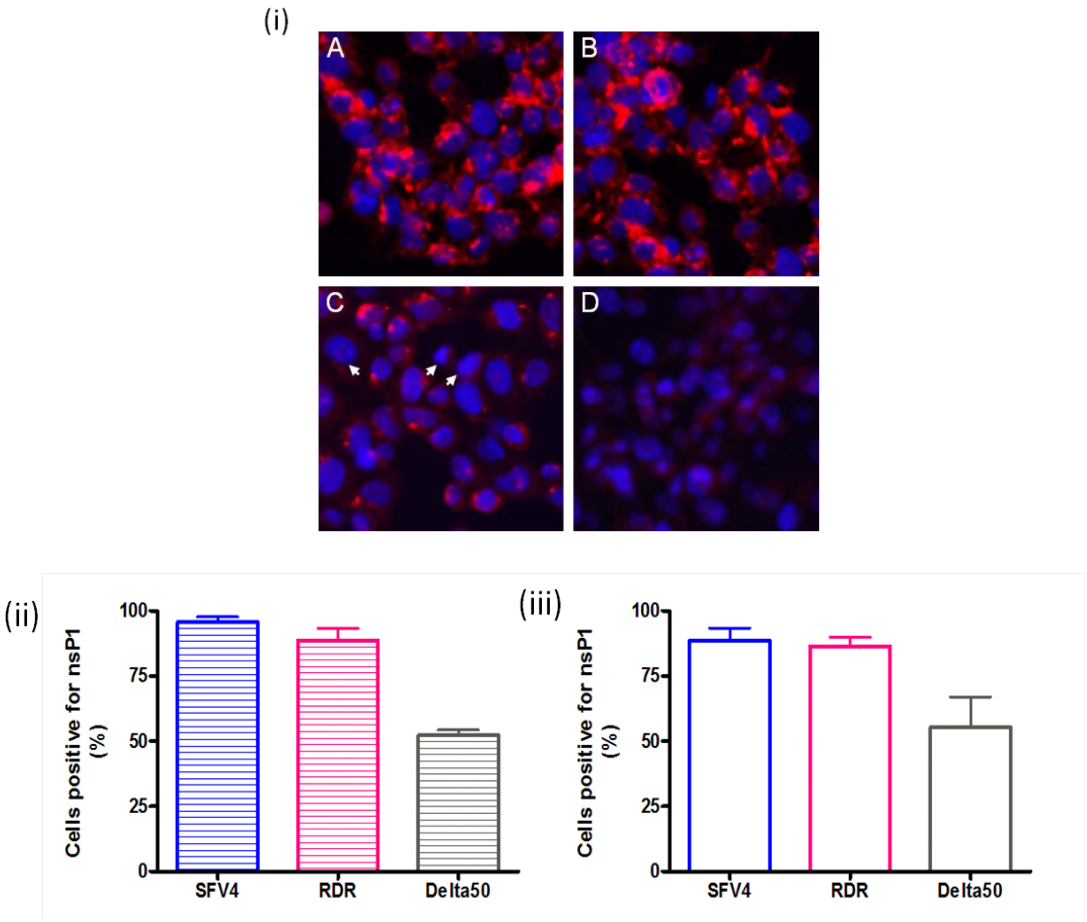

Figure 5.1: Extent of infection of 2fTGH and L929 cells with SFV4, SFV4-RDR or SFV4nsP3Δ50

(i) 2fTGH cells were infected with SFV4 (A), SFV4-RDR (B), SFV4nsP3Δ50 (C) at MOI 5 for 24 h or mock-infected (D) and immunostained for virus nsP1 (red). Nuclei are stained blue. Arrows identify nsP1-negative cells. (ii) 2fTGH cells positive for nsP1 were calculated as a percentage of the total number of cells. Bars are the mean of 15 microscope fields; error bars are standard deviations of the mean. (iii) The experiment was repeated in L929 cells.

To investigate the effect of nsP2RDR and nsP3Δ50 on IFN induction, human fibroblast cell lines 2fTGH and Hs 633T and mouse fibroblast cell lines L929 and NIH 3T3 were infected at MOI 5 with SFV4, SFV4-RDR or SFV4nsP3Δ50 for 24 h. The supernatant was analysed for infectious virus (plaque assay) and the amount of IFN (IFN bioassay) (2.2.9, 2.4). SeV was included to demonstrate the amount of IFN that the cells were capable of producing during a virus infection. No infectious virus was detected in mock-infected cells (data not shown). The experiment was carried out three times and the results combined. In general, SFV4 produced higher titres of

infectious virus than SFV4-RDR or SFV4nsP3Δ50 (Fig. 5.2). The difference between SFV4 and SFV4-RDR was significant in both human cell lines ($p<0.05$ by the Mann-Whitney test), but not in either mouse cell line. The difference between SFV4 and SFV4nsP3Δ50 was significant in L929 cells and Hs 633T cells ($p<0.05$ by the Mann-Whitney) (Fig. 5.2.ii and 5.2.iii). As in chapter 4, NIH 3T3 cells showed the greatest variability between replicates and no significant differences between viruses (Fig. 5.2.iv). In Hs 633T cells, production of infectious virus with all three strains was reduced by >90 % compared to the other cell lines (Fig. 5.2.iii).

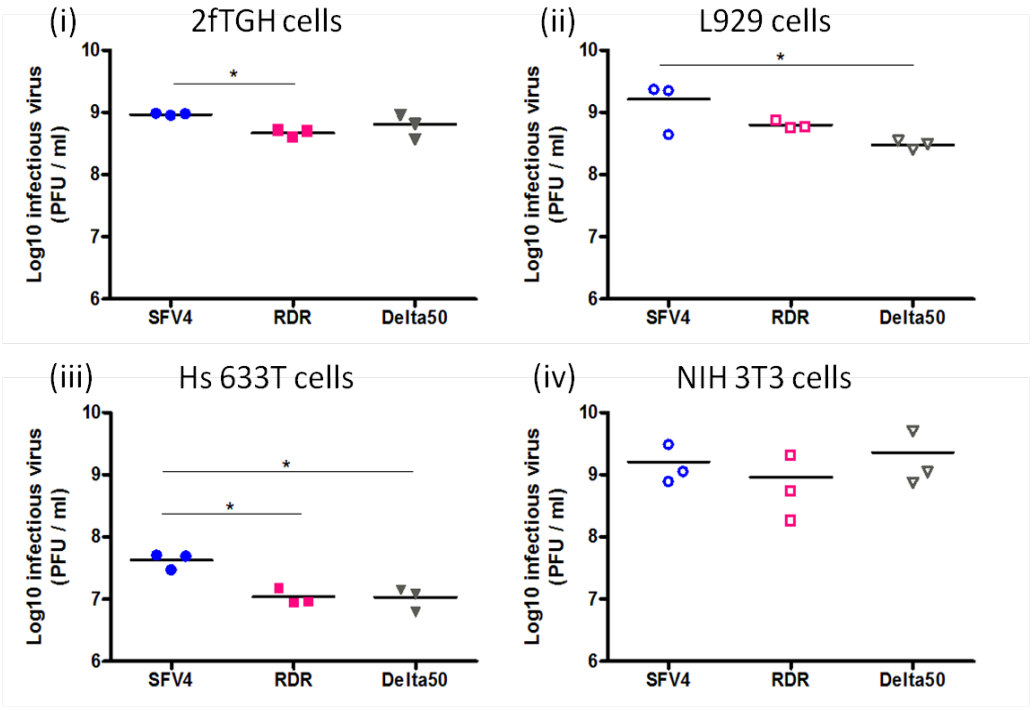

Figure 5.2: Infectious virus titres in fibroblasts infected with SFV4, SFV4-RDR or SFV4nsP3Δ50

(i) 2fTGH cells, (ii) L929 cells, (iii) Hs 633T cells or (iv) NIH 3T3 cells were infected with SFV4 (blue circle), SFV4-RDR (RDR, pink square) or SFV4nsP3Δ50 (Delta50, grey triangle) at MOI 5 for 24 h and infectious virus measured by plaque assay. Each symbol represents one experiment. The experiment was repeated three times and combined. * significant difference ($p <0.05$ by the Mann-Whitney test).

IFN induction during infection with SFV4 or SFV4-RDR at MOI 5 was compared (Fig. 5.3). SFV4-RDR induced significantly higher levels of IFN than SFV4 in all four cell lines ($p <0.05$ by the Mann-Whitney test). In two of the cell lines, SFV4-RDR induced similar levels of IFN to infection with SeV. This induction was not dependent on whether the cells were human or mouse.

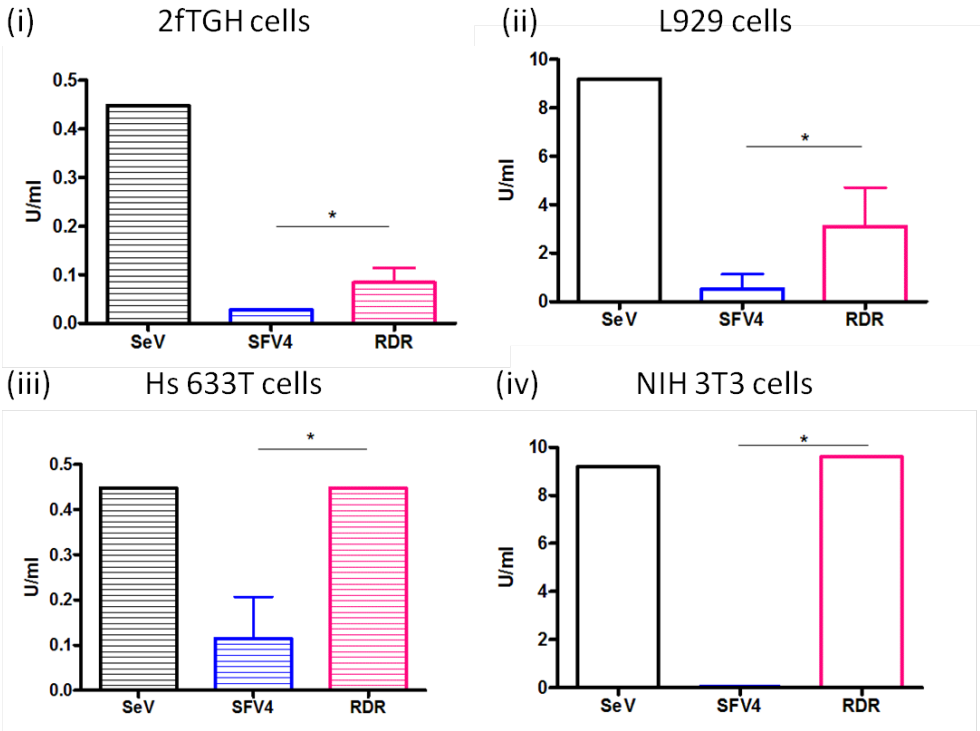

Figure 5.3: IFN production by fibroblasts infected with SeV, SFV4 or SFV4-RDR

(i) 2fTGH cells, (ii) L929 cells, (iii) Hs 633T cells or (iv) NIH 3T3 cells were infected with SeV (SeV, Black), SFV4 (blue) or SFV4-RDR (RDR, pink) at MOI 5 for 24 h and IFN levels were measured using the IFN bioassay. Striped columns are human cell lines (i & iii) and clear columns are mouse cell lines (ii & iv). Each column represents the mean of three experiments; bars are standard deviations of the mean. * significant difference ($p < 0.05$ by the Mann-Whitney test).

Next, IFN induction during infection at MOI 5 with SFV4 or SFV4nsP3Δ50 was compared. Both SFV4 and SFV4nsP3Δ50 induced much lower levels of IFN than SeV in all four cells lines (Fig. 5.4). In general, SFV4nsP3Δ50 induced more IFN than SFV4. This was significant in mouse L929 and NIH 3T3 cells ($p < 0.05$ by the Mann-Whitney test). In Hs 633T cells, SFV4 induced more IFN than SFV4nsP3Δ50. This was in contrast to 2fTGH, L929 or NIH 3T3 cell cultures. One possible explanation is that SFV4nsP3Δ50 only replicates in Hs 633T at low levels (Fig. 5.2), which in turn may only induce small amounts of IFN.

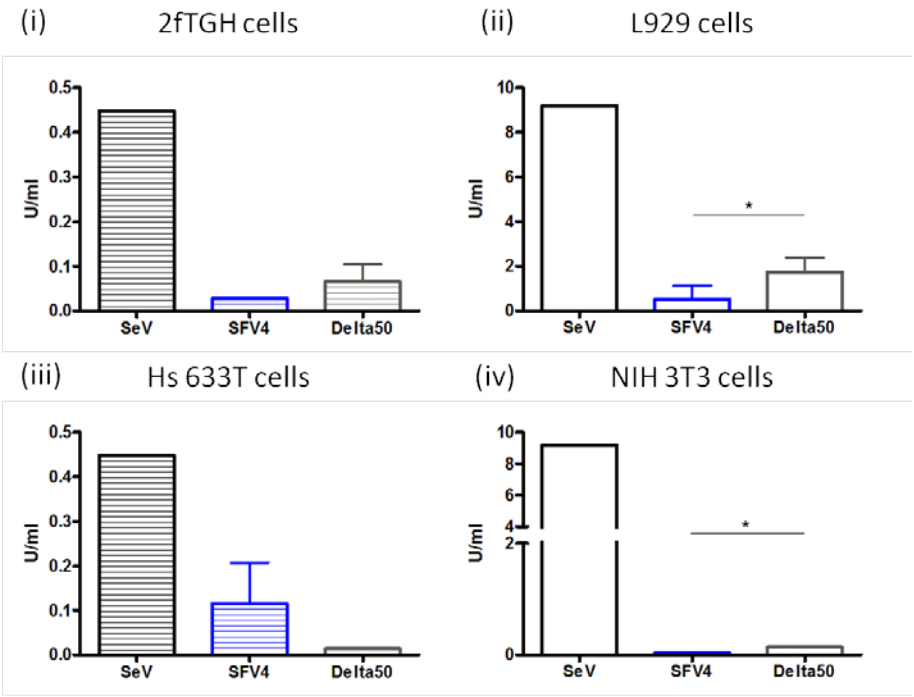

Figure 5.4: IFN production by fibroblasts infected with SFV4 or SFV4nsP3Δ50

(i) 2fTGH cells, (ii) L929 cells, (iii) Hs 633T cells or (iv) NIH 3T3 cells were infected with SeV (SeV), SFV4 (blue) or SFV4nsP3Δ50 (Delta50, grey) at MOI 5 for 24 h and IFN levels were measured using the IFN bioassay. Striped columns are human cell lines (i & iii) and clear columns are mouse cell lines (ii & iv). Each column represents the mean of three experiments; bars are standard deviations of the mean. * significant difference ($p < 0.05$ by the Mann-Whitney test).

To investigate whether SFV4, SFV4-RDR and SFV4nsP3Δ50 infect Hs 633T cells less efficiently than 2fTGH cells; 2fTGH and Hs 633T cells were infected with SFV4, SFV4-RDR and SFV4nsP3Δ50 at MOI 5 for 24 h and immunostained for nsP1. In Hs 633T cells, ≥50 % less of the cell monolayer stained positive for nsP1 compared to in 2fTGH cells in SFV4, SFV4-RDR and SFV4nsP3Δ50 infections (Fig. 5.5). In both 2fTGH and Hs 633T cells, nsP1 was detected in fewer cells in cultures infected with SFV4nsP3Δ50 than SFV4. In Hs 633T cells, nsP1 was only detected in ≤10 % cells infected with SFV4nsP3Δ50. The results in Fig. 5.5 support the data presented in Fig. 5.2. Taken together, the data in Figs 5.2 and 5.5 indicate that SFV4nsP3Δ50 infects Hs 633T at low levels, which may explain why this virus induces less IFN than SFV in this cell line. If the values in Fig. 5.4 are normalised to the extent of infection given in Fig. 5.5, for these cell lines, in 2fTGH cells

SFV4nsP3Δ50 induces 3 times more IFN than SFV4, while in Hs 633T cells SFV4 induces 3 times more IFN than SFV4nsP3Δ50.

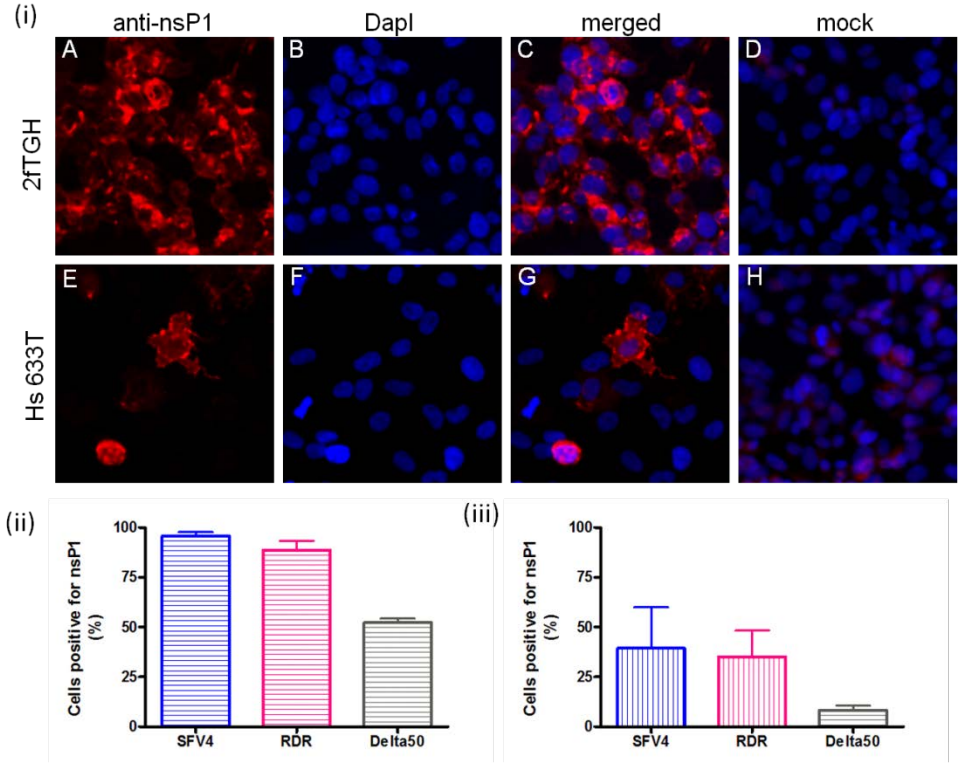

Figure 5.5: Comparison of SFV4, SFV4-RDR and SFV4nsP3Δ50 infection in 2fTGH and Hs 633T cells

(i) 2fTGH cells or Hs 633T cells were infected with SFV4 at MOI 5 for 24 h or mock-infected (D & H) and immunostained for virus nsP1. NsP1 is stained red (A & E). The nuclei are stained blue (B & F). Merged images (C & G). (ii) 2fTGH (horizontal stripes) and (iii) Hs 633T (vertical stripes) cells infected with SFV4, SFV4-RDR or SFV4nsP3Δ50 that stained positive for nsP1 were calculated as a percentage of the total number of cells as determined by counting nuclei (blue). Bars are the mean of 15 microscope fields; error bars are standard deviations of the mean.

In conclusion, SFV4-RDR and SFV4nsP3Δ50, in general, induce greater levels of IFN than WT SFV4 in both mouse and human fibroblasts.

5.3.2 Comparison of the effect of IFN on SFV4, SFV4-RDR and SFV4nsP3Δ50 virus production in fibroblasts

An IFN sensitivity assay was carried out to compare the effect of IFN pre-treatment on the replication of SFV4, SFV4-RDR and SFV4nsP3Δ50 at MOI 5 in 2fTGH, L929, Hs 633T and NIH 3T3 cells (2.5). SFV4 was first compared to SFV4-RDR and a mock-infected control (Fig. 5.6). No infectious virus was detected in the mock-infected control (data not shown). Following IFN pre-treatment, both SFV4 and

SFV4-RDR showed a reduction in infectious virus titre of ≥75 % relative to the mock-treated control. SFV4-RDR appeared to be less affected by IFN pre-treatment than SFV4 (Fig. 5.6.i, ii and iv).

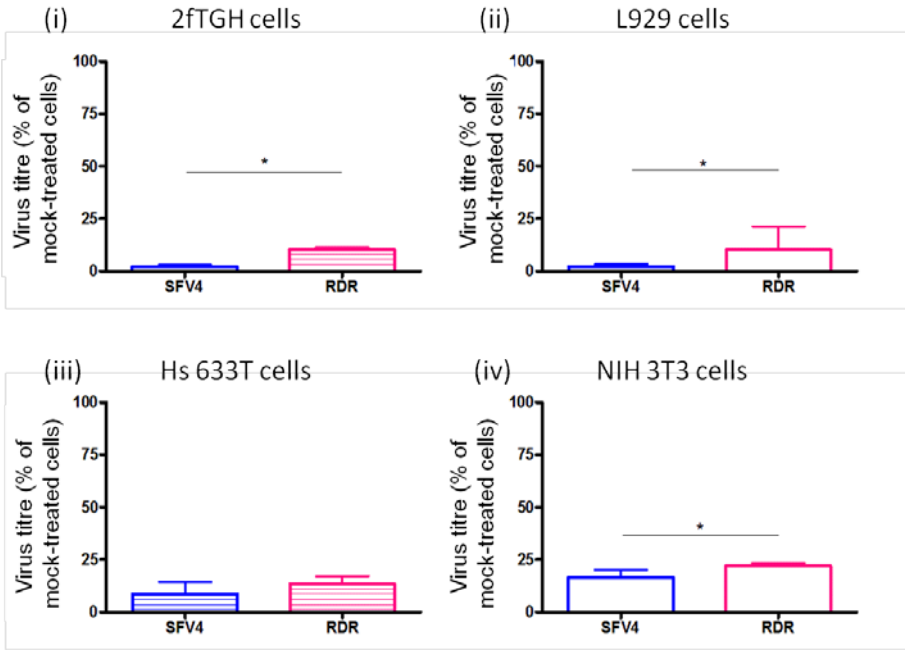

Figure 5.6: Effect of IFN pre-treatment on SFV4 and SFVnsP2RDR replication in fibroblasts

The IFN sensitivity assay was carried out on (i) 2fTGH cells, (ii) L929 cells, (iii) Hs 633T cells or (iv) NIH 3T3 cells infected with SFV4 (blue) or SFV4-RDR (RDR, pink). Infectious virus titres in IFN treated cells were normalised to mock-treated cells infected with virus. Striped columns are human cell lines (i & iii) and clear columns mouse cell lines (ii & iv). Each column represents the mean of three experiments; bars are standard deviations of the mean. * significance ($p < 0.05$ and by the Mann-Whitney test).

The IFN sensitivity assay was carried out on SFV4, SFV4nsP3Δ50 at MOI 5 or a mock-infected control (2.5). No infectious virus was detected in the mock-infected control (data not shown). Following IFN treatment, both SFV4 and SFV4nsP3Δ50 showed a reduction in infectious virus titre of ≥75 % relative to the mock-treated control (Fig. 5.7). One possible explanation for the apparent different sensitivity of SFV4, SFV4-RDR and SFV4nsP3Δ50 to IFN pre-treatment is that SFV4-RDR and SFV4nsP3Δ50 initially infects fewer cells in the culture than SFV4, which is, in part, due to the IFN response (Breakwell *et al.*, 2007). IFN pre-treatment renders the majority of the culture into an antiviral state. The difference between IFN treated and untreated cultures would be more apparent in SFV4 infections compared

to SFV4-RDR or SFV4nsP3Δ50, as a greater percentage of cells were initially infected by SFV4 and would now be protected. Taken together, the mutant viruses and SFV4 were sensitive to IFN pre-treatment and this sensitivity was not dependent on whether the cells were human or mouse (Figs 5.6 and 5.7).

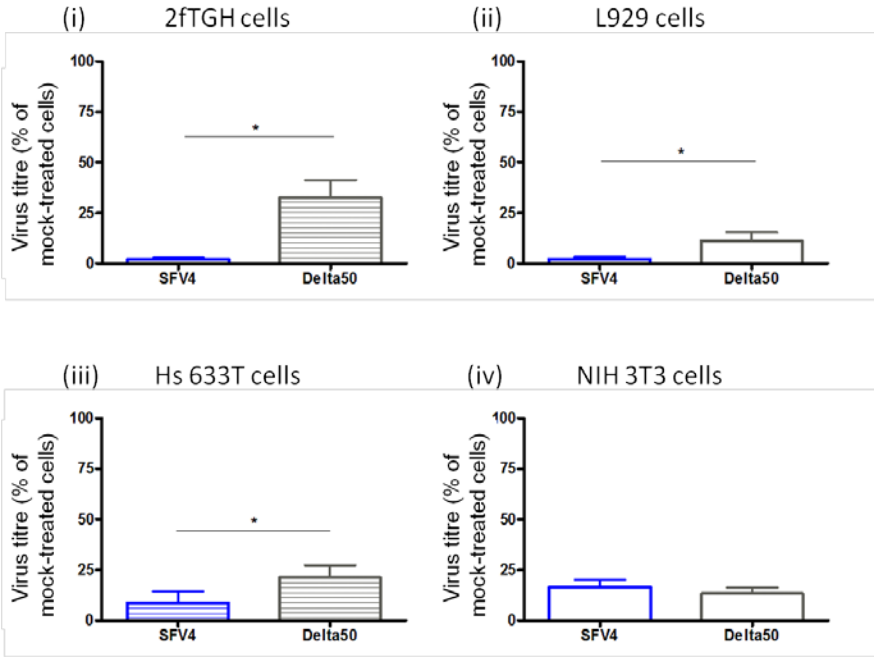

Figure 5.7: Effect of IFN pre-treatment on SFV4 and SFVnsP3Δ50 replication in fibroblasts

The IFN sensitivity assay was carried out on (i) 2fTGH cells, (ii) L929 cells, (iii) Hs 633T cells or (iv) NIH 3T3 cells infected with SFV4 (blue) or SFV4nsP3Δ50 (Delta50, grey). Infectious virus titres in the IFN treated cells were normalised to the mock treated cells. Striped columns are human cell lines (i & iii) and clear columns are mouse cell lines (ii & iv). Each column represents the mean of three experiments; bars are standard deviations of the mean. * significant ($p < 0.05$ by the Mann-Whitney test).

5.2.2 Do SFV4, SFV L10 or SFV A7(74) inhibit the phosphorylation of STAT1 during the infection of fibroblasts?

In chapter 4 it was demonstrated that strains of SFV induced the production of low levels of functional IFN in fibroblasts relative to SeV. This data suggests that SFV may antagonise the IFN system, either at the signalling or, most likely, the induction phase. The ability of SFV to antagonise IFN induction has been previously investigated in this laboratory (Breakwell *et al*., 2007). However, IFN signalling in SFV infected cells has not been analysed. Recent studies have shown that the related alphaviruses CHIKV and SINV can inhibit IFN signalling by inhibiting the phosphorylation of STAT1. The phosphorylation of STAT1 is essential for IFN

signalling (Fros *et al.*, 2010; Simmons *et al.*, 2010). To determine if SFV also inhibits the phosphorylation of STAT1 and, therefore, IFN signalling, a Western blot was carried out on 2fTGH, Hs 633T, L929 and NIH 3T3 cells infected with SFV4, SFV L10 or SFV A7(74) to detect phosphorylated STAT1. MOI 30 was used in order to infect all the cells at the same time. Cells were lysed at 10 h post-infection as IFN is produced early after infection with SFV (Breakwell *et al*., 2007) and any phosphorylation of STAT1 should have occurred by this time. At 10 h post-infection, cultures were treated with IFN-α for 45 minutes to induce STAT1 phosphorylation or with PBSA as a negative control. Blots were probed for phosphorylated STAT1, and then β-actin as a loading control. Mock-infected and mock-treated cell lysates were included as a negative control. Mock-infected lysates treated with IFN were included as a positive control to show the amount of phosphorylated STAT1 possible within the cell culture. The experiment was repeated three times with each cell line and representative blots are shown in Fig. 5.8.

In all four cell lines, no phosphorylated STAT1 was detected in the negative control (Fig. 5.8). STAT1 was the expected size (STAT1α is 91 kDa and STAT1β is 84 kDa). The β-actin bands were the correct size (42 kDa) and generally uniform in each blot indicating that similar amounts of protein were loaded into each lane. In all four cell lines, SFV4, SFV L10 and SFV A7(74) infection resulted in no detectable phosphorylated STAT1. In all four cell lines, SFV4, SFV L10 and SFV A7(74) infected cells treated with IFN had less phosphorylated STAT1 than uninfected cells treated with IFN. The SFV4 lanes on the blot from the NIH 3T3 lysates shown in Fig. 5.8.iv were damaged, however, in other blots SFV4 IFN treated cells induced low levels of phosphorylated STAT1 in NIH 3T3 cells relative to the positive control. These results indicate that all three viruses specifically inhibited the IFN signalling pathway in fibroblasts at or upstream of the phosphorylation of STAT1.

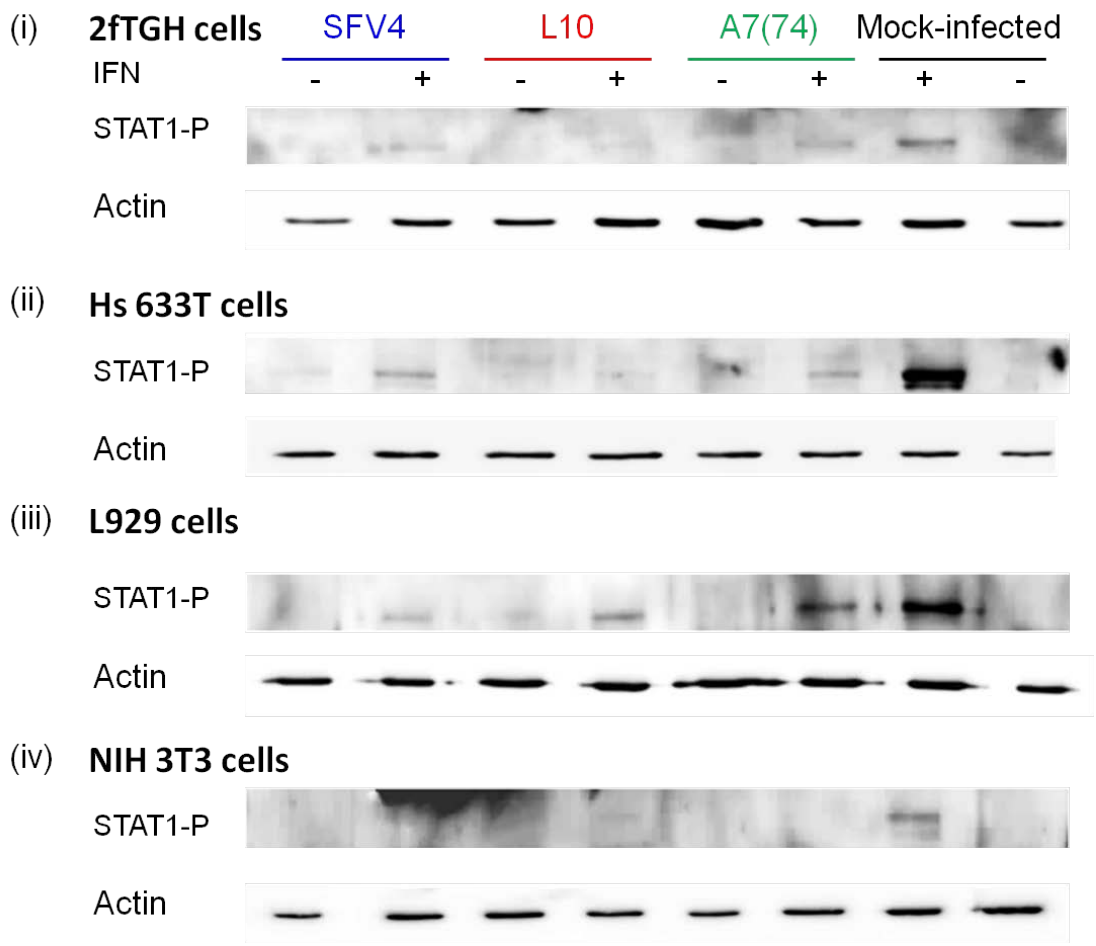

Figure 5.8: Western blot for phosphorylated STAT1 in fibroblast cells infected with SFV4, SFV L10 or SFV A7(74)
(i) 2fTGH, (ii) Hs 633T, (iii) L929 and (iv) NIH 3T3 cells were infected with SFV4, SFV L10 or SFV A7(74) at MOI 30 for 10 h or mock-infected and then treated with IFN-α (+) mock treated (-). A Western blot was carried out using the cell lysates and the blot was probed for phosphorylated STAT1 (STAT1-P) and then β-actin (Actin). Each experiment was repeated three times and a representative blot is shown.

The Western blots in Fig. 5.8 showed a difference in the amount of phosphorylated STAT1 induced by infection with SFV L10 compared to SFV4 or SFV A7(74) in the 2fTGH and Hs 633T cells, which was not observed in mouse cells. The band intensity on these blots was quantified and compared using ImageJ (2.6.6). The phosphorylated STAT1 bands were normalised to the corresponding band intensity of β-actin. The STAT1 band intensity was greatest in SFV4 infected cells and lowest in SFV L10 infected cells (Fig. 5.9). This suggests that SFV L10 either induces less phosphorylation of STAT1 or is more efficient at inhibiting the phosphorylation of STAT1 in human cells than SFV4 and SFV A7(74).

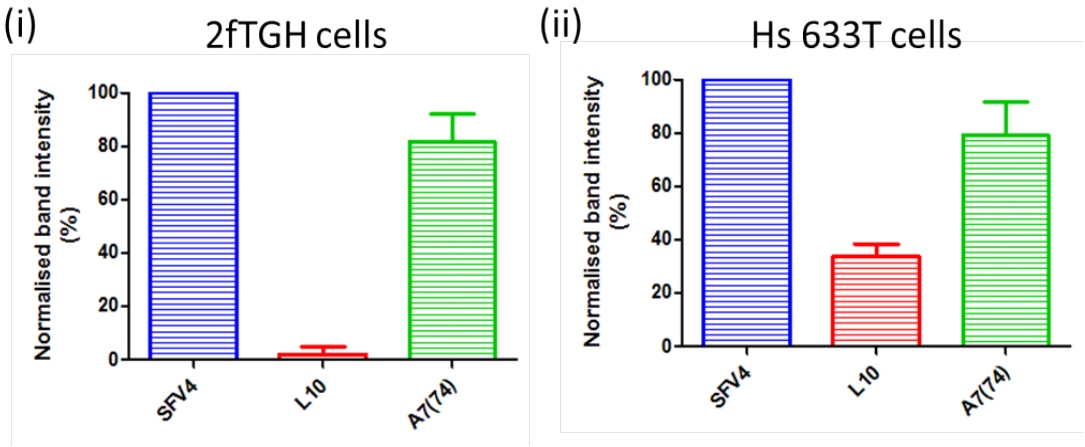

Figure 5.9: There are lower levels of phosphorylated STAT1 in SFV L10 infected 2fTGH and Hs 633T cells compared to SFV4 and SFV A7(74)
The intensity of bands from three 2fTGH and Hs 633T Western blots were determined using ImageJ and band intensity was normalised to actin for each lane and then compared to SFV4 to generate relative band intensities.

The levels of phosphorylated STAT1 during infection with SFV could be affected by virus degradation of STAT1. The levels of phosphorylated STAT1 would decrease as a result of a total decrease in STAT1 levels. To investigate this possibility, a Western blot was carried out on the lysates from 2fTGH and L929 cells infected with SFV L10, SFV A7(74) and SFV4 at MOI 30 for 10 h. Blots were probed for STAT1 and then β-actin as a loading control. Each phosphorylated STAT1 band was normalised to the corresponding β-actin to account for loading discrepancies and relative values are shown in Fig. 5.10. Similar levels of STAT1 were detected in cells infected with SFV L10, SFV A7(74) and SFV4. The strains do not appear to be degrading STAT1, which suggests that the observed decrease in phosphorylated STAT1 is a result of SFV directly affecting the phosphorylation of STAT1. This could either be due to differential induction or differential suppression of the phosphorylation of STAT1.

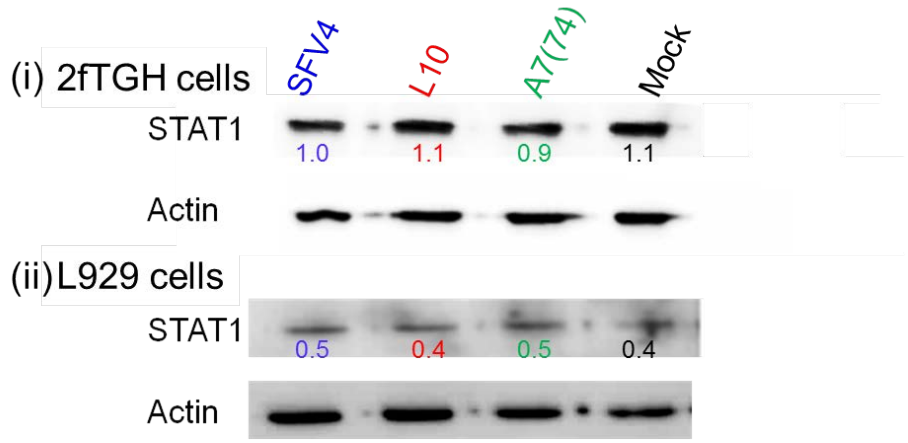

Figure 5.10: Western blot for STAT1 in 2fTGH and L929 cells infected with SFV4, SFV L10 or SFV A7(74)
A Western blot was carried out on cell lysates from (i) 2fTGH and (ii) L929 cells infected with SFV4, SFV L10 or SFV A7(74) at MOI 30 for 10 h or mock-infected. Blots were probed for STAT1 and then β-actin (Actin). Each experiment was repeated three times and a representative blot is shown. Each STAT1 band was normalised to the corresponding β-actin band using ImageJ and the relative band intensity value is shown.

In conclusion, strains of SFV inhibited the phosphorylation of STAT1 in both human and mouse fibroblasts. One possibility is that SFV infection does not induce IFN production and, therefore, no IFN is present to induce the IFN signalling pathway and produce the phosphorylation of STAT1. An alternative hypothesis is that strains of SFV prevent the phosphorylation of STAT1 by directly antagonising the IFN signalling pathway. The result that IFN treatment of cells already infected with SFV does not induce the phosphorylation of STAT1 indicates that SFV is antagonising the IFN signalling pathway. However, it would be useful to confirm that SFV inhibits the IFN signalling pathway, perhaps by using STAT1 or Jak1 reporter plasmids.

5.2.3 Comparison of the levels of phosphorylated STAT1 in fibroblasts infected with SFV4, SFV4-RDR and SFV4nsP3Δ50

In fibroblasts, SFV L10, SFV A7(74) and SFV4 either directly inhibit the phosphorylation of STAT1 or act upstream to reduce phosphorylated STAT1 levels(Fig. 5.8). To analyse the effect of the nsP2RDR and nsP3Δ50 genetic changes

of levels of phosphorylated STAT1, a Western blot was carried out on 2fTGH, Hs 633T, L929 and NIH 3T3 cells infected with SFV4, SFV4-RDR or SFV4nsP3Δ50 at MOI 30 for 10 h. At 10 h post-infection, cultures were treated with IFN-α for 45 minutes to induce STAT1 phosphorylation or with PBSA as a negative control. Blots were probed for phosphorylated STAT1, and then β-actin as a loading control. Mock-infected and mock-treated cell lysates were included as a negative control. Mock-infected lysates treated with IFN were included as a positive control. The experiment was repeated three times with each cell line and representative blots are shown in Figs 5.11, 5.12, 5.13 and 5.14. Band intensities on the blot were compared using ImageJ (2.6.6). Each phosphorylated STAT1 band was normalised to the corresponding β-actin band and then compared to the phosphorylated STAT1 band intensity in the IFN control. Relative intensity values are shown in the graph below each blot.

In 2fTGH cells, no phosphorylated STAT1 was detected in the cells with no virus and no IFN (Fig. 5.11). Phosphorylated STAT1 was barely detectable in SFV4 infected cells, but was clearly present following addition of IFN following IFN challenge. In contrast to Fig. 5.8, in this experiment SFV4 infected cells had similar level of phosphorylated STAT1 following IFN treatment as the IFN control. Essentially, similar results to SFV4 were observed in lysates from 2fTGH cells infected with SFV4nsP3Δ50. In contrast, good levels of phosphorylated STAT1 was detected in 2fTGH cells infected with SFV4-RDR and these were increased only slightly following IFN treatment.

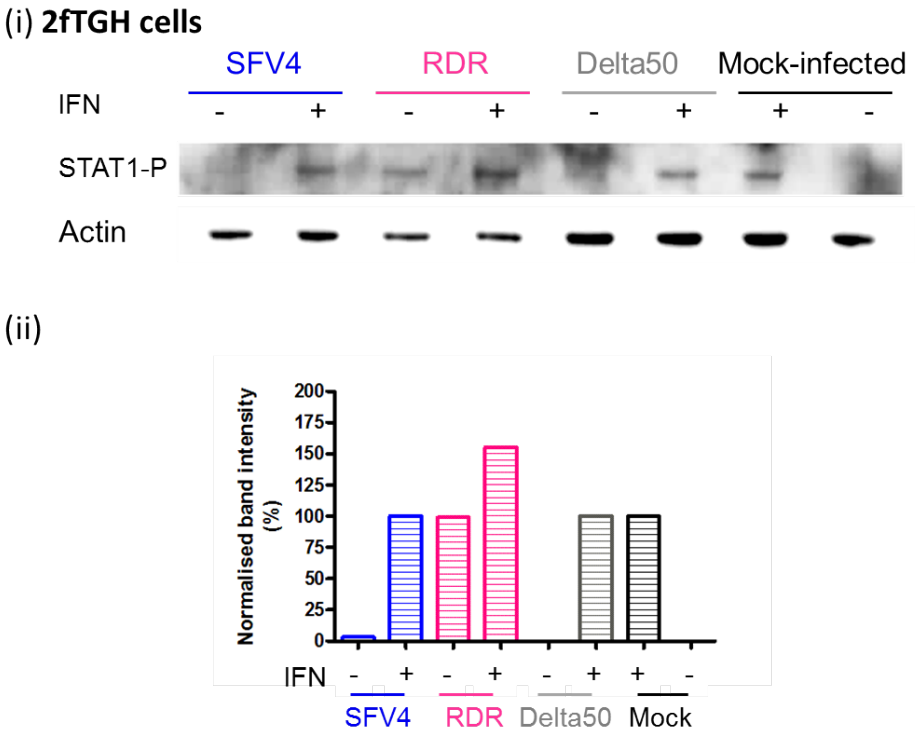

Figure 5.11: Western blot for phosphorylated STAT1 in 2fTGH cells infected with SFV4, SFV4-RDR or SFV4nsP3Δ50

(i) 2fTGH cells were infected with SFV4, SFV4-RDR or SFV4nsP3Δ50 at MOI 30 for 10 h or mock-infected and then treated with IFN-α (+) mock treated (-). A Western blot was carried out using the cell lysates and immunostained for phosphorylated STAT1 (STAT1-P) and then β-actin (Actin). The experiment was repeated three times and a representative blot is shown. (ii) The intensity of the bands on the blot was normalised to actin in each lane and then compared to the IFN control using ImageJ and a relative intensity graph was created.

The experiment was repeated in Hs 633T cells. Similar results were observed on Western blots using Hs 633T cells infected with SFV4, SFV4-RDR or SFV4nsP3Δ50 as described above (Fig. 5.12). As in the previous experiment (Fig. 5.8), SFV4 induced lower levels of phosphorylated STAT1 compared to the positive control. The SFV4 infected and IFN treated lysate band was approximately 30 % of the intensity of the positive control (Fig. 5.12.ii). Again, strong bands for phosphorylated STAT1 were detected in Hs 633T cells infected with SFV4-RDR both with and without IFN treatment.

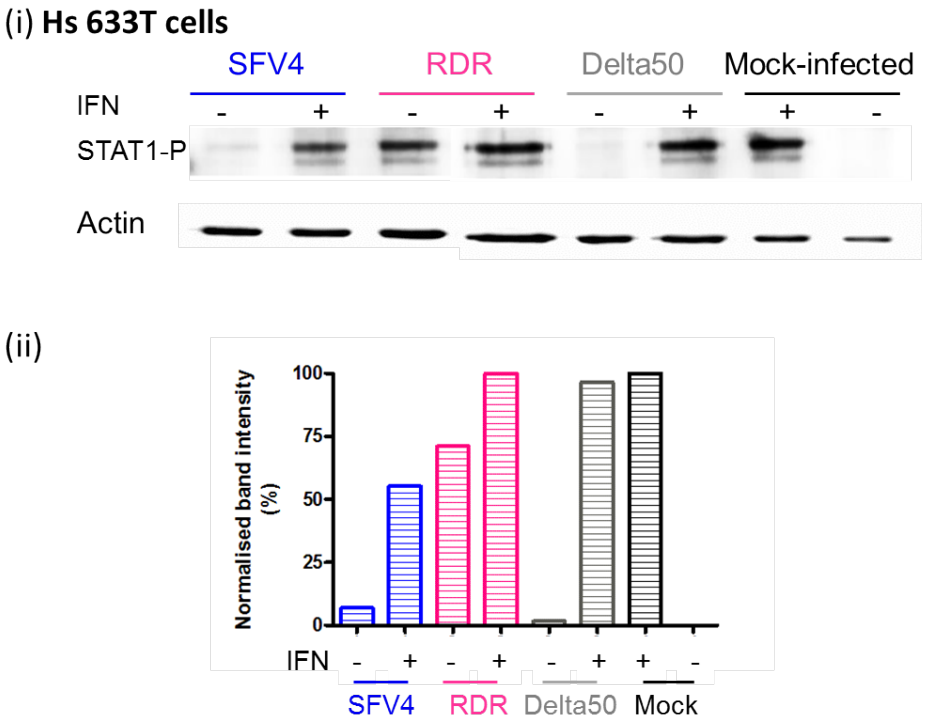

Figure 5.12: Western blot for phosphorylated STAT1 in Hs 633T cells infected with SFV4, SFV4-RDR or SFV4nsP3Δ50
(i) Hs 633T cells were infected with SFV4, SFV4-RDR or SFV4nsP3Δ50 at MOI 30 for 10 h or mock-infected and then treated with IFN-α (+) mock treated (-). A Western blot was carried out using the cell lysates and immunostained for phosphorylated STAT1 (STAT1-P) and then β-actin (Actin). The experiment was repeated three times and a representative blot is shown. (ii) The intensity of the bands on the blot was normalised to actin in each lane and then compared to the IFN control using ImageJ and a relative intensity graph was created.

To investigate if similar results would be observed in mouse fibroblasts, the experiment was repeated using L929 and NIH 3T3 cells. Similar results to 2fTGH and Hs 633T cells were observed in both cell lines (Figs 5.11, 5.12, 5.13 and 5.14). Phosphorylated STAT1 was only detected in cells infected with SFV4nsP3Δ50 following IFN treatment, apart from in the L929 cells (Figs 5.11, 5.12, 5.13 and 5.14). In NIH 3T3 cells, the results were more dramatic and no phosphorylated STAT1 was detected in SFV4 infected cultures even following IFN treatment (Fig. 5.14).

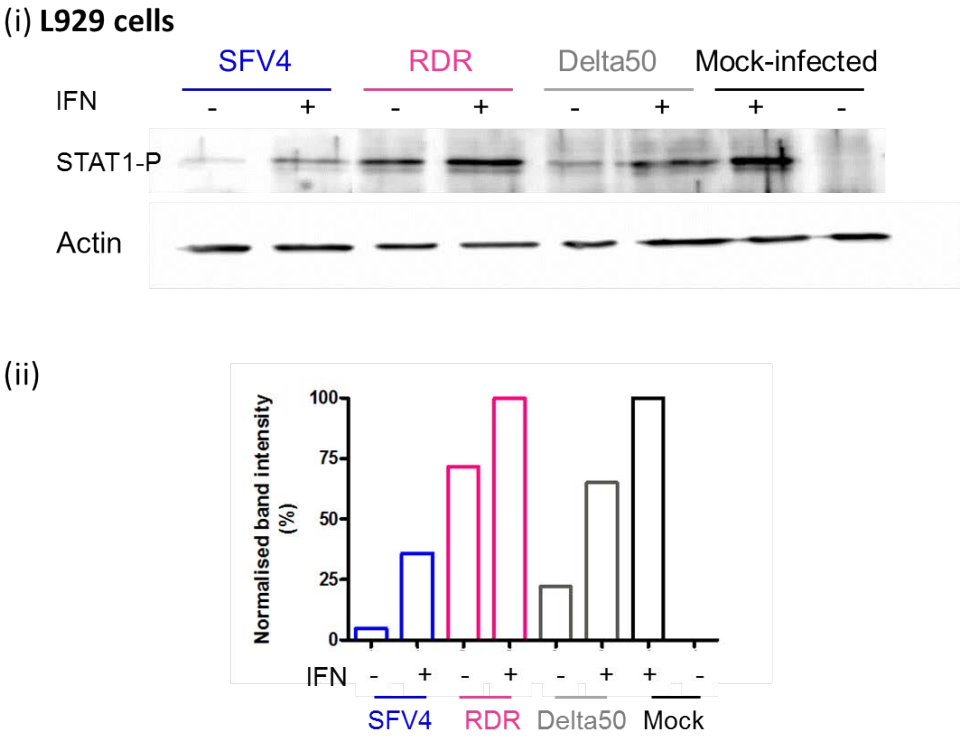

Figure 5.13: Western blot for phosphorylated STAT1 in L929 cells infected with SFV4, SFV4-RDR or SFV4nsP3Δ50

(i) L929 cells were infected with SFV4, SFV4-RDR or SFV4nsP3Δ50 at MOI 30 for 10 h or mock-infected and then treated with IFN-α (+) mock treated (-). A Western blot was carried out using the cell lysates and immunostained for phosphorylated STAT1 (STAT1-P) and then β-actin (Actin). The experiment was repeated three times and a representative blot is shown. (ii) The intensity of the bands on the blot was normalised to actin in each lane and then compared to the IFN control using ImageJ and a relative intensity graph was created.

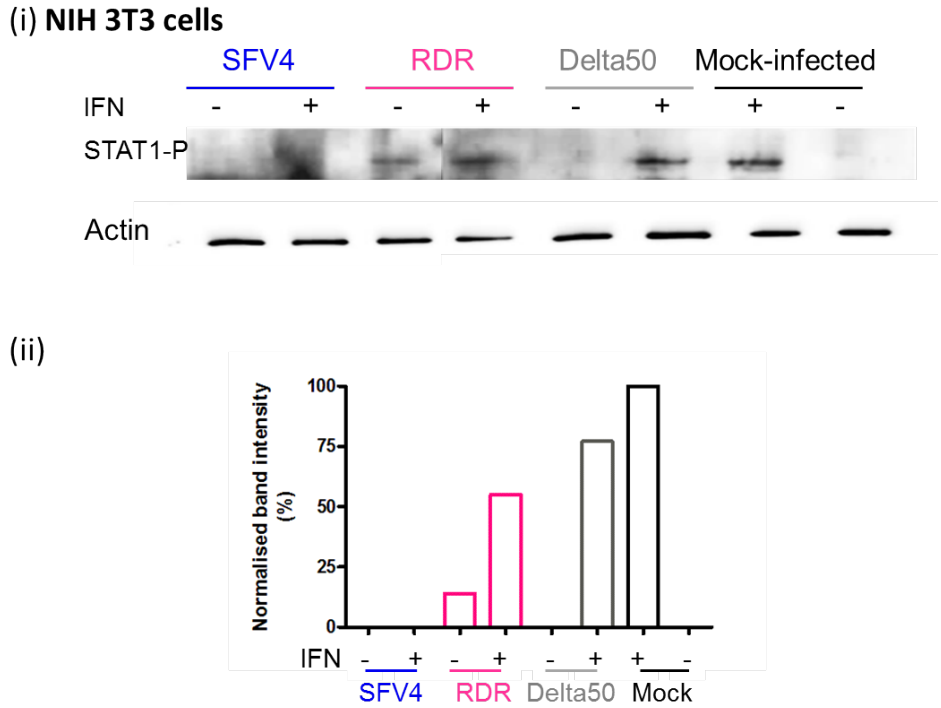

Figure 5.14: Western blot for phosphorylated STAT1 in NIH 3T3 cells infected with SFV4, SFV4-RDR or SFV4nsP3Δ50
(i) NIH 3T3 cells were infected with SFV4, SFV4-RDR or SFV4nsP3Δ50 at MOI 30 for 10 h or mock-infected and then treated with IFN-α (+) mock treated (-). A Western blot was carried out using the cell lysates and immunostained for phosphorylated STAT1 (STAT1-P) and then β-actin (Actin). The experiment was repeated three times and a representative blot is shown. (ii) The intensity of the bands on the blot was normalised to actin in each lane and then compared to the IFN control using ImageJ and a relative intensity graph was created.

In conclusion, in both human and mouse fibroblasts, infection with SFV4, SFV L10 or A7(74) results in no or only very low levels of phosphorylated STAT1 and SFV infection prevents IFN induced increase in levels of phosphorylated STAT1. The nsP2 NLS sequence is important in this suppression. NsP3 may also be involved.

5.2.4 Summary of findings

- In human and mouse fibroblasts, SFV4-RDR and SFV4nsP3Δ50 infection induced more IFN than SFV4 infection.
- Following pre-treatment of human and mouse fibroblasts with IFN; SFV4, SFV4-RDR and SFV4nsP3Δ50 showed a large reduction in replication. This

reduction was less extreme in SFV4-RDR and SFV4nsP3Δ50 infection than in SFV4 infection.

- In human and mouse fibroblasts, SFV4, SFV L10 and SFV A7(74) infection give rise to no or very low levels of phosphorylated STAT-1 and prevent an increase in these levels in response to IFN treatment.
- In human fibroblasts, SFV L10 infection induced lower levels of phosphorylated STAT1 than either SFV4 or SFV A7(74).
- In human and mouse fibroblasts, SFV4-RDR infection induced greater levels of phosphorylated STAT1 than SFV4. SFV4-RDR induced phosphorylation of STAT1 even without IFN treatment.
- SFV4nsP3Δ50 infection induced phosphorylation of STAT1 following IFN treatment. In general, SFV4nsP3Δ50 induced greater levels of phosphorylated STAT1 than SFV4.

5.3 Discussion

In chapter 4 it was demonstrated that strains of SFV induced the production of low levels of functional IFN in fibroblasts relative to SeV (Figs 4.6 and 4.7). This data suggests that SFV may antagonise the IFN system, either at the signalling or, most likely, the induction phase. The ability of SFV to antagonise IFN induction has been previously investigated in this laboratory (Breakwell *et al*., 2007). During SFV4 infection in MEFs, NF-$_K$B and IRF-3 both enter the nucleus, but fewer IFN-β transcripts are produced in comparison to the SFV4 mutant SFV4-RDR (Breakwell *et al*., 2007). The mechanism by which SFV antagonises the IFN induction pathway remains unclear and would be an interesting area of future research. IFN signalling in SFV infected cells has not been analysed. Recent studies have shown that the related alphaviruses CHIKV and SINV can inhibit IFN signalling by preventing the phosphorylation of STAT1 (Fros *et al.*, 2010; Simmons *et al.*, 2010). Phosphorylation of STAT1 is essential for IFN signalling. In this chapter, experiments were carried out to determine if SFV also inhibits the phosphorylation of STAT1 and, therefore, IFN signalling.

In the experiments presented here, all three strains were shown to inhibit the phosphorylation of STAT1 in four different fibroblast cell lines (Fig. 5.8). One possible explanation is that SFV infection does not induce IFN production and, therefore, no IFN is present to activate the IFN signalling pathway. An alternative explanation is that strains of SFV prevent the phosphorylation of STAT1 by directly antagonising the IFN signalling pathway. In general, levels of phosphorylated STAT1 were lower in SFV infected cells treated with IFN than in uninfected cells treated with IFN (Fig. 5.8). This data suggests that SFV can directly antagonise IFN signalling. However, experiments are required in the future to confirm that SFV can antagonise IFN signalling, perhaps using STAT1 or JAK1 reporter plasmids.

In human fibroblast cells, following SFV4, SFV L10 and SFV A7(74) infection different amounts of phosphorylated of STAT1 were detected (Fig. 5.8). Lower levels of phosphorylated STAT1 were detected following infection with SFV L10 than either SFV A7(74) or SFV4 (Fig. 5.9). In SINV infection, the virulence of different strains has been attributed to their ability to inhibit the phosphorylation of STAT1 (Simmons *et al.*, 2010). The ability of SFV L10 to inhibit the phosphorylation of STAT1 could explain the increased virulence of SFV L10 compared to SFV A7(74) or SFV4. In this hypothesis, SFV L10 inhibits the phosphorylation of STAT1 preventing IFN signalling and induction of the antiviral state more efficiently than SFV4 or SFV A7(74). However, similar results were not observed in mouse fibroblasts (Fig. 5.8). One possible explanation for this result is that the strains of SFV interact with the IFN system differently in human cells compared to in mouse cells.

In the data presented, all three strains of SFV were found to limit the phosphorylation of STAT1, either through antagonising IFN induction or IFN signalling. The decrease in phosphorylated STAT1 was not due to degradation of STAT1, as observed with paramyxoviruses (Fig. 5.10) (Young *et al.*, 2000;Andrejeva *et al.*, 2002;Parisien *et al.*, 2002). The flaviviruses WNV (Guo *et al.*, 2005), JEV (Lin *et al.*, 2004), Langat virus (Best *et al.*, 2005) and DENV (Ho *et al.*, 2005) all inhibit the phosphorylation of STAT1 and IFN signalling. The flavivirus protein NS5 inhibits the phosphorylation of STAT1 by preventing the activation of proteins upstream in the pathway (Lin *et al.*, 2004;Ho *et al.*, 2005;Guo *et al.*, 2005;Best *et al.*, 2005). NS5 can also inhibit IFN signalling by binding to STAT2 and sequestering the protein for degradation (Ashour *et al.*, 2009). In DENV infection, another protein called NS4B also prevents the phosphorylation of STAT1 (Munoz-Jordan *et al.*, 2003).

The mechanism by which alphaviruses may inhibit the phosphorylation of STAT1 and the virus proteins involved remain to be elucidated. The literature suggests a role for nsP2 in CHIKV infection (Fros *et al.*, 2010) and nsP1 in SINV infection (Simmons *et al.*, 2010). To investigate the potential role of SFV nsP2, a mutant with a point mutation in the NLS, SFV4-RDR, was utilised (Rikkonen *et al.*, 1992). SFV4 and SFV4-RDR both have similar replication kinetics in BHK-21 cells

(Rikkonen *et al.*, 1992), both induce protein shutoff at similar rates (Breakwell *et al.*, 2007) and neither virus inhibits the translocation of the transcription factors NF-$_k$B and IRF-3 to the nucleus (Breakwell *et al.*, 2007). However, SFV4-RDR replicates less efficiently and induces more IFN than SFV4 in MEFs (Breakwell *et al.*, 2007). Furthermore, SFV4-RDR is less virulent in mice than SFV4 (Fazakerley *et al.*, 2002). These results suggest that (i) SFV4-RDR cannot inhibit the IFN pathway, either induction or signalling, as efficiently as SFV4, (ii) nsP2 is important in mediating the interaction of SFV with the IFN pathway and (iii) the difference in IFN induction between SFV4-RDR and SFV4 is not due to differences in the translocation of the transcription factors or host protein shutoff. In the data presented here, SFV4-RDR induced significantly more IFN than SFV4 in four different fibroblast cell lines as expected (Fig. 5.3). SFV4-RDR also induced greater levels of phosphorylated STAT1 than SFV4 in four different fibroblast cell lines, even without the addition of IFN (Figs 5.11, 12, 13 and 14). This data suggests that WT nsP2 is required to prevent IFN signalling, either through differing induction or differing antagonism of the IFN signalling pathway relative to SFV4. NsP2 is a multifunctional protein that probably interacts with the type-I IFN pathway at various stages.

The mechanism by which WT nsP2 inhibits the phosphorylation of STAT1 is an exciting area of research within our laboratory. One possible mechanism by which nsP2 could inhibit STAT1 phosphorylation is that nsP2 enters the nucleus and inhibits IFN induction, probably via shutoff of transcription, and prevents the downstream phosphorylation of STAT1. SFV4-RDR nsP2 only enters the nucleus at low levels (Rikkonen *et al.*, 1992) and, therefore, would be less efficient at inhibiting this process. A recent study on SINV infection in NIH 3T3 cells demonstrated that inhibition of IFN production occurs at approximately 2 h post-infection, while the phosphorylation of STAT1 is inhibited at between 6 to 8 h post-infection (Frolov *et al.*, 2012). The authors suggest that SINV can inhibit the IFN response, probably via shutoff of transcription, before preventing the phosphorylation of STAT1. Another possible mechanism is that nsP2 binds STAT1 or a protein important in STAT1 phosphorylation in the cytoplasm and this inhibits the phosphorylation of STAT1. In SFV4-RDR, the structure of nsP2 is altered which may affect its ability to interact

with other proteins. Current experiments in our laboratory provide strong evidence for the second mechanism (Dr. Gerald Barry, personal communication).

The role of SFV nsP3 as a virulence determinant is not fully elucidated. The literature suggests that nsP3 functions in replication of the virus genome (Peranen *et al.*, 1988;Hahn *et al.*, 1989;de Groot *et al.*, 1990;Peranen, 1991;Lemm & Rice, 1993;Lemm *et al.*, 1994;Shirako & Strauss, 1994;Wang *et al.*, 1994;Strauss & Strauss, 1994;LaStarza *et al.*, 1994a;Peranen *et al.*, 1995;Salonen *et al.*, 2003;Neuvonen *et al.*, 2011) and as a virulence determinant (Tarbatt *et al.*, 1997;Tuittila *et al.*, 2000;Tuittila & Hinkkanen, 2003). In this chapter, the mutant virus SFV4nsP3Δ50 was utilised to investigate the hyperphosphorylated region of nsP3. SFV4nsP3Δ50, which has a deletion of 50 amino acids in the hypervariable domain of nsP3, replicates less efficiently *in vitro* and is less virulent *in vivo* than SFV4 (Vihinen *et al.*, 2001). One possible explanation for the difference between SFV4 and SFV4nP3Δ50 is that SFV4nsP3Δ50 does not inhibit the IFN response as efficiently as SFV4. In the data presented here, SFV4nsP3Δ50 generally induced significantly more IFN production than SFV4 in fibroblasts (Fig. 5.4). However, unlike SFV4-RDR, phosphorylated STAT1 was normally detected in cells infected with SFV4nsP3Δ50 only following IFN treatment (Figs 5.11, 5.12, 5.13 and 5.14). This suggests that if nsP3 interacts with the IFN system, it is by a different mechanism from that of nsP2.

One possible explanation for the difference in IFN induction between SFV4 and SFV4nsP3Δ50 is that the hypervariable region of nsP3 inhibits proteins within the IFN induction and/or signalling pathways. Yeast-2-hybrid assays are underway within our laboratory to investigate which cellular proteins SFV nsP3 and, in addition, CHIKV nsP3 bind to. It will be interesting to see if the proteins identified are involved in the IFN response. An alternative explanation for the difference in IFN induction between SFV4 and SFV4nsP3Δ50 is that SFV4nsP3Δ50 replicates less efficiently than SFV4. A recent report suggests that the hyperphosphorylated region is important for replication of the virus genome (Neuvonen *et al.*, 2011). It would be extremely interesting to investigate SFV4nsP3Δ50 further and determine how it is affecting IFN induction.

One objective of this chapter was to investigate whether SFV4-RDR and SFV4nsP3Δ50 differed in their sensitivity to IFN compared to SFV4. Both SFV4-RDR and SFV4nsP3Δ50 are less virulent compared to SFV4 *in vivo* (Vihinen *et al.*, 2001). Therefore, it was hypothesised that SFV4-RDR and SFV4nsP3Δ50 would be more sensitive to the effects of IFN pre-treatment than SFV4 and that this would explain the virulence in mice. However, SFV4-RDR and SFV4nsP3Δ50 appeared to be less affected by IFN pre-treatment than SFV4 (Figs 5.6 and 5.7). One possible explanation for the apparent different sensitivity of SFV4 and the mutant viruses to IFN pre-treatment is that the mutant viruses initially infect fewer cells in culture that SFV4 which is, in part, due to the IFN response (Breakwell *et al.*, 2007). IFN pre-treatment renders the majority of the culture into an antiviral state. The difference between IFN treated and untreated cultures would be more apparent in SFV4 infections compared to SFV4-RDR, as a greater percentage of cells were initially infected by SFV4 and would now be protected.

5.3.1 Final summary

The data presented in chapter 4 and 5 suggests that SFV may antagonise the IFN pathway at both the induction and signalling stage. SFV appears to directly inhibit IFN signalling by limiting the phosphorylation of STAT1, either by directly binding STAT1 or by preventing upstream events. The NLS motif in nsP2 was required for this function, as demonstrated using SFV4-RDR. This finding could explain why SFV4-RDR is less virulent in mice than SFV4. The role of nsP3 remains unclear, but the data presented here enhances our understanding. SFV4nsP3Δ50 replicated less efficiently and induced more IFN than SFV4. Future studies could include determining (i) how SFV inhibits IFN induction; (ii) the mechanism by which SFV inhibits IFN signalling and (iii) the interaction of nsP3 with the IFN pathway.

Chapter 6: Comparison of the genetic sequences of SFV4, SFV L10 and SFV A7(74).

Contents

6.1 Introduction

SFV was one of the first viruses to be sequenced. In 1980 the structural protein ORF of Prototype virus was sequenced, followed by the nsP ORF in 1986 (Garoff *et al.*, 1980;Takkinen, 1986). However, these sequences were generated using the technology available at the time and subsequent studies have identified several mistakes. Newer sequences have been generated and published in online databases; in 2002 the original Prototype sequence (accession number J02361.1) was replaced with an SFV sequence labelled SFV 42S RNA genome (accession number X04129) in the NCBI database. To allow accurate comparisons between studies in the literature, it is important to identify the original SFV isolate(s) and the laboratory where the various strains of SFV were derived. This thesis has focused on the laboratory strains of SFV held at the University of Edinburgh (EDI): SFV L10, SFV A7(74) and SFV4. The history of each of these strains is summarised below and in Table 6.1.

6.1.1 SFV L10

SFV L10 was isolated from a pool of 130 *Aedes africanus* mosquitoes captured in the Semliki Forest, Uganda (Smithburn & Haddow, 1944) and passaged eight times by *ic* inoculation in adult mouse brains followed by two passages *ic* in neonatal mouse brains (Bradish *et al.*, 1971). Prototype virus was isolated from the same mosquito sample as SFV L10 and passaged 4 times by *ic* inoculation in mice (Bradish *et al.*, 1971). Historically, the literature has referred to SFV L10 and Prototype virus interchangeably. However, the strains underwent different passaging conditions, as mentioned above, which may have selected for differences in the genetic sequence (Bradish *et al.*, 1971). There are no published studies that analyse the genetic sequence of SFV L10.

The laboratory strain of SFV L10 used in EDI was provided by Prof. H.E. Webb, St. Thomas' Hospital, London, England and has been stored at -80^{o}C with minimum passage. This virus was obtained by Prof. Webb from Dr C. Bradish at Porton Down. This SFV L10 has been used in several studies both in EDI and previously at St Thomas' Hospital (Oaten *et al.*, 1980;Amor & Webb, 1986;Khalili-Shirazi *et al.*, 1988;Fazakerley *et al.*, 1993;Fazakerley, 2002). The stock of SFV L10 held at EDI, referred to in this chapter as L10-EDI, has not been sequenced. An SFV

sequence labelled ‘L10’ was deposited in the NCBI database, accession number Ay112987, by Logue *et al*., 2002 from Trinity College Dublin, Ireland (IRE). The provenance of this L10-IRE is unclear.

6.1.2 SFV4

SFV4 was generated as a molecular cDNA clone of Prototype virus expressed under the control of a SP6 promoter (also known as SP6-SFV4) (Liljestrom *et al.*, 1991). Since the creation of SFV4, multiple studies have used it to generate mutant viruses, such as SFV4-RDR and SFV4nsP3Δ50 (Rikkonen *et al.*, 1992;Vihinen *et al.*, 2001). SFV L10 and SFV4 have similar replication kinetics in cell culture. SFV4 is virulent in adult mice following *ic* inoculation or *in* inoculation at high dose. However, unlike L10-EDI, *ip* inoculation with SFV4 is avirulent in adult mice, unless administered at high dose (Glasgow *et al*., 1991;Fazakerley, 2002).

Our plasmid stock of SFV4 was obtained from Prof. A. Merits, Institute of Technology, University of Tartu, Estonia. Prof. Merits has compiled and verified the sequence of SFV4 by Solexa (Illumina) sequencing and this sequence will be termed SFV4-EST. The SFV4-EST plasmid originated from the Karoliska institute in Sweden and was created by Liljestrom *et al* (1991). The published sequence of this will be termed SFV4-SWE.

6.1.3 SFV A7(74)

The SFV strain AR2006 was isolated from *Aedes argenteopunctatus* mosquitoes in Mozambique (McIntosh *et al.*, 1961). SFV A7 was derived from the AR2006 strain of SFV by passaging seven times by *ic* inoculation in neonatal mice. SFV A7(74) was derived from the AR2006 strain of SFV by passaging seven times by *ic* inoculation in neonatal mice, followed by two clonal selections from plaques in monolayers of primary chick embryo cells (CEFs) (Bradish *et al.*, 1971).

One sequence for SFV A7(74) is available in the literature: SFV A7(74) determined by Santagati *et al* (1994), University of Turku, Finland. This sequence was supplied by Dr. A. Hinkkanen, University of Turku, Finland. A sequence for SFV A7 is also available; published by Tarbatt *et al*., (1997), Trinity College, Dublin, Ireland. In this chapter the sequences generated in Finland and Ireland will be termed A7(74)-FIN and A7-IRE respectively. A7(74)-FIN was obtained from Prof. Webb, St. Thomas’ Hospital, London, England who received the virus from Dr.

Bradish, Porton Down, England. The source of A7-IRE in Tarbatt *et al* (1997) was not reported. Another strain of SFV A7(74) referenced in the literature was obtained from Prof. H. Smith, University of Birmingham, England. This will be referred to as A7(74)-BIR (Logue *et al.*, 2008). The sequence of A7(74)-BIR is not available in the NCBI database.

The version of SFV A7(74) held at EDI, like A7(74)-FIN, was obtained from Prof. Webb, St. Thomas' Hospital, London, England, and has since been used in many studies (Fazakerley & Webb, 1987;Fazakerley *et al.*, 1988;Fazakerley *et al.*, 1993). This version of SFV A7(74), termed A7(74)-EDI, has not been sequenced. However, a considerable body of research exists on this virus. A7(74)-EDI is virulent in mice under 11 days old and, like L10-EDI, rapidly spreads throughout the brain. However, as mice become older the spread of A7(74)-EDI is restricted, at least in the brain, to perivascular foci and the mice survive (Pathak & Webb, 1974;Fleming, 1977;Fazakerley *et al.*, 1993;Oliver *et al.*, 1997;Oliver & Fazakerley, 1998).

6.1.4 Objectives

1. Sequence L10-EDI and A7(74)-EDI by Solexa (Illumina) sequencing and confirm sequences using PCR.
2. Align and compare the genetic sequence of L10-IRE with L10-EDI at the nucleotide and amino acid level to identify differences.
3. Align and compare the genetic sequence of A7-IRE and A7(74)-FIN with A7(74)-EDI at the nucleotide and amino acid level to identify differences.
4. Align and compare the genetic sequence of L10-EDI and A7(74)-EDI with SFV4-EST at the nucleotide and amino acid level to identify differences.

6.2.1 Solexa (Illumina) sequencing of SFV4-EST, L10-EDI and A7(74)-EDI

Details of the virus strains used in the following section are provided in Table 6.1. A schematic diagram depicting the genome of SFV is shown in Fig. 1.1.

Table 6.1: Strains of SFV referred to in chapter 6.

Virus	Name in chapter 6	Background	References
Prototype virus	Prototype virus	Isolated from a pool of 130 *Aedes africanus* mosquitoes captured in the Semliki Forest, Uganda and passaged 4 times by *ic* inoculation in mice. Complete genome sequenced, accession number X04129.	(Smithburn & Haddow, 1944;Bradish *et al.*, 1971;Garoff *et al.*, 1980;Takkinen, 1986).
SFV L10	L10-EDI	Edinburgh stock. Isolated from a pool of 130 *Aedes africanus* mosquitoes captured in the Semliki Forest, Uganda and passaged eight times by *ic* inoculation in adult mouse brains followed by two passages *ic* in neonatal mouse brains. Obtained from, Prof. Webb, St. Thomas' Hospital, London, England, who received it from Dr. Bradish, Porton Down, England. Not sequenced.	(Smithburn & Haddow, 1944;Bradish *et al.*, 1971)
SFV L10	L10-IRE	Unknown origin. Accession number AY112987.	(Logue *et al.*, 2002)
SFV4	SFV4-SWE	cDNA clone generated from Prototype virus.	(Liljestrom *et al.*, 1991)
SFV4	SFV4-EST	Edinburgh stock. cDNA clone of Prototype virus obtained from Prof. P. Liljestrom, Karolinska Insitute, Stockholm, Sweden and sequenced by Prof. Merits, Institute of Technology, University of Tartu, Estonia.	
SFV A7(74)	A7(74)-EDI	Edinburgh stock. Derived from the AR2006 strain of SFV that was isolated from *Aedes argenteopunctatus* mosquitoes in Mozambique. AR2006 was passaged seven times by *ic* inoculation in neonatal mice, followed by clonal selection from plaques in monolayers of primary CEFs to give SFV A7(74). Obtained from Prof. Webb, St. Thomas' Hospital, London, England, who received it from Dr. Bradish, Porton Down, England. Not sequenced.	(McIntosh *et al.*, 1961;Bradish *et al.*, 1971)
SFV A7(74)	A7(74)-FIN	Same background as A7(74)-EDI, which is described above. Sequenced by Santagati *et al* (1994), University of Turku, Finland. Sequence from Dr. Hinkkanen, University of Turku, Finland.	(Santagati *et al.*, 1994)
SFV A7(74)	A7(74)-BIR	Unknown origin. Obtained from Prof. Smith, University of Birmingham, UK and the 5' UTR was sequenced by Logue *et al* (2008).	(Logue *et al.*, 2008).
SFV A7	A7-IRE	Unknown origin. Accession number Z48163.	(Tarbatt *et al.*, 1997)

The complete genomes of L10-EDI and A7(74)-EDI were determined using Solexa (Illumina) sequencing at the Roslin Institute's ARKgenomics facility (2.13.2). The sequences generated were named ARKL10-EDI for L10-EDI and ARKA7(74)-EDI for A7(74)-EDI. The complete sequences are shown in Appendix 1.

6.2.2 Comparison of the nsP2 and nsP3 sequences generated by Solexa (Illumina) sequencing and by PCR sequencing

To confirm that the sequences of ARKL10-EDI and ARKA7(74)-EDI generated by Solexa (Illumina) sequencing and subsequent bioinformatic analysis were correct, PCR sequencing was carried out to determine the sequences of nsP2 and nsP3 in L10-EDI and A7(74)-EDI (2.13.1). SFV4-EST was included to confirm the sequence of SFV4-EST. NsP2 and nsP3 were chosen for PCR sequencing, as these proteins were studied in chapter 5.

At the amino acid level, the nsP2 and nsP3 PCR derived sequence for A7(74)-EDI aligned perfectly to ARKA7(74)-EDI (data not shown). Similarly, the nsP2 and nsP3 PCR derived amino acid sequence for SFV4-EST aligned perfectly to SFV4-EST (data not shown). The amino acid PCR derived sequence for L10-EDI nsP3 also aligned perfectly to ARKL10-EDI nsP3 (data not shown). However, the L10-EDI PCR derived amino acid sequence for nsP2 had a single difference at position 754 compared to ARKL10-EDI. The PCR was repeated and this result was confirmed. This variation at amino acid 754 is likely to represent genetic variation within the population. Solexa (Illumina) sequencing identifies all RNA sequences in the sample, while PCR often amplifies one genotype. Both amino acids at position 754 were hydrophilic (aspartic acid in ARKL10-EDI and asparagine in L10-EDI). This substitution is unlikely to affect the secondary structure of nsP2. Taken together, this data confirms the accuracy of the Solexa (Illumina) sequences of nsP2 and nsP3 in L10-EDI, A7(74)-EDI and SFV4-EST.

6.2.3 Comparison of the genetic sequences of L10-IRE to L10-EDI at the nucleotide and amino acid level.

The complete genetic sequences of ARKL10-EDI and L10-IRE were aligned and compared for nucleotide differences (Table 6.2). Across the genome, 19 nucleotide differences were identified between ARKL10-EDI and L10-IRE. These differences mainly mapped to nsP2. The structural ORF sequence was identical between both strains. Nucleotide position 1 in L10-IRE was G. This was not present in ARKL10-

EDI and may be an error in the L10-IRE sequence. The L10-IRE sequence was most likely generated from cDNA cloned into a DNA vector and the extra G is probably the last nucleotide of the SP6 vector promoter.

Table 6.2: Nucleotide changes in L10-IRE compared to ARKL10-EDI.
Numbering is according to the nucleotide (nt) position in ARKL10-EDI. -, gap in sequence.

nt Position	L10-EDI	L10-IRE	Region
0	-	G	5' UTR
101	C	T	nsP1
1016	G	A	nsP1
1066	C	A	nsP1
1084	C	A	nsP1
- (2375 in L10-IRE)	-	G	nsP2
- (2376 in L10-IRE)	-	A	nsP2
2388	C	-	nsP2
2398	G	-	nsP2
2534	G	A	nsP2
2562	T	C	nsp2
2612	C	A	nsP2
2661	C	G	nsP2
3858	G	-	nsP2
3859	C	-	nsP2
3860	C	-	nsP2
5847	C	G	nsP4
5898	T	C	nsP4
6348	C	A	nsP4

Next, the genetic sequence of ARKL10-EDI and L10-IRE were compared at the amino acid level (Table 6.3). Between ARKL10-EDI and L10-IRE, 18 amino acid differences were identified of which 11 produced a change in biochemistry. Amino acids 227 – 234 in nsP2 are probably the result of a frame-shift (personal communication with Prof. Merits). Most noteworthy is the substitution of a ^{103}arginine residue in L10-IRE to a ^{103}proline residue in L10-EDI, which is located in nsP4. Proline disrupts the secondary structure of proteins and is normally located at the end of α-helices or β-sheets.

The replicase region of L10-IRE differed substantially from L10-EDI at both the nucleotide and amino acid level (Tables 6.2 and 6.3). Possible explanations for

the sequence differences between ARKL10-EDI and L10-IRE include (i) the strains were passaged differently and this selected for differences in the genetic sequence or, more likely, (ii) there are errors in the L10-IRE replicase sequence.

Table 6.3: Amino acid changes in L10-IRE compared to ARKL10-EDI.
Numbering is according to the amino acid (aa)[1] position in ARKL10-EDI or aa[2] position in individual ARKL10-EDI proteins. Dark grey, hydrophilic amino acid residue; light grey, hydrophobic amino acid residue; white, weakly hydrophilic and -, gap in sequence.

Region	nsP1	
aa position[1]	6	311
aa position[2]	6	311
L10-EDI	H	E
L10-IRE	Y	K

Region	nsP2												
aa position[1]	764	765	766	767	768	770	771	817	826	843	859	1258	1259
aa position[2]	227	228	229	230	231	233	234	280	289	306	322	721	722
L10-EDI	L	D	I	Q	A	T	V	D	M	H	S	S	L
L10-IRE	N	W	T	S	R	N	S	N	T	N	C	-	I

Region	nsP4		
aa position[1]	1921	1938	2088
aa position[2]	103	120	270
L10-EDI	P	V	A
L10-IRE	R	A	D

6.2.4 Comparison of the genetic sequences of A7(74)-FIN and A7-IRE to A7(74)-EDI at the nucleotide and amino acid level.

Much of our understanding about SFV A7(74) is from studies using A7(74)-EDI, A7(74)-FIN and A7-IRE (Glasgow *et al.*, 1994;Santagati *et al.*, 1995;Tarbatt *et al.*, 1997;Tuittila *et al.*, 2000;Tuittila & Hinkkanen, 2003;Neuvonen *et al.*, 2011). To determine if ARKA7(74)-EDI, A7(74)-FIN and A7-IRE have similar sequences, the complete genetic sequences of the three strains were aligned and compared for nucleotide differences (Table 6.4). Across the genome, five nucleotide differences were identified between ARKA7(74)-EDI and A7(74)-FIN. One difference was at position 21 in the 5' untranslated region (UTR) where ARKA7(74)-EDI encoded G and A7(74)-FIN A. However, the A in A7(74)-FIN is likely to be a sequencing error; in Logue *et al* (2008), it is reported that A7(74)-FIN contains G at nucleotide position 21 not A.

On comparing the genetic sequence of ARKA7(74)-EDI and A7-IRE, 11 nucleotide differences were identified, these were located throughout the genome. In addition, A7-IRE encoded an extra 2771 nucleotides in the 3' UTR, which were not present in ARKA7(74)-EDI. On blasting the 2771 nucleotide sequence in the NCBI database, the sequence had 99 % homology to the pSP64 cloning vector. Therefore, these additional nucleotides are actually part of the cloning vector and not the A7-IRE sequence. Possible explanations for the other genetic differences between ARKA7(74)-EDI and A7-IRE include (i) the strains were passaged differently in the laboratory and this selected for differences in the genetic sequence or (ii) errors were made during sequencing of A7-IRE, possibly during reverse transcription or the PCR stage.

Table 6.4: Nucleotide changes in A7(74)-FIN and A7-IRE compared to ARKA7(74)-EDI.

Numbering is according to the nucleotide (nt) position in ARKA7(74)-EDI. Red highlights nucleotide differences compared to the ARKA7(74)-EDI sequence.

nt position	A7(74)-EDI	A7(74)-FIN	A7-IRE	Region
21	G	A	A	5' UTR
35	A	A	T	5' UTR
42	T	T	C	5' UTR
223	T	T	C	nsP1
256	T	T	C	nsP1
3701	A	A	G	nsP2
3883	C	T	C	nsP2
4124	A	G	A	nsP3
5881	A	T	A	nsP4
6313	T	T	A	nsP4
6721	A	G	A	nsP4
7183	C	C	T	capsid
10802	C	C	A	E1
11336	T	T	C	E1
11704	A	A	G	E1
11758 – 14529	-	-	2771 nt	3’ UTR

Next the genetic sequence of ARKA7(74)-EDI, A7(74)-FIN and A7-IRE were compared at the amino acid level (Table 6.5). Only one amino acid substitution was identified between ARKA7(74)-EDI and A7(74)-FIN; nsP3 at position 11 is isoleucine in ARKA7(74)-EDI and valine in A7(74)-FIN. As isoleucine and valine are both hydrophobic amino acids, this substitution is unlikely to affect the structure and function of nsP3. The high sequence similarity between ARKA7(74)-EDI and A7(74)-FIN suggests that observations made using A7(74)-FIN virus would be applicable to A7(74)-EDI virus and the single amino acid difference fits well with the very close ancestry of these viruses (both from Prof. Webb in London).

At the amino acid level ARKA7(74)-EDI and A7-IRE were also extremely similar with only two amino acid differences; of which only one is likely to produce a change in biochemistry. In nsP2 at amino acid position 669, ARKA7(74)-EDI had a

serine while A7-IRE had a glycine. Glycine is a small amino acid, which can have a large impact on the secondary structure of proteins.

Table 6.5: Amino acid changes in A7(74)-FIN and A7-IRE compared to ARKA7(74)-EDI.
Numbering is according to the amino acid (aa)[1] position in ARKA7(74)-EDI and aa[2] position in individual ARKA7(74)-EDI proteins. Dark grey, hydrophilic amino acid residue; light grey, hydrophobic amino acid residue and white, weakly hydrophilic.

Region	nsP2	nsP3	E1
aa position[1]	**1206**	**1347**	**1134**
aa position[2]	**669**	**11**	**319**
A7(74)-EDI	S	I	T
A7(74)-FIN	S	V	T
A7-IRE	G	I	K

In conclusion, the high sequence similarity between ARKA7(74)-EDI, A7-IRE and, in particular, A7(74)-FIN suggests that observations made using these viruses are applicable to A7(74)-EDI.

6.2.5 Comparison of the sequences of L10-EDI and A7(74)-EDI to SFV4-EST at the nucleotide and amino acid level.

Most of the SFV pathogenesis work has been done using L10-EDI, A7(74)-EDI and SFV4-EST and it is for these viruses that there is a need to relate phenotype to genotype. The complete genetic sequences of ARKL10-EDI, ARKA7(74)-EDI and SFV4-EST will first be compared at the amino acid level. Amino acid substitutions resulting in a change in the biochemistry of the amino acid are potentially the most important as these could affect the secondary and tertiary structure of the protein and, therefore, its function. Following consideration of changes at the protein level, change in the 5' and 3' UTR and the inter-genic region between the two ORFs will be considered.

SFV4-EST and ARKL10-EDI were almost identical across the genomes. In the replicase region, ARKL10-EDI had only one amino acid substitution compared to

SFV4-EST. This was in nsP3 at amino acid position 48 (Table 6.6). The expression of a hydrophobic amino acid in ARKL10-EDI (^{48}alanine) compared to a hydrophilic amino acid in SFV4-EST (^{48}glutamic acid) could alter the structure of nsP3. This difference is analysed further in section 6.2.7. In the structural region, 5 amino acid substitutions were identified between SFV4-EST and ARKL10-EDI. These were located in the capsid protein and envelope glycoprotein (E) 2. Biochemically, the greatest difference was between a hydrophilic amino acid and a neutral amino acid in the capsid protein: ^{63}arginine in SFV4-EST and ^{63}glycine in ARKL10-EDI. The capsid protein facilitates the packaging of viral RNA (Frolova *et al*., 1997). The change of glycine to arginine at position 63 could affect this process. The amino acid substitutions identified in nsP3 and capsid are likely determinants of the virulence difference between SFV4-EST and L10-EDI in adult mice (L10-EDI is virulent following low dose extraneural inoculation whereas SFV4-EST is not).

The sequence of ARKA7(74)-EDI differed substantially from SFV4-EST. Across the genome, ARKA7(74)-EDI had 36 different amino acid residues, a deletion of seven amino acids and an opal stop codon compared to SFV4-EST. Most of these differences mapped to nsP3. In nsP1, two substitutions replaced a hydrophobic amino acid residue with a hydrophilic one; ^{237}cysteine in SFV4-EST and ^{237}serine in ARKA7(74)-EDI; ^{308}tyrosine in SFV4-EST and ^{308}histidine in ARKA7(74)-EDI. Cysteine can make covalent bonds while histidine is charged, therefore these could be particularly important substitutions. In nsP2, the greatest biochemical change was ^{515}valine in SFV4-EST to ^{515}glutamic acid in ARKA7(74)-EDI. This changes a hydrophobic residue to a charged hydrophilic one. Amino acid 515 is located in the nsP2 protease domain and is associated with cleavage of the replicase polyprotein (Merits *et al.*, 2001). This difference is analysed further in section 6.2.6. In nsP3, four substitutions produced large changes in the amino acid biochemistry. These substitutions were located in the macro domain (positions 48 and 70) and the hypervariable domain (positions 394 and 442). In addition, ARKA7(74)-EDI nsP3 had an opal codon at position 476, which was not present in SFV4-EST or ARKL10-

EDI. In SFV4-EST and ARKL10-EDI the opal codon was replaced by an arginine codon. ARKA7(74)-EDI had a deletion of seven amino acids (^{386}A – GIADLA) in the nsP3 hypervariable domain. The differences in nsP3 between SFV4-EST (or ARKL10-EDI) and ARKA7(74)-EDI were substantial at the biochemical level and may be responsible for the difference in virulence in adult mice between these strains. In nsP4, two amino acid substitutions were identified. These were very conservative changes; aspartic acid to glutamic acid, both of which are negatively charged, arginine to lysine, both of which are positively charged.

In the capsid protein, one amino acid difference was identified between SFV4-EST and ARKA7(74)-EDI, which replaced a hydrophobic amino acid for a hydrophilic or neutral one: ^{62}arginine in SFV4-EST and ^{62}glycine in ARKA7(74)-EDI. In E3, one amino acid substitution switched a hydrophobic residue for a hydrophilic one (^{12}alanine in SFV4-EST and ^{12}threonine in ARKA7(74)-EDI). In E2, only one amino change was non-conservative; ^{215}methionine in SFV4-EST to ^{215}lysine in ARKA7(74)-EDI. Finally, in E1, three amino acid changes substituted a hydrophobic amino acid residue for a hydrophilic one: ^{65}arginine in SFV4-EST and ^{65}serine in ARKA7(74)-EDI, ^{228}methionine in SFV4-EST and ^{228}threonine in ARKA7(74)-EDI, and ^{297}isoleucine in SFV4-EST and ^{297}threonine in ARKA7(74)-EDI.

Table 6.6: Amino acid changes in ARKL10-EDI and ARKA7(74)-EDI compared to SFV4-EST.
Numbering is according to the amino acid (aa)[1] position in SFV4-EST and aa[2] position in individual SFV4-EST proteins. Dark grey, hydrophilic amino acid residue; light grey, hydrophobic amino acid residue; white, weakly hydrophilic; -, gap in sequence and *, opal codon. Circles identify changes ARKA7(74)-EDI most likely to affect structure and function: red, ARKL10-EDI compared to SFV4-EST; green, ARKA7(74)-EDI compared to SFV4-EST.

Region	nsP1						nsP2			
aa position[1]	237	308	387	427	484	534	679	1052	1216	1258
aa position[2]	237	308	387	427	484	534	142	515	679	721
SFV4	C	Y	I	R	V	H	V	V	F	S
L10	C	Y	I	R	V	H	V	V	F	S
A7(74)	S	H	V	K	A	R	I	E	Y	N

Region	nsP3															nsP4	
aa position[1]	1384	1406	1537	1585	1722	1723	1724	1725	1726	1727	1728	1730	1778	1785	1812	1974	2429
aa position[2]	48	70	201	249	386	387	388	389	390	391	392	394	442	449	476	156	611
SFV4	E	A	F	N	A	G	I	A	D	L	A	D	A	L	R	D	R
L10	A	A	F	N	A	G	I	A	D	L	A	D	A	L	R	D	R
A7(74)	A	G	L	D		-	-	-	-	-		A	T	F	*	E	K

Region	Capsid			E3		E2								E1				
aa position[1]	62	63	85	279	291	370	437	495	545	548	700	704	722	880	930	1043	1112	1188
aa position[2]	62	63	85	12	24	37	104	162	212	215	367	371	389	65	115	228	297	373
SFV4	A	R	N	A	V	V	K	K	N	M	V	V	V	A	R	M	I	R
L10	A	G	K	A	V	I	T	E	N	M	V	V	V	A	R	M	I	R
A7(74)	T	R	K	T	A	I	T	E	S	K	A	A	A	S	K	T	T	K

In addition to the replicase and structural ORF, the alphavirus genome contains a 5' UTR, an inter-genic nucleotide sequence between the ORFs and a 3' UTR. These regions can affect the secondary structure of the genome and have been associated with enhancing replication and virulence in several alphaviruses including SFV (Kuhn *et al.*, 1992;Atkins *et al.*, 1999;Fayzulin & Frolov, 2004;Logue *et al.*, 2008). The nucleotide sequences of these three regions in SFV4-EST, ARKL10-EDI and ARKA7(74)-EDI were aligned and compared. In the 5' UTR, SFV4-EST differed from SFVL10-EDI at one nucleotide, position 59 (Fig. 6.1.i). Comparison of the 5' UTR between SFV4-EST and ARKA7(74)-EDI identified four substitutions at positions 21, 35, 42 and 59. Three of these substitutions were also observed in two published studies, one of which compared A7(74)-FIN to Prototype virus while the other compared SFV4-SWE to A7(74)-BIR (Santagati *et al.*, 1994;Logue *et al.*, 2008). Chimera studies in which the 5' UTR nucleotides at position 21, 35 and 42 in SFV4-SWE were replaced with those from A7(74)-BIR attenuated the virulence of SFV4-SWE in adult mice (Logue *et al.*, 2008).

No differences were detected between the three strains in the inter-genic region. In the 3' UTR, ARKL10-EDI had 36 fewer nucleotides at the C-terminus than SFV4-EST (Fig. 6.1.ii). The 3' UTR differed substantially between SFV4-EST and ARKA7(74)-EDI. One previous study reported that A7(74)-FIN encodes 334 additional nucleotides in the 3' UTR compared to Prototype virus (Santagati *et al.*, 1994). These additional nucleotides contain 5 repeating motifs (Santagati *et al.*, 1994). As shown in Fig. 6.1.ii, extra nucleotides and repeating motifs were detected in the 3' UTR of ARKA7(74)-EDI, but not in SFV4-EST. This is in agreement with Santagati *et al*. (1994).

(i)

(ii)

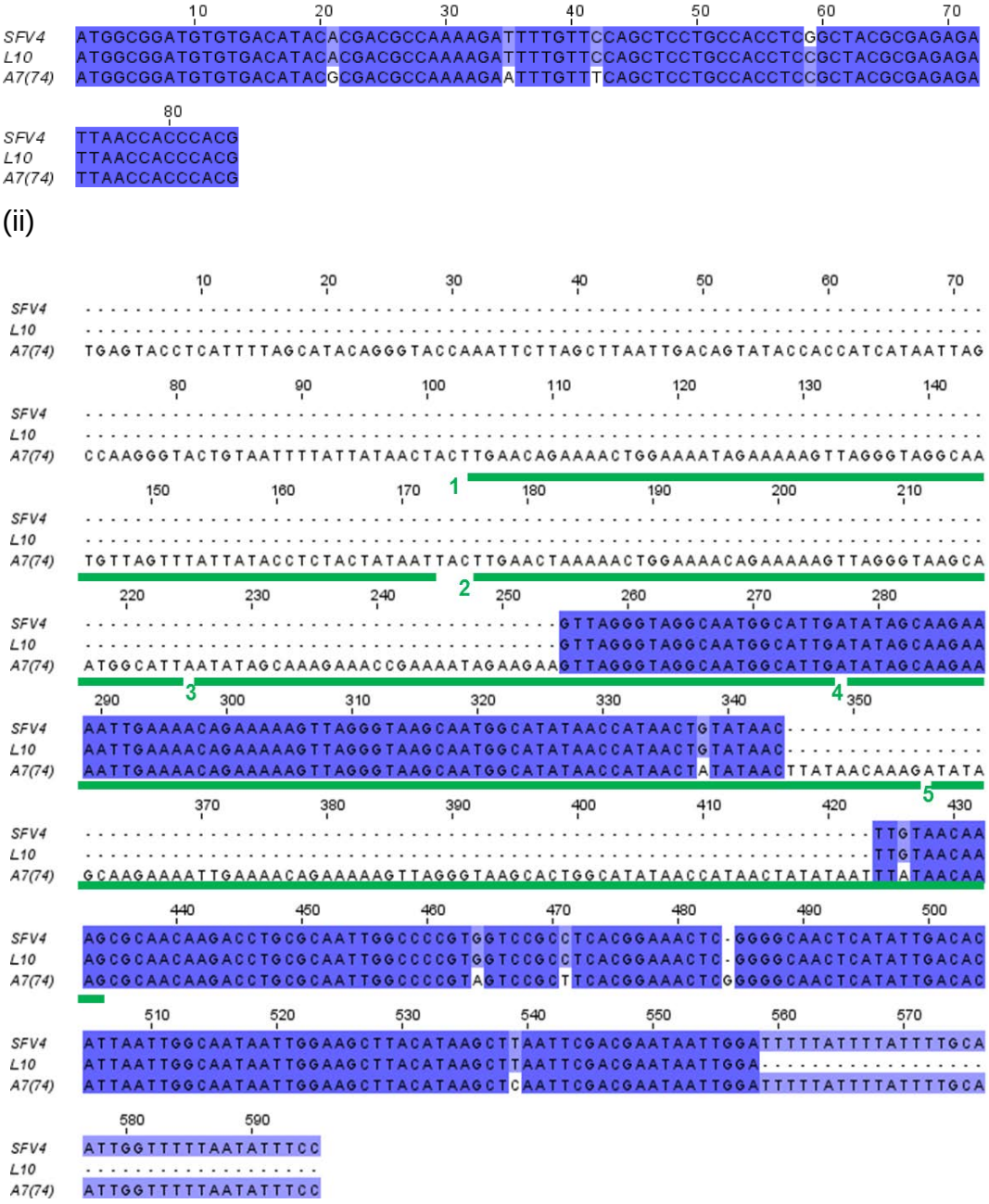

Figure 6.1: Comparison of the nucleotide sequence of the 5' UTR and 3' UTR of ARKL10-EDI and ARKA7(74)-EDI compared to SFV4-EST.
The (i) 5' UTR and (ii) 3' URT of SFV4 (SFV4-EST), L10 (ARKL10-EDI) and A7(74) (ARKA7(74)-EDI) were aligned and compared for percentage similarity using Jalview 2.7. Colours range from dark blue (highly conserved) to white (variable). The green lines mark tandem repeats 1 to 5.

In conclusion, the data presented here indicate high sequence conservation throughout the genome between SFV4-EST and ARKL10-EDI; only 7 differences were identified which were located in the 5' UTR, nsP3, capsid and E2. In addition,

ARKL10-EDI had 37 fewer nucleotides in the 3'UTR compared to SFV4-EST. In contrast, several amino acid differences were identified between the genetic sequence of ARKA7(74)-EDI and SFV4-EST.

6.2.6 Comparison of the sequences encoding nsP2 and nsP3 in SFV4-EST, L10-EDI and A7(74)-EDI

The data presented in chapter 5 indicated the importance of nsP3 and, in particular, nsP2 in the interaction of SFV with the IFN response. Therefore, the amino acid sequences for SFV4-EST, L10-EDI and A7(74)-EDI nsP2 and nsP3 were analysed in greater depth using the Solexa (Illumina) generated sequences. The sequences encoding SFV4-EST, ARKL10-EDI and ARKA7(74)-EDI nsP2 and nsP3 were compared for evolutionary divergence at the nucleotide and the amino acid level using Mega5 (2.13.2), as shown in Table 6.7. The evolutionary divergence between SFV4-EST and ARKL10-EDI was very low in both nsP2 and nsP3 at the nucleotide and amino acid level (≤ 0.1 divergence). SFV4-EST was engineered from Prototype virus, which was isolated from the same mosquito sample as SFV L10. Therefore SFV4-EST would be expected to be similar to ARKL10-EDI. ARKA7(74)-EDI had greater evolutionary divergence from ARKL10-EDI and SFV4-EST, especially in nsP3 (≤ 3.5 at the nucleotide level and ≤ 1.5 at the amino acid level compared to ARKL10-EDI), which is expected considering the viruses were isolated from different pools of mosquitoes.

Table 6.7: Estimates of the evolutionary divergence between SFV4-EST, ARKL10-EDI and ARKA7(74)-EDI nsP2 and nsP3 at the nucleotide and amino acid level.

The percentage of nucleotide (nt and amino acid (aa) differences per site in nsP2 and nsP3 between SFV4-EST, ARKL10-EDI and ARKA7(74)-EDI are shown. A value of 0 suggests no evolutionary divergence. The analyses were conducted in Mega5.

	nt level			aa level		
	SFV4/L10	**SFV4/A7(74)**	**L10/A7(74)**	**SFV4/L10**	**SFV4/A7(74)**	**L10/A7(74)**
nsP2	0.1	1.3	1.3	0.1	0.5	0.6
nsP3	0.1	3.5	3.4	0.1	1.5	1.3

One amino difference between SFV4-EST and ARKL10-EDI was identified in nsP3, while several differences were observed between SFV4-EST and ARKA7(74)-EDI in nsP2 and nsP3 (Table 6.6). To investigate the potential

importance of these amino acid substitutions, the amino acid sequences of SFV4-EST, ARKL10-EDI and ARKA7(74)-EDI nsP2 and nsP3 were compared to a panel of alphaviruses using Jalview 2.7 (2.13.2). Viruses selected for this comparison were the closely related CHIKV, O'nyong-nyong virus, Mayaro virus, Barmah Forest virus and the more distantly related WEEV and VEEV.

Nine different alphavirus nsP2 amino acid sequences were aligned and analysed for the percentage of amino acid similarity using Jalview 2.7 (Fig. 6.2). Percentage similarity is indicated by colour, ranging from highly conserved (dark blue), through to variable (white). Conserved amino acid sequences could be identified in all nine viruses. These regions are likely to be important in the function of nsP2, for example in processing the replicase polyprotein. SFV4-EST, ARKL10-EDI and ARKA7(74)-EDI appeared to be more similar to each other than to the other viruses, as expected; for example at amino acid position 112 the three strains of SFV express serine while all the other alphaviruses studied express alanine. The ^{650}RRR nuclear localisation signal (NLS) was identified in SFV4-EST, ARKL10-EDI and ARKA7(74)-EDI, but not in the other alphaviruses analysed.

In Table 6.6, the greatest biochemical difference identified in nsP2 between SFV4-EST and ARKA7(74)-EDI was at position 1052 (amino acid position 515 in nsP2); SFV4-EST expressed a valine while ARKA7(74)-EDI expressed glutamic acid. The other alphaviruses analysed, like ARKA7(74), all had ^{515}glutamic acid. This amino acid is located in the protease domain of nsP2 (Merits *et al.*, 2001).

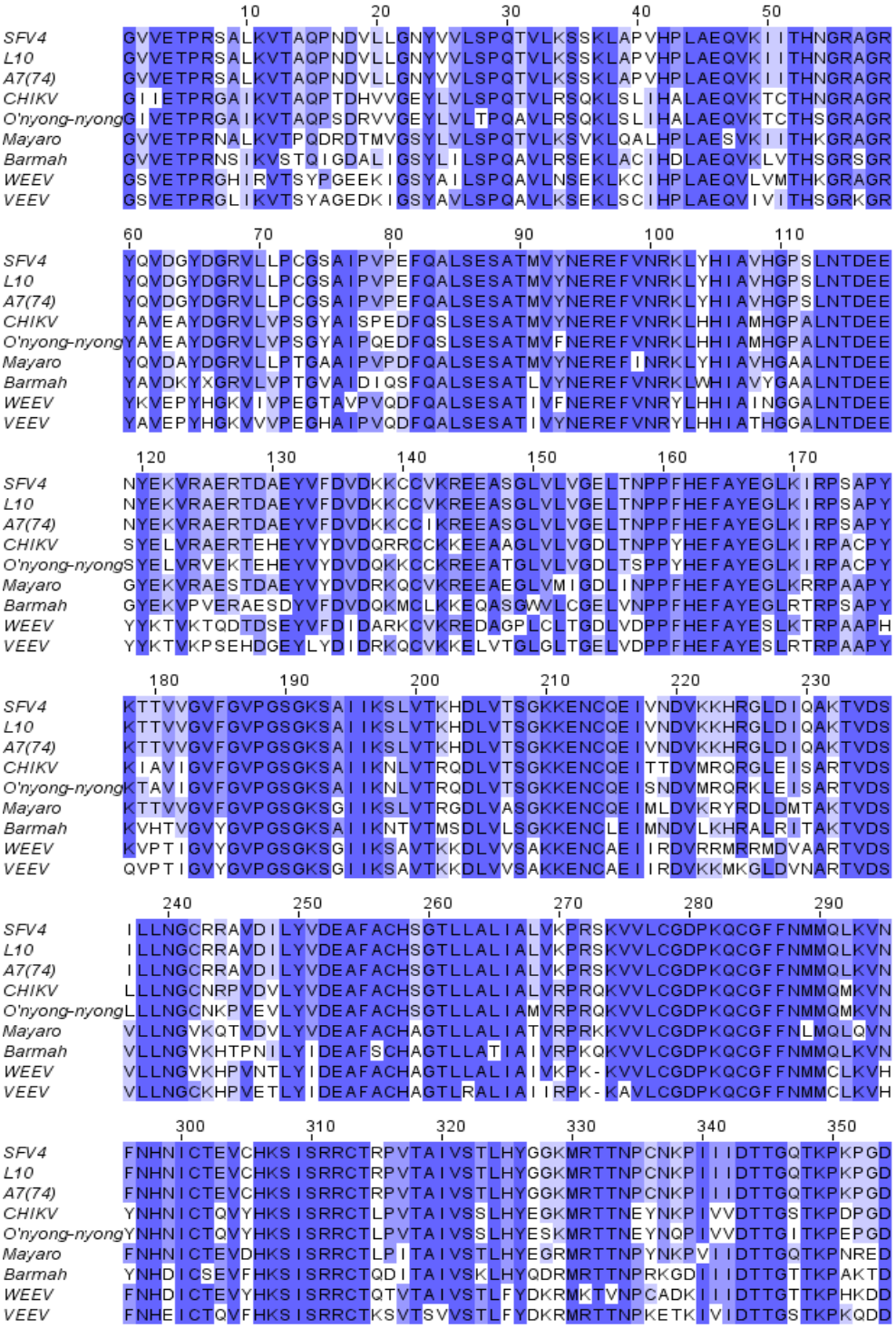
10 20 30 40 50
SFV4 GVVETPRSALKVTAQPNDVLLGNYVVLSPQTVLKSSKLAPVHPLAEQVKIITHNGRAGR
L10 GVVETPRSALKVTAQPNDVLLGNYVVLSPQTVLKSSKLAPVHPLAEQVKIITHNGRAGR
A7(74) GVVETPRSALKVTAQPNDVLLGNYVVLSPQTVLKSSKLAPVHPLAEQVKIITHNGRAGR
CHIKV GIIETPRGAIKVTAQPTDHVVGEYLVLSPQTVLRSQKLSLIHALAEQVKTCTHNGRAGR
O'nyong-nyong GIVETPRGAIKVTAQPSDRVVGEYLVLTPQAVLRSQKLSLIHALAEQVKTCTHSGRAGR
Mayaro GVVETPRNALKVTPQDRDTMVGSYLVLSPQTVLKSVKLQALHPLAESVKIITHKGRAGR
Barmah GVVETPRNSIKVSTQIGDALIGSYLILSPQAVLRSEKLACIHDLAEQVKLVTHSGRSGR
WEEV GSVETPRGHIRVTSYPGEEKIGSYAILSPQAVLNSEKLKCIHPLAEQVLVMTHKGRAGR
VEEV GSVETPRGLIKVTSYAGEDKIGSYAVLSPQAVLKSEKLSCIHPLAEQVIVITHSGRKGR
60 70 80 90 100 110
SFV4 YQVDGYDGRVLLPCGSAIPVPEFQALSESATMVYNEREFVNRKLYHIAVHGPSLNTDEE
L10 YQVDGYDGRVLLPCGSAIPVPEFQALSESATMVYNEREFVNRKLYHIAVHGPSLNTDEE
A7(74) YQVDGYDGRVLLPCGSAIPVPEFQALSESATMVYNEREFVNRKLYHIAVHGPSLNTDEE
CHIKV YAVEAYDGRVLVPSGYAISPEDFQSLSESATMVYNEREFVNRKLHHIAMHGPALNTDEE
O'nyong-nyong YAVEAYDGRVLVPSGYAIPQEDFQSLSESATMVFNEREFVNRKLHHIAMHGPALNTDEE
Mayaro YQVDAYDGRVLLPTGAAIPVPDFQALSESATMVYNEREFINRKLYHIAVHGAALNTDEE
Barmah YAVDKYXGRVLVPTGVAIDIQSFQALSESATLVYNEREFVNRKLWHIAVYGAALNTDEE
WEEV YKVEPYHGKVIVPEGTAVPVQDFQALSESATIVFNEREFVNRYLHHIAINGGALNTDEE
VEEV YAVEPYHGKVVVPEGHAIPVQDFQALSESATIVYNEREFVNRYLHHIATHGGALNTDEE
120 130 140 150 160 170
SFV4 NYEKVRAERTDAEYVFDVDKKCCVKREEASGLVLVGELTNPPFHEFAYEGLKIRPSAPY
L10 NYEKVRAERTDAEYVFDVDKKCCVKREEASGLVLVGELTNPPFHEFAYEGLKIRPSAPY
A7(74) NYEKVRAERTDAEYVFDVDKKCCIKREEASGLVLVGELTNPPFHEFAYEGLKIRPSAPY
CHIKV SYELVRAERTEHEYVYDVDQRRCCKKEEAAGLVLVGDLTNPPYHEFAYEGLKIRPACPY
O'nyong-nyong SYELVRVEKTEHEYVYDVDQKKCCKREEATGLVLVGDLTSPPYHEFAYEGLKIRPACPY
Mayaro GYEKVRAESTDAEYVYDVDRKQCVKREEAEGLVMIGDLINPPFHEFAYEGLKRRPAAPY
Barmah GYEKVPVERAESDYVFDVDQKMCLKKEQASGWVLCGELVNPPFHEFAYEGLRTRPSAPY
WEEV YYKTVKTQDTDSEYVFDIDARKCVKREDAGPLCLTGDLVDPPFHEFAYESLKTRPAAPH
VEEV YYKTVKPSEHDGEYLYDIDRKQCVKKELVTGLGLTGELVDPPFHEFAYESLRTRPAAPY
180 190 200 210 220 230
SFV4 KTTVVGVFGVPGSGKSAIIKSLVTKHDLVTSGKKENCQEIVNDVKKHRGLDIQAKTVDS
L10 KTTVVGVFGVPGSGKSAIIKSLVTKHDLVTSGKKENCQEIVNDVKKHRGLDIQAKTVDS
A7(74) KTTVVGVFGVPGSGKSAIIKSLVTKHDLVTSGKKENCQEIVNDVKKHRGLDIQAKTVDS
CHIKV KIAVIGVFGVPGSGKSAIIKNLVTRQDLVTSGKKENCQEITTDVMRQRGLEISARTVDS
O'nyong-nyong KTAVIGVFGVPGSGKSAIIKNLVTRQDLVTSGKKENCQEISNDVMRQRKLEISARTVDS
Mayaro KTTVVGVFGVPGSGKSGIIKSLVTRGDLVASGKKENCQEIMLDVKRYRDLDMTAKTVDS
Barmah KVHTVGVYGVPGSGKSAIIKNTVTMSDLVLSGKKENCLEIMNDVLKHRALRITAKTVDS
WEEV KVPTIGVYGVPGSGKSGIIKSAVTKKDLVVSAKKENCAEIIRDVRRMRRMDVAARTVDS
VEEV QVPTIGVYGVPGSGKSGIIKSAVTKKDLVVSAKKENCAEIIRDVKKMKGLDVNARTVDS
240 250 260 270 280 290
SFV4 ILLNGCRRAVDILYVDEAFACHSGTLLALIALVKPRSKVVLCGDPKQCGFFNMMQLKVN
L10 ILLNGCRRAVDILYVDEAFACHSGTLLALIALVKPRSKVVLCGDPKQCGFFNMMQLKVN
A7(74) ILLNGCRRAVDILYVDEAFACHSGTLLALIALVKPRSKVVLCGDPKQCGFFNMMQLKVN
CHIKV LLLNGCNRPVDVLYVDEAFACHSGTLLALIALVRPRQKVVLCGDPKQCGFFNMMQMKVN
O'nyong-nyong LLLNGCNKPVEVLYVDEAFACHSGTLLALIAMVRPRQKVVLCGDPKQCGFFNMMQMKVN
Mayaro VLLNGVKQTVDVLYVDEAFACHAGTLLALIATVRPRKKVVLCGDPKQCGFFNLMQLQVN
Barmah VLLNGVKHTPNILYIDEAFSCHAGTLLATIAIVRPKQKVVLCGDPKQCGFFNMMQLKVN
WEEV VLLNGVKHPVNTLYIDEAFACHAGTLLALIAIVKPK-KVVLCGDPKQCGFFNMMCLKVH
VEEV VLLNGCKHPVETLYIDEAFACHAGTLRALIAIIRPK-KAVLCGDPKQCGFFNMMCLKVH
300 310 320 330 340 350
SFV4 FNHNICTEVCHKSISRRCTRPVTAIVSTLHYGGKMRTTNPCNKPIIIDTTGQTKPKPGD
L10 FNHNICTEVCHKSISRRCTRPVTAIVSTLHYGGKMRTTNPCNKPIIIDTTGQTKPKPGD
A7(74) FNHNICTEVCHKSISRRCTRPVTAIVSTLHYGGKMRTTNPCNKPIIIDTTGQTKPKPGD
CHIKV YNHNICTQVYHKSISRRCTLPVTAIVSSLHYEGKMRTTNEYNKPIVVDTTGSTKPDPGD
O'nyong-nyong YNHNICTQVYHKSISRRCTLPVTAIVSSLHYESKMRTTNEYNQPIVVDTTGITKPEPGD
Mayaro FNHNICTEVDHKSISRRCTLPITAIVSTLHYEGRMRTTNPYNKPVIIDTTGQTKPNRED
Barmah YNHDICSEVFHKSISRRCTQDITAIVSKLHYQDRMRTTNPRKGDIIIDTTGTTKPAKTD
WEEV FNHDICTEVYHKSISRRCTQTVTAIVSTLFYDKRMKTVNPCADKIIIDTTGTTKPHKDD
VEEV FNHEICTQVFHKSISRRCTKSVTSVVSTLFYDKRMRTTNPKETKIVIDTTGSTKPKQDD

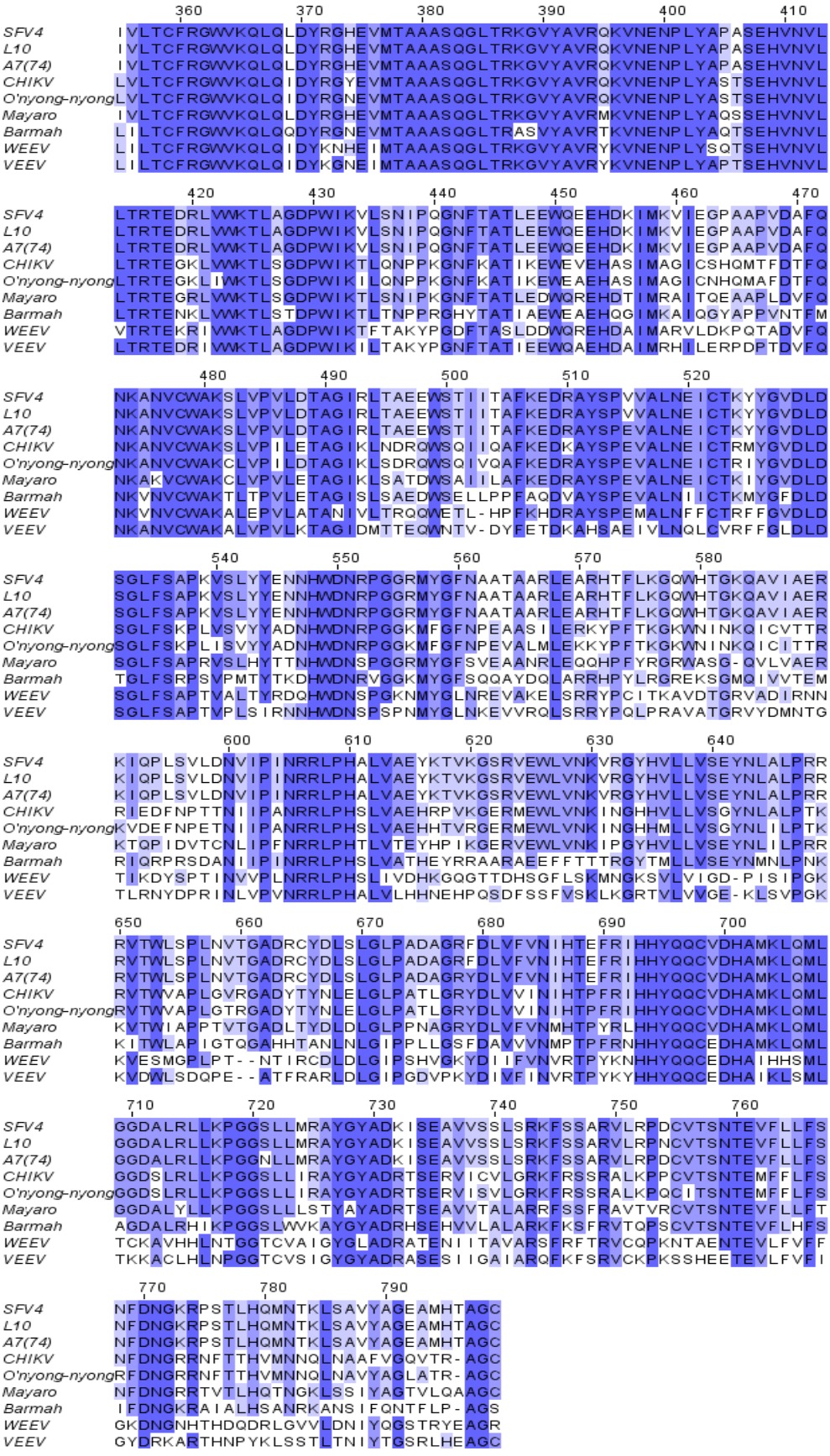
SFV4
L10
A7(74)
CHIKV
O'nyong-nyong
Mayaro
Barmah
WEEV
VEEV

Figure 6.2: Comparison of the amino acid sequence of the nsP2 in a panel of alphaviruses.
The nsP2 amino acid sequence of SFV4-EST (SFV4), ARKL10-EDI (L10), ARKA7(74)-EDI (A7(74)), CHIKV, O'nyong-nyong virus, Mayaro virus, Barmah Forest virus, WEEV and VEEV were aligned and compared for percentage similarity using Jalview 2.7. Colours range from dark blue (highly conserved) to white (variable).

Crystal structures of the CHIKV and VEEV nsP2 protease domains are available in the Protein Data Bank, 3TRK and 2HWK respectively (www.rcsb.org/). 3D structures of the SFV4-EST and ARKA7(74)-EDI nsP2 protease domains were predicted using the program Phyre2 (2.14). SFV4-EST and ARKA7(74)-EDI were modelled to the crystal structure of the CHIKV nsP2 protease domain with 100 % confidence. The predicted 3D structure of the SFV4 nsP2 protease domain is shown in Fig. 6.3.

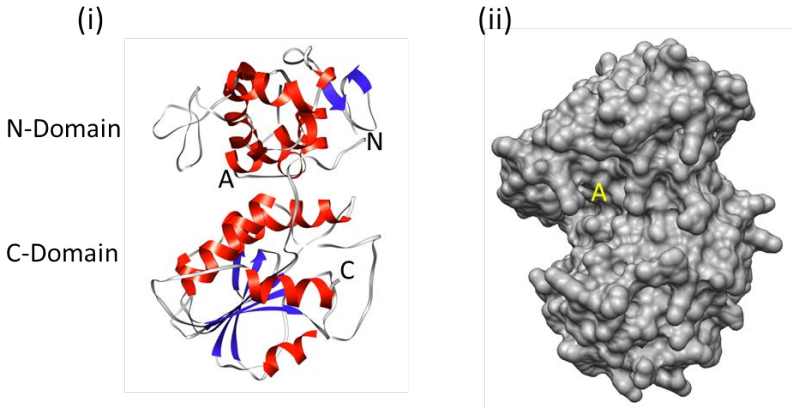

Figure 6.3: Predicted structure of the SFV4 nsP2 protease domain.
(i) Ribbon diagram of the nsP2 protease domain showing the N-terminus (N), C-terminus (C) and the active site (A). The nsP2 protease domain consists of a α-helices rich N-domain and a α-helices and β-sheet rich C-domain. (ii) Surface representation of the nsP2 protease domain. Structures were generated using Phyre2 and formatted using UCSF Chimera.

The nsP2 protease structure consists of two domains: the N-terminal domain and the C-terminal domain. The N-terminal domain is largely helical and is a cysteine protease domain, while the C-terminus is a combination of α-helices and β-sheets and is a methyltransferase-like domain (Russo *et al.*, 2006). The active site is located adjacent to the interface between the two domains and amino acids predominately from the N-domain are associated with its function in processing the replicase polyprotein (Merits *et al.*, 2001;Russo *et al.*, 2006;Russo *et al.*, 2010).

To predict the importance of amino acid 515 on the function of nsP2, the position and orientation of amino acid 515 was identified in the predicted 3D structure of the SFV4-EDI and ARKA7(74)-EDI nsP2 protease domain (Fig. 6.4). Amino acid 515 was located close to the active site and orientated outwards (Fig. 6.4). This data indicates that amino acids 515 is likely to affect replication by altering the interaction of nsP2 with the replicase polyprotein cleavage sites. In conclusion, amino acid 515 probably affects the replication and virulence of SFV4-EST and ARKA7(74)-EDI.

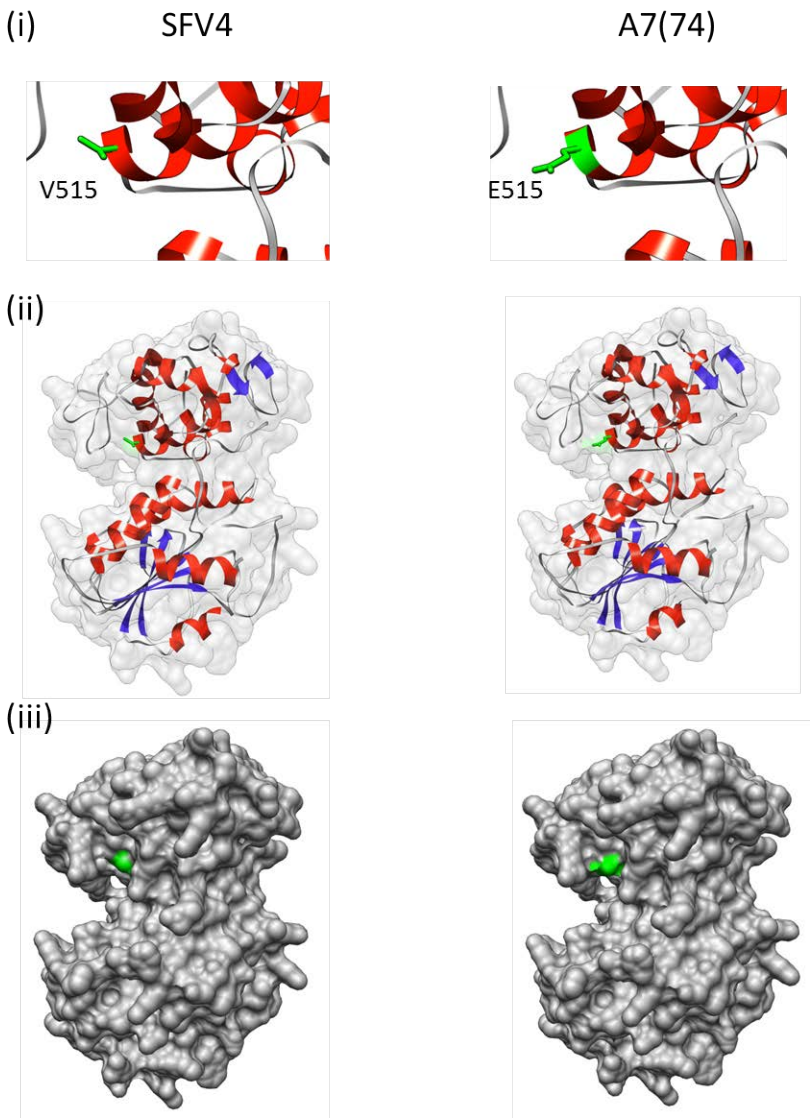

Figure 6.4: Predicted structures of the SFV4-EDI and ARKA7(74)-EDI nsP2 protease domain.
(i) Sections of the ribbon structures of SFV4-EDI and ARKA7(74)-EDI nsP2 protease domains showing the location of amino acid 515 (green); valine (V) and glutamic acid (E). (ii) Combined ribbon and surface structure of SFV4-EDI and ARKA7(74)-EDI nsP2 protease domains. (iii) Surface structure of SFV4-EDI and ARKA7(74)-EDI nsP2 protease domains. Structures were generated using Phyre2 and formatted using UCSF Chimera.

Next, the nsP3 amino acid sequences of SFV4-EST, ARKL10-EDI and ARKA7(74)-EDI were analysed. The nsP3 amino acid sequences from the nine alphavirus used previously were aligned and analysed for the percentage of amino acid similarity (Fig. 6.5). The conserved macro domain (largely highly conserved - dark blue), and the hypervariable domain (largely variable – white), were apparent. In Table 6.6, one amino acid differences was observed between SFV4-EST and

ARKL10-EDI in the nsP3 macro domain at position 48; glutamic acid in SFV4-EST and alanine in ARKL10-EDI. Amino acid 48 varied between the nine alphaviruses studied, although alanine was most common at this position (Fig. 6.5).

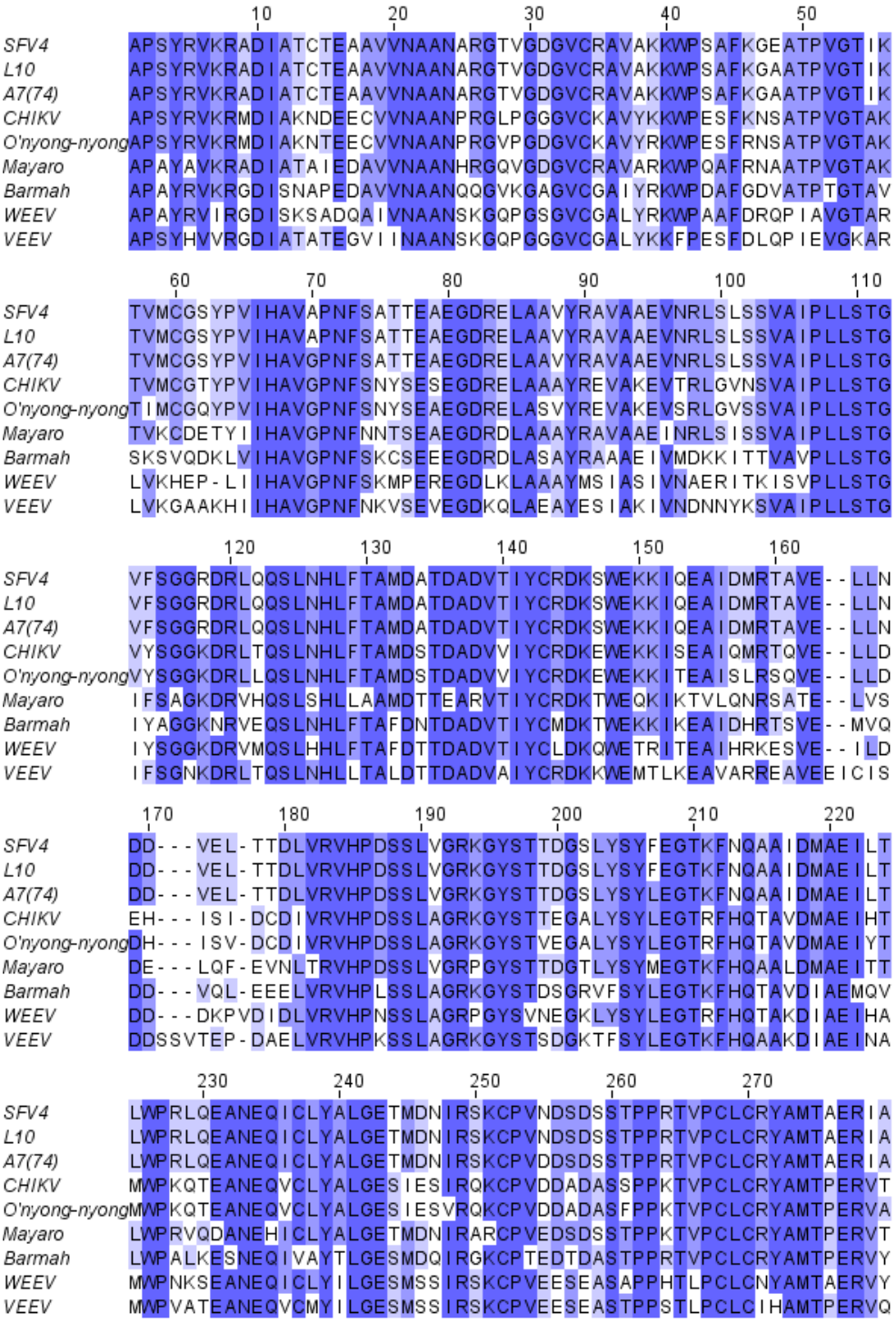
10 20 30 40 50
SFV4 APSYRVKRADIATCTEAAVVNAANARGTVGDGVCRAVAKKWPSAFKGEATPVGTIK
L10 APSYRVKRADIATCTEAAVVNAANARGTVGDGVCRAVAKKWPSAFKGAATPVGTIK
A7(74) APSYRVKRADIATCTEAAVVNAANARGTVGDGVCRAVAKKWPSAFKGAATPVGTIK
CHIKV APSYRVKRMDIAKNDEECVVNAANPRGLPGGGVCKAVYKKWPESFKNSATPVGTAK
O'nyong-nyong APSYRVKRMDIAKNTEECVVNAANPRGVPGDGVCKAVYRKWPESFRNSATPVGTAK
Mayaro APAYAVKRADIATAIEDAVVNAANHRGQVGDGVCRAVARKWPQAFRNAATPVGTAK
Barmah APAYRVKRGDISNAPEDAVVNAANQQGVKGAGVCGAIYRKWPDAFGDVATPTGTAV
WEEV APAYRVIRGDISKSADQAIVNAANSKGQPGSGVCGALYRKWPAAFDRQPIAVGTAR
VEEV APSYHVVRGDIATATEGVIINAANSKGQPGGGVCGALYKKFPESFDLQPIEVGKAR
60 70 80 90 100 110
SFV4 TVMCGSYPVIHAVAPNFSATTEAEGDRELAAVYRAVAAEVNRLSLSSVAIPLLSTG
L10 TVMCGSYPVIHAVAPNFSATTEAEGDRELAAVYRAVAAEVNRLSLSSVAIPLLSTG
A7(74) TVMCGSYPVIHAVGPNFSATTEAEGDRELAAVYRAVAAEVNRLSLSSVAIPLLSTG
CHIKV TVMCGTYPVIHAVGPNFSNYSESEGDRELAAAYREVAKEVTRLGVNSVAIPLLSTG
O'nyong-nyong TIMCGQYPVIHAVGPNFSNYSEAEGDRELASVYREVAKEVSRLGVSSVAIPLLSTG
Mayaro TVKCDETYIIHAVGPNFNNTSEAEGDRDLAAAYRAVAAEINRLSISSVAIPLLSTG
Barmah SKSVQDKLVIHAVGPNFSKCSEEEGDRDLASAYRAAAEIVMDKKITTVAVPLLSTG
WEEV LVKHEP-LIIHAVGPNFSKMPEREGDLKLAAAYMSIASIVNAERITKISVPLLSTG
VEEV LVKGAAKHIIHAVGPNFNKVSEVEGDKQLAEAYESIAKIVNDNNYKSVAIPLLSTG
120 130 140 150 160
SFV4 VFSGGRDRLQQSLNHLFTAMDATDADVTIYCRDKSWEKKIQEAIDMRTAVE--LLN
L10 VFSGGRDRLQQSLNHLFTAMDATDADVTIYCRDKSWEKKIQEAIDMRTAVE--LLN
A7(74) VFSGGRDRLQQSLNHLFTAMDATDADVTIYCRDKSWEKKIQEAIDMRTAVE--LLN
CHIKV VYSGGKDRLTQSLNHLFTAMDSTDADVVIYCRDKEWEKKISEAIQMRTQVE--LLD
O'nyong-nyong VYSGGKDRLLQSLNHLFTAMDSTDADVVIYCRDKEWEKKITEAISLRSQVE--LLD
Mayaro IFSAGKDRVHQSLSHLLAAMDTTEARVTIYCRDKTWEQKIKTVLQNRSATE--LVS
Barmah IYAGGKNRVEQSLNHLFTAFDNTDADVTIYCMDKTWEKKIKEAIDHRTSVE--MVQ
WEEV IYSGGKDRVMQSLHHLFTAFDTTDADVTIYCLDKQWETRITEAIHRKESVE--ILD
VEEV IFSGNKDRLTQSLNHLLTALDTTDADVAIYCRDKKWEMTLKEAVARREAVEEICIS
170 180 190 200 210 220
SFV4 DD---VEL-TTDLVRVHPDSSLVGRKGYSTTDGSLYSYFEGTKFNQAAIDMAEILT
L10 DD---VEL-TTDLVRVHPDSSLVGRKGYSTTDGSLYSYFEGTKFNQAAIDMAEILT
A7(74) DD---VEL-TTDLVRVHPDSSLVGRKGYSTTDGSLYSYLEGTKFNQAAIDMAEILT
CHIKV EH---ISI-DCDIVRVHPDSSLAGRKGYSTTEGALYSYLEGTRFHQTAVDMAEIHT
O'nyong-nyong DH---ISV-DCDIVRVHPDSSLAGRKGYSTVEGALYSYLEGTRFHQTAVDMAEIYT
Mayaro DE---LQF-EVNLTRVHPDSSLVGRPGYSTTDGTLYSYMEGTKFHQAALDMAEITT
Barmah DD---VQL-EEELVRVHPLSSLAGRKGYSTDSGRVFSYLEGTKFHQTAVDIAEMQV
WEEV DD---DKPVDIDLVRVHPNSSLAGRPGYSVNEGKLYSYLEGTRFHQTAKDIAEIHA
VEEV DDSSVTEP-DAELVRVHPKSSLAGRKGYSTSDGKTFSYLEGTKFHQAAKDIAEINA
230 240 250 260 270
SFV4 LWPRLQEANEQICLYALGETMDNIRSKCPVNDSDSSTPPRTVPCLCRYAMTAERIA
L10 LWPRLQEANEQICLYALGETMDNIRSKCPVNDSDSSTPPRTVPCLCRYAMTAERIA
A7(74) LWPRLQEANEQICLYALGETMDNIRSKCPVDDSDSSTPPRTVPCLCRYAMTAERIA
CHIKV MWPKQTEANEQVCLYALGESIESIRQKCPVDDADASSPPKTVPCLCRYAMTPERVT
O'nyong-nyong MWPKQTEANEQVCLYALGESIESVRQKCPVDDADASFPPKTVPCLCRYAMTPERVA
Mayaro LWPRVQDANEHICLYALGETMDNIRARCPVEDSDSSTPPKTVPCLCRYAMTPERVT
Barmah LWPALKESNEQIVAYTLGESMDQIRGKCPTEDTDASTPPRTVPCLCRYAMTPERVY
WEEV MWPNKSEANEQICLYILGESMSSIRSKCPVEESEASAPPHTLPCLCNYAMTAERVY
VEEV MWPVATEANEQVCMYILGESMSSIRSKCPVEESEASTPPSTLPCLCIHAMTPERVQ

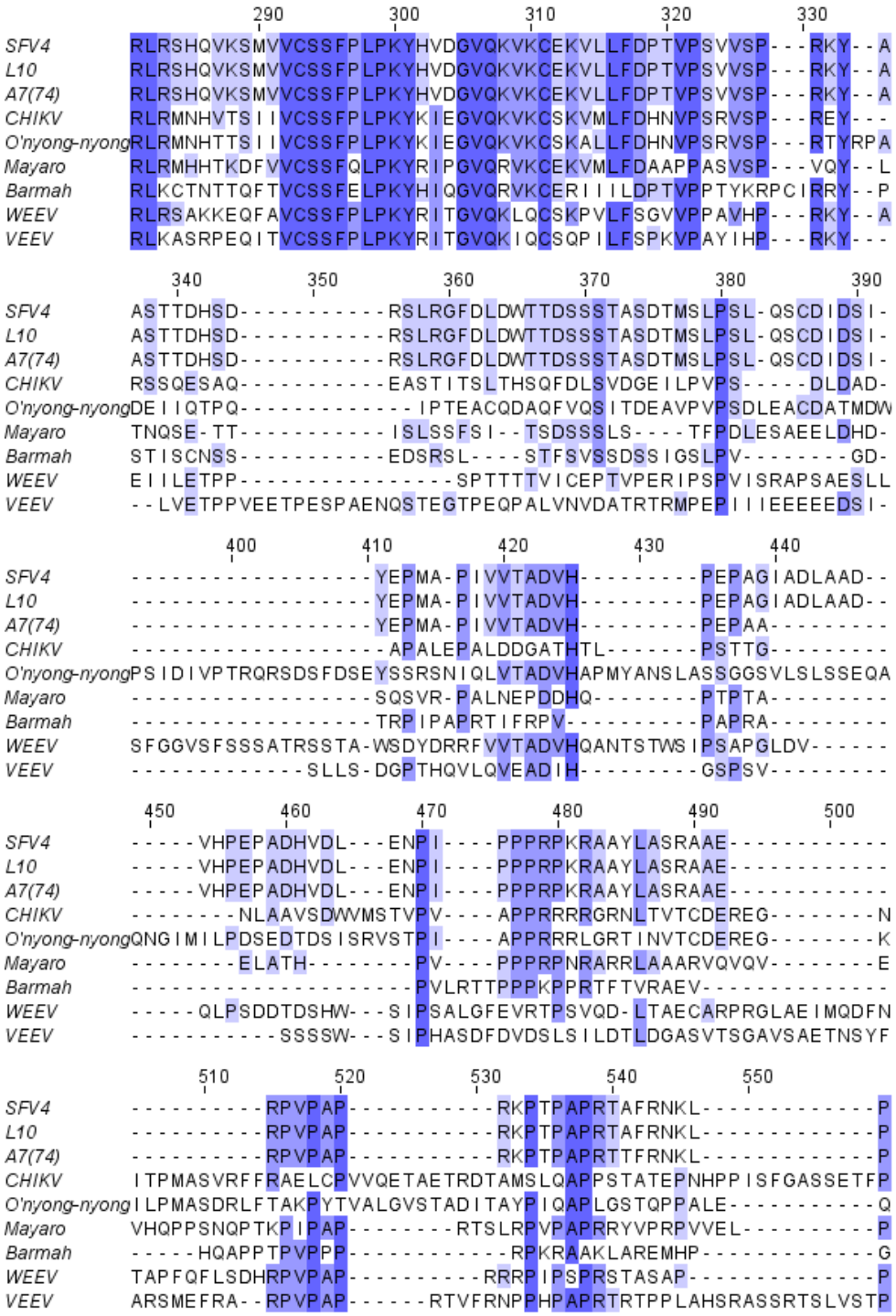
290 300 310 320 330
SFV4 RLRSHQVKSMVVCSSFPLPKYHVDGVQKVKCEKVLLFDPTVPSVVSP---RKY--A
L10 RLRSHQVKSMVVCSSFPLPKYHVDGVQKVKCEKVLLFDPTVPSVVSP---RKY--A
A7(74) RLRSHQVKSMVVCSSFPLPKYHVDGVQKVKCEKVLLFDPTVPSVVSP---RKY--A
CHIKV RLRMNHVTSIIVCSSFPLPKYKIEGVQKVKCSKVMLFDHNVPSRVSP---REY---
O'nyong-nyong RLRMNHTTSIIVCSSFPLPKYKIEGVQKVKCSKALLFDHNVPSRVSP---RTYRPA
Mayaro RLRMHHTKDFVVCSSFQLPKYRIPGVQRVKCEKVMLFDAAPPASVSP---VQY--L
Barmah RLKCTNTTQFTVCSSFELPKYHIQGVQRVKCERIIILDPTVPPTYKRPCIRRY--P
WEEV RLRSAKKEQFAVCSSFPLPKYRITGVQKLQCSKPVLFSGVVPPAVHP---RKY--A
VEEV RLKASRPEQITVCSSFPLPKYRITGVQKIQCSQPILFSPKVPAYIHP---RKY---
340 350 360 370 380 390
SFV4 ASTTDHSD----------RSLRGFDLDWTTDSSSTASDTMSLPSL-QSCDIDSI-
L10 ASTTDHSD----------RSLRGFDLDWTTDSSSTASDTMSLPSL-QSCDIDSI-
A7(74) ASTTDHSD----------RSLRGFDLDWTTDSSSTASDTMSLPSL-QSCDIDSI-
CHIKV RSSQESAQ----------EASTITSLTHSQFDLSVDGEILPVPS-----DLDAD-
O'nyong-nyong DEIIQTPQ----------IPTEACQDAQFVQSITDEAVPVPSDLEACDATMDW
Mayaro TNQSE-TT----------ISLSSFSI--TSDSSSLS----TFPDLESAEELDHD-
Barmah STISCNSS----------EDSRSL----STFSVSSDSSIGSLPV--------GD-
WEEV EIILETPP----------SPTTTTVICEPTVPERIPSPVISRAPSAESLL
VEEV --LVETPPVEETPESPAENQSTEGTPEQPALVNVDATRTRMPEPIIIEEEEEDSI-
400 410 420 430 440
SFV4 ----------YEPMA-PIVVTADVH---------PEPAGIADLAAD--
L10 ----------YEPMA-PIVVTADVH---------PEPAGIADLAAD--
A7(74) ----------YEPMA-PIVVTADVH---------PEPAA---------
CHIKV ----------APALEPALDDGATHTL-------PSTTG---------
O'nyong-nyong PSIDIVPTRQRSDSFDSEYSSRSNIQLVTADVHAPMYANSLASSGGSVLSLSSEQA
Mayaro ----------SQSVR-PALNEPDDHQ--------PTPTA---------
Barmah ----------TRPIPAPRTIFRPV----------PAPRA---------
WEEV SFGGVSFSSSATRSSTA-WSDYDRRFVVTADVHQANTSTWSIPSAPGLDV------
VEEV ----------SLLS-DGPTHQVLQVEADIH---------GSPSV---------
450 460 470 480 490 500
SFV4 -----VHPEPADHVDL---ENPI----PPPRPKRAAYLASRAAE----------
L10 -----VHPEPADHVDL---ENPI----PPPRPKRAAYLASRAAE----------
A7(74) -----VHPEPADHVDL---ENPI----PPPRPKRAAYLASRAAE----------
CHIKV --------NLAAVSDWVMSTVPV----APPRRRRGRNLTVTCDEREG--------N
O'nyong-nyong QNGIMILPDSEDTDSISRVSTPI----APPRRRLGRTINVTCDEREG--------K
Mayaro --------ELATH--------PV----PPPRPNRARRLAAARVQVQV--------E
Barmah ----------PVLRTTPPPKPPRTFTVRAEV----------
WEEV -----QLPSDDTDSHW---SIPSALGFEVRTPSVQD-LTAECARPRGLAEIMQDFN
VEEV ----------SSSSW---SIPHASDFDVDSLSILDTLDGASVTSGAVSAETNSYF
510 520 530 540 550
SFV4 ----------RPVPAP----------RKPTPAPRTAFRNKL----------P
L10 ----------RPVPAP----------RKPTPAPRTAFRNKL----------P
A7(74) ----------RPVPAP----------RKPTPAPRTTFRNKL----------P
CHIKV ITPMASVRFFRAELCPVVQETAETRDTAMSLQAPPSTATEPNHPPISFGASSETFP
O'nyong-nyong ILPMASDRLFTAKPYTVALGVSTADITAYPIQAPLGSTQPPALE----------Q
Mayaro VHQPPSNQPTKPIPAP--------RTSLRPVPAPRRYVPRPVVEL----------P
Barmah -----HQAPPTPVPPP----------RPKRAAKLAREMHP----------G
WEEV TAPFQFLSDHRPVPAP----------RRRPIPSPRSTASAP----------P
VEEV ARSMEFRA--RPVPAP------RTVFRNPPHPAPRTRTPPLAHSRASSRTSLVSTP

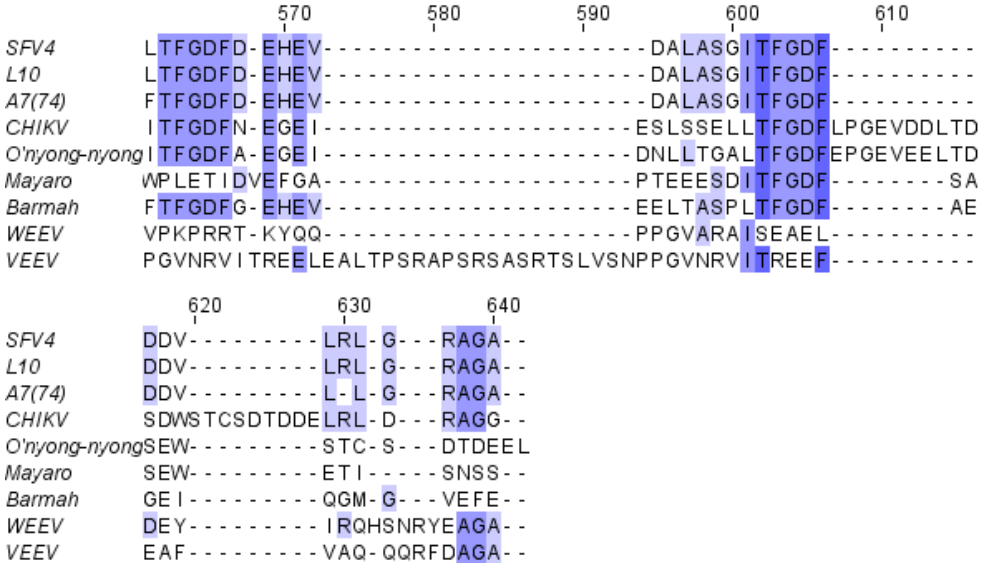

Figure 6.5: Comparison of the amino acid sequence of the nsP3 in a panel of alphaviruses.

The nsP3 amino acid sequence of SFV4-EST (SFV4), ARKL10-EDI (L10), ARKA7(74)-EDI (A7(74)), CHIKV, O'nyong-nyong virus, Mayaro virus, Barmah Forest virus, WEEV and VEEV were aligned and compared for percentage similarity using Jalview 2.7. Colours range from dark blue (highly conserved) to white (variable).

The nsP3 macro domain crystal structures are available in the Protein Data Bank for CHIKV and VEEV, 3PG and 3GQE respectively (www.rcsb.org). 3D structures of the SFV4-EST, ARKL10-EDI and, also, ARKA7(74)-EDI nsP3 macro domains were predicted using the program Phyre2 (2.14). SFV4-EST and ARKA7(74)-EDI were modelled to the crystal structure of the CHIKV nsP3 macro domain with 100 % confidence. The predicted 3D structure of the SFV4 nsP3 macro domain is shown in Fig. 6.6.

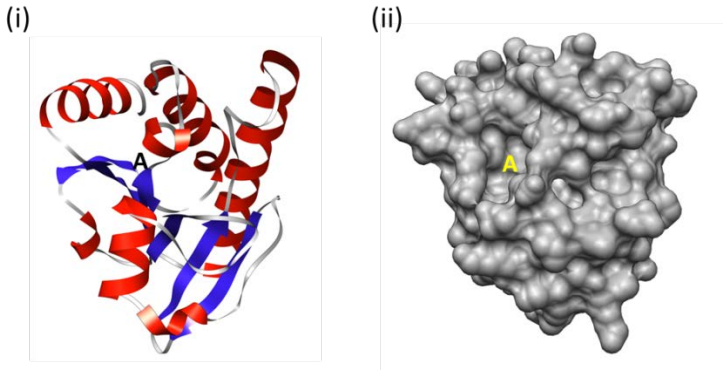

Figure 6.6: Predicted structure of the SFV4 nsP3 macro domain.
(i) Ribbon and (ii) Surface representation diagrams of the nsP3 macro domain showing the active site (A). Structures were generated using Phyre2 and formatted using UCSF Chimera.

The nsP3 macro domain is comprised of six β-sheets surrounded by four α-helices. The active site is an adenosine binding pocket (Malet *et al.*, 2009). To predict the importance of amino acid 48 on the function of nsP3, the position and orientation of amino acid 48 was identified in the 3D structure of SFV4-EDI and ARKL10-EDI nsP3 macro domain (Fig. 6.7). Amino acid 48 was located in a loop orientated inwards, away from the active site (Fig. 6.7). Taken together, amino acid 48 is unlikely to affect the function of nsP3, at least in the macro domain.

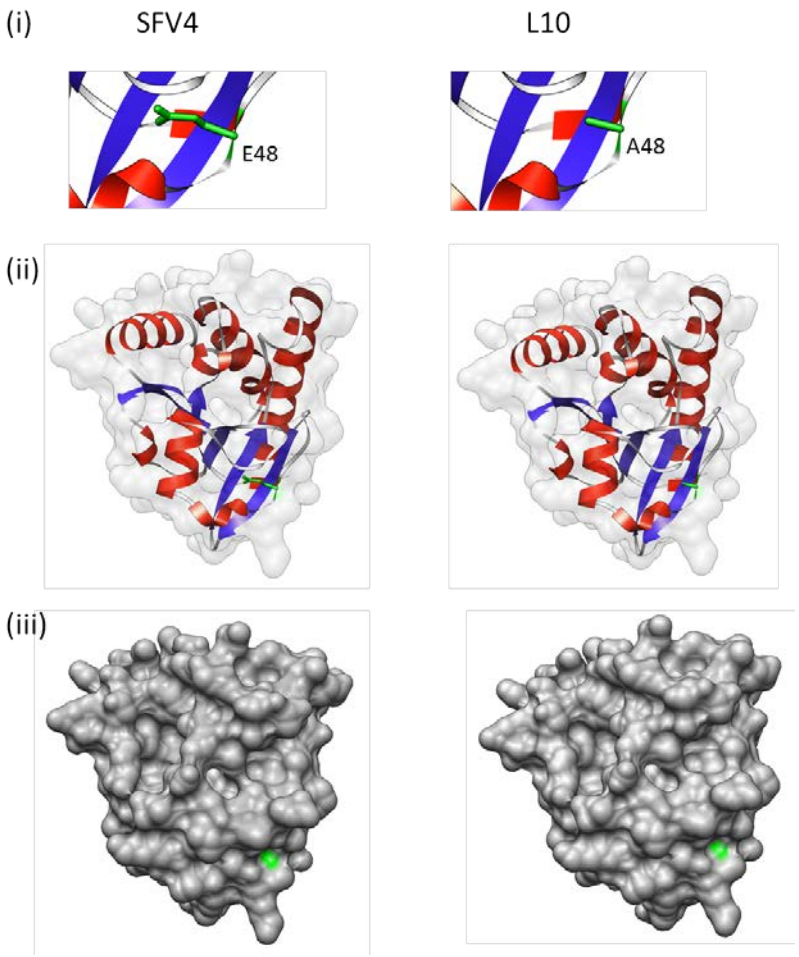

Figure 6.7: Predicted structures of the SFV4-EDI and ARKL10-EDI nsP3 macro domain.
(i) Sections of the ribbon structures of SFV4-EDI and ARKL10-EDI nsP3 macro domains showing the location of amino acid 48 (green); glutamic acid (E) and alanine (A). (ii) Combined ribbon and surface structures of SFV4-EDI and ARKL10-EDI nsP3 macro domains. (iii) Surface structures of SFV4-EDI and ARKL10-EDI nsP3 macro domains. Structures were generated using Phyre2 and formatted using UCSF Chimera.

In Table 6.6, most amino acid differences between SFV4-EST and ARKA7(74)-EDI mapped to nsP3. Biochemically, the most important amino acid substitutions in the macro domain were at positions 48 and 70. Amino acid 48 has been analysed in detail above in the context of SFV4-EST and ARKL10-EDI and the results can be applied to ARKA7(74)-EDI (Fig. 6.7). At amino acid position 70, SFV4-EST expressed alanine and ARKA7(74)-EDI glycine. Analysis of a panel of alphaviruses demonstrated that all alphaviruses apart from SFV4-EST and ARKL10-EDI expressed ^{70}glycine (Fig. 6.8). ^{70}glycine is a completely different size and structure to ^{70}alanine. In addition, amino acid 70 is located close to the active site

(Fig. 6.8). The data indicate that amino acid 70 is likely to affect the function of nsP3 and, therefore, virulence of SFV4-EST and ARKA7(74)-EDI.

Other potentially important differences between SFV4-EST and ARKA7(74)-EDI were located in the nsP3 hypervariable domain. Seven amino acids were identified in SFV4-EST and ARKL10-EDI (^{386}A – GIADLA), which were not present in ARKA7(74)-EDI or any other alphavirus studied (Fig. 6.8). The hypervariable domain is predicted to be highly disordered and no crystal structure is currently available. Therefore, it is difficult to predict how changes in this region affect the structure and function of nsP3.

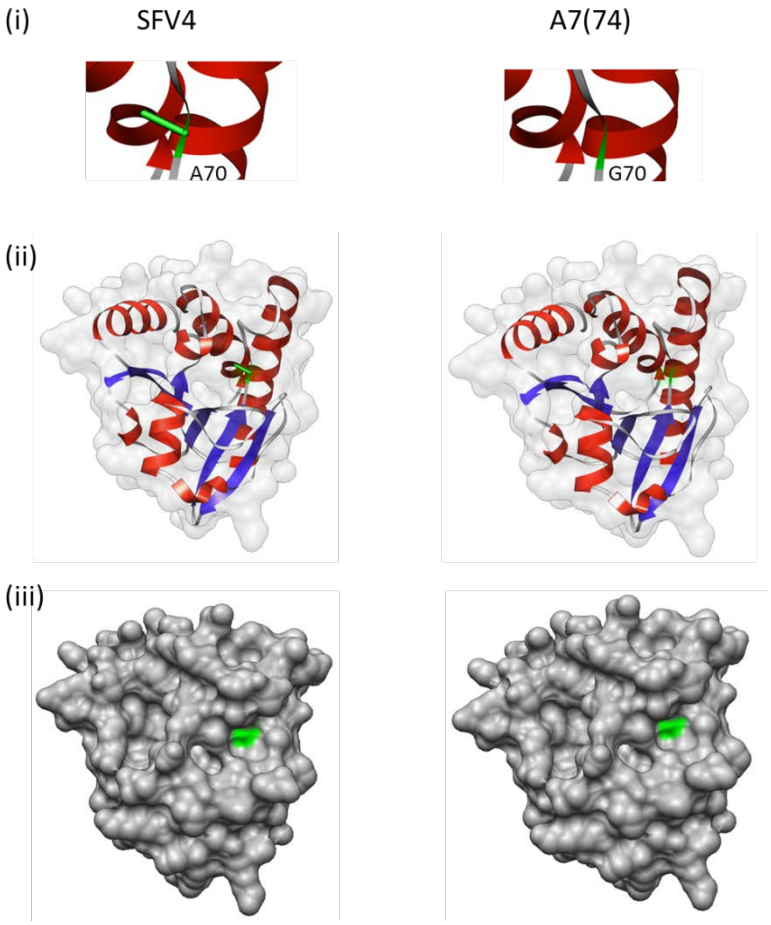

Figure 6.8: Predicted structures of the SFV4-EDI and ARKA7(74)-EDI nsP3 macro domain.
(i) Sections of the ribbon structures of the SFV4-EDI and ARKA7(74)-EDI nsP3 macro domain showing the location of amino acid 70 (green); alanine (A) and glycine (G). (ii) Combined ribbon and surface structures of the SFV4-EDI and ARKA7(74)-EDI nsP3 macro domains. (iii) Surface structures of the SFV4-EDI and ARKA7(74)-EDI nsP3 macro domains. Structures were generated using Phyre2 and formatted using UCSF Chimera.

In conclusion, the amino acid sequence of SFV4-EST differed from ARKL10-EDI at position 48 in nsP3. However, the results presented here indicate that this amino acid is unlikely to affect the function of nsP3 and, therefore, the virulence of SFV4-EST and ARKL10-EDI. Biochemically important amino acid substitutions between SFV4-EST and ARKA7(74)-EDI were identified at position 515 in nsP2 and positions 48 and 70 in nsP3. Further analysis, using the predicted 3D structure of the ARKA7(74)-EDI nsP2 protease domain, indicated that amino acid 515 is most likely to affect the function of ARKA7(74)-EDI nsP2 and SFV4-EDI, which could affect virulence.

6.2.7 Summary of findings

- The complete genomes of L10-EDI and A7(74)-EDI were sequenced using Solexa (Illumina) sequencing.
- The genetic sequence of L10-IRE was compared to L10-EDI. The replicase region of L10-IRE had 19 nucleotide differences compared to L10-EDI, of which 12 produced amino acid changes with large changes in the biochemistry. The structural region was identical between L10-EDI and L10-IRE at both the nucleotide and amino acid level.
- The genetic sequence of A7(74)-FIN and A7(74)-EDI were compared and are very similar at both the nucleotide and amino acid level. Five nucleotide differences were identified, of which only one produced an amino change. This difference was located in nsP3 at position 11.
- The genetic sequence of A7-IRE was compared to A7(74)-EDI. Across the genome, 11 nucleotide differences were identified and an additional 2771 nucleotides were encoded by A7-IRE in the 3’ UTR which were not present in A7(74)-EDI. However, at the amino acid level only two amino acid differences were identified. These were located in nsP2 and E1 at position 669 and 319 respectively.
- The genetic sequence of SFV4-EST and L10-EDI were compared. Across the genome seven substitutions were identified that were located in the 5’ UTR, nsP3, capsid and E2. L10-EDI had 37 fewer nucleotides in the 3’UTR compared

to SFV4-EDI. In nsP3, the amino acid difference was located at position 48 in the macro domain. 3D modelling suggests this change is unlikely to affect function.

- Several differences were identified throughout the genetic sequence of ARKA7(74)-EDI compared to SFV4-EST. In nsP2 and nsP3, three biochemically important changes were identified. These were in the nsP2 protease domain at position 515 and in the nsP3 macro domain at positions 48 and 70. NsP2 515 is located close to the protease domain active site, orientated outwards and therefore likely to affect function. In the nsP3 macro domain, amino acid 48 is located in a loop away from the active site. In contrast, amino acid 70 is located closer to the active site, is a large change in biochemistry and is likely to be more important in affecting the function of nsP3 than amino acid 48.

6.3 Discussion

In this chapter the genetic sequences of L10-EDI, A7(74)-EDI and SFV4-EST, in particular the genes encoding nsP2 and nsP3, were determined and compared. SFV L10 and SFV A7(74) differ in virulence in adult mice (Bradish *et al.*, 1971), however the genetic factor(s) behind this are unknown. SFV4 is a molecular cDNA clone of Prototype virus, which is closely related to SFV L10 (Liljestrom *et al.*, 1991). However, during the cloning process an unknown genetic change must have occurred since after *ip* inoculation SFV4 is avirulent in adult mice, while SFV L10 is virulent (Glasgow *et al.*, 1991;Fazakerley, 2002).

The genetic sequences of L10-EDI (ARKL10-EDI) and A7(74)-EDI (ARKA7(74)-EDI) were generated by Solexa (Illumina) sequencing and confirmed in part (nsP2/nsP3) using PCR sequencing (2.13.1, 2.13.2). Solexa (Illumina) sequencing is a powerful tool that sequences all DNA in a sample to generate a consensus sequence with a high confidence. In contrast, traditional PCR rapidly sequences a single genotype in the population. Both techniques are useful depending on the aim. The sequence of SFV4, referred to here as SFV4-EST, was recently generated by Prof. Merits, Institute of Technology, University of Tartu, Estonia. PCR sequencing confirmed the sequences of nsP2 and nsP3 in SFV4-EST and SFV A7(74)-EDI (obtained by Solexa (Illumina) sequencing). However, in L10-EDI, the amino acid sequence of nsP2 differed at position 754 between the sequence generated by Solexa (Illumina) sequencing and PCR. The amino acids are both hydrophilic and, therefore, constitute a minor change which is unlikely to affect the secondary structure of nsP2. One possible explanation for the difference between the Solexa (Illumina) sequencing results and the PCR sequencing results is that both sequences are present in the virus population. Potentially, the sequence identified by PCR was present at a lower abundance than that identified by Solexa (Illumina) sequencing. In HCV infections, deep sequencing technology has facilitated the detection of a master sequence and quasispecies within a sample. Quasispecies are viral subpopulations that have small sequence variations compared to the master sequence (Ruiz-Jarabo *et al.*, 2000;Domingo & Wain-Hobson, 2009;Verbinnen *et al.*, 2010).

There is one sequence for SFV L10 available on the NCBI database, L10-IRE. However, comparison of the genetic sequences of ARKL10-EDI and L10-IRE identified 19 nucleotide differences resulting in 18 amino acid changes (Tables 6.2 and 6.6). All the differences identified were located in the replicase ORF and most mapped to nsP2. The majority of these amino acid differences appear to be due to a frame-shift (discussion with Prof. Merits). Possible explanations for the differences between ARKL10-EDI and L10-IRE include (i) L10-IRE has a different passage history to ARKL10-EDI that selected for genetic changes or, more likely, (ii) there were mistakes during the sequencing of L10-IRE. This data indicate that experiments using L10-IRE cannot be directly applied to ARKL10-EDI and that these two stocks of virus both labelled SFV L10 must be considered different.

Much of our understanding about SFV A7(74) comes from studies using A7(74)-EDI, A7(74)-FIN and A7-IRE (Glasgow *et al.*, 1994;Santagati *et al.*, 1995;Tarbatt *et al.*, 1997;Tuittila *et al.*, 2000;Tuittila & Hinkkanen, 2003;Neuvonen *et al.*, 2011). The genetic sequences of A7(74)-FIN and A7-IRE were compared to A7(74)-EDI at both the nucleotide and amino acid level. The amino acid sequences of A7(74)-FIN and A7-IRE were extremely similar to A7(74)-EDI; one amino acid difference was identified between A7(74)-EDI and A7(74)-FIN and two amino acid differences between A7(74)-EDI and A7-IRE (Table 6.5). This data indicate that the observations made with A7(74)-FIN and A7-IRE can be applied to A7(74)-EDI.

Next, the genetic sequences of SFV4-EST and L10-EDI were compared. The sequences were highly conserved with only seven substitutions identified (Table 6.6). These were located in the 5' UTR, nsP3, capsid and E2 (Table 6.6 and Fig. 6.1). In addition, L10-EDI encoded 37 fewer nucleotides than SFV4-EST in the 3'UTR. In nsP3, the amino acid substitution was located in the macro domain at amino acid position 48; SFV4-EST expressed glutamic acid and ARKL10-EDI expressed alanine. The macro domain is highly conserved between alphaviruses, rubella virus, HEV and the coronaviruses, although its function remains to be fully elucidated (Koonin & Dolja, 1993;Pehrson & Fuji, 1998;Neuvonen & Ahola, 2009). During alphavirus infection, the macro domain is associated with replication of the virus genome and in attachment of replication complexes to cellular membranes (Peranen *et al.*, 1988;Peranen, 1991;Peranen *et al.*, 1995;Salonen *et al.*, 2003;Tuittila &

Hinkkanen, 2003). It is difficult to predict the importance of amino acid 48 on nsP3 function and the virulence of SFV-EST and ARKL10-EDI. Amino acid position 48 is highly variable between alphaviruses (Fig. 6.5). In addition, amino acid 48 is located in a loop, orientated inwards, away from the active site (Fig. 6.7). Furthermore, deletion of nsP3 residues 25 – 49 in SFV4-EST had a limited affect on virus replication in BHK-21 cells (Lulla *et al.*, 2012). In contrast, in one study, substitution of ^{48}glutamic acid in SFV4-SWE for ^{48}alanine in A7(74)-FIN produced a virus incapable of replication *in vitro* (Tuittila & Hinkkanen, 2003). Taken together, this data indicate that amino acid 48 is unlikely to affect SFV replication. However, one possibility is that amino acid 48 affects the interaction of nsP3 with the host immune system, as opposed to directly altering virus replication. In MHV (coronavirus) infection, the macro domain functions as an IFN antagonist (Eriksson *et al.*, 2008). In Lulla *et al* (2012), BHK-21 cells were used to assess the replication of SFV4-EST and SFV4-EST with a deletion of nsP3 residues 25 – 49. BHK-21 cells are IFN incompetent and, therefore, if the nsP3 macrodomain is important in controlling the host IFN response this would not be seen in this experimental design.

Based on this information it is difficult to predict how important amino acid 48 is for SFV virulence. Engineering of SFV4-EST constructs is currently underway in the laboratory of Prof. Merits to produce clones of SFV4-EST with different combinations of amino acids identified in ARKL10-EDI. Further analysis of other amino acid substitutions was beyond the scope of this thesis. The pathogenesis of these constructs will then be assessed in adult mice by our laboratory in Edinburgh and functional IFN levels will be measured.

The genetic sequence of ARKA7(74)-EDI had several changes compared to SFV4-EST, which mostly mapped to nsP3 (Table 6.6). This has been previously reported for A7(74)-FIN compared to SFV4-SWE (Tarbatt *et al.*, 1997;Tuittila *et al.*, 2000). Several studies suggest that nsP3 is a virulence determinant in A7(74)-FIN infection (Tarbatt *et al.*, 1997;Tuittila *et al.*, 2000;Tuittila & Hinkkanen, 2003). In nsP3, the important biochemical differences identified in this study between A7(74)-EDI and SFV4-EST were amino acid substitutions at positions 48 (glutamic acid in SFV4-EST and alanine in ARKA7(74)-EDI), 70 (arginine in SFV4-EST and glycine in A7(74)-EDI), 394 (aspartic acid in SFV4-EST and alanine in ARKA7(74)-EDI)

and 442 (alanine in SFV4-EST and threonine in ARKA7(74)-EDI) a deletion of 7 amino acids in A7(74)-EDI and an opal codon in ARKA7(74)-EDI not identified in SFV4-EST (Table 6.6). Amino acid 48 and 70 are located within the macro domain. Amino acid 48 has been discussed above. In the panel of alphaviruses, only SFV4-EST and ARKL10-EDI expressed ^{70}glycine (Fig. 6.2). This amino acid difference between SFV4-EST and ARKA7(74)-EDI is likely to affect the function of nsP3 due to (i) glycine is smaller and has a completely different structure to alanine and (ii) amino acid 70 is located relatively close to the active site (Fig. 6.4). Indeed, a clone based on A7(74)-FIN engineered to express ^{70}glycine produced mild to severe paralysis in adult mice following *ip* inoculation (A7(74)-FIN is avirulent in adult mice) (Tuittila & Hinkkanen, 2003). The role of the nsP3 macro domain and, in particular, this amino acid during SFV infection remains unclear. This would be an interesting area for future work. Amino acids 394 and 442 are located in the hypervariable domain. The hypervariable is predicted to be highly disordered and no crystal structure is currently available. Therefore, it is difficult to predict how changes in this region affect the structure and function of nsP3 without mouse experiments.

In chapter 5, nsP2 was shown to be important in determining the virulence of SFV4-EST. Therefore, the nsP2 amino acid sequence was analysed further. The nsP2 amino sequence of SFV4-EST and ARKL10-EDI were identical, while the amino acid sequence of SFV4-EST and ARKA7(74)-EDI differed on four occasions. One biochemically important amino acid substitution was identified at position 515, valine was identified in SFV4-EST and glutamic acid in ARKA7(74)-EDI (Table 6.6). In the panel of alphaviruses, only SFV4-EST expressed ^{515}glutamic acid. Amino acid 515 is located in the active site of the nsP2 protease domain (Fig. 6.4). The protease domain is associated with cleavage of the polyprotein and replication of the virus genome (Suopanki *et al.*, 1998;Vasiljeva *et al.*, 2003;Russo *et al.*, 2006). However, a specific role for this amino acid during SFV replication has not been described. This amino acid could potentially be involved in replication efficiency through processing the replicase polyprotein and/or in interaction with the immune system. It would be interesting to substitute the amino acid at position 515 in A7(74)-

EDI nsP2 with the amino acid in SFV4-EST and investigate how this affects the pathogenesis of the virus in mice.

In conclusion, the sequence analysis presented here demonstrates the similarity of SFV4-EST to L10-EDI and suggests amino acids that may determine the virulence of SFV L10 relative to SFV4 in adult mice. The data confirms reports that the genetic sequence of SFV A7(74) differs from SFV4 on multiple occasions and suggests amino acid substitutions that may be important in determining SFV virulence in adult mice.

6.3.1 Final summary

For the first time two strains of SFV held at EDI, L10-EDI and A7(74)-EDI, were sequenced and compared to other database sequences. The results comparing L10-EDI to SFV4-EST were extremely interesting; only seven differences were identified. These substitutions are currently under investigation. Multiple amino acid differences were identified between A7(74)-EDI and SFV4-EST, as expected. One particularly interesting amino acid difference was located in the active site of the nsP2 protease domain at position 515. This data suggests avenues for future work.

Chapter 7: Final discussion

This thesis investigated the interaction of SFV with host cell stress responses, in particular the autophagy and type-I IFN responses. The cell stress response is employed by cells to control internal conditions following a stressful stimulus, such as virus infection. Cell stress responses include the type-I IFN response, autophagy, UPR and, if the cell cannot recover, apoptosis. Previous studies have demonstrated that SFV infection induces the type-I IFN response, the UPR, apoptosis and, more recently, autophagy (Bradish *et al.*, 1975;Barry *et al.*, 2010;Eng *et al.*, 2012). At the beginning of this thesis three hypotheses were set out: (i) SFV infection induces autophagy in cell culture utilises this response to enhance virus replication and (ii) the quality, quantity and/or protective efficacy of the IFN response differ between strains of SFV and between human and murine cells and (iii) the replicase proteins nsP2 and/or nsP3 antagonise the IFN response.

In chapter 3 the hypothesis that 'SFV infection induces autophagy in cell culture and subverts autophagy to enhance virus replication' was investigated. Strains of SFV rapidly induced the accumulation of autophagosomes by 1 h post-infection in Huh7 cells. Most RNA viruses studied to date induce autophagy in cell culture. Autophagy enhances the replication of CHIKV, which is closely related to SFV, in HEK293 cells (Krejbich-Trotot *et al.*, 2011). Similarly, autophagy enhances the replication of PV (Jackson *et al.*, 2005), Coxsachievirus B3 virus (Wong *et al.*, 2008), FMDV (O'Donnell *et al.*, 2011), DENV (Lee *et al.*, 2008), JEV (Li *et al.*, 2012a), SARS-CoV (Prentice *et al.*, 2004) and HCV (Dreux & Chisari, 2009). In contrast, during SINV infection autophagy appears to selectively target capsid protein for degradation in autolysosomes, although replication is unaffected (Orvedahl *et al.*, 2010). Other studies have shown that autophagy has no affect on the replication of MHV and HRV2 (Brabec-Zaruba *et al.*, 2007;Zhao *et al.*, 2007b).

In the data presented here neither the inhibition nor the induction of autophagy affected SFV replication at a high MOI of 5. In addition, the autophagosome marker GFP-LC3 colocalised with nsP3 or dsRNA in <5 % of cells in

the monolayer at 6 and 24 h post-infection. Similar results were observed for capsid and GFP-LC3 colocalisation experiments. However, at a low MOI of 0.01, rapamycin induction of autophagy appeared to reduce SFV replication at 5 and 6 h post-infection; the opposite effect on replication was observed with 3MA inhibition of autophagy. This effect at high MOI, when all cells are infected, suggests that autophagy does not function either as a site of replication for SFV or, to a large extent, as a mechanism to degrade SFV proteins. Similar results were observed by Eng *et al* (2012), who investigated the interaction of SFV with autophagy in HOS and MEFs. The results at a low MOI, when only a few cells are infected, could indicate that rapamycin pre-treatment is delaying virus release or reducing numbers of infectious viruses released, while 3MA enhances this. Indeed, 5 – 6 h post-infection is consistent with the time at which the second round of virus infection is expected. In conclusion, SFV induces the accumulation of autophagosomes *in vitro*, which has an antiviral effect on SFV replication only at a low MOI.

The hypothesis that 'the quality and/or the quantity and/or the protective efficacy of the IFN response differ between strains of SFV and between human and murine cells' was investigated in chapters 4 and 5. The results were complicated, which indicates the complexity of the type-I IFN response. Three strains of SFV were investigated that differ in virulence in adult mice: virulent SFV L10 and avirulent SFV A7(74) and SFV4. The experiments were carried out in both human and mouse fibroblasts that are believed to have an intact type-I IFN response. In chapter 4, all three strains were shown to be highly sensitive to both human and mouse IFN-α pre-treatment, as demonstrated by a reduction in titre of >75 %. The strains did not differ in sensitivity to IFN-α pre-treatment, disagreeing with the hypothesis suggested in (ii). These results differed from a study by Deuber and Pavlovic (2007) in which a virulent strain of SFV (SFV L10) was less sensitive to IFN pre-treatment than an avirulent strain of SFV (SFV V42); SFV L10 replicated to higher titres than SFV V42 following IFN pre-treatment. The differing results between Deuber and Pavlovic (2007) and the data presented here could be due to (i) differences between V42 and

SFV4 and SFV A7(74), (ii) variations between the cells used and/or (iii) differences in the experimental protocol. Based on these results, it is unlikely that IFN induction is responsible for the mild infection of SFV in humans suggested in hypothesis (ii). However, the results presented here do not exclude the possibility that IFN does determine the pathogenesis of other alphaviruses, such as CHIKV, in mice. CHIKV is avirulent in mice unless the mice are deficient in the type-I IFN system (Couderc *et al.*, 2008). It would be interesting to directly compare CHIKV and SFV induction of IFN and sensitivity to the effects of IFN in both human and mouse cells. This experiment was planned as part of the present study, but was not carried out due to the unavailability of containment level 3 laboratory spaces.

In another experiment, human and mouse fibroblasts were infected with the three strains of SFV and the amount of functional IFN produced was measured. Two particularly interesting observations were made, (i) SFV4 induced more functional IFN than SFV L10 in mouse fibroblasts and (ii) strains of SFV induced less functional IFN than SeV in fibroblasts. SFV4 was derived from Prototype virus, which was isolated from the same pool of mosquitoes as SFV L10 (SMITHBURN & Harrow, 1944;Liljestrom *et al.*, 1991). However, during the cloning process the virulence of SFV4 following *ip* inoculation in adult mice was lost (Glasgow *et al.*, 1991;Fazakerley, 2002). The results presented here indicate that changes in the sequence of SFV4 have made it less efficient at inhibiting the IFN response than SFV L10. This could explain the difference in pathogenesis between the strains in adult mice.

In chapter 6, Solexa (Illumina) sequencing and PCR facilitated the comparison of our laboratory strains of SFV L10 and SFV A7(74) with the molecular clone SFV4 at the nucleotide and amino acid level. Sequence comparison of SFV4 and SFV L10 at the amino acid level identified 9 substitutions located in the 5’ UTR, nsP3, capsid, E1 and E2. Biochemical analysis of the amino acid residues predicted that the substitutions with the greatest impact on function were in nsP3 and capsid. Comparison of the amino acid 48 in nsP3 between members of the alphavirus genus

indicated that this is a variable position and may, therefore, have a limited affect on virulence. However, amino acid 48 proved vital for SFV A7(74) replication (Tuittila & Hinkkanen, 2003). Without analysing the affect of these changes *in vivo* it is difficult to predict their importance to virulence. Currently, a series of SFV4 constructs are being created by our collaborators in the laboratory of Prof. Andres Merits, Institute of Technology, University of Tartu, Estonia that will encode the SFV L10 amino acid substitutions. These will be compared by our laboratory in adult mice for virulence and IFN production. This experiment should determine the difference(s) between SFV4 and SFV L10 that dictate virulence in adult mice.

The second observation, that strains of SFV induce less functional IFN than SeV, has been reported for other alphaviruses, including CHIKV and SINV (Burke *et al.*, 2009). Another study demonstrated that SFV4 induces less functional IFN and fewer IFN-β transcripts than SFV4 with a mutation in nsP2, termed SFV4-RDR (Breakwell *et al.*, 2007). Taken together, these data indicate that SFV can inhibit the IFN, either at the induction or signalling stage. The mechanism by which SFV inhibits the IFN signalling pathway was investigated in chapter 5. A panel of fibroblasts was infected with the three strains of SFV and then challenged with IFN-α treatment 10 h later. All three strains of SFV restricted the phosphorylation of STAT1 compared to the uninfected IFN-treated control. Inhibition of STAT1 phosphorylation was reported for cells infected with CHIKV and SINV (Simmons *et al.*, 2010; Fros *et al.*, 2010). Several viruses target and inhibit the type-I IFN signalling pathway through different mechanisms. The paramyxovirus PIV5 expresses V protein that promotes the polyubiquitylation of STAT1 and targets STAT1 for degradation (Didcock *et al.*, 1999;Andrejeva *et al.*, 2002;Ulane & Horvath, 2002;Precious *et al.*, 2005). HeV and MV sequester STAT1 into cytoplasmic high molecular complexes (Rodriguez *et al.*, 2003;Palosaari *et al.*, 2003). Flaviviruses, such as DENV and JEV, express the protein NS5 that directly disrupts the phosphorylation and activation of STAT1 (Munoz-Jordan *et al.*, 2003;Lin *et al.*, 2004;Guo *et al.*, 2005;Ho *et al.*, 2005;Best *et al.*, 2005;Ashour *et al.*, 2009). SARS-CoV indirectly inhibits STAT1

activity by the virus protein ORF6 binding nuclear transport protein karyopherin α2, which prevents the nuclear translocation of STAT1 (Frieman *et al.*, 2007). In addition, the inhibition of IFN-β induction by viruses prevents all downstream processes, including STAT1 phosphorylation. SFV does not induce total STAT1 degradation, as demonstrated by Western blot. Therefore, SFV does not appear to antagonise STAT1 phosphorylation through the same mechanism as PIV5.

The hypothesis that 'the replicase proteins nsP2 and/or nsP3 antagonise the IFN response' was also investigated in chapter 5. Experiments demonstrated that the NLS motif in nsP2 was required to inhibit STAT1 phosphorylation; greater levels of STAT1 phosphorylation were detected in lysates from cells infected with SFV4-RDR compared to WT SFV4. One possible mechanism by which nsP2 could inhibit STAT1 phosphorylation is that nsP2 enters the nucleus and disrupts the IFN-β promoter, which is downstream of the transcription factors IRF-3 and NF-$_K$B. nsP2RDR is largely restricted to the cytoplasm and would not efficiently disrupt the IFN-β promoter. SFV4-RDR induces the production of more functional IFN than SFV4 (chapter 4). Therefore, the high levels of phosphorylated STAT1 during SFV4-RDR infection may be the result of increased IFN signalling, relative to SFV4. A recent study suggested that inhibition of the type-I IFN response during SINV infection *in vitro* occurred prior to the inhibition of STAT1 phosphorylation (Frolov *et al.*, 2012). An alternative mechanism is that nsP2 binds STAT1 or a protein important in STAT1 phosphorylation in the cytoplasm and this inhibits STAT1 phosphorylation. The levels of phosphorylated STAT1 detected during SFV4 infection remained low, even after IFN stimulation. This could indicate a specific role of SFV4 and perhaps nsP2 in antagonising the IFN signalling pathway. In SFV4-RDR, the structure of nsP2 is altered which may affect its ability to interact with other proteins. Current experiments in our laboratory provide strong evidence for the second mechanism (Dr. Gerald Barry, personal communication).

In conclusion, nsP2 is a multifunctional protein that probably interacts with the type-I IFN pathway at various stages. These results highlight the importance of

controlling the type-I IFN response for SFV replication and spread. Future research could focus on investigating the interaction of nsP2 with other proteins involved in the type-I IFN response and comparing this to nsP2 encoded by other alphaviruses, such as CHIKV.

In chapter 5, the potential role of nsP3 in antagonising the type-I IFN response was also investigated. NsP3 is implicated in virus replication, association of the RC with cellular membranes and as a virulence determinant (Hahn *et al.*, 1989;Lemm & Rice, 1993;Lemm *et al.*, 1994;Shirako & Strauss, 1994;Wang *et al.*, 1994;LaStarza *et al.*, 1994a;Tarbatt *et al.*, 1997;Tuittila *et al.*, 2000;Tuittila & Hinkkanen, 2003). The interaction of nsP3 with the type-I IFN response has not previously been investigated. NsP3 can be divided into 3 domains: the macrodomain towards the N-terminus, the domain conserved between alphaviruses and the hypervariable domain towards the C-terminus (Koonin & Dolja, 1993; Pehrson & Fuji, 1998; Neuvonen & Ahola, 2009; Peranen, 1991; Vihinen & Saarinen, 2000). The interaction of nsP3, and in particular the hypervariable domain, with the type-I IFN response was analysed using the mutant SFV4nsP3Δ50, which has a deletion of 50 amino acids in the hyperphosphorylated region. SFV4nsP3Δ50 replicates less efficiently *in vitro* and is less virulent *in vivo* than WT SFV4 (Vihinen *et al.*, 2001). In the data presented here, SFV4nsP3Δ50 replicated less efficiently in cell culture and induced significantly more IFN than WT SFV4. Higher levels of STAT1 phosphorylation were detected in lysates from cells infected with SFV4nsP3Δ50 compared to SFV4. However, the trend observed by Western blot was different to SFV4-RDR: SFV4-RDR induced STAT1 phosphorylation even without IFN-α challenge, while SFV4nsP3Δ50 only induced STAT phosphorylation following IFN-α challenge. This observation indicates that SFV4-RDR and SFV4nsP3Δ50 interact with the type-I IFN response via different mechanisms.

One hypothesis for the difference in IFN induction between WT SFV4 and SFV4nsP3Δ50 is that the hypervariable region of nsP3 inhibits proteins within the IFN induction and/or signalling pathways. An alternative hypothesis is that

SFV4nsP3Δ50 replicates less efficiently than SFV4 and, therefore, (i) does not enter the spherules (invaginations in cytoplasmic cell membranes) as efficiently for replication and does not 'hide' from the immune response and/or (ii) does not produce as many virus proteins that inhibit the immune response and/or (iii) does not induce host cell macromolecular synthesis shutoff as efficiently as WT SFV4. In a recent study, the hyperphosphorylated region was identified to have SH2 domains which are suggested to target the RC to cellular membranes (Neuvonen *et al.*, 2011). In SFV4nsP3Δ50 this region is lost, which would affect replication. The data presented here offer a greater insight into the role of nsP3 and the hyperphosphorylated region during SFV infection, although much is still unknown about nsP3. Future studies could focus on why SFV4nsP3Δ50 induces more IFN that WT SFV4 and with which cellular proteins nsP3 interacts. It would be interesting to compare the activity of nsP3 between different alphaviruses, in particular CHIKV.

This thesis enhances SFV research by providing a comprehensive comparison of three commonly used strains of SFV: SFV L10, SFV A7(74) and SFV4 and their interaction with the autophagy and the type-I IFN responses. This thesis demonstrates a novel mechanism by which strains of SFV can antagonise the type-I IFN pathway by inhibiting STAT1 phosphorylation and further elucidates the role of nsP2 and nsP3 during infection. Overall, the studies presented here provide a greater understanding of the interaction of SFV with the cell stress responses autophagy and type-I IFN.

Appendix

SFV L10 complete genome

ATGGCGGATGTGTGACATACACGACGCCAAAAGATTTTGTTCCAGCTCCTGCCACCT
CCGCTACGCGAGAGATTAACCACCCACGATGGCCGCCAAAGTGCATGTTGATATTGA
GGCTGACAGCCCATTCATCAAGTCTTTGCAGAAGGCATTTCCGTCGTTCGAGGTGGA
GTCATTGCAGGTCACACCAAATGACCATGCAAATGCCAGAGCATTTTCGCACCTGGC
TACCAAATTGATCGAGCAGGAGACTGACAAAGACACACTCATCTTGGATATCGGCAG
TGCGCCTTCCAGGAGAATGATGTCTACGCACAAATACCACTGCGTATGCCCTATGCG
CAGCGCAGAAGACCCCGAAAGGCTCGTATGCTACGCAAAGAAACTGGCAGCGGCCTC
CGGGAAGGTGCTGGATAGAGAGATCGCAGGAAAAATCACCGACCTGCAGACCGTCAT
GGCTACGCCAGACGCTGAATCTCCTACCTTTTGCCTGCATACAGACGTCACGTGTCG
TACGGCAGCCGAAGTGGCCGTATACCAGGACGTGTATGCTGTACATGCACCAACATC
GCTGTACCATCAGGCGATGAAAGGTGTCAGAACGGCGTATTGGATTGGGTTTGACAC
CACCCCGTTTATGTTTGACGCGCTAGCAGGCGCGTATCCAACCTACGCCACAAACTG
GGCCGACGAGCAGGTGTTACAGGCCAGGAACATAGGACTGTGTGCAGCATCCTTGAC
TGAGGGAAGACTCGGCAAACTGTCCATTCTCCGCAAGAAGCAATTGAAACCTTGCGA
CACAGTCATGTTCTCGGTAGGATCTACATTGTACACTGAGAGCAGAAAGCTACTGAG
GAGCTGGCACTTACCCTCCGTATTCCACCTGAAAGGTAAACAATCCTTTACCTGTAG
GTGCGATACCATCGTATCATGTGAAGGGTACGTAGTTAAGAAAATCACTATGTGCCC
CGGCCTGTACGGTAAAACGGTAGGGTACGCCGTGACGTATCACGCGGAGGGATTCCT
AGTGTGCAAGACCACAGACACTGTCAAAGGAGAAAGAGTCTCATTCCCTGTATGCAC
CTACGTCCCCTCAACCATCTGTGATCAAATGACTGGCATACTAGCGACCGACGTCAC
ACCGGAGGACGCACAGAAGTTGTTAGTGGGATTGAATCAGAGGATAGTTGTGAACGG
AAGAACACAGCGAAACACTAACACGATGAAGAACTATCTGCTTCCGATTGTGGCCGT
CGCATTTAGCAAGTGGGCGAGGGAATACAAGGCAGACCTTGATGATGAAAAACCTCT
GGGTGTCCGAGAGAGGTCACTTACTTGCTGCTGCTTGTGGGCATTTAAAACGAGGAA
GATGCACACCATGTACAAGAAACCAGACACCCAGACAATAGTGAAGGTGCCTTCAGA
GTTTAACTCGTTCGTCATCCCGAGCCTATGGTCTACAGGCCTCGCAATCCCAGTCAG
ATCACGCATTAAGATGCTTTTGGCCAAGAAGACCAAGCGAGAGTTAATACCTGTTCT
CGACGCGTCGTCAGCCAGGGATGCTGAACAAGAGGAGAAGGAGAGGTTGGAGGCCGA
GCTGACTAGAGAAGCCTTACCACCCCTCGTCCCCATCGCGCCGGCGGAGACGGGAGT
CGTCGACGTCGACGTTGAAGAACTAGAGTATCACGCAGGTGCAGGGGTCGTGGAAAC
ACCTCGCAGCGCGTTGAAAGTCACCGCACAGCCGAACGACGTACTACTAGGAAATTA
CGTAGTTCTGTCCCCGCAGACCGTGCTCAAGAGCTCCAAGTTGGCCCCCGTGCACCC
TCTAGCAGAGCAGGTGAAAATAATAACACATAACGGGAGGGCCGGCCGTTACCAGGT
CGACGGATATGACGGCAGGGTCCTACTACCATGTGGATCGGCCATTCCGGTCCCTGA
GTTTCAAGCTTTGAGCGAGAGCGCCACTATGGTGTACAACGAAAGGGAGTTCGTCAA
CAGGAAACTATACCATATTGCCGTTCACGGACCGTCGCTGAACACCGACGAGGAGAA
CTACGAGAAAGTCAGAGCTGAAAGAACTGACGCCGAGTACGTGTTCGACGTAGATAA
AAAATGCTGCGTCAAGAGAGAGGAAGCGTCGGGTTTGGTGTTGGTGGGAGAGCTAAC
CAACCCCCCGTTCCATGAATTCGCCTACGAAGGGCTGAAGATCAGGCCGTCGGCACC
ATATAAGACTACAGTAGTAGGAGTCTTTGGGGTTCCGGGATCAGGCAAGTCTGCTAT
TATTAAGAGCCTCGTGACCAAACACGATCTGGTCACCAGCGGCAAGAAGGAGAACTG
CCAGGAAATAGTCAACGACGTGAAGAAGCACCGCGGACTGGACATCCAGGCAAAAAC
AGTGGACTCCATCCTGCTAAACGGGTGTCGTCGTGCCGTGGACATCCTATATGTGGA
CGAGGCTTTCGCTTGCCATTCCGGTACTCTGCTGGCCCTAATTGCTCTTGTTAAACC
TCGGAGCAAAGTGGTGTTATGCGGAGACCCCAAGCAATGCGGATTCTTCAATATGAT
GCAGCTTAAGGTGAACTTCAACCACAACATCTGCACTGAAGTATGTCATAAAAGTAT

ATCCAGACGTTGCACGCGTCCAGTCACGGCCATCGTGTCTACGTTGCACTACGGAGG
CAAGATGCGCACGACCAACCCGTGCAACAAACCCATAATCATAGACACCACAGGACA
GACCAAGCCCAAGCCAGGAGACATCGTGTTAACATGCTTCCGAGGCTGGGTAAAGCA
GCTGCAGTTGGACTACCGTGGACACGAAGTCATGACAGCAGCAGCATCTCAGGGCCT
CACCCGCAAAGGGGTATACGCCGTAAGGCAGAAGGTGAATGAAAATCCCTTGTATGC
CCCTGCGTCGGAGCACGTGAATGTACTGCTGACGCGCACTGAGGATAGGCTGGTGTG
GAAAACGCTGGCCGGCGATCCCTGGATTAAGGTCCTATCAAACATTCCACAGGGTAA
CTTTACGGCCACATTGGAAGAATGGCAAGAAGAACACGACAAAATAATGAAGGTGAT
TGAAGGACCGGCTGCGCCTGTGGACGCGTTCCAGAACAAAGCGAACGTGTGTTGGGC
GAAAAGCCTGGTGCCTGTCCTGGACACTGCCGGAATCAGATTGACAGCAGAGGAGTG
GAGCACCATAATTACAGCATTTAAGGAGGACAGAGCTTACTCTCCAGTGGTGGCCTT
GAATGAAATTTGCACCAAGTACTATGGAGTTGACCTGGACAGTGGCCTGTTTTCTGC
CCCGAAGGTGTCCCTGTATTACGAGAACAACCACTGGGATAACAGACCTGGTGGAAG
GATGTATGGATTCAATGCCGCAACAGCTGCCAGGCTGGAAGCTAGACATACCTTCCT
GAAGGGGCAGTGGCATACGGGCAAGCAGGCAGTTATCGCAGAAAGAAAAATCCAACC
GCTTTCTGTGCTGGACAATGTAATTCCTATCAACCGCAGGCTGCCGCACGCCCTGGT
GGCTGAGTACAAGACGGTTAAAGGCAGTAGGGTTGAGTGGCTGGTCAATAAAGTAAG
AGGGTACCACGTCCTGCTGGTGAGTGAGTACAACCTGGCTTTGCCTCGACGCAGGGT
CACTTGGTTGTCACCGCTGAATGTCACAGGCGCCGATAGGTGCTACGACCTAAGTTT
AGGACTGCCGGCTGACGCCGGCAGGTTCGACTTGGTCTTTGTGAACATTCACACGGA
ATTCAGAATCCACCACTACCAGCAGTGTGTCGACCACGCCATGAAGCTGCAGATGCT
TGGGGGAGATGCGCTACGACTGCTAAAACCCGGCGGCAGCCTCTTGATGAGAGCTTA
CGGATACGCCGATAAAATCAGCGAAGCCGTTGTTTCCTCCTTAAGCAGAAAGTTCTC
GTCTGCAAGAGTGTTGCGCCCGGATTGTGTCACCAGCAATACAGAAGTGTTCTTGCT
GTTCTCCAACTTTGACAACGGAAAGAGACCCTCTACGCTACACCAGATGAATACCAA
GCTGAGTGCCGTGTATGCCGGAGAAGCCATGCACACGGCCGGGTGTGCACCATCCTA
CAGAGTTAAGAGAGCAGACATAGCCACGTGCACAGAAGCGGCTGTGGTTAACGCAGC
TAACGCCCGTGGAACTGTAGGGGATGGCGTATGCAGGGCCGTGGCGAAGAAATGGCC
GTCAGCCTTTAAGGGAGCAGCAACACCAGTGGGCACAATTAAAACAGTCATGTGCGG
CTCGTACCCCGTCATCCACGCTGTAGCGCCTAATTTCTCTGCCACGACTGAAGCGGA
AGGGGACCGCGAATTGGCCGCTGTCTACCGGGCAGTGGCCGCCGAAGTAAACAGACT
GTCACTGAGCAGCGTAGCCATCCCGCTGCTGTCCACAGGAGTGTTCAGCGGCGGAAG
AGATAGGCTGCAGCAATCCCTCAACCATCTATTCACAGCAATGGACGCCACGGACGC
TGACGTGACCATCTACTGCAGAGACAAAAGTTGGGAGAAGAAAATCCAGGAAGCCAT
AGACATGAGGACGGCTGTGGAGTTGCTCAATGATGACGTGGAGCTGACCACAGACTT
GGTGAGAGTGCACCCGGACAGCAGCCTGGTGGGTCGTAAGGGCTACAGTACCACTGA
CGGGTCGCTGTACTCGTACTTTGAAGGTACGAAATTCAACCAGGCTGCTATTGATAT
GGCAGAGATACTGACGTTGTGGCCCAGACTGCAAGAGGCAAACGAACAGATATGCCT
ATACGCGCTGGGCGAAACAATGGACAACATCAGATCCAAATGTCCGGTGAACGATTC
CGATTCATCAACACCTCCCAGGACAGTGCCCTGCCTGTGCCGCTACGCAATGACAGC
AGAACGGATCGCCCGCCTTAGGTCACACCAAGTTAAAAGCATGGTGGTTTGCTCATC
TTTTCCCCTCCCGAAATACCATGTAGATGGGGTGCAGAAGGTAAAGTGCGAGAAGGT
TCTCCTGTTCGACCCGACGGTACCTTCAGTGGTTAGTCCGCGGAAGTATGCCGCATC
TACGACGGACCACTCAGATCGGTCGTTACGAGGGTTTGACTTGGACTGGACCACCGA
CTCGTCTTCCACTGCCAGCGATACCATGTCGCTACCCAGTTTGCAGTCGTGTGACAT
CGACTCGATCTACGAGCCAATGGCTCCCATAGTAGTGACGGCTGACGTACACCCTGA
ACCCGCAGGCATCGCGGACCTGGCGGCAGATGTGCATCCTGAACCCGCAGACCATGT
GGACCTCGAGAACCCGATTCCTCCACCGCGCCCGAAGAGAGCTGCATACCTTGCCTC
CCGCGCGGCGGAGCGACCGGTGCCGGCGCCGAGAAAGCCGACGCCTGCCCCAAGGAC
TGCGTTTAGGAACAAGCTGCCTTTGACGTTCGGCGACTTTGACGAGCACGAGGTCGA
TGCGTTGGCCTCCGGGATTACTTTCGGAGACTTCGACGACGTCCTGCGACTAGGCCG

CGCGGGTGCATATATTTTCTCCTCGGACACTGGCAGCGGACATTTACAACAAAAATC
CGTTAGGCAGCACAATCTCCAGTGCGCACAACTGGATGCGGTCGAGGAGGAGAAAAT
GTACCCGCCAAAATTGGATACTGAGAGGGAGAAGCTGTTGCTGCTGAAAATGCAGAT
GCACCCATCGGAGGCTAATAAGAGTCGATACCAGTCTCGCAAAGTGGAGAACATGAA
AGCCACGGTGGTGGACAGGCTCACATCGGGGGCCAGATTGTACACGGGAGCGGACGT
AGGCCGCATACCAACATACGCGGTTCGGTACCCCCGCCCCGTGTACTCCCCTACCGT
GATCGAAAGATTCTCAAGCCCCGATGTAGCAATCGCAGCGTGCAACGAATACCTATC
CAGAAATTACCCAACAGTGGCGTCGTACCAGATAACAGATGAATACGACGCATACTT
GGACATGGTTGACGGGTCGGATAGTTGCTTGGACAGAGCGACATTCTGCCCGGCGAA
GCTCCGGTGCTACCCGAAACATCATGCGTACCACCAGCCGACTGTACGCAGTGCCGT
CCCGTCACCCTTTCAGAACACACTACAGAACGTGCTAGCGGCCGCCACCAAGAGAAA
CTGCAACGTCACGCAAATGCGAGAACTACCCACCATGGACTCGGCAGTGTTCAACGT
GGAGTGCTTCAAGCGCTATGCCTGCTCCGGAGAATATTGGGAAGAATATGCTAAACA
ACCTATCCGGATAACCACTGAGAACATCACTACCTATGTGACCAAATTGAAAGGCCC
GAAAGCTGCTGCCTTGTTCGCTAAGACCCACAACTTGGTTCCGCTGCAGGAGGTTCC
CATGGACAGATTCACGGTCGACATGAAACGAGATGTCAAAGTCACTCCAGGGACGAA
ACACACAGAGGAAAGACCCAAAGTCCAGGTAATTCAAGCAGCGGAGCCATTGGCGAC
CGCTTACCTGTGCGGCATCCACAGGGAATTAGTAAGGAGACTAAATGCTGTGTTACG
CCCTAACGTGCACACATTGTTTGATATGTCGGCCGAAGACTTTGACGCGATCATCGC
CTCTCACTTCCACCCAGGAGACCCGGTTCTAGAGACGGACATTGCATCATTCGACAA
AAGCCAGGACGACTCCTTGGCTCTTACAGGTTTAATGATCCTCGAAGATCTAGGGGT
GGATCAGTACCTGCTGGACTTGATCGAGGCAGCCTTTGGGGAAATATCCAGCTGTCA
CCTACCAACTGGCACGCGCTTCAAGTTCGGAGCTATGATGAAATCGGGCATGTTTCT
GACTTTGTTTATTAACACTGTTTTGAACATCACCATAGCAAGCAGGGTACTGGAGCA
GAGACTCACTGACTCCGCCTGTGCGGCCTTCATCGGCGACGACAACATCGTTCACGG
AGTGATCTCCGACAAGCTGATGGCGGAGAGGTGCGCGTCGTGGGTCAACATGGAGGT
GAAGATCATTGACGCTGTCATGGGCGAAAAACCCCCATATTTTTGTGGGGGATTCAT
AGTTTTTGACAGCGTCACACAGACCGCCTGCCGTGTTTCAGACCCACTTAAGCGCCT
GTTCAAGTTGGGTAAGCCGCTAACAGCTGAAGACAAGCAGGACGAAGACAGGCGACG
AGCACTGAGTGACGAGGTTAGCAAGTGGTTCCGGACAGGCTTGGGGGCCGAACTGGA
GGTGGCACTAACATCTAGGTATGAGGTAGAGGGCTGCAAAAGTATCCTCATAGCCAT
GGCCACCTTGGCGAGGGACATTAAGGCGTTTAAGAAATTGAGAGGACCTGTTATACA
CCTCTACGGCGGTCCTAGATTGGTGCGTTAATACACAGAATTCTGATTATAGCGCAC
TATTATAGCACCATGAATTACATCCCTACGCAAACGTTTTACGGCCGCCGGTGGCGC
CCGCGCCCGGCGGCCCGTCCCTGGCCGTTGCAGGCCACTCCGGTGGCTCCCGTCGTC
CCCGACTTCCAGGCCCAGCAGATGCAGCAACTCATCAGCGCCGTAAATGCGCTGACA
ATGAGACAGAACGCAATTGCTCCTGCTGGGCCTCCCAAACCAAAGAAGAAGAAGACA
ACCAAACCAAAGCCGAAAACGCAGCCCAAGAAGATCAAAGGAAAAACGCAGCAGCAA
AAGAAGAAAGACAAGCAAGCCGACAAGAAGAAGAAGAAACCCGGAAAAAGAGAAAGA
ATGTGCATGAAGATTGAAAATGACTGTATCTTCGAAGTCAAACACGAAGGAAAGGTC
ACTGGGTACGCCTGCCTGGTGGGCGACAAAGTCATGAAACCTGCCCACGTGAAAGGA
GTCATCGACAACGCGGACCTGGCAAAGCTAGCTTTCAAGAAATCGAGCAAGTATGAC
CTTGAGTGTGCCCAGATACCAGTTCACATGAGGTCGGATGCCTCAAAGTACACGCAT
GAGAAGCCCGAGGGACACTATAACTGGCACCACGGGGCTGTTCAGTACAGCGGAGGT
AGGTTCACTATACCGACAGGAGCGGGCAAACCGGGAGACAGTGGCCGGCCCATCTTT
GACAACAAGGGGAGGGTAGTCGCTATCGTCCTGGGCGGGGCCAACGAGGGCTCACGC
ACAGCACTGTCGGTGGTCACCTGGAACAAAGATATGGTGACTAGAGTGACCCCCGAG
GGGTCCGAAGAGTGGTCCGCCCCGCTGATTACTGCCATGTGTGTCCTTGCCAATGCT
ACCTTCCCGTGCTTCCAGCCCCCGTGTGTACCTTGCTGCTATGAAAACAACGCAGAG
GCCACACTACGGATGCTCGAGGATAACGTGGATAGGCCAGGGTACTACGACCTCCTT
CAGGCAGCCTTGACGTGCCGAAACGGAACAAGACACCGGCGCAGCGTGTCGCAACAC

TTCAACGTGTATAAGGCTACACGCCCTTACATCGCGTACTGCGCCGACTGCGGAGCA
GGGCACTCGTGTCATAGCCCCGTAGCAATTGAAGCGATCAGGTCCGAAGCTACCGAC
GGGATGCTGAAGATTCAGTTCTCGGCACAAATTGGCATAGATAAGAGTGACAATCAT
GACTACACGAAGATAAGGTACGCAGACGGGCACGCCATTGAGAATGCCGTCCGGTCA
TCTTTGAAGGTAGCCACCTCCGGAGACTGTTTCGTCCATGGCACAATGGGACATTTC
ATACTGGCAACGTGCCCACCGGGTGAATTCCTGCAGGTCTCGATCCAGGACACCAGA
AACGCGGTCCGTGCCTGCAGAATACAATATCATCATGACCCTCAACCGGTGGGTAGA
GAAAAATTTACAATTAGACCACACTATGGAAAAGAGATCCCTTGCACCACTTATCAA
CAGACCACAGCGGAGACCGTGGAGGAAATCGACATGCATATGCCGCCAGATACGCCG
GACAGGACGTTGCTATCACAGCAATCTGGCAATGTAAAGATCACAGTCGGAGGAAAG
AAGGTGAAATACAACTGCACCTGTGGAACCGGAAACGTTGGCACTACTAATTCGGAC
ATGACGATCAACACGTGTCTAATAGAGCAGTGCCACGTCTCAGTGACGGACCATAAG
AAATGGCAGTTCAACTCACCTTTCGTCCCGAGAGCCGACGAACCGGCTAGAAAAGGC
AAAGTCCATATCCCATTCCCGTTGGACAACATCACATGCAGAGTTCCAATGGCGCGC
GAACCAACCGTCATCCACGGCAAAAGAGAAGTGACACTGCACCTTCACCCAGATCAT
CCCACGCTCTTTTCCTACCGCACACTGGGTGAGGACCCGCAGTATCACGAGGAATGG
GTGACAGCGGCGGTGGAACGGACCATACCCGTACCAGTGGACGGGATGGAGTACCAC
TGGGGAAACAACGACCCAGTGAGGCTTTGGTCTCAACTCACCACTGAAGGGAAACCG
CACGGCTGGCCGCATCAGATCGTACAGTACTACTATGGGCTTTACCCGGCCGCTACA
GTATCCGCGGTCGTCGGGATGAGCTTACTGGCGTTGATATCGATCTTCGCGTCGTGC
TACATGCTGGTTGCGGCCCGCAGTAAGTGCTTGACCCCTTATGCTTTAACACCAGGA
GCTGCAGTTCCGTGGACGCTGGGGATACTCTGCTGCGCCCCGCGGGCGCACGCAGCT
AGTGTGGCAGAGACTATGGCCTACTTGTGGGACCAAAACCAAGCGTTGTTCTGGTTG
GAGTTTGCGGCCCCTGTTGCCTGCATCCTCATCATCACGTATTGCCTCAGAAACGTG
CTGTGTTGCTGTAAGAGCCTTTCTTTTTTAGTGCTACTGAGCCTCGGGGCAACCGCC
AGAGCTTACGAACATTCGACAGTAATGCCGAACGTGGTGGGGTTCCCGTATAAGGCT
CACATTGAAAGGCCAGGATATAGCCCCCTCACTTTGCAGATGCAGGTTGTTGAAACC
AGCCTCGAACCAACCCTTAATTTGGAATACATAACCTGTGAGTACAAGACGGTCGTC
CCGTCGCCGTACGTGAAGTGCTGCGGCGCCTCAGAGTGCTCCACTAAAGAGAAGCCT
GACTACCAATGCAAGGTTTACACAGGCGTGTACCCGTTCATGTGGGGAGGGGCATAT
TGCTTCTGCGACTCAGAAAACACGCAACTCAGCGAGGCGTACGTCGATCGATCGGAC
GTATGCAGGCATGATCACGCATCTGCTTACAAAGCCCATACAGCATCGCTGAAGGCC
AAAGTGAGGGTTATGTACGGCAACGTAAACCAGACTGTGGATGTTTACGTGAACGGA
GACCATGCCGTCACGATAGGGGGTACTCAGTTCATATTCGGGCCGCTGTCATCGGCC
TGGACCCCGTTCGACAACAAGATAGTCGTGTACAAAGACGAAGTGTTCAATCAGGAC
TTCCCGCCGTACGGATCTGGGCAACCAGGGCGCTTCGGCGACATCCAAAGCAGAACA
GTGGAGAGTAACGACCTGTACGCGAACACGGCACTGAAGCTGGCACGCCCTTCACCC
GGCATGGTCCATGTACCGTACACACAGACACCTTCAGGGTTCAAATATTGGCTAAAG
GAAAAAGGGACAGCCCTAAATACGAAGGCTCCTTTTGGCTGCCAAATCAAAACGAAC
CCTGTCAGGGCCATGAACTGCGCCGTGGGAAACATCCCTGTCTCCATGAATTTGCCT
GACAGCGCCTTTACCCGCATTGTCGAGGCGCCGACCATCATTGACCTGACTTGCACA
GTGGCTACCTGTACGCACTCCTCGGATTTCGGCGGCGTCTTGACACTGACGTACAAG
ACCGACAAGAACGGGGACTGCTCTGTACACTCGCACTCTAACGTAGCTACTCTACAG
GAGGCCACAGCAAAAGTGAAGACAGCAGGTAAGGTTACCTTACACTTCTCCACGGCA
AGCGCATCACCTTCTTTTGTGGTGTCGCTATGCAGTGCTAGGGCCACCTGTTCAGCG
TCGTGTGAGCCCCCGAAAGACCACATAGTCCCATATGCGGCTAGCCACAGTAACGTA
GTGTTTCCAGACATGTCGGGCACCGCACTATCATGGGTGCAGAAAATCTCGGGTGGT
CTGGGGGCCTTCGCAATCGGCGCTATCCTGGTGCTGGTTGTGGTCACTTGCATTGGG
CTCCGCAGATAAGTTAGGGTAGGCAATGGCATTGATATAGCAAGAAAATTGAAAACA
GAAAAAGTTAGGGTAAGCAATGGCATATAACCATAACTGTATAACTTGTAACAAAGC
GCAACAAGACCTGCGCAATTGGCCCCGTGGTCCGCCTCACGGAAACTCGGGGCAACT

CATATTGACACATTAATTGGCAATAATTGGAAGCTTACATAAGCTTAATTCGACGAA
TAATTGGATTTTTATTTTATTTTGCAATTGGTTTTTAATATTTCC

SFV A7(74) complete genome

ATGGCGGATGTGTGACATACGCGACGCCAAAAGAATTTGTTTCAGCTCCTGCCACCT
CCGCTACGCGAGAGATTAACCACCCACGATGGCCGCCAAAGTGCATGTTGATATTGA
GGCTGACAGCCCATTCATCAAGTCTTTGCAGAAGGCATTTCCGTCGTTCGAGGTGGA
GTCATTGCAGGTCACACCAAATGACCATGCAAATGCCAGAGCATTTTCGCATCTGGC
TACCAAATTGATCGAGCAGGAGACTGATAAAGACACACTCATCTTGGATATCGGCAG
TGCGCCTTCCAGGAGAATGATGTCTACGCACAAATACCACTGCGTATGCCCTATGCG
CAGCGCAGAAGATCCCGAAAGGCTCGTATGCTACGCAAAGAAACTGGCAGCGGCCTC
CGGGAAGGTGCTGGATAGAGAGATCGCAGGGAAAATCACCGACCTGCAGACCGTCAT
GGCTACGCCAGACGCTGAATCTCCTACCTTTTGTCTGCATACAGACGTCACATGTCG
TACGGCAGCTGAAGTGGCCGTATACCAGGACGTGTATGCTGTACATGCACCAACATC
GCTGTACCATCAGGCGATGAAAGGTGTCAGGACGGCGTATTGGATTGGGTTTGACAC
CACCCCGTTTATGTTTGACGCGCTTGCAGGCGCGTATCCAACCTACGCCACAAACTG
GGCCGACGAGCAGGTGTTACAGGCCAGGAACATAGGACTGTGTGCAGCATCCTTGAC
TGAGGGAAGACTCGGCAAACTGTCCATTCTCCGCAAGAAGCAATTGAAACCTAGCGA
CACAGTCATGTTCTCGGTAGGATCTACCTTGTACACTGAGAGCAGAAAGCTACTGAG
GAGCTGGCACTTACCCTCCGTATTCCACCTGAAAGGGAAACAATCCTTTACCTGTAG
GTGCGATACCATCGTATCATGTGAAGGGTATGTAGTTAAGAAAATCACTATGTGCCC
CGGCCTGTACGGTAAAACGGTAGGGTACGCCGTGACGCATCACGCGGAGGGATTCCT
AGTGTGCAAGACCACAGACACCGTCAAAGGAGAAAGAGTCTCATTCCCTGTATGCAC
CTACGTCCCCTCAACCATCTGTGATCAAATGACTGGTATATTAGCGACTGATGTCAC
ACCGGAGGACGCACAGAAGTTGTTAGTGGGATTGAATCAGAGGATAGTTGTGAACGG
AAGAACACAGCGAAACACTAACACGATGAAGAACTATCTGCTTCCGGTTGTGGCTGT
CGCATTTAGCAAGTGGGCGAGGGAATATAAGGCAGACCTTGATGATGAAAAACCACT
GGGTGTCCGAGAGAGGTCACTTACTTGCTGCTGCTTGTGGGCATTTAAAACAAAGAA
AATGCACACCATGTACAAGAAACCAGACACCCAGACAATAGTGAAGGTGCCTTCAGA
GTTCAACTCGTTCGTCATCCCGAGCCTATGGTCTACAGGCCTCGCAATCCCAGTCAG
ATCACGCATTAAGATGCTTTTGGCCAAGAAGACCAAGCGAGAGTTAATACCTGCTCT
CGACGCGTCGTCAGCCAGGGATGCTGAACAAGAGGAGAAGGAGAGGTTGGAGGCCGA
GCTGACTAGAGAAGCCTTACCACCCCTCGTCCCCATCGCGCCGGCGGAGACGGGAGT
CGTCGACGTCGACGTTGAAGAACTAGAGTATCGCGCAGGTGCAGGGGTCGTGGAAAC
ACCCCGCAGCGCGTTGAAAGTCACCGCACAGCCGAACGACGTACTACTAGGAAATTA
CGTAGTTCTGTCCCCGCAGACCGTGCTCAAGAGCTCCAAGCTGGCCCCCGTGCACCC
TCTAGCAGAGCAGGTGAAAATAATAACGCATAACGGGAGGGCTGGCCGTTACCAGGT
CGACGGATATGACGGCAGGGTCCTACTACCATGTGGATCGGCCATTCCGGTCCCTGA
GTTCCAAGCTTTGAGCGAGAGCGCCACTATGGTGTACAACGAAAGGGAGTTCGTCAA
CAGGAAACTATACCATATTGCCGTTCACGGACCGTCGTTGAACACCGACGAGGAGAA
CTACGAGAAAGTCAGAGCTGAAAGAACTGACGCCGAGTACGTGTTCGACGTAGACAA
AAAATGCTGCATCAAGAGAGAGGAAGCGTCGGGTTTGGTGTTGGTGGGAGAGCTAAC
CAACCCCCCGTTCCATGAATTCGCTTACGAAGGGCTGAAGATCAGGCCGTCGGCACC
ATATAAGACTACAGTAGTAGGAGTCTTTGGGGTTCCGGGATCAGGCAAGTCTGCTAT
TATCAAGAGCCTCGTGACCAAACACGACCTGGTCACCAGCGGCAAGAAGGAGAACTG
CCAGGAAATAGTCAACGACGTGAAGAAGCACCGCGGACTGGACATCCAGGCAAAAAC
AGTGGACTCCATCCTGCTAAACGGGTGTCGTCGCGCCGTGGACATCCTATATGTGGA
CGAGGCTTTTGCTTGCCATTCCGGTACTCTGCTGGCCCTAATTGCTCTTGTTAAACC
TCGGAGCAAAGTGGTGTTATGCGGAGACCCCAAGCAATGCGGATTCTTCAATATGAT
GCAGCTTAAGGTGAACTTCAACCATAACATCTGCACTGAAGTATGTCATAAAAGTAT
ATCCAGACGTTGCACGCGTCCAGTCACGGCCATCGTGTCTACGTTGCACTACGGAGG
CAAGATGCGCACGACCAACCCGTGTAACAAACCCATAATTATAGACACCACAGGACA
GACCAAGCCCAAGCCAGGAGACATTGTGTTAACATGCTTCCGAGGCTGGGTAAAGCA

GCTGCAATTGGACTATCGTGGACACGAAGTCATGACAGCAGCAGCATCTCAGGGCCT
CACCCGCAAAGGGGTATACGCCGTAAGGCAGAAGGTGAATGAAAATCCCTTGTATGC
CCCTGCGTCGGAGCACGTGAATGTACTGCTGACGCGCACTGAGGATAGGCTGGTGTG
GAAAACGCTGGCCGGCGATCCCTGGATTAAGGTCCTATCAAACATTCCACAGGGTAA
CTTTACGGCCACATTGGAAGAATGGCAAGAAGAACACGACAAAATAATGAAGGTGAT
TGAAGGACCGGCTGCGCCTGTGGACGCGTTCCAGAACAAAGCGAACGTGTGTTGGGC
GAAAAGCCTGGTGCCTGTCCTGGACACTGCCGGAATCAGATTGACAGCAGAGGAGTG
GAGTACCATAATTACAGCATTTAAGGAGGACAGAGCTTACTCTCCAGAGGTGGCCTT
GAATGAAATTTGCACCAAGTACTATGGAGTCGACCTGGACAGTGGCCTGTTTTCTGC
CCCGAAGGTGTCCCTGTATTACGAGAACAACCACTGGGATAACAGACCAGGTGGAAG
GATGTATGGATTCAATGCCGCAACAGCTGCCAGGCTGGAAGCTAGACATACCTTCCT
GAAGGGGCAGTGGCATACGGGCAAGCAGGCAGTAATCGCAGAAAGAAAAATCCAACC
GCTTTCTGTGCTGGACAATGTGATTCCCATCAACCGCAGGCTACCGCACGCCCTGGT
GGCTGAGTACAAGACGGTTAAAGGCAGTAGGGTTGAGTGGCTGGTCAATAAAGTAAG
AGGGTACCACGTCCTGCTGGTGAGCGAGTACAACCTGGCTTTGCCTCGACGCAGGGT
CACTTGGCTGTCACCGCTGAATGTCACAGGTGCCGATAGGTGCTACGACCTAAGTTT
AGGACTGCCGGCTGACGCCGGCAGATACGACTTGGTCTTTGTGAACATTCACACGGA
ATTCAGAATCCACCACTACCAGCAGTGTGTCGACCACGCTATGAAGCTGCAGATGCT
GGGGGGAGATGCACTACGACTGCTAAAACCCGGCGGCAACCTCTTGATGAGAGCTTA
CGGATACGCCGACAAAATCAGCGAAGCCGTTGTTTCCTCCTTAAGCAGAAAGTTCTC
GTCTGCAAGAGTACTGCGCCCGGATTGTGTCACCAGCAATACAGAAGTGTTCTTGCT
GTTTTCCAACTTTGACAATGGAAAGAGACCCTCTACGCTACACCAGATGAACACCAA
GCTGAGTGCCGTGTATGCCGGAGAAGCCATGCACACAGCCGGGTGCGCACCATCCTA
CAGAGTTAAGAGAGCAGACATAGCCACGTGTACAGAAGCGGCTGTGGTTAACGCAGC
TAACGCCCGTGGAACTGTAGGGGACGGTGTATGCAGGGCCGTGGCGAAGAAATGGCC
GTCAGCCTTTAAGGGAGCAGCAACACCAGTGGGCACAATTAAAACAGTCATGTGCGG
CTCGTATCCGGTCATCCATGCCGTAGGGCCTAATTTCTCTGCCACGACTGAAGCGGA
AGGGGACCGCGAACTGGCCGCTGTCTATCGGGCAGTGGCCGCCGAAGTAAACAGACT
GTCATTGAGCAGCGTAGCCATCCCGCTGCTGTCCACAGGAGTGTTCAGCGGCGGAAG
AGATAGGCTGCAGCAGTCCCTCAACCATCTATTCACAGCAATGGACGCCACGGACGC
TGACGTGACCATCTACTGCAGAGACAAAAGTTGGGAGAAGAAAATCCAGGAAGCCAT
AGACATGAGGACGGCTGTGGAGTTGCTCAATGATGACGTGGAGCTGACCACAGACTT
GGTGAGAGTGCACCCGGATAGCAGCCTGGTGGGACGTAAGGGCTACAGTACCACTGA
CGGGTCGCTGTACTCGTACTTGGAAGGTACGAAATTCAACCAGGCTGCCATTGATAT
GGCAGAGATACTGACGTTGTGGCCCAGACTGCAAGAGGCAAACGAACAGATATGCCT
ATACGCACTGGGCGAAACAATGGATAACATCAGATCCAAATGTCCGGTGGACGATTC
CGATTCGTCAACACCTCCCAGGACAGTGCCCTGCCTGTGCCGCTACGCAATGACAGC
AGAACGGATTGCCCGCCTTAGGTCACACCAAGTTAAAAGCATGGTGGTTTGCTCATC
TTTTCCCCTCCCGAAATACCATGTAGATGGGGTGCAGAAGGTAAAATGCGAGAAGGT
TCTCCTGTTCGACCCGACAGTACCTTCAGTGGTTAGTCCGCGGAAGTATGCCGCCTC
GACGACGGACCACTCAGACCGGTCGCTACGAGGGTTCGACTTGGATTGGACCACCGA
CTCGTCTTCGACTGCCAGCGATACCATGTCGCTACCCAGTTTGCAGTCGTGTGACAT
CGACTCGATCTACGAGCCAATGGCTCCCATAGTAGTGACGGCTGACGTGCACCCTGA
ACCCGCAGCTGTGCACCCTGAACCCGCAGACCATGTGGACCTTGAGAACCCGATTCC
TCCACCGCGCCCGAAGAGAGCTGCATACCTTGCCTCCCGCGCGGCGGAGCGACCAGT
GCCGGCGCCGAGAAAACCGACGCCTGCCCCAAGGACTACGTTTAGGAACAAGCTGCC
TTTTACGTTCGGCGACTTTGATGAGCACGAAGTCGATGCGTTGGCCTCCGGGATTAC
TTTCGGAGACTTCGACGATGTCCTGTGACTAGGCCGCGCGGGTGCATATATTTTCTC
CTCGGACACTGGCAGCGGACATTTACAACAAAAATCCGTTAGGCAACACAATCTCCA
GTGTGCACAACTGGATGCGGTCGAGGAGGAGAAAATGTACCCGCCGAAATTGGATAC
TGAGAGGGAGAAGCTGTTGCTGCTGAAAATGCAGATGCACCCATCGGAAGCTAATAA

GAGTCGATACCAGTCTCGCAAGGTGGAGAACATGAAAGCCACGGTGGTGGACAGGCT
CACATCGGGGGCCAGATTGTACACGGGAGCGGACGTAGGCCGCATACCAACATACGC
GGTTCGGTACCCCCGCCCCGTGTACTCCCCTACCGTGATCGAAAGATTCTCAAGCCC
CGATGTAGCAATCGCAGCGTGCAACGAATACCTATCCAGAAATTACCCAACAGTGGC
GTCGTACCAGATAACAGATGAATACGACGCATACTTGGACATGGTTGACGGGTCGGA
GAGTTGCCTGGACAGAGCGACATTCTGCCCGGCGAAGCTCCGGTGCTATCCAAAACA
TCATGCGTACCACCAGCCGACTGTACGCAGTGCCGTCCCGTCACCCTTTCAGAACAC
ACTACAGAACGTGCTAGCGGCCGCCACCAAGAGAAACTGCAACGTCACGCAAATGCG
AGAACTACCTACCATGGACTCGGCAGTGTTCAATGTGGAGTGCTTCAAGCGCTATGC
CTGCTCCGGAGAATATTGGGAAGAATACGCTAAACAACCTATCCGGATAACCACTGA
GAACATCACTACCTATGTAACCAAACTGAAAGGCCCGAAAGCTGCCGCCTTGTTTGC
TAAGACCCACAACTTGGTTCCGCTGCAGGAGGTTCCCATGGACAGATTCACAGTCGA
CATGAAACGAGATGTCAAAGTCACCCCAGGGACGAAACACACAGAGGAAAGACCCAA
AGTCCAGGTAATTCAAGCAGCGGAGCCACTGGCGACCGCTTACCTGTGTGGCATCCA
CAGGGAATTAGTAAGGAGGTTAAACGCTGTGTTACGTCCTAACGTGCACACATTGTT
TGATATGTCGGCCGAAGACTTCGACGCGATCATCGCCTCTCACTTCCACCCAGGAGA
CCCGGTTCTAGAGACGGACATTGCATCATTCGACAAAAGCCAGGACGACTCCTTGGC
TCTTACAGGTTTAATGATCCTCGAAGATCTAGGGGTGGATCAGTACCTGCTAGACTT
GATCGAGGCAGCCTTTGGGGAAATATCCAGCTGTCACCTACCAACTGGCACGCGCTT
CAAGTTCGGAGCCATGATGAAATCAGGCATGTTTCTGACTTTGTTCATTAACACTGT
TTTGAACATCACCATAGCAAGCAGGGTACTGGAGCAGAGACTCACTGACTCCGCCTG
TGCAGCCTTTATCGGCGACGACAATATCGTTCACGGAGTGATCTCCGACAAGCTGAT
GGCTGAGAGGTGCGCGTCGTGGGTCAACATGGAGGTGAAGATCATTGACGCTGTCAT
GGGCGAAAAACCCCCATATTTTTGTGGGGGATTCATAGTTTTTGACAGCGTCACACA
GACCGCCTGCCGTGTTTCAGACCCACTCAAACGCTTGTTCAAGTTGGGTAAGCCGTT
AACAGCTGAAGACAAGCAGGACGAAGACAGGCGACGAGCATTGAGCGACGAGGTCAG
CAAGTGGTTCCGGACAGGCTTGGGGGCCGAACTGGAGGTGGCGCTAACATCTAGGTA
TGAGGTAGAGGGCTGCAAGAGTATCCTCATAGCCATGGCCACCCTGGCAAGGGACAT
TAAGGCGTTTAAGAAATTGAGAGGACCTGTTATACACCTCTACGGCGGTCCTAAATT
GGTGCGTTAATACACAGAATTCTGATTATAGCGCACTATTATAGCACCATGAATTAC
ATCCCTACGCAAACGTTCTACGGCCGCCGGTGGCGCCCGCGCCCGGCGGCCCGTCCC
TGGCCGTTGCAGGCCACTCCGGTGGCTCCCGTCGTCCCCGACTTCCAGGCCCAGCAG
ATGCAGCAACTCATCAGCGCCGTAAATGCGCTGACAATGAGACAGAACGCAATTGCT
CCTACTAGGCCTCCCAAACCAAAGAAGAAGAAGACGACCAAACCAAAGCCGAAAACG
CAGCCTAAGAAGATTAAAGGAAAAACGCAGCAGCAAAAGAAGAAAGACAAGCAAGCC
GACAAGAAGAAGAAGAAACCCGGAAAAAGAGAACGAATGTGCATGAAGATTGAAAAT
GACTGTATCTTCGAAGTCAAACATGAAGGAAAGGTCACTGGGTACGCCTGCCTGGTG
GGCGACAAAGTCATGAAACCTGCCCACGTGAAAGGAGTCATCGACAACGCGGACCTG
GCAAAACTAGCTTTCAAGAAATCGAGCAAGTATGACCTTGAGTGTGCCCAGATACCA
GTTCACATGAGGTCGGATGCTTCAAAGTACACGCATGAGAAGCCCGAGGGACACTAT
AACTGGCACCACGGGGCCGTTCAGTACAGCGGAGGCAGGTTCACTATACCGACAGGA
GCGGGCAAACCGGGAGACAGTGGCCGGCCCATTTTTGACAACAAGGGGAGGGTAGTC
GCTATCGTCCTGGGCGGGGCCAACGAGGGCTCACGCACAGCACTGTCGGTGGTCACC
TGGAACAAAGATATGGTGACTAGAGTGACCCCAGAGGGGTCCGAAGAGTGGTCCGCC
CCGCTGATTACTGCCATGTGTGTCCTTACCAATGCTACCTTCCCGTGCTTCCAGCCC
CCGTGTGCACCTTGCTGCTACGAAAACAACGCAGAGGCTACACTACGGATGCTCGAG
GATAACGTGGATAGGCCAGGGTACTACGACCTCCTTCAGGCAGCCTTGACGTGCCGA
AACGGAACAAGACACCGGCGCAGCGTGTCGCAACACTTTAACGTGTATAAGGCTACA
CGCCCTTACATCGCGTACTGCGCCGACTGCGGAGCAGGGCACTCGTGTCATAGCCCC
GTAGCAATTGAAGCGATCAGGTCCGAGGCTACCGACGGGATGCTGAAGATTCAGTTC
TCGGCACAAATTGGCATAGATAAGAGTGACAATCATGACTACACGAAGATAAGGTAC

GCAGACGGGCACGCCATTGAGAACGCCGTCCGGTCATCTTTGAAGGTAGCCACCTCC
GGAGATTGTTTCGTCCATGGCACAATGGGACACTTCATACTGGCAACGTGCCCACCG
GGTGAATTTCTACAGGTTTCGATCCAGGACACTAGAAATGCGGTCCGTGCCTGCAGG
ATACAATACCATCATGACCCTCAACCGGTGGGGAGAGAAAAATTTACAATTAGACCA
CACTATGGAAAAGAGATCCCTTGCACCACTTATCAGCAAACCACAGCGGAGACCGTG
GAGGAAATCGACATGCATATGCCGCCAGATACGCCGGACAGGACGTTGCTATCACAG
CAATCTGGTAACGTAAAGATCACAGTCGGAGGAAAGAAGGTAAAATACAACTGCACC
TGTGGAACCGGAAACGTTGGCACTACTAGTTCGGACAAGACGATCAACACGTGTCTA
ATAGAGCAGTGCCACGTCTCAGTGACAGACCATAAGAAATGGCAGTTCAACTCACCT
TTTGTCCCGAGAGCCGACGAACCGGCTAGAAAAGGCAAAGTCCATATCCCGTTCCCG
TTGGACAATATCACATGTAGAGTTCCAATGGCGCGCGAACCAACTGTCATCCACGGC
AAAAGAGAAGTGACACTGCACCTTCACCCAGATCATCCCACGCTCTTTTCCTACCGC
ACACTGGGCGAGGACCCGCAGTATCACGAGGAATGGGTGACAGCGGCGGTGGAACGG
ACCATACCCGTACCAGTGGACGGGATGGAGTACCACTGGGGAAACAACGACCCAGTG
AGGCTTTGGTCTCAACTCACCACTGAAGGGAAACCGCACGGCTGGCCGCATCAGATC
GTACAGTACTACTATGGGCTTTACCCGGCCGCTACAGCATCCGCGGTCGCCGGGATG
AGCTTACTGGCGTTGATATCGATCTTCGCGTCGTGCTACATGCTGGCTGCGGCCCGC
AGCAAGTGTTTGACCCCTTATGCTTTAACACCAGGAGCTGCAGTTCCGTGGACGCTG
GGGATACTCTGCTGCGCCCCACGGGCGCATGCAGCCAGTGTGGCAGAGACTATGGCC
TACTTGTGGGACCAAAACCAAGCGCTGTTCTGGTTGGAGTTTGCGGCCCCTGTTGCC
TGCATCCTCATCATCACGTATTGCCTCAGAAACGTGCTGTGTTGCTGTAAGAGCCTT
TCTTTTTTAGTGCTACTGAGCCTCGGGGCCACCGCCAGAGCTTACGAACATTCGACA
GTAATGCCGAACGTGGTGGGGTTCCCGTATAAGGCTCACATTGAAAGGCCAGGATAT
AGCCCCCTCACTCTGCAGATGCAGGTTGTAGAAACCAGCCTTGAACCAACCCTTAAT
TTGGAATACATAACCTGTGAGTACAAGACGGTCGTCCCGTCGCCGTACGTGAAGTGC
TGCGGCTCCTCAGAGTGCTCCACTAAAGAGAAGCCTGACTATCAATGCAAGGTTTAC
ACAGGCGTGTACCCATTCATGTGGGGTGGGGCATATTGCTTCTGCGACTCAGAAAAC
ACGCAACTCAGCGAGGCGTACGTCGATCGATCGGACGTATGCAAGCATGATCACGCA
TCTGCTTACAAAGCCCACACAGCATCGCTGAAGGCCAAAGTGAGAGTTATGTACGGC
AACGTAAACCAGACCGTGGATGTTTACGTGAACGGAGACCATGCCGTCACGATAGGG
GGTACTCAGTTCATATTCGGGCCGCTGTCATCGGCCTGGACGCCGTTCGACAACAAG
ATAGTCGTGTACAAAGACGAAGTGTTCAATCAGGACTTCCCGCCGTACGGATCTGGG
CAACCAGGGCGCTTCGGCGACATCCAAAGCAGAACGGTGGAGAGTAATGACCTGTAC
GCGAACACGGCACTGAAGCTGGCGCGCCCTTCACCCGGCACGGTCCATGTACCTTAC
ACACAGACACCTTCAGGGTTCAAATATTGGCTAAAGGAAAAAGGGACAGCCCTAAAT
ACGAAGGCTCCATTTGGCTGCCAAATCAAAACAAACCCTGTCAGGGCCATGAACTGC
GCCGTGGGAAACATCCCTGTCTCCATGAATTTGCCTGACAGCGCCTTTACTCGCATT
GTTGAGGCACCGACCATCACTGACCTGACTTGCACAGTGGCTACCTGTACGCACTCC
TCGGATTTCGGCGGCGTCTTGACATTGACGTACAAAACCGACAAGAACGGGGACTGC
TCTGTACACTCACACTCTAACGTAGCTACTCTGCAGGAGGCCACAGCAAAAGTGAAG
ACAGCAGGTAAGGTGACCTTACACTTCTCCACGGCAAGCGCATCACCTTCTTTTGTG
GTGTCGCTATGCAGTGCCAAGGCCACCTGTTCAGCGTCGTGTGAGCCCCCGAAAGAC
CACATAGTCCCATATGCGGCTAGCCACAGTAACGTAGTGTTCCCAGACATGTCGGGC
ACCGCACTATCATGGGTGCAGAAAATCTCGGGTGGTCTGGGGGCCTTCGCAATCGGC
GCTATTCTGGTGCTAGTTGTGGTCACTTGCATTGGACTCCGCAGATAATGAGTACCT
CATTTTAGCATACAGGGTACCAAATTCTTAGCTTAATTGACAGTATACCACCATCAT
AATTAGCCAAGGGTACTGTAATTTTATTATAACTACTTGAACAGAAAACTGGAAAAT
AGAAAAAGTTAGGGTAGGCAATGTTAGTTTATTATACCTCTACTATAATTACTTGAA
CTAAAAACTGGAAAACAGAAAAAGTTAGGGTAAGCAATGGCATTAATATAGCAAAGA
AACCGAAAATAGAAGAAGTTAGGGTAGGCAATGGCATTGATATAGCAAGAAAATTGA
AAACAGAAAAAGTTAGGGTAAGCAATGGCATATAACCATAACTATATAACTTATAAC

AAAGATATAGCAAGAAAATTGAAAACAGAAAAAGTTAGGGTAAGCACTGGCATATAA
CCATAACTATATAATTTATAACAAAGCGCAACAAGACCTGCGCAATTGGCCCCGTAG
TCCGCTTCACGGAAACTCGGGGGCAACTCATATTGACACATTAATTGGCAATAATTG
GAAGCTTACATAAGCTCAATTCGACGAATAATTGGATTTTTATTTTATTTTGCAATT
GGTTTTTAATATTTCC

SFV4 complete genome

ATGGCCGCCAAAGTGCATGTTGATATTGAGGCTGACAGCCCATTCATCAAGTCTTTG
CAGAAGGCATTTCCGTCGTTCGAGGTGGAGTCATTGCAGGTCACACCAAATGACCAT
GCAAATGCCAGAGCATTTTCGCACCTGGCTACCAAATTGATCGAGCAGGAGACTGAC
AAAGACACACTCATCTTGGATATCGGCAGTGCGCCTTCCAGGAGAATGATGTCTACG
CACAAATACCACTGCGTATGCCCTATGCGCAGCGCAGAAGACCCCGAAAGGCTCGTA
TGCTACGCAAAGAAACTGGCAGCGGCCTCCGGGAAGGTGCTGGATAGAGAGATCGCA
GGAAAAATCACCGACCTGCAGACCGTCATGGCTACGCCAGACGCTGAATCTCCTACC
TTTTGCCTGCATACAGACGTCACGTGTCGTACGGCAGCCGAAGTGGCCGTATACCAG
GACGTGTATGCTGTACATGCACCAACATCGCTGTACCATCAGGCGATGAAAGGTGTC
AGAACGGCGTATTGGATTGGGTTTGACACCACCCCGTTTATGTTTGACGCGCTAGCA
GGCGCGTATCCAACCTACGCCACAAACTGGGCCGACGAGCAGGTGTTACAGGCCAGG
AACATAGGACTGTGTGCAGCATCCTTGACTGAGGGAAGACTCGGCAAACTGTCCATT
CTCCGCAAGAAGCAATTGAAACCTTGCGACACAGTCATGTTCTCGGTAGGATCTACA
TTGTACACTGAGAGCAGAAAGCTACTGAGGAGCTGGCACTTACCCTCCGTATTCCAC
CTGAAAGGTAAACAATCCTTTACCTGTAGGTGCGATACCATCGTATCATGTGAAGGG
TACGTAGTTAAGAAAATCACTATGTGCCCCGGCCTGTACGGTAAAACGGTAGGGTAC
GCCGTGACGTATCACGCGGAGGGATTCCTAGTGTGCAAGACCACAGACACTGTCAAA
GGAGAAAGAGTCTCATTCCCTGTATGCACCTACGTCCCCTCAACCATCTGTGATCAA
ATGACTGGCATACTAGCGACCGACGTCACACCGGAGGACGCACAGAAGTTGTTAGTG
GGATTGAATCAGAGGATAGTTGTGAACGGAAGAACACAGCGAAACACTAACACGATG
AAGAACTATCTGCTTCCGATTGTGGCCGTCGCATTTAGCAAGTGGGCGAGGGAATAC
AAGGCAGACCTTGATGATGAAAAACCTCTGGGTGTCCGAGAGAGGTCACTTACTTGC
TGCTGCTTGTGGGCATTTAAAACGAGGAAGATGCACACCATGTACAAGAAACCAGAC
ACCCAGACAATAGTGAAGGTGCCTTCAGAGTTTAACTCGTTCGTCATCCCGAGCCTA
TGGTCTACAGGCCTCGCAATCCCAGTCAGATCACGCATTAAGATGCTTTTGGCCAAG
AAGACCAAGCGAGAGTTAATACCTGTTCTCGACGCGTCGTCAGCCAGGGATGCTGAA
CAAGAGGAGAAGGAGAGGTTGGAGGCCGAGCTGACTAGAGAAGCCTTACCACCCCTC
GTTCCCATCGCGCCGGCGGAGACGGGAGTCGTCGACGTCGACGTTGAAGAACTAGAG
TATCACGCAGGTGCAGGGGTCGTGGAAACACCTCGCAGCGCGTTGAAAGTCACCGCA
CAGCCGAACGACGTACTACTAGGAAATTACGTAGTTCTGTCCCCGCAGACCGTGCTC
AAGAGCTCCAAGTTGGCCCCCGTGCACCCTCTAGCAGAGCAGGTGAAAATAATAACA
CATAACGGGAGGGCCGGCCGTTACCAGGTCGACGGATATGACGGCAGGGTCCTACTA
CCATGTGGATCGGCCATTCCGGTCCCTGAGTTTCAAGCTTTGAGCGAGAGCGCCACT
ATGGTGTACAACGAAAGGGAGTTCGTCAACAGGAAACTATACCATATTGCCGTTCAC
GGACCGTCGCTGAACACCGACGAGGAGAACTACGAGAAAGTCAGAGCTGAAAGAACT
GACGCCGAGTACGTGTTCGACGTAGATAAAAAATGCTGCGTCAAGAGAGAGGAAGCG
TCGGGTTTGGTGTTGGTGGGAGAGCTAACCAACCCCCCGTTCCATGAATTCGCCTAC
GAAGGGCTGAAGATCAGGCCGTCGGCACCATATAAGACTACAGTAGTAGGAGTCTTT
GGGGTTCCGGGATCAGGCAAGTCTGCTATTATTAAGAGCCTCGTGACCAAACACGAT
CTGGTCACCAGCGGCAAGAAGGAGAACTGCCAGGAAATAGTCAACGACGTGAAGAAG
CACCGCGGACTGGACATCCAGGCAAAAACAGTGGACTCCATCCTGCTAAACGGGTGT
CGTCGTGCCGTGGACATCCTATATGTGGACGAGGCTTTCGCTTGCCATTCCGGTACT
CTGCTAGCCCTAATTGCTCTTGTTAAACCTCGGAGCAAAGTGGTGTTATGCGGAGAC
CCCAAGCAATGCGGATTCTTCAATATGATGCAGCTTAAGGTGAACTTCAACCACAAC
ATCTGCACTGAAGTATGTCATAAAAGTATATCCAGACGTTGCACGCGTCCAGTCACG
GCCATCGTGTCTACGTTGCACTACGGAGGCAAGATGCGCACGACCAACCCGTGCAAC
AAACCCATAATCATAGACACCACAGGACAGACCAAGCCCAAGCCAGGAGACATCGTG
TTAACATGCTTCCGAGGCTGGGTAAAGCAGCTGCAGTTGGACTACCGTGGACACGAA
GTCATGACAGCAGCAGCATCTCAGGGCCTCACCCGCAAAGGGGTATACGCCGTAAGG

CAGAAGGTGAATGAAAATCCCTTGTATGCCCCTGCGTCGGAGCACGTGAATGTACTG
CTGACGCGCACTGAGGATAGGCTGGTGTGGAAAACGCTGGCCGGCGATCCCTGGATT
AAGGTCCTATCAAACATTCCACAGGGTAACTTTACGGCCACATTGGAAGAATGGCAA
GAAGAACACGACAAAATAATGAAGGTGATTGAAGGACCGGCTGCGCCTGTGGACGCG
TTCCAGAACAAAGCGAACGTGTGTTGGGCGAAAAGCCTGGTGCCTGTCCTGGACACT
GCCGGAATCAGATTGACAGCAGAGGAGTGGAGCACCATAATTACAGCATTTAAGGAG
GACAGAGCTTACTCTCCAGTGGTGGCCTTGAATGAAATTTGCACCAAGTACTATGGA
GTTGACCTGGACAGTGGCCTGTTTTCTGCCCCGAAGGTGTCCCTGTATTACGAGAAC
AACCACTGGGATAACAGACCTGGTGGAAGGATGTATGGATTCAATGCCGCAACAGCT
GCCAGGCTGGAAGCTAGACATACCTTCCTGAAGGGGCAGTGGCATACGGGCAAGCAG
GCAGTTATCGCAGAAAGAAAAATCCAACCGCTTTCTGTGCTGGACAATGTAATTCCT
ATCAACCGCAGGCTGCCGCACGCCCTGGTGGCTGAGTACAAGACGGTTAAAGGCAGT
AGGGTTGAGTGGCTGGTCAATAAAGTAAGAGGGTACCACGTCCTGCTGGTGAGTGAG
TACAACCTGGCTTTGCCTCGACGCAGGGTCACTTGGTTGTCACCGCTGAATGTCACA
GGCGCCGATAGGTGCTACGACCTAAGTTTAGGACTGCCGGCTGACGCCGGCAGGTTC
GACTTGGTCTTTGTGAACATTCACACGGAATTCAGAATCCACCACTACCAGCAGTGT
GTCGACCACGCCATGAAGCTGCAGATGCTTGGGGGAGATGCGCTACGACTGCTAAAA
CCCGGCGGCAGCCTCTTGATGAGAGCTTACGGATACGCCGATAAAATCAGCGAAGCC
GTTGTTTCCTCCTTAAGCAGAAAGTTCTCGTCTGCAAGAGTGTTGCGCCCGGATTGT
GTCACCAGCAATACAGAAGTGTTCTTGCTGTTCTCCAACTTTGACAACGGAAAGAGA
CCCTCTACGCTACACCAGATGAATACCAAGCTGAGTGCCGTGTATGCCGGAGAAGCC
ATGCACACGGCCGGGTGTGCACCATCCTACAGAGTTAAGAGAGCAGACATAGCCACG
TGCACAGAAGCGGCTGTGGTTAACGCAGCTAACGCCCGTGGAACTGTAGGGGATGGC
GTATGCAGGGCCGTGGCGAAGAAATGGCCGTCAGCCTTTAAGGGAGAAGCAACACCA
GTGGGCACAATTAAAACAGTCATGTGCGGCTCGTACCCCGTCATCCACGCTGTAGCG
CCTAATTTCTCTGCCACGACTGAAGCGGAAGGGGACCGCGAATTGGCCGCTGTCTAC
CGGGCAGTGGCCGCCGAAGTAAACAGACTGTCACTGAGCAGCGTAGCCATCCCGCTG
CTGTCCACAGGAGTGTTCAGCGGCGGAAGAGATAGGCTGCAGCAATCCCTCAACCAT
CTATTCACAGCAATGGACGCCACGGACGCTGACGTGACCATCTACTGCAGAGACAAA
AGTTGGGAGAAGAAAATCCAGGAAGCCATAGACATGAGGACGGCTGTGGAGTTGCTC
AATGATGACGTGGAGCTGACCACAGACTTGGTGAGAGTGCACCCGGACAGCAGCCTG
GTGGGTCGTAAGGGCTACAGTACCACTGACGGGTCGCTGTACTCGTACTTTGAAGGT
ACGAAATTCAACCAGGCTGCTATTGATATGGCAGAGATACTGACGTTGTGGCCCAGA
CTGCAAGAGGCAAACGAACAGATATGCCTATACGCGCTGGGCGAAACAATGGACAAC
ATCAGATCCAAATGTCCGGTGAACGATTCCGATTCATCAACACCTCCCAGGACAGTG
CCCTGCCTGTGCCGCTACGCAATGACAGCAGAACGGATCGCCCGCCTTAGGTCACAC
CAAGTTAAAAGCATGGTGGTTTGCTCATCTTTTCCCCTCCCGAAATACCATGTAGAT
GGGGTGCAGAAGGTAAAGTGCGAGAAGGTTCTCCTGTTCGACCCGACGGTACCTTCA
GTGGTTAGTCCGCGGAAGTATGCCGCATCTACGACGGACCACTCAGATCGGTCGTTA
CGAGGGTTTGACTTGGACTGGACCACCGACTCGTCTTCCACTGCCAGCGATACCATG
TCGCTACCCAGTTTGCAGTCGTGTGACATCGACTCGATCTACGAGCCAATGGCTCCC
ATAGTAGTGACGGCTGACGTACACCCTGAACCCGCAGGCATCGCGGACCTGGCGGCA
GATGTGCATCCTGAACCCGCAGACCATGTGGACCTCGAGAACCCGATTCCTCCACCG
CGCCCGAAGAGAGCTGCATACCTTGCCTCCCGCGCGGCGGAGCGACCGGTGCCGGCG
CCGAGAAAGCCGACGCCTGCCCCAAGGACTGCGTTTAGGAACAAGCTGCCTTTGACG
TTCGGCGACTTTGACGAGCACGAGGTCGATGCGTTGGCCTCCGGGATTACTTTCGGA
GACTTCGACGACGTCCTGCGACTAGGCCGCGCGGGTGCATATATTTTCTCCTCGGAC
ACTGGCAGCGGACATTTACAACAAAAATCCGTTAGGCAGCACAATCTCCAGTGCGCA
CAACTGGATGCGGTCGAGGAGGAGAAAATGTACCCGCCAAAATTGGATACTGAGAGG
GAGAAGCTGTTGCTGCTGAAAATGCAGATGCACCCATCGGAGGCTAATAAGAGTCGA
TACCAGTCTCGCAAAGTGGAGAACATGAAAGCCACGGTGGTGGACAGGCTCACATCG

GGGGCCAGATTGTACACGGGAGCGGACGTAGGCCGCATACCAACATACGCGGTTCGG
TACCCCCGCCCCGTGTACTCCCCTACCGTGATCGAAAGATTCTCAAGCCCCGATGTA
GCAATCGCAGCGTGCAACGAATACCTATCCAGAAATTACCCAACAGTGGCGTCGTAC
CAGATAACAGATGAATACGACGCATACTTGGACATGGTTGACGGGTCGGATAGTTGC
TTGGACAGAGCGACATTCTGCCCGGCGAAGCTCCGGTGCTACCCGAAACATCATGCG
TACCACCAGCCGACTGTACGCAGTGCCGTCCCGTCACCCTTTCAGAACACACTACAG
AACGTGCTAGCGGCCGCCACCAAGAGAAACTGCAACGTCACGCAAATGCGAGAACTA
CCCACCATGGACTCGGCAGTGTTCAACGTGGAGTGCTTCAAGCGCTATGCCTGCTCC
GGAGAATATTGGGAAGAATATGCTAAACAACCTATCCGGATAACCACTGAGAACATC
ACTACCTATGTGACCAAATTGAAAGGCCCGAAAGCTGCTGCCTTGTTCGCTAAGACC
CACAACTTGGTTCCGCTGCAGGAGGTTCCCATGGACAGATTCACGGTCGACATGAAA
CGAGATGTCAAAGTCACTCCAGGGACGAAACACACAGAGGAAAGACCCAAAGTCCAG
GTAATTCAAGCAGCGGAGCCATTGGCGACCGCTTACCTGTGCGGCATCCACAGGGAA
TTAGTAAGGAGACTAAATGCTGTGTTACGCCCTAACGTGCACACATTGTTTGATATG
TCGGCCGAAGACTTTGACGCGATCATCGCCTCTCACTTCCACCCAGGAGACCCGGTT
CTAGAGACGGACATTGCATCATTCGACAAAAGCCAGGACGACTCCTTGGCTCTTACA
GGTTTAATGATCCTCGAAGATCTAGGGGTGGATCAGTACCTGCTGGACTTGATCGAG
GCAGCCTTTGGGGAAATATCCAGCTGTCACCTACCAACTGGCACGCGCTTCAAGTTC
GGAGCTATGATGAAATCGGGCATGTTTCTGACTTTGTTTATTAACACTGTTTTGAAC
ATCACCATAGCAAGCAGGGTACTGGAGCAGAGACTCACTGACTCCGCCTGTGCGGCC
TTCATCGGCGACGACAACATCGTTCACGGAGTGATCTCCGACAAGCTGATGGCGGAG
AGGTGCGCGTCGTGGGTCAACATGGAGGTGAAGATCATTGACGCTGTCATGGGCGAA
AAACCCCCATATTTTTGTGGGGGATTCATAGTTTTTGACAGCGTCACACAGACCGCC
TGCCGTGTTTCAGACCCACTTAAGCGCCTGTTCAAGTTGGGTAAGCCGCTAACAGCT
GAAGACAAGCAGGACGAAGACAGGCGACGAGCACTGAGTGACGAGGTTAGCAAGTGG
TTCCGGACAGGCTTGGGGGCCGAACTGGAGGTGGCACTAACATCTAGGTATGAGGTA
GAGGGCTGCAAAAGTATCCTCATAGCCATGGCCACCTTGGCGAGGGACATTAAGGCG
TTTAAGAAATTGAGAGGACCTGTTATACACCTCTACGGCGGTCCTAGATTGGTGCGT
TAATACACAGAATTCTGATTATAGCGCACTATTATAGCACCATGAATTACATCCCTA
CGCAAACGTTTTACGGCCGCCGGTGGCGCCCGCGCCCGGCGGCCCGTCCTTGGCCGT
TGCAGGCCACTCCGGTGGCTCCCGTCGTCCCCGACTTCCAGGCCCAGCAGATGCAGC
AACTCATCAGCGCCGTAAATGCGCTGACAATGAGACAGAACGCAATTGCTCCTGCTA
GGCCTCCCAAACCAAAGAAGAAGAAGACAACCAAACCAAAGCCGAAAACGCAGCCCA
AGAAGATCAACGGAAAAACGCAGCAGCAAAAGAAGAAAGACAAGCAAGCCGACAAGA
AGAAGAAGAAACCCGGAAAAAGAGAAAGAATGTGCATGAAGATTGAAAATGACTGTA
TCTTCGAAGTCAAACACGAAGGAAAGGTCACTGGGTACGCCTGCCTGGTGGGCGACA
AAGTCATGAAACCTGCCCACGTGAAAGGAGTCATCGACAACGCGGACCTGGCAAAGC
TAGCTTTCAAGAAATCGAGCAAGTATGACCTTGAGTGTGCCCAGATACCAGTTCACA
TGAGGTCGGATGCCTCAAAGTACACGCATGAGAAGCCCGAGGGACACTATAACTGGC
ACCACGGGGCTGTTCAGTACAGCGGAGGTAGGTTCACTATACCGACAGGAGCGGGCA
AACCGGGAGACAGTGGCCGGCCCATCTTTGACAACAAGGGGAGGGTAGTCGCTATCG
TCCTGGGCGGGGCCAACGAGGGCTCACGCACAGCACTGTCGGTGGTCACCTGGAACA
AAGATATGGTGACTAGAGTGACCCCCGAGGGGTCCGAAGAGTGGTCCGCCCCGCTGA
TTACTGCCATGTGTGTCCTTGCCAATGCTACCTTCCCGTGCTTCCAGCCCCCGTGTG
TACCTTGCTGCTATGAAAACAACGCAGAGGCCACACTACGGATGCTCGAGGATAACG
TGGATAGGCCAGGGTACTACGACCTCCTTCAGGCAGCCTTGACGTGCCGAAACGGAA
CAAGACACCGGCGCAGCGTGTCGCAACACTTCAACGTGTATAAGGCTACACGCCCTT
ACATCGCGTACTGCGCCGACTGCGGAGCAGGGCACTCGTGTCATAGCCCCGTAGCAA
TTGAAGCGGTCAGGTCCGAAGCTACCGACGGGATGCTGAAGATTCAGTTCTCGGCAC
AAATTGGCATAGATAAGAGTGACAATCATGACTACACGAAGATAAGGTACGCAGACG
GGCACGCCATTGAGAATGCCGTCCGGTCATCTTTGAAGGTAGCCACCTCCGGAGACT

GTTTCGTCCATGGCACAATGGGACATTTCATACTGGCAAAGTGCCCACCGGGTGAAT
TCCTGCAGGTCTCGATCCAGGACACCAGAAACGCGGTCCGTGCCTGCAGAATACAAT
ATCATCATGACCCTCAACCGGTGGGTAGAGAAAAATTTACAATTAGACCACACTATG
GAAAAGAGATCCCTTGCACCACTTATCAACAGACCACAGCGAAGACCGTGGAGGAAA
TCGACATGCATATGCCGCCAGATACGCCGGACAGGACGTTGCTATCACAGCAATCTG
GCAATGTAAAGATCACAGTCGGAGGAAAGAAGGTGAAATACAACTGCACCTGTGGAA
CCGGAAACGTTGGCACTACTAATTCGGACATGACGATCAACACGTGTCTAATAGAGC
AGTGCCACGTCTCAGTGACGGACCATAAGAAATGGCAGTTCAACTCACCTTTCGTCC
CGAGAGCCGACGAACCGGCTAGAAAAGGCAAAGTCCATATCCCATTCCCGTTGGACA
ACATCACATGCAGAGTTCCAATGGCGCGCGAACCAACCGTCATCCACGGCAAAAGAG
AAGTGACACTGCACCTTCACCCAGATCATCCCACGCTCTTTTCCTACCGCACACTGG
GTGAGGACCCGCAGTATCACGAGGAATGGGTGACAGCGGCGGTGGAACGGACCATAC
CCGTACCAGTGGACGGGATGGAGTACCACTGGGGAAACAACGACCCAGTGAGGCTTT
GGTCTCAACTCACCACTGAAGGGAAACCGCACGGCTGGCCGCATCAGATCGTACAGT
ACTACTATGGGCTTTACCCGGCCGCTACAGTATCCGCGGTCGTCGGGATGAGCTTAC
TGGCGTTGATATCGATCTTCGCGTCGTGCTACATGCTGGTTGCGGCCCGCAGTAAGT
GCTTGACCCCTTATGCTTTAACACCAGGAGCTGCAGTTCCGTGGACGCTGGGGATAC
TCTGCTGCGCCCCGCGGGCGCACGCAGCTAGTGTGGCAGAGACTATGGCCTACTTGT
GGGACCAAAACCAAGCGTTGTTCTGGTTGGAGTTTGCGGCCCCTGTTGCCTGCATCC
TCATCATCACGTATTGCCTCAGAAACGTGCTGTGTTGCTGTAAGAGCCTTTCTTTTT
TAGTGCTACTGAGCCTCGGGGCAACCGCCAGAGCTTACGAACATTCGACAGTAATGC
CGAACGTGGTGGGGTTCCCGTATAAGGCTCACATTGAAAGGCCAGGATATAGCCCCC
TCACTTTGCAGATGCAGGTTGTTGAAACCAGCCTCGAACCAACCCTTAATTTGGAAT
ACATAACCTGTGAGTACAAGACGGTCGTCCCGTCGCCGTACGTGAAGTGCTGCGGCG
CCTCAGAGTGCTCCACTAAAGAGAAGCCTGACTACCAATGCAAGGTTTACACAGGCG
TGTACCCGTTCATGTGGGGAGGGGCATATTGCTTCTGCGACTCAGAAAACACGCAAC
TCAGCGAGGCGTACGTCGATCGATCGGACGTATGCAGGCATGATCACGCATCTGCTT
ACAAAGCCCATACAGCATCGCTGAAGGCCAAAGTGAGGGTTATGTACGGCAACGTAA
ACCAGACTGTGGATGTTTACGTGAACGGAGACCATGCCGTCACGATAGGGGGTACTC
AGTTCATATTCGGGCCGCTGTCATCGGCCTGGACCCCGTTCGACAACAAGATAGTCG
TGTACAAAGACGAAGTGTTCAATCAGGACTTCCCGCCGTACGGATCTGGGCAACCAG
GGCGCTTCGGCGACATCCAAAGCAGAACAGTGGAGAGTAACGACCTGTACGCGAACA
CGGCACTGAAGCTGGCACGCCCTTCACCCGGCATGGTCCATGTACCGTACACACAGA
CACCTTCAGGGTTCAAATATTGGCTAAAGGAAAAAGGGACAGCCCTAAATACGAAGG
CTCCTTTTGGCTGCCAAATCAAAACGAACCCTGTCAGGGCCATGAACTGCGCCGTGG
GAAACATCCCTGTCTCCATGAATTTGCCTGACAGCGCCTTTACCCGCATTGTCGAGG
CGCCGACCATCATTGACCTGACTTGCACAGTGGCTACCTGTACGCACTCCTCGGATT
TCGGCGGCGTCTTGACACTGACGTACAAGACCGACAAGAACGGGGACTGCTCTGTAC
ACTCGCACTCTAACGTAGCTACTCTACAGGAGGCCACAGCAAAAGTGAAGACAGCAG
GTAAGGTGACCTTACACTTCTCCACGGCAAGCGCATCACCTTCTTTTGTGGTGTCGC
TATGCAGTGCTAGGGCCACCTGTTCAGCGTCGTGTGAGCCCCCGAAAGACCACATAG
TCCCATATGCGGCTAGCCACAGTAACGTAGTGTTTCCAGACATGTCGGGCACCGCAC
TATCATGGGTGCAGAAAATCTCGGGTGGTCTGGGGGCCTTCGCAATCGGCGCTATCC
TGGTGCTGGTTGTGGTCACTTGCATTGGGCTCCGCAGATAAGTTAGGGTAGGCAATG
GCATTGATATAGCAAGAAAATTGAAAACAGAAAAAGTTAGGGTAAGCAATGGCATAT
AACCATAACTGTATAACTTGTAACAAAGCGCAACAAGACCTGCGCAATTGGCCCCGT
GGTCCGCCTCACGGAAACTCGGGGCAACTCATATTGACACATTAATTGGCAATAATT
GGAAGCTTACATAAGCTTAATTCGACGAATAATTGGATTTTTATTTTATTTTGCAAT
TGGTTTTTAATATTTC

Reference List

Agarraberes, F. A., Terlecky, S. R. & Dice, J. F. (1997). An intralysosomal hsp70 is required for a selective pathway of lysosomal protein degradation. *J Cell Biol* **137**, 825-834.

Aguilar, P. V., Weaver, S. C. & Basler, C. F. (2007). Capsid protein of eastern equine encephalitis virus inhibits host cell gene expression. *J Virol* **81**, 3866-3876.

Akahata, W., Yang, Z. Y., Andersen, H., Sun, S., Holdaway, H. A., Kong, W. P., Lewis, M. G., Higgs, S., Rossmann, M. G., Rao, S. & Nabel, G. J. (2010).A virus-like particle vaccine for epidemic Chikungunya virus protects nonhuman primates against infection. *Nat Med* **16**, 334-338.

Akira, S. (2000). The role of IL-18 in innate immunity. *Curr Opin Immunol* **12**, 59-63.

Alexopoulou, L., Holt, A. C., Medzhitov, R. & Flavell, R. A. (2001). Recognition of double-stranded RNA and activation of NF-kappaB by Toll-like receptor 3. *Nature* **413**, 732-738.

Aliperti, G. & Schlesinger, M. J. (1978). Evidence for an autoprotease activity of sindbis virus capsid protein. *Virology* **90**, 366-369.

Alonso, G., Prieto, M. & Chauvet, N. (1999). Tangential migration of young neurons arising from the subventricular zone of adult rats is impaired by surgical lesions passing through their natural migratory pathway. *Journal Of Comparative Neurology* **405**, 508-528.

Amor, S., Scallan, M. F., Morris, M. M., Dyson, H. & Fazakerley, J. K. (1996). Role of immune responses in protection and pathogenesis during Semliki Forest virus encephalitis. *J Gen Virol* **77 (Pt 2)**, 281-291.

Amor, S. & Webb, H. E. (1986). Use of N-acetylethyleneimine [AEI] for the inactivation of Semliki Forest virus in vitro. *J Med Virol* **19**, 367-376.

Andrade, R. M., Wessendarp, M., Gubbels, M. J., Striepen, B. & Subauste, C. S. (2006).CD40 induces macrophage anti-Toxoplasma gondii activity by triggering autophagy-dependent fusion of pathogen-containing vacuoles and lysosomes. *J Clin Invest* **116**, 2366-2377.

Andrejeva, J., Childs, K. S., Young, D. F., Carlos, T. S., Stock, N., Goodbourn, S. & Randall, R. E. (2004). The V proteins of paramyxoviruses bind the IFN-inducible RNA helicase, mda-5, and inhibit its activation of the IFN-beta promoter. *Proc Natl Acad Sci U S A* **101**, 17264-17269.

Andrejeva, J., Young, D. F., Goodbourn, S. & Randall, R. E. (2002). Degradation of STAT1 and STAT2 by the V proteins of simian virus 5 and human parainfluenza virus type 2, respectively: consequences for virus replication in the presence of alpha/beta and gamma interferons. *J Virol* **76**, 2159-2167.

Ank, N., West, H., Bartholdy, C., Eriksson, K., Thomsen, A. R. & Paludan, S. R. (2006). Lambda interferon (IFN-lambda), a type III IFN, is induced by viruses and IFNs and displays potent antiviral activity against select virus infections in vivo. *J Virol* **80**, 4501-4509.

Ashford, T. P. & Porter, K. R. (1962). Cytoplasmic components in hepatic cell lysosomes. *J Cell Biol* **12**, 198-202.

Ashour, J., Laurent-Rolle, M., Shi, P. Y. & Garcia-Sastre, A. (2009).NS5 of dengue virus mediates STAT2 binding and degradation. *J Virol* **83**, 5408-5418.

Asselin-Paturel, C., Boonstra, A., Dalod, M., Durand, I., Yessaad, N., Dezutter-Dambuyant, C., Vicari, A., O'Garra, A., Biron, C., Briere, F. & Trinchieri, G. (2001). Mouse type I IFN-producing cells are immature APCs with plasmacytoid morphology. *Nat Immunol* **2**, 1144-1150.

Asselin-Paturel, C., Brizard, G., Pin, J. J., Briere, F. & Trinchieri, G. (2003). Mouse strain differences in plasmacytoid dendritic cell frequency and function revealed by a novel monoclonal antibody. *J Immunol* **171**, 6466-6477.

Atkins, G. J., Sheahan, B. J. & Liljestrom, P. (1996). Manipulation of the Semliki Forest virus genome and its potential for vaccine construction. *Mol Biotechnol* **5**, 33-38.

Atkins, G. J., Sheahan, B. J. & Liljestrom, P. (1999). The molecular pathogenesis of Semliki Forest virus: a model virus made useful. *Journal of General Virology* **80**, 2287-2297.

Au, W. C., Moore, P. A., Lowther, W., Juang, Y. T. & Pitha, P. M. (1995). Identification of a member of the interferon regulatory factor family that binds to the interferon-stimulated response element and activates expression of interferon-induced genes. *Proc Natl Acad Sci U S A* **92**, 11657-11661.

Axe, E. L., Walker, S. A., Manifava, M., Chandra, P., Roderick, H. L., Habermann, A., Griffiths, G. & Ktistakis, N. T. (2008). Autophagosome formation from membrane compartments enriched in phosphatidylinositol 3-phosphate and dynamically connected to the endoplasmic reticulum. *J Cell Biol* **182**, 685-701.

Bach, E. A., Aguet, M. & Schreiber, R. D. (1997). The IFN gamma receptor: a paradigm for cytokine receptor signaling. *Annu Rev Immunol* **15**, 563-591.

Baeuerle, P. A. & Henkel, T. (1994). Function and activation of NF-kappa B in the immune system. *Annu Rev Immunol* **12**, 141-179.

Balluz, I. M., Glasgow, G. M., Killen, H. M., Mabruk, M. J., Sheahan, B. J. & Atkins, G. J. (1993). Virulent and avirulent strains of Semliki Forest virus show similar cell tropism for the murine central nervous system but differ in the severity and rate of induction of cytolytic damage. *Neuropathology And Applied Neurobiology* **19**, 233-239.

Bampton, E. T., Goemans, C. G., Niranjan, D., Mizushima, N. & Tolkovsky, A. M. (2005). The dynamics of autophagy visualized in live cells: from autophagosome formation to fusion with endo/lysosomes. *Autophagy* **1**, 23-36.

Banninger, G. & Reich, N. C. (2004).STAT2 nuclear trafficking. *J Biol Chem* **279**, 39199-39206.

Barchet, W., Cella, M., Odermatt, B., Asselin-Paturel, C., Colonna, M. & Kalinke, U. (2002). Virus-induced interferon alpha production by a dendritic cell subset in the absence of feedback signaling in vivo. *J Exp Med* **195**, 507-516.

Barry, G., Breakwell, L., Fragkoudis, R., ttarzadeh-Yazdi, G., Rodriguez-Andres, J., Kohl, A. & Fazakerley, J. K. (2009).PKR acts early in infection to suppress Semliki Forest virus production and strongly enhances the type I interferon response. *J Gen Virol* **90**, 1382-1391.

Barry, G., Fragkoudis, R., Ferguson, M. C., Lulla, A., Merits, A., Kohl, A. & Fazakerley, J. K. (2010). Semliki forest virus-induced endoplasmic reticulum stress accelerates apoptotic death of mammalian cells. *J Virol* **84**, 7369-7377.

Beg, A. A. & Baldwin, A. S., Jr. (1993). The I kappa B proteins: multifunctional regulators of Rel/NF-kappa B transcription factors. *Genes Dev* **7**, 2064-2070.

Bekisz, J., Schmeisser, H., Hernandez, J., Goldman, N. D. & Zoon, K. C. (2004). Human interferons alpha, beta and omega. *Growth Factors* **22**, 243-251.

Belsham, G. J. & Sonenberg, N. (2000). Picornavirus RNA translation: roles for cellular proteins. *Trends Microbiol* **8**, 330-335.

Bennett-Lovsey, R. M., Herbert, A. D., Sternberg, M. J. & Kelley, L. A. (2008). Exploring the extremes of sequence/structure space with ensemble fold recognition in the program Phyre. *Proteins* **70**, 611-625.

Berkowitz, B., Huang, D. B., Chen-Park, F. E., Sigler, P. B. & Ghosh, G. (2002). The x-ray crystal structure of the NF-kappa B p50.p65 heterodimer bound to the interferon beta -kappa B site. *J Biol Chem* **277**, 24694-24700.

Best, S. M., Morris, K. L., Shannon, J. G., Robertson, S. J., Mitzel, D. N., Park, G. S., Boer, E., Wolfinbarger, J. B. & Bloom, M. E. (2005). Inhibition of interferon-stimulated JAK-STAT signaling by a tick-borne flavivirus and identification of NS5 as an interferon antagonist. *J Virol* **79**, 12828-12839.

Bhattacharya, S., Eckner, R., Grossman, S., Oldread, E., Arany, Z., D'Andrea, A. & Livingston, D. M. (1996). Cooperation of Stat2 and p300/CBP in signalling induced by interferon-alpha. *Nature* **383**, 344-347.

Bieback, K., Lien, E., Klagge, I. M., Avota, E., Schneider-Schaulies, J., Duprex, W. P., Wagner, H., Kirschning, C. J., ter, M., V & Schneider-Schaulies, S. (2002). Hemagglutinin protein of wild-type measles virus activates toll-like receptor 2 signaling. *J Virol* **76**, 8729-8736.

Billecocq, A., Spiegel, M., Vialat, P., Kohl, A., Weber, F., Bouloy, M. & Haller, O. (2004).NSs protein of Rift Valley fever virus blocks interferon production by inhibiting host gene transcription. *J Virol* **78**, 9798-9806.

Birmingham, C. L., Smith, A. C., Bakowski, M. A., Yoshimori, T. & Brumell, J. H. (2006). Autophagy controls Salmonella infection in response to damage to the Salmonella-containing vacuole. *J Biol Chem* **281**, 11374-11383.

Biron, C. A. (2001). Interferons alpha and beta as immune regulators--a new look. *Immunity* **14**, 661-664.

Bjorck, P. (2001). Isolation and characterization of plasmacytoid dendritic cells from Flt3 ligand and granulocyte-macrophage colony-stimulating factor-treated mice. *Blood* **98**, 3520-3526.

Black, T. L., Barber, G. N. & Katze, M. G. (1993). Degradation of the interferon-induced 68,000-M(r) protein kinase by poliovirus requires RNA. *J Virol* **67**, 791-800.

Blommaart, E. F., Krause, U., Schellens, J. P., Vreeling-Sindelarova, H. & Meijer, A. J. (1997). The phosphatidylinositol 3-kinase inhibitors wortmannin and LY294002 inhibit autophagy in isolated rat hepatocytes. *Eur J Biochem* **243**, 240-246.

Bode, J. G., Ludwig, S., Ehrhardt, C., Albrecht, U., Erhardt, A., Schaper, F., Heinrich, P. C. & Haussinger, D. (2003).IFN-alpha antagonistic activity of HCV core protein involves induction of suppressor of cytokine signaling-3. *FASEB J* **17**, 488-490.

Boehm, U., Klamp, T., Groot, M. & Howard, J. C. (1997). Cellular responses to interferon-gamma. *Annu Rev Immunol* **15**, 749-795.

Bonatti, S., Migliaccio, G., Blobel, G. & Walter, P. (1984). Role of signal recognition particle in the membrane assembly of Sindbis viral glycoproteins. *Eur J Biochem* **140**, 499-502.

Brabec-Zaruba, M., Berka, U., Blaas, D. & Fuchs, R. (2007). Induction of autophagy does not affect human rhinovirus type 2 production. *J Virol* **81**, 10815-10817.

Bradish, C. J., Allner, K. & Fitzgeorge, R. (1975). Immunomodification and the expression of virulence in mice by defined strains of Semliki Forest virus: the effects of cyclophosphamide. *J Gen Virol* **28**, 225-237.

Bradish, C. J., Allner, K. & Maber, H. B. (1971). The virulence of original and derived strains of Semliki forest virus for mice, guinea-pigs and rabbits. *J Gen Virol* **12**, 141-160.

Bradish, C. J. & Titmuss, D. (1981). The effects of interferon and double-stranded RNA upon the virus-host interaction: studies with togavirus strains in mice. *J Gen Virol* **53**, 21-30.

Brand, S. R., Kobayashi, R. & Mathews, M. B. (1997). The Tat protein of human immunodeficiency virus type 1 is a substrate and inhibitor of the interferon-induced, virally activated protein kinase, PKR. *J Biol Chem* **272**, 8388-8395.

Breakwell, L., Dosenovic, P., Karlsson Hedestam, G. B., D'Amato, M., Liljestrom, P., Fazakerley, J. & McInerney, G. M. (2007). Semliki Forest virus nonstructural protein 2 is involved in suppression of the type I interferon response. *J Virol* **81**, 8677-8684.

Brehin, A. C., Casademont, I., Frenkiel, M. P., Julier, C., Sakuntabhai, A. & Despres, P. (2009). The large form of human 2',5'-Oligoadenylate Synthetase (OAS3) exerts antiviral effect against Chikungunya virus. *Virology* **384**, 216-222.

Bromberg, J. & Wang, T. C. (2009). Inflammation and cancer: IL-6 and STAT3 complete the link. *Cancer Cell* **15**, 79-80.

Bromberg, J. F., Horvath, C. M., Besser, D., Lathem, W. W. & Darnell, J. E., Jr. (1998). Stat3 activation is required for cellular transformation by v-src. *Mol Cell Biol* **18**, 2553-2558.

Bromberg, J. F., Horvath, C. M., Wen, Z., Schreiber, R. D. & Darnell, J. E., Jr. (1996). Transcriptionally active Stat1 is required for the antiproliferative effects of both interferon alpha and interferon gamma. *Proc Natl Acad Sci U S A* **93**, 7673-7678.

Burke, C. W., Gardner, C. L., Steffan, J. J., Ryman, K. D. & Klimstra, W. B. (2009). Characteristics of alpha/beta interferon induction after infection of murine fibroblasts with wild-type and mutant alphaviruses. *Virology*.

Cadwell, K. (2010). Crohn's disease susceptibility gene interactions, a NOD to the newcomer ATG16L1. *Gastroenterology* **139**, 1448-1450.

Cadwell, K., Liu, J. Y., Brown, S. L., Miyoshi, H., Loh, J., Lennerz, J. K., Kishi, C., Kc, W., Carrero, J. A., Hunt, S., Stone, C. D., Brunt, E. M., Xavier, R. J., Sleckman, B. P., Li, E., Mizushima, N., Stappenbeck, T. S. & Virgin, H. W. (2008).A key role for autophagy and the autophagy gene Atg16l1 in mouse and human intestinal Paneth cells. *Nature* **456**, 259-263.

Capon, D. J., Shepard, H. M. & Goeddel, D. V. (1985). Two distinct families of human and bovine interferon-alpha genes are coordinately expressed and encode functional polypeptides. *Mol Cell Biol* **5**, 768-779.

Carnaud, C., Lee, D., Donnars, O., Park, S. H., Beavis, A., Koezuka, Y. & Bendelac, A. (1999). Cutting edge: Cross-talk between cells of the innate immune system: NKT cells rapidly activate NK cells. *J Immunol* **163**, 4647-4650.

Caro, L. H., Plomp, P. J., Wolvetang, E. J., Kerkhof, C. & Meijer, A. J. (1988).3-Methyladenine, an inhibitor of autophagy, has multiple effects on metabolism. *Eur J Biochem* **175**, 325-329.

Cella, M., Jarrossay, D., Facchetti, F., Alebardi, O., Nakajima, H., Lanzavecchia, A. & Colonna, M. (1999). Plasmacytoid monocytes migrate to

inflamed lymph nodes and produce large amounts of type I interferon. *Nat Med* **5**, 919-923.

Chang, H. C., Sehra, S., Goswami, R., Yao, W., Yu, Q., Stritesky, G. L., Jabeen, R., McKinley, C., Ahyi, A. N., Han, L., Nguyen, E. T., Robertson, M. J., Perumal, N. B., Tepper, R. S., Nutt, S. L. & Kaplan, M. H. (2010). The transcription factor PU.1 is required for the development of IL-9-producing T cells and allergic inflammation. *Nat Immunol* **11**, 527-534.

Cheshire, J. L., Williams, B. R. & Baldwin, A. S., Jr. (1999). Involvement of double-stranded RNA-activated protein kinase in the synergistic activation of nuclear factor-kappaB by tumor necrosis factor-alpha and gamma-interferon in preneuronal cells. *J Biol Chem* **274**, 4801-4806.

Chien, C. Y., Xu, Y., Xiao, R., Aramini, J. M., Sahasrabudhe, P. V., Krug, R. M. & Montelione, G. T. (2004). Biophysical characterization of the complex between double-stranded RNA and the N-terminal domain of the NS1 protein from influenza A virus: evidence for a novel RNA-binding mode. *Biochemistry* **43**, 1950-1962.

Chiu, M. I., Katz, H. & Berlin, V. (1994).RAPT1, a mammalian homolog of yeast Tor, interacts with the FKBP12/rapamycin complex. *Proc Natl Acad Sci U S A* **91**, 12574-12578.

Choi, E. A., Lei, H., Maron, D. J., Wilson, J. M., Barsoum, J., Fraker, D. L., El-Deiry, W. S. & Spitz, F. R. (2003). Stat1-dependent induction of tumor necrosis factor-related apoptosis-inducing ligand and the cell-surface death signaling pathway by interferon beta in human cancer cells. *Cancer Res* **63**, 5299-5307.

Chu, W. M., Ostertag, D., Li, Z. W., Chang, L., Chen, Y., Hu, Y., Williams, B., Perrault, J. & Karin, M. (1999).JNK2 and IKKbeta are required for activating the innate response to viral infection. *Immunity* **11**, 721-731.

Chung, C. D., Liao, J., Liu, B., Rao, X., Jay, P., Berta, P. & Shuai, K. (1997). Specific inhibition of Stat3 signal transduction by PIAS3. *Science* **278**, 1803-1805.

Clark, M. E., Lieberman, P. M., Berk, A. J. & Dasgupta, A. (1993). Direct cleavage of human TATA-binding protein by poliovirus protease 3C in vivo and in vitro. *Mol Cell Biol* **13**, 1232-1237.

Clark, S. L. J. (1957). Cellular differentiation in the kidneys of newborn mice studies with the electron microscope. *J Biophys Biochem Cytol* **3**, 349-362.

Clemens, M. J., Hershey, J. W., Hovanessian, A. C., Jacobs, B. C., Katze, M. G., Kaufman, R. J., Lengyel, P., Samuel, C. E., Sen, G. C. & Williams, B. R. (1993).PKR: proposed nomenclature for the RNA-dependent protein kinase induced by interferon. *J Interferon Res* **13**, 241.

Colamonici, O. R., Uyttendaele, H., Domanski, P., Yan, H. & Krolewski, J. J. (1994).p135tyk2, an interferon-alpha-activated tyrosine kinase, is physically associated with an interferon-alpha receptor. *J Biol Chem* **269**, 3518-3522.

Couderc, T., Chretien, F., Schilte, C., Disson, O., Brigitte, M., Guivel-Benhassine, F., Touret, Y., Barau, G., Cayet, N., Schuffenecker, I., Despres, P., renzana-Seisdedos, F., Michault, A., Albert, M. L. & Lecuit, M. (2008).A mouse model for Chikungunya: young age and inefficient type-I interferon signaling are risk factors for severe disease. *PLoS Pathog* **4**, e29.

Cuervo, A. M. & Dice, J. F. (1996).A receptor for the selective uptake and degradation of proteins by lysosomes. *Science* **273**, 501-503.

Cuervo, A. M. & Dice, J. F. (2000). Age-related decline in chaperone-mediated autophagy. *J Biol Chem* **275**, 31505-31513.

Cusson-Hermance, N., Khurana, S., Lee, T. H., Fitzgerald, K. A. & Kelliher, M. A. (2005). Rip1 mediates the Trif-dependent toll-like receptor 3- and 4-induced NF-{kappa}B activation but does not contribute to interferon regulatory factor 3 activation. *J Biol Chem* **280**, 36560-36566.

Dalod, M., Salazar-Mather, T. P., Malmgaard, L., Lewis, C., Asselin-Paturel, C., Briere, F., Trinchieri, G. & Biron, C. A. (2002). Interferon alpha/beta and interleukin 12 responses to viral infections: pathways regulating dendritic cell cytokine expression in vivo. *J Exp Med* **195**, 517-528.

Dardalhon, V., Awasthi, A., Kwon, H., Galileos, G., Gao, W., Sobel, R. A., Mitsdoerffer, M., Strom, T. B., Elyaman, W., Ho, I. C., Khoury, S., Oukka, M. & Kuchroo, V. K. (2008).IL-4 inhibits TGF-beta-induced Foxp3+ T cells and, together with TGF-beta, generates IL-9+ IL-10+ Foxp3(-) effector T cells. *Nat Immunol* **9**, 1347-1355.

Das, S. & Dasgupta, A. (1993). Identification of the cleavage site and determinants required for poliovirus 3CPro-catalyzed cleavage of human TATA-binding transcription factor TBP. *J Virol* **67**, 3326-3331.

David, M., Grimley, P. M., Finbloom, D. S. & Larner, A. C. (1993).A nuclear tyrosine phosphatase downregulates interferon-induced gene expression. *Mol Cell Biol* **13**, 7515-7521.

de Groot, R. J., Hardy, W. R., Shirako, Y. & Strauss, J. H. (1990). Cleavage-site preferences of Sindbis virus polyproteins containing the non-structural proteinase. Evidence for temporal regulation of polyprotein processing in vivo. *EMBO J* **9**, 2631-2638.

De, D. C. & Wattiaux, R. (1966). Functions of lysosomes. *Annu Rev Physiol* **28**, 435-492.

Decker, T., Lew, D. J. & Darnell, J. E., Jr. (1991). Two distinct alpha-interferon-dependent signal transduction pathways may contribute to activation of transcription of the guanylate-binding protein gene. *Mol Cell Biol* **11**, 5147-5153.

Degenhardt, K., Mathew, R., Beaudoin, B., Bray, K., Anderson, D., Chen, G., Mukherjee, C., Shi, Y., Gelinas, C., Fan, Y., Nelson, D. A., Jin, S. & White, E. (2006). Autophagy promotes tumor cell survival and restricts necrosis, inflammation, and tumorigenesis. *Cancer Cell* **10**, 51-64.

Delgado, M. A., Elmaoued, R. A., Davis, A. S., Kyei, G. & Deretic, V. (2008). Toll-like receptors control autophagy. *EMBO J* **27**, 1110-1121.

Deng, L., Wang, C., Spencer, E., Yang, L., Braun, A., You, J., Slaughter, C., Pickart, C. & Chen, Z. J. (2000). Activation of the IkappaB kinase complex by TRAF6 requires a dimeric ubiquitin-conjugating enzyme complex and a unique polyubiquitin chain. *Cell* **103**, 351-361.

Der, S. D., Zhou, A., Williams, B. R. & Silverman, R. H. (1998). Identification of genes differentially regulated by interferon alpha, beta, or gamma using oligonucleotide arrays. *Proc Natl Acad Sci U S A* **95**, 15623-15628.

Deuber, S. A. & Pavlovic, J. (2007). Virulence of a mouse-adapted Semliki Forest virus strain is associated with reduced susceptibility to interferon. *J Gen Virol* **88**, 1952-1959.

Devaney, M. A., Vakharia, V. N., Lloyd, R. E., Ehrenfeld, E. & Grubman, M. J. (1988). Leader protein of foot-and-mouth disease virus is required for cleavage of the p220 component of the cap-binding protein complex. *J Virol* **62**, 4407-4409.

Dice, J. F. & Chiang, H. L. (1989). Lysosomal degradation of microinjected proteins. *Revis Biol Celular* **20**, 13-33.

Didcock, L., Young, D. F., Goodbourn, S. & Randall, R. E. (1999). The V protein of simian virus 5 inhibits interferon signalling by targeting STAT1 for proteasome-mediated degradation. *J Virol* **73**, 9928-9933.

Diebold, S. S., Kaisho, T., Hemmi, H., Akira, S. & Reis e Sousa (2004). Innate antiviral responses by means of TLR7-mediated recognition of single-stranded RNA. *Science* **303**, 1529-1531.

Ding, W. X., Ni, H. M., Gao, W., Yoshimori, T., Stolz, D. B., Ron, D. & Yin, X. M. (2007). Linking of autophagy to ubiquitin-proteasome system is important for the regulation of endoplasmic reticulum stress and cell viability. *Am J Pathol* **171**, 513-524.

Djavaheri-Mergny, M., Amelotti, M., Mathieu, J., Besancon, F., Bauvy, C., Souquere, S., Pierron, G. & Codogno, P. (2006).NF-kappaB activation represses tumor necrosis factor-alpha-induced autophagy. *J Biol Chem* **281**, 30373-30382.

Domingo, E. & Wain-Hobson, S. (2009). The 30th anniversary of quasispecies. Meeting on 'Quasispecies: past, present and future'. *EMBO Rep* **10**, 444-448.

Donnelly, R. P., Sheikh, F., Kotenko, S. V. & Dickensheets, H. (2004). The expanded family of class II cytokines that share the IL-10 receptor-2 (IL-10R2) chain. *J Leukoc Biol* **76**, 314-321.

Doyle, S. E., Schreckhise, H., Khuu-Duong, K., Henderson, K., Rosler, R., Storey, H., Yao, L., Liu, H., Barahmand-pour, F., Sivakumar, P., Chan, C., Birks, C., Foster, D., Clegg, C. H., Wietzke-Braun, P., Mihm, S. & Klucher, K. M. (2006). Interleukin-29 uses a type 1 interferon-like program to promote antiviral responses in human hepatocytes. *Hepatology* **44**, 896-906.

Dragan, A. I., Hargreaves, V. V., Makeyeva, E. N. & Privalov, P. L. (2007). Mechanisms of activation of interferon regulator factor 3: the role of C-terminal domain phosphorylation in IRF-3 dimerization and DNA binding. *Nucleic Acids Res* **35**, 3525-3534.

Dreux, M. & Chisari, F. V. (2009). Autophagy proteins promote hepatitis C virus replication. *Autophagy* **5**, 1224-1225.

Dumoutier, L., Tounsi, A., Michiels, T., Sommereyns, C., Kotenko, S. V. & Renauld, J. C. (2004). Role of the interleukin (IL)-28 receptor tyrosine residues for antiviral and antiproliferative activity of IL-29/interferon-lambda 1: similarities with type I interferon signaling. *J Biol Chem* **279**, 32269-32274.

Duong, F. H., Filipowicz, M., Tripodi, M., La, M. N. & Heim, M. H. (2004). Hepatitis C virus inhibits interferon signaling through up-regulation of protein phosphatase 2A. *Gastroenterology* **126**, 263-277.

Dupuis, S., Dargemont, C., Fieschi, C., Thomassin, N., Rosenzweig, S., Harris, J., Holland, S. M., Schreiber, R. D. & Casanova, J. L. (2001). Impairment of mycobacterial but not viral immunity by a germline human STAT1 mutation. *Science* **293**, 300-303.

Dupuis, S., Jouanguy, E., Al-Hajjar, S., Fieschi, C., Al-Mohsen, I. Z., Al-Jumaah, S., Yang, K., Chapgier, A., Eidenschenk, C., Eid, P., Al, G. A., Tufenkeji, H., Frayha, H., Al-Gazlan, S., Al-Rayes, H., Schreiber, R. D., Gresser, I. & Casanova, J. L. (2003). Impaired response to interferon-alpha/beta and lethal viral disease in human STAT1 deficiency. *Nat Genet* **33**, 388-391.

Dupuis-Maguiraga, L., Noret, M., Brun, S., Le, G. R., Gras, G. & Roques, P. (2012). Chikungunya disease: infection-associated markers from the acute to the chronic phase of arbovirus-induced arthralgia. *PLoS Negl Trop Dis* **6**, e1446.

Durbin, J. E., Hackenmiller, R., Simon, M. C. & Levy, D. E. (1996). Targeted disruption of the mouse Stat1 gene results in compromised innate immunity to viral disease. *Cell* **84**, 443-450.

Ea, C. K., Deng, L., Xia, Z. P., Pineda, G. & Chen, Z. J. (2006). Activation of IKK by TNFalpha requires site-specific ubiquitination of RIP1 and polyubiquitin binding by NEMO. *Mol Cell* **22**, 245-257.

Edelman, R., Ascher, M. S., Oster, C. N., Ramsburg, H. H., Cole, F. E. & Eddy, G. A. (1979). Evaluation in humans of a new, inactivated vaccine for Venezuelan equine encephalitis virus (C-84). *J Infect Dis* **140**, 708-715.

Edelman, R., Wasserman, S. S., Bodison, S. A., Perry, J. G., O'Donnoghue, M. & DeTolla, L. J. (2003). Phase II safety and immunogenicity study of type F botulinum toxoid in adult volunteers. *Vaccine* **21**, 4335-4347.

Ellis, M. J. & Goodbourn, S. (1994).NF-kappa B-independent activation of beta-interferon expression in mouse F9 embryonal carcinoma cells. *Nucleic Acids Res* **22**, 4489-4496.

Endo, T. A., Masuhara, M., Yokouchi, M., Suzuki, R., Sakamoto, H., Mitsui, K., Matsumoto, A., Tanimura, S., Ohtsubo, M., Misawa, H., Miyazaki, T., Leonor, N., Taniguchi, T., Fujita, T., Kanakura, Y., Komiya, S. & Yoshimura, A. (1997).A new protein containing an SH2 domain that inhibits JAK kinases. *Nature* **387**, 921-924.

Eng, K. E., Panas, M. D., Hedestam, G. B. & McInerney, G. M. (2010).A novel quantitative flow cytometry-based assay for autophagy. *Autophagy* **6**.

Eng, K. E., Panas, M. D., Murphy, D., Karlsson Hedestam, G. B. & McInerney, G. M. (2012). Accumulation of autophagosomes in semliki forest virus-infected cells is dependent on expression of the viral glycoproteins. *J Virol* **86**, 5674-5685.

English, L., Chemali, M., Duron, J., Rondeau, C., Laplante, A., Gingras, D., Alexander, D., Leib, D., Norbury, C., Lippe, R. & Desjardins, M. (2009). Autophagy enhances the presentation of endogenous viral antigens on MHC class I molecules during HSV-1 infection. *Nat Immunol* **10**, 480-487.

Enninga, J., Levy, D. E., Blobel, G. & Fontoura, B. M. (2002). Role of nucleoporin induction in releasing an mRNA nuclear export block. *Science* **295**, 1523-1525.

Enserink, M. (2007). Infectious diseases. Chikungunya: no longer a third world disease. *Science* **318**, 1860-1861.

Ericsson, J. L. (1969). Studies on induced cellular autophagy. II. Characterization of the membranes bordering autophagosomes in parenchymal liver cells. *Exp Cell Res* **56**, 393-405.

Eriksson, K. K., Cervantes-Barragan, L., Ludewig, B. & Thiel, V. (2008). Mouse hepatitis virus liver pathology is dependent on ADP-ribose-1"-phosphatase, a viral function conserved in the alpha-like supergroup. *J Virol* **82**, 12325-12334.

Etchison, D., Milburn, S. C., Edery, I., Sonenberg, N. & Hershey, J. W. (1982). Inhibition of HeLa cell protein synthesis following poliovirus infection correlates with the proteolysis of a 220,000-dalton polypeptide associated with eucaryotic initiation factor 3 and a cap binding protein complex. *J Biol Chem* **257**, 14806-14810.

Fauconnier, B. (1969). Enhancing effect of interferon antiserum on viral growth. *Nature* **222**, 185-186.

Fauconnier, B. (1971).[Effect of an anti-interferon serum on experimental viral pathogenicity in vivo]. *Pathol Biol (Paris)* **19**, 575-578.

Fayzulin, R. & Frolov, I. (2004). Changes of the secondary structure of the 5' end of the Sindbis virus genome inhibit virus growth in mosquito cells and lead to accumulation of adaptive mutations. *J Virol* **78**, 4953-4964.

Fazakerley, J. K. (2002). Pathogenesis of Semliki Forest virus encephalitis. *J Neurovirol* **8 Suppl 2**, 66-74.

Fazakerley, J. K., Boyd, A., Mikkola, M. L. & Kaariainen, L. (2002).A single amino acid change in the nuclear localization sequence of the nsP2 protein affects the neurovirulence of Semliki Forest virus. *J Virol* **76**, 392-396.

Fazakerley, J. K., Cotterill, C. L., Lee, G. & Graham, A. (2006). Virus tropism, distribution, persistence and pathology in the corpus callosum of the Semliki Forest virus-infected mouse brain: a novel system to study virus-oligodendrocyte interactions. *Neuropathol Appl Neurobiol* **32**, 397-409.

Fazakerley, J. K., Khalili-Shirazi, A. & Webb, H. E. (1988). Semliki Forest virus (A7[74]) infection of adult mice induces an immune-mediated demyelinating encephalomyelitis. *Ann N Y Acad Sci* **540**, 672-673.

Fazakerley, J. K., Pathak, S., Scallan, M., Amor, S. & Dyson, H. (1993). Replication of the A7(74) strain of Semliki Forest virus is restricted in neurons. *Virology* **195**, 627-637.

Fazakerley, J. K. & Webb, H. E. (1987). Semliki Forest virus-induced, immune-mediated demyelination: adoptive transfer studies and viral persistence in nude mice. *J Gen Virol* **68 (Pt 2)**, 377-385.

Feinstein, S. I., Mory, Y., Chernajovsky, Y., Maroteaux, L., Nir, U., Lavie, V. & Revel, M. (1985). Family of human alpha-interferon-like sequences. *Mol Cell Biol* **5**, 510-517.

Fenner, J. E., Starr, R., Cornish, A. L., Zhang, J. G., Metcalf, D., Schreiber, R. D., Sheehan, K., Hilton, D. J., Alexander, W. S. & Hertzog, P. J. (2006). Suppressor of cytokine signaling 1 regulates the immune response to infection by a unique inhibition of type I interferon activity. *Nat Immunol* **7**, 33-39.

Ferreon, J. C., Ferreon, A. C., Li, K. & Lemon, S. M. (2005). Molecular determinants of TRIF proteolysis mediated by the hepatitis C virus NS3/4A protease. *J Biol Chem* **280**, 20483-20492.

Fimia, G. M., Stoykova, A., Romagnoli, A., Giunta, L., Di, B. S., Nardacci, R., Corazzari, M., Fuoco, C., Ucar, A., Schwartz, P., Gruss, P., Piacentini, M., Chowdhury, K. & Cecconi, F. (2007). Ambra1 regulates autophagy and development of the nervous system. *Nature* **447**, 1121-1125.

Finkelman, F. D., Shea-Donohue, T., Morris, S. C., Gildea, L., Strait, R., Madden, K. B., Schopf, L. & Urban, J. F., Jr. (2004). Interleukin-4- and interleukin-13-mediated host protection against intestinal nematode parasites. *Immunol Rev* **201**, 139-155.

Finter, N. B. (1966). Interferon as an antiviral agent in vivo: quantitative and temporal aspects of the protection of mice against Semliki Forest virus. *Br J Exp Pathol* **47**, 361-371.

Fitzgerald, K. A., McWhirter, S. M., Faia, K. L., Rowe, D. C., Latz, E., Golenbock, D. T., Coyle, A. J., Liao, S. M. & Maniatis, T. (2003).IKKepsilon and TBK1 are essential components of the IRF3 signaling pathway. *Nat Immunol* **4**, 491-496.

Fleming, P. (1977). Age-dependent and strain-related differences of virulence of Semliki Forest virus in mice. *J Gen Virol* **37**, 93-105.

Flores, I., Mariano, T. M. & Pestka, S. (1991). Human interferon omega (omega) binds to the alpha/beta receptor. *J Biol Chem* **266**, 19875-19877.

Floyd-Smith, G., Slattery, E. & Lengyel, P. (1981). Interferon action: RNA cleavage pattern of a (2'-5')oligoadenylate--dependent endonuclease. *Science* **212**, 1030-1032.

Foti, M., Granucci, F. & Ricciardi-Castagnoli, P. (2004).A central role for tissue-resident dendritic cells in innate responses. *Trends Immunol* **25**, 650-654.

Foy, E., Li, K., Sumpter, R., Jr., Loo, Y. M., Johnson, C. L., Wang, C., Fish, P. M., Yoneyama, M., Fujita, T., Lemon, S. M. & Gale, M., Jr. (2005). Control of antiviral defenses through hepatitis C virus disruption of retinoic acid-inducible gene-I signaling. *Proc Natl Acad Sci U S A* **102**, 2986-2991.

Fragkoudis, R., Breakwell, L., McKimmie, C., Boyd, A., Barry, G., Kohl, A., Merits, A. & Fazakerley, J. K. (2007). The type I interferon system protects mice from Semliki Forest virus by preventing widespread virus dissemination in extraneural tissues, but does not mediate the restricted replication of avirulent virus in central nervous system neurons. *J Gen Virol* **88**, 3373-3384.

Fredericksen, B. L., Keller, B. C., Fornek, J., Katze, M. G. & Gale, M., Jr. (2008). Establishment and maintenance of the innate antiviral response to West Nile Virus involves both RIG-I and MDA5 signaling through IPS-1. *J Virol* **82**, 609-616.

Frieman, M., Yount, B., Heise, M., Kopecky-Bromberg, S. A., Palese, P. & Baric, R. S. (2007). Severe acute respiratory syndrome coronavirus ORF6 antagonizes STAT1 function by sequestering nuclear import factors on the rough endoplasmic reticulum/Golgi membrane. *J Virol* **81**, 9812-9824.

Frolov, I., Akhrymuk, M., Akhrymuk, I., Atasheva, S. & Frolova, E. I. (2012). Early events in alphavirus replication determine the outcome of infection. *J Virol* **86**, 5055-5066.

Frolov, I. & Schlesinger, S. (1994). Comparison of the effects of Sindbis virus and Sindbis virus replicons on host cell protein synthesis and cytopathogenicity in BHK cells. *J Virol* **68**, 1721-1727.

Frolova, E. I., Fayzulin, R. Z., Cook, S. H., Griffin, D. E., Rice, C. M. & Frolov, I. (2002). Roles of nonstructural protein nsP2 and Alpha/Beta interferons in determining the outcome of Sindbis virus infection. *J Virol* **76**, 11254-11264.

Fros, J. J., Liu, W. J., Prow, N. A., Geertsema, C., Ligtenberg, M., Vanlandingham, D. L., Schnettler, E., Vlak, J. M., Suhrbier, A., Khromykh, A. A. & Pijlman, G. P. (2010). Chikungunya virus nonstructural protein 2 inhibits type I/II interferon-stimulated JAK-STAT signaling. *J Virol*.

Froshauer, S., Kartenbeck, J. & Helenius, A. (1988). Alphavirus RNA replicase is located on the cytoplasmic surface of endosomes and lysosomes. *J Cell Biol* **107**, 2075-2086.

Frucht, D. M., Fukao, T., Bogdan, C., Schindler, H., O'Shea, J. J. & Koyasu, S. (2001).IFN-gamma production by antigen-presenting cells: mechanisms emerge. *Trends Immunol* **22**, 556-560.

Fu, X. Y. (1992).A transcription factor with SH2 and SH3 domains is directly activated by an interferon alpha-induced cytoplasmic protein tyrosine kinase(s). *Cell* **70**, 323-335.

Fu, X. Y., Kessler, D. S., Veals, S. A., Levy, D. E. & Darnell, J. E., Jr. (1990).ISGF3, the transcriptional activator induced by interferon alpha, consists of multiple interacting polypeptide chains. *Proc Natl Acad Sci U S A* **87**, 8555-8559.

Fu, X. Y., Schindler, C., Improta, T., Aebersold, R. & Darnell, J. E., Jr. (1992). The proteins of ISGF-3, the interferon alpha-induced transcriptional activator, define a gene family involved in signal transduction. *Proc Natl Acad Sci U S A* **89**, 7840-7843.

Fujita, N., Itoh, T., Omori, H., Fukuda, M., Noda, T. & Yoshimori, T. (2008). The Atg16L complex specifies the site of LC3 lipidation for membrane biogenesis in autophagy. *Mol Biol Cell* **19**, 2092-2100.

Fukao, T., Matsuda, S. & Koyasu, S. (2000). Synergistic effects of IL-4 and IL-18 on IL-12-dependent IFN-gamma production by dendritic cells. *J Immunol* **164**, 64-71.

Fuller, S. D., Berriman, J. A., Butcher, S. J. & Gowen, B. E. (1995). Low pH induces swiveling of the glycoprotein heterodimers in the Semliki Forest virus spike complex. *Cell* **81**, 715-725.

Ganchi, P. A., Sun, S. C., Greene, W. C. & Ballard, D. W. (1993).A novel NF-kappa B complex containing p65 homodimers: implications for transcriptional control at the level of subunit dimerization. *Mol Cell Biol* **13**, 7826-7835.

Garcin, D., Marq, J. B., Strahle, L., le, M. P. & Kolakofsky, D. (2002). All four Sendai Virus C proteins bind Stat1, but only the larger forms also induce its mono-ubiquitination and degradation. *Virology* **295**, 256-265.

Garmashova, N., Atasheva, S., Kang, W., Weaver, S. C., Frolova, E. & Frolov, I. (2007a). Analysis of Venezuelan equine encephalitis virus capsid protein function in the inhibition of cellular transcription. *J Virol* **81**, 13552-13565.

Garmashova, N., Gorchakov, R., Frolova, E. & Frolov, I. (2006). Sindbis virus nonstructural protein nsP2 is cytotoxic and inhibits cellular transcription. *J Virol* **80**, 5686-5696.

Garmashova, N., Gorchakov, R., Volkova, E., Paessler, S., Frolova, E. & Frolov, I. (2007b). The Old World and New World alphaviruses use different virus-specific proteins for induction of transcriptional shutoff. *J Virol* **81**, 2472-2484.

Garoff, H., Frischauf, A. M., Simons, K., Lehrach, H. & Delius, H. (1980). Nucleotide sequence of cdna coding for Semliki Forest virus membrane glycoproteins. *Nature* **288**, 236-241.

Gauzzi, M. C., Velazquez, L., McKendry, R., Mogensen, K. E., Fellous, M. & Pellegrini, S. (1996). Interferon-alpha-dependent activation of Tyk2 requires phosphorylation of positive regulatory tyrosines by another kinase. *J Biol Chem* **271**, 20494-20500.

Geigenmuller-Gnirke, U., Weiss, B., Wright, R. & Schlesinger, S. (1991). Complementation between Sindbis viral RNAs produces infectious particles with a bipartite genome. *Proc Natl Acad Sci U S A* **88**, 3253-3257.

Gibbs, E. P. (1976). Equine viral encephalitis. *Equine Vet J* **8**, 66-71.

Gil, J. & Esteban, M. (2000). The interferon-induced protein kinase (PKR), triggers apoptosis through FADD-mediated activation of caspase 8 in a manner independent of Fas and TNF-alpha receptors. *Oncogene* **19**, 3665-3674.

Gimenez-Barcons, M., Wang, C., Chen, M., Sanchez-Tapias, J. M., Saiz, J. C. & Gale, M., Jr. (2005). The oncogenic potential of hepatitis C virus NS5A sequence variants is associated with PKR regulation. *J Interferon Cytokine Res* **25**, 152-164.

Gitlin, L., Barchet, W., Gilfillan, S., Cella, M., Beutler, B., Flavell, R. A., Diamond, M. S. & Colonna, M. (2006). Essential role of mda-5 in type I IFN responses to polyriboinosinic:polyribocytidylic acid and encephalomyocarditis picornavirus. *Proc Natl Acad Sci U S A* **103**, 8459-8464.

Glasgow, G. M., Killen, H. M., Liljestrom, P., Sheahan, B. J. & Atkins, G. J. (1994).A single amino acid change in the E2 spike protein of a virulent strain of Semliki Forest virus attenuates pathogenicity. *J Gen Virol* **75 (Pt 3)**, 663-668.

Glasgow, G. M., McGee, M. M., Sheahan, B. J. & Atkins, G. J. (1997). Death mechanisms in cultured cells infected by Semliki Forest virus. *J Gen Virol* **78 (Pt 7)**, 1559-1563.

Glasgow, G. M., Sheahan, B. J., Atkins, G. J., Wahlberg, J. M., Salminen, A. & Liljestrom, P. (1991). Two mutations in the envelope glycoprotein E2 of Semliki Forest virus affecting the maturation and entry patterns of the virus alter pathogenicity for mice. *Virology* **185**, 741-748.

Golab, J., Zagozdzon, Stoklosal, T., Kaminski, R., Kozar, K. & Jakobisiak, M. (2000). Direct stimulation of macrophages by IL-12 and IL-18--a bridge too far? *Immunol Lett* **72**, 153-157.

Gomez de, C. M., Ehsani, N., Mikkola, M. L., Garcia, J. A. & Kaariainen, L. (1999).RNA helicase activity of Semliki Forest virus replicase protein NSP2. *FEBS Lett* **448**, 19-22.

Grandadam, M., Caro, V., Plumet, S., Thiberge, J. M., Souares, Y., Failloux, A. B., Tolou, H. J., Budelot, M., Cosserat, D., Leparc-Goffart, I. & Despres, P. (2011). Chikungunya virus, southeastern France. *Emerg Infect Dis* **17**, 910-913.

Grimley, P. M., Berezesky, I. K. & Friedman, R. M. (1968). Cytoplasmic structures associated with an arbovirus infection: loci of viral ribonucleic acid synthesis. *J Virol* **2**, 1326-1338.

Guo, J. T., Hayashi, J. & Seeger, C. (2005). West Nile virus inhibits the signal transduction pathway of alpha interferon. *J Virol* **79**, 1343-1350.

Guo, Z., Chen, L. M., Zeng, H., Gomez, J. A., Plowden, J., Fujita, T., Katz, J. M., Donis, R. O. & Sambhara, S. (2007).NS1 protein of influenza A virus inhibits the function of intracytoplasmic pathogen sensor, RIG-I. *Am J Respir Cell Mol Biol* **36**, 263-269.

Gutierrez, M. G., Master, S. S., Singh, S. B., Taylor, G. A., Colombo, M. I. & Deretic, V. (2004). Autophagy is a defense mechanism inhibiting BCG and Mycobacterium tuberculosis survival in infected macrophages. *Cell* **119**, 753-766.

Hacker, H., Redecke, V., Blagoev, B., Kratchmarova, I., Hsu, L. C., Wang, G. G., Kamps, M. P., Raz, E., Wagner, H., Hacker, G., Mann, M. & Karin, M. (2006). Specificity in Toll-like receptor signalling through distinct effector functions of TRAF3 and TRAF6. *Nature* **439**, 204-207.

Hahn, Y. S., Strauss, E. G. & Strauss, J. H. (1989). Mapping of RNA- temperature-sensitive mutants of Sindbis virus: assignment of complementation groups A, B, and G to nonstructural proteins. *J Virol* **63**, 3142-3150.

Hailey, D. W., Rambold, A. S., Satpute-Krishnan, P., Mitra, K., Sougrat, R., Kim, P. K. & Lippincott-Schwartz, J. (2010). Mitochondria supply membranes for autophagosome biogenesis during starvation. *Cell* **141**, 656-667.

Haines, G. K., III, Becker, S., Ghadge, G., Kies, M., Pelzer, H. & Radosevich, J. A. (1993). Expression of the double-stranded RNA-dependent protein kinase (p68) in squamous cell carcinoma of the head and neck region. *Arch Otolaryngol Head Neck Surg* **119**, 1142-1147.

Han, J. Q., Wroblewski, G., Xu, Z., Silverman, R. H. & Barton, D. J. (2004). Sensitivity of hepatitis C virus RNA to the antiviral enzyme ribonuclease L is determined by a subset of efficient cleavage sites. *J Interferon Cytokine Res* **24**, 664-676.

Hanada, T., Noda, N. N., Satomi, Y., Ichimura, Y., Fujioka, Y., Takao, T., Inagaki, F. & Ohsumi, Y. (2007). The Atg12-Atg5 conjugate has a novel E3-like activity for protein lipidation in autophagy. *J Biol Chem* **282**, 37298-37302.

Hara, T., Takamura, A., Kishi, C., Iemura, S., Natsume, T., Guan, J. L. & Mizushima, N. (2008).FIP200, a ULK-interacting protein, is required for autophagosome formation in mammalian cells. *J Cell Biol* **181**, 497-510.

Hardy, M. P., Owczarek, C. M., Jermiin, L. S., Ejdeback, M. & Hertzog, P. J. (2004). Characterization of the type I interferon locus and identification of novel genes. *Genomics* **84**, 331-345.

Harris, D. P., Haynes, L., Sayles, P. C., Duso, D. K., Eaton, S. M., Lepak, N. M., Johnson, L. L., Swain, S. L. & Lund, F. E. (2000). Reciprocal regulation of polarized cytokine production by effector B and T cells. *Nat Immunol* **1**, 475-482.

Harris, J., De Haro, S. A., Master, S. S., Keane, J., Roberts, E. A., Delgado, M. & Deretic, V. (2007).T helper 2 cytokines inhibit autophagic control of intracellular Mycobacterium tuberculosis. *Immunity* **27**, 505-517.

Hassel, B. A., Zhou, A., Sotomayor, C., Maran, A. & Silverman, R. H. (1993).A dominant negative mutant of 2-5A-dependent RNase suppresses antiproliferative and antiviral effects of interferon. *EMBO J* **12**, 3297-3304.

Hauptmann, R. & Swetly, P. (1985).A novel class of human type I interferons. *Nucleic Acids Res* **13**, 4739-4749.

Hayashi-Nishino, M., Fujita, N., Noda, T., Yamaguchi, A., Yoshimori, T. & Yamamoto, A. (2009).A subdomain of the endoplasmic reticulum forms a cradle for autophagosome formation. *Nat Cell Biol* **11**, 1433-1437.

Heil, F., Hemmi, H., Hochrein, H., Ampenberger, F., Kirschning, C., Akira, S., Lipford, G., Wagner, H. & Bauer, S. (2004). Species-specific recognition of single-stranded RNA via toll-like receptor 7 and 8. *Science* **303**, 1526-1529.

Heim, M. H., Moradpour, D. & Blum, H. E. (1999). Expression of hepatitis C virus proteins inhibits signal transduction through the Jak-STAT pathway. *J Virol* **73**, 8469-8475.

Helenius, A., Marsh, M. & White, J. (1980). The entry of viruses into animal cells. *Trends Biochem* **5**, 104-106.

Helenius, A., Marsh, M. & White, J. (1982). Inhibition of Semliki forest virus penetration by lysosomotropic weak bases. *J Gen Virol* **58 Pt 1**, 47-61.

Hemmi, H., Kaisho, T., Takeda, K. & Akira, S. (2003). The roles of Toll-like receptor 9, MyD88, and DNA-dependent protein kinase catalytic subunit in the effects of two distinct CpG DNAs on dendritic cell subsets. *J Immunol* **170**, 3059-3064.

Hemmi, H., Takeuchi, O., Kawai, T., Kaisho, T., Sato, S., Sanjo, H., Matsumoto, M., Hoshino, K., Wagner, H., Takeda, K. & Akira, S. (2000).A Toll-like receptor recognizes bacterial DNA. *Nature* **408**, 740-745.

Henderson, B. E., Metselaar, D., Kirya, G. B. & Timms, G. L. (1970). Investigations into yellow fever virus and other arboviruses in the northern regions of Kenya. *Bull World Health Organ* **42**, 787-795.

Henry, G. L., McCormack, S. J., Thomis, D. C. & Samuel, C. E. (1994). Mechanism of interferon action. Translational control and the RNA-dependent protein kinase (PKR): antagonists of PKR enhance the translational activity of mRNAs that include a 161 nucleotide region from reovirus S1 mRNA. *J Biol Regul Homeost Agents* **8**, 15-24.

Hewson, C. A., Jardine, A., Edwards, M. R., Laza-Stanca, V. & Johnston, S. L. (2005). Toll-like receptor 3 is induced by and mediates antiviral activity against rhinovirus infection of human bronchial epithelial cells. *J Virol* **79**, 12273-12279.

Hilton, L., Moganeradj, K., Zhang, G., Chen, Y. H., Randall, R. E., McCauley, J. W. & Goodbourn, S. (2006). The NPro product of bovine viral diarrhea virus inhibits DNA binding by interferon regulatory factor 3 and targets it for proteasomal degradation. *J Virol* **80**, 11723-11732.

Ho, L. J., Hung, L. F., Weng, C. Y., Wu, W. L., Chou, P., Lin, Y. L., Chang, D. M., Tai, T. Y. & Lai, J. H. (2005). Dengue virus type 2 antagonizes IFN-alpha but not IFN-gamma antiviral effect via down-regulating Tyk2-STAT signaling in the human dendritic cell. *J Immunol* **174**, 8163-8172.

Hochrein, H., Shortman, K., Vremec, D., Scott, B., Hertzog, P. & O'Keeffe, M. (2001). Differential production of IL-12, IFN-alpha, and IFN-gamma by mouse dendritic cell subsets. *J Immunol* **166**, 5448-5455.

Honda, K., Yanai, H., Takaoka, A. & Taniguchi, T. (2005). Regulation of the type I IFN induction: a current view. *Int Immunol* **17**, 1367-1378.

Hornung, V., Ellegast, J., Kim, S., Brzozka, K., Jung, A., Kato, H., Poeck, H., Akira, S., Conzelmann, K. K., Schlee, M., Endres, S. & Hartmann, G. (2006).5'-Triphosphate RNA is the ligand for RIG-I. *Science* **314**, 994-997.

Horvath, C. M., Stark, G. R., Kerr, I. M. & Darnell, J. E., Jr. (1996). Interactions between STAT and non-STAT proteins in the interferon-stimulated gene factor 3 transcription complex. *Mol Cell Biol* **16**, 6957-6964.

Horwood, C. M. & Bi, P. (2005). The incidence of Ross River virus disease in South Australia, 1992 to 2003. *Commun Dis Intell* **29**, 291-296.

Hosokawa, N., Sasaki, T., Iemura, S., Natsume, T., Hara, T. & Mizushima, N. (2009). Atg101, a novel mammalian autophagy protein interacting with Atg13. *Autophagy* **5**, 973-979.

Huang, S., Bucana, C. D., Van, A. M. & Fidler, I. J. (2002). Stat1 negatively regulates angiogenesis, tumorigenicity and metastasis of tumor cells. *Oncogene* **21**, 2504-2512.

Huang, S., Hendriks, W., Althage, A., Hemmi, S., Bluethmann, H., Kamijo, R., Vilcek, J., Zinkernagel, R. M. & Aguet, M. (1993). Immune response in mice that lack the interferon-gamma receptor. *Science* **259**, 1742-1745.

Huber, S., Hoffmann, R., Muskens, F. & Voehringer, D. (2010). Alternatively activated macrophages inhibit T-cell proliferation by Stat6-dependent expression of PD-L2. *Blood* **116**, 3311-3320.

Hwa, V., Nadeau, K., Wit, J. M. & Rosenfeld, R. G. (2011).STAT5b deficiency: lessons from STAT5b gene mutations. *Best Pract Res Clin Endocrinol Metab* **25**, 61-75.

Ichimura, Y., Kirisako, T., Takao, T., Satomi, Y., Shimonishi, Y., Ishihara, N., Mizushima, N., Tanida, I., Kominami, E., Ohsumi, M., Noda, T. & Ohsumi, Y. (2000).A ubiquitin-like system mediates protein lipidation. *Nature* **408**, 488-492.

Imakawa, K., Hansen, T. R., Malathy, P. V., Anthony, R. V., Polites, H. G., Marotti, K. R. & Roberts, R. M. (1989). Molecular cloning and characterization of complementary deoxyribonucleic acids corresponding to bovine trophoblast protein-1: a comparison with ovine trophoblast protein-1 and bovine interferon-alpha II. *Mol Endocrinol* **3**, 127-139.

Imakawa, K. & Roberts, R. M. (1989). Interferons and maternal recognition of pregnancy. *Prog Clin Biol Res* **294**, 347-358.

Improta, T., Schindler, C., Horvath, C. M., Kerr, I. M., Stark, G. R. & Darnell, J. E., Jr. (1994). Transcription factor ISGF-3 formation requires phosphorylated Stat91 protein, but Stat113 protein is phosphorylated independently of Stat91 protein. *Proc Natl Acad Sci U S A* **91**, 4776-4780.

Iordanov, M. S., Ryabinina, O. P., Wong, J., Dinh, T. H., Newton, D. L., Rybak, S. M. & Magun, B. E. (2000). Molecular determinants of apoptosis induced

by the cytotoxic ribonuclease onconase: evidence for cytotoxic mechanisms different from inhibition of protein synthesis. *Cancer Res* **60**, 1983-1994.

Iordanov, M. S., Wong, J., Bell, J. C. & Magun, B. E. (2001). Activation of NF-kappaB by double-stranded RNA (dsRNA) in the absence of protein kinase R and RNase L demonstrates the existence of two separate dsRNA-triggered antiviral programs. *Mol Cell Biol* **21**, 61-72.

Isaacs, A. & Lindenmann, J. (1957). Virus Interference. I. Interferon. *J Interferon Res* **7**, 429-438.

Itakura, E., Kishi, C., Inoue, K. & Mizushima, N. (2008). Beclin 1 forms two distinct phosphatidylinositol 3-kinase complexes with mammalian Atg14 and UVRAG. *Mol Biol Cell* **19**, 5360-5372.

Jackson, D., Killip, M. J., Galloway, C. S., Russell, R. J. & Randall, R. E. (2010). Loss of function of the influenza A virus NS1 protein promotes apoptosis but this is not due to a failure to activate phosphatidylinositol 3-kinase (PI3K). *Virology* **396**, 94-105.

Jackson, W. T., Giddings, T. H., Jr., Taylor, M. P., Mulinyawe, S., Rabinovitch, M., Kopito, R. R. & Kirkegaard, K. (2005). Subversion of cellular autophagosomal machinery by RNA viruses. *PLoS Biol* **3**, e156.

Jagannath, C., Lindsey, D. R., Dhandayuthapani, S., Xu, Y., Hunter, R. L., Jr. & Eissa, N. T. (2009). Autophagy enhances the efficacy of BCG vaccine by increasing peptide presentation in mouse dendritic cells. *Nat Med* **15**, 267-276.

Jewell, N. A., Cline, T., Mertz, S. E., Smirnov, S. V., Flano, E., Schindler, C., Grieves, J. L., Durbin, R. K., Kotenko, S. V. & Durbin, J. E. (2010). Lambda interferon is the predominant interferon induced by influenza A virus infection in vivo. *J Virol* **84**, 11515-11522.

Jiang, Z., Mak, T. W., Sen, G. & Li, X. (2004). Toll-like receptor 3-mediated activation of NF-kappaB and IRF3 diverges at Toll-IL-1 receptor domain-containing adapter inducing IFN-beta. *Proc Natl Acad Sci U S A* **101**, 3533-3538.

Johnston, L. J., Halliday, G. M. & King, N. J. (1996). Phenotypic changes in Langerhans' cells after infection with arboviruses: a role in the immune response to epidermally acquired viral infection? *J Virol* **70**, 4761-4766.

Johnston, L. J., Halliday, G. M. & King, N. J. (2000). Langerhans cells migrate to local lymph nodes following cutaneous infection with an arbovirus. *J Invest Dermatol* **114**, 560-568.

Jounai, N., Takeshita, F., Kobiyama, K., Sawano, A., Miyawaki, A., Xin, K. Q., Ishii, K. J., Kawai, T., Akira, S., Suzuki, K. & Okuda, K. (2007). The Atg5 Atg12 conjugate associates with innate antiviral immune responses. *Proc Natl Acad Sci U S A* **104**, 14050-14055.

Jung, C. H., Jun, C. B., Ro, S. H., Kim, Y. M., Otto, N. M., Cao, J., Kundu, M. & Kim, D. H. (2009).ULK-Atg13-FIP200 complexes mediate mTOR signaling to the autophagy machinery. *Mol Biol Cell* **20**, 1992-2003.

Justesen, J., Hartmann, R. & Kjeldgaard, N. O. (2000). Gene structure and function of the 2'-5'-oligoadenylate synthetase family. *Cell Mol Life Sci* **57**, 1593-1612.

Kaariainen, L., Takkinen, K., Keranen, S. & Soderlund, H. (1987). Replication of the genome of alphaviruses. *J Cell Sci Suppl* **7**, 231-250.

Kabeya, Y., Mizushima, N., Ueno, T., Yamamoto, A., Kirisako, T., Noda, T., Kominami, E., Ohsumi, Y. & Yoshimori, T. (2000).LC3, a mammalian homologue of yeast Apg8p, is localized in autophagosome membranes after processing. *EMBO J* **19**, 5720-5728.

Kamer, G. & Argos, P. (1984). Primary structural comparison of RNA-dependent polymerases from plant, animal and bacterial viruses. *Nucleic Acids Res* **12**, 7269-7282.

Kaplan, M. H., Sun, Y. L., Hoey, T. & Grusby, M. J. (1996). Impaired IL-12 responses and enhanced development of Th2 cells in Stat4-deficient mice. *Nature* **382**, 174-177.

Karin, M. & Ben-Neriah, Y. (2000). Phosphorylation meets ubiquitination: the control of NF-[kappa]B activity. *Annu Rev Immunol* **18**, 621-663.

Kato, H., Takeuchi, O., Sato, S., Yoneyama, M., Yamamoto, M., Matsui, K., Uematsu, S., Jung, A., Kawai, T., Ishii, K. J., Yamaguchi, O., Otsu, K., Tsujimura, T., Koh, C. S., Reis e Sousa, Matsuura, Y., Fujita, T. & Akira, S. (2006). Differential roles of MDA5 and RIG-I helicases in the recognition of RNA viruses. *Nature* **441**, 101-105.

Kawai, T., Takahashi, K., Sato, S., Coban, C., Kumar, H., Kato, H., Ishii, K. J., Takeuchi, O. & Akira, S. (2005).IPS-1, an adaptor triggering RIG-I- and Mda5-mediated type I interferon induction. *Nat Immunol* **6**, 981-988.

Kawamoto, S., Oritani, K., Asada, H., Takahashi, I., Ishikawa, J., Yoshida, H., Yamada, M., Ishida, N., Ujiie, H., Masaie, H., Tomiyama, Y. & Matsuzawa, Y. (2003). Antiviral activity of limitin against encephalomyocarditis virus, herpes simplex virus, and mouse hepatitis virus: diverse requirements by limitin and alpha interferon for interferon regulatory factor 1. *J Virol* **77**, 9622-9631.

Kedersha, N. L., Gupta, M., Li, W., Miller, I. & Anderson, P. (1999).RNA-binding proteins TIA-1 and TIAR link the phosphorylation of eIF-2 alpha to the assembly of mammalian stress granules. *J Cell Biol* **147**, 1431-1442.

Keranen, S. & Kaariainen, L. (1979). Functional defects of RNA-negative temperature-sensitive mutants of Sindbis and Semliki Forest viruses. *J Virol* **32**, 19-29.

Kerr, I. M. & Brown, R. E. (1978).pppA2'p5'A2'p5'A: an inhibitor of protein synthesis synthesized with an enzyme fraction from interferon-treated cells. *Proc Natl Acad Sci U S A* **75**, 256-260.

Kessler, D. S., Veals, S. A., Fu, X. Y. & Levy, D. E. (1990). Interferon-alpha regulates nuclear translocation and DNA-binding affinity of ISGF3, a multimeric transcriptional activator. *Genes Dev* **4**, 1753-1765.

Khalili-Shirazi, A., Gregson, N. & Webb, H. E. (1988). Immunocytochemical evidence for Semliki Forest virus antigen persistence in mouse brain. *J Neurol Sci* **85**, 17-26.

Kim, K. H., Rumenapf, T., Strauss, E. G. & Strauss, J. H. (2004). Regulation of Semliki Forest virus RNA replication: a model for the control of alphavirus pathogenesis in invertebrate hosts. *Virology* **323**, 153-163.

Kimura, S., Noda, T. & Yoshimori, T. (2007). Dissection of the autophagosome maturation process by a novel reporter protein, tandem fluorescent-tagged LC3. *Autophagy* **3**, 452-460.

Kirchhoff, S., Wilhelm, D., Angel, P. & Hauser, H. (1999).NFkappaB activation is required for interferon regulatory factor-1-mediated interferon beta induction. *Eur J Biochem* **261**, 546-554.

Kirchweger, R., Ziegler, E., Lamphear, B. J., Waters, D., Liebig, H. D., Sommergruber, W., Sobrino, F., Hohenadl, C., Blaas, D., Rhoads, R. E. & . (1994). Foot-and-mouth disease virus leader proteinase: purification of the Lb form and determination of its cleavage site on eIF-4 gamma. *J Virol* **68**, 5677-5684.

Kirkin, V., Lamark, T., Sou, Y. S., Bjorkoy, G., Nunn, J. L., Bruun, J. A., Shvets, E., McEwan, D. G., Clausen, T. H., Wild, P., Bilusic, I., Theurillat, J. P., Overvatn, A., Ishii, T., Elazar, Z., Komatsu, M., Dikic, I. & Johansen, T. (2009).A role for NBR1 in autophagosomal degradation of ubiquitinated substrates. *Mol Cell* **33**, 505-516.

Klimstra, W. B., Ryman, K. D., Bernard, K. A., Nguyen, K. B., Biron, C. A. & Johnston, R. E. (1999). Infection of neonatal mice with sindbis virus results in a systemic inflammatory response syndrome. *J Virol* **73**, 10387-10398.

Komatsu, M., Waguri, S., Ueno, T., Iwata, J., Murata, S., Tanida, I., Ezaki, J., Mizushima, N., Ohsumi, Y., Uchiyama, Y., Kominami, E., Tanaka, K. & Chiba, T. (2005). Impairment of starvation-induced and constitutive autophagy in Atg7-deficient mice. *J Cell Biol* **169**, 425-434.

Koonin, E. V. & Dolja, V. V. (1993). Evolution and taxonomy of positive-strand RNA viruses: implications of comparative analysis of amino acid sequences. *Crit Rev Biochem Mol Biol* **28**, 375-430.

Kotenko, S. V., Gallagher, G., Baurin, V. V., Lewis-Antes, A., Shen, M., Shah, N. K., Langer, J. A., Sheikh, F., Dickensheets, H. & Donnelly, R. P. (2003).IFN-lambdas mediate antiviral protection through a distinct class II cytokine receptor complex. *Nat Immunol* **4**, 69-77.

Kourtis, N. & Tavernarakis, N. (2009). Autophagy and cell death in model organisms. *Cell Death Differ* **16**, 21-30.

Krause, C. D. & Pestka, S. (2005). Evolution of the Class 2 cytokines and receptors, and discovery of new friends and relatives. *Pharmacol Ther* **106**, 299-346.

Krejbich-Trotot, P., Gay, B., Li-Pat-Yuen, G., Hoarau, J. J., Jaffar-Bandjee, M. C., Briant, L., Gasque, P. & Denizot, M. (2011). Chikungunya triggers an autophagic process which promotes viral replication. *Virol J* **8**, 432.

Krug, A., French, A. R., Barchet, W., Fischer, J. A., Dzionek, A., Pingel, J. T., Orihuela, M. M., Akira, S., Yokoyama, W. M. & Colonna, M. (2004).TLR9-dependent recognition of MCMV by IPC and DC generates coordinated cytokine responses that activate antiviral NK cell function. *Immunity* **21**, 107-119.

Krug, A., Uppaluri, R., Facchetti, F., Dorner, B. G., Sheehan, K. C., Schreiber, R. D., Cella, M. & Colonna, M. (2002).IFN-producing cells respond to CXCR3 ligands in the presence of CXCL12 and secrete inflammatory chemokines upon activation. *J Immunol* **169**, 6079-6083.

Ku, B., Woo, J. S., Liang, C., Lee, K. H., Hong, H. S., E X, Kim, K. S., Jung, J. U. & Oh, B. H. (2008). Structural and biochemical bases for the inhibition of autophagy and apoptosis by viral BCL-2 of murine gamma-herpesvirus 68. *PLoS Pathog* **4**, e25.

Kuhen, K. L. & Samuel, C. E. (1997). Isolation of the interferon-inducible RNA-dependent protein kinase Pkr promoter and identification of a novel DNA element within the 5'-flanking region of human and mouse Pkr genes. *Virology* **227**, 119-130.

Kuhn, R. J., Griffin, D. E., Zhang, H., Niesters, H. G. & Strauss, J. H. (1992). Attenuation of Sindbis virus neurovirulence by using defined mutations in nontranslated regions of the genome RNA. *J Virol* **66**, 7121-7127.

Kujala, P., Ikaheimonen, A., Ehsani, N., Vihinen, H., Auvinen, P. & Kaariainen, L. (2001). Biogenesis of the Semliki Forest virus RNA replication complex. *J Virol* **75**, 3873-3884.

Kumar, A., Haque, J., Lacoste, J., Hiscott, J. & Williams, B. R. (1994). Double-stranded RNA-dependent protein kinase activates transcription factor NF-kappa B by phosphorylating I kappa B. *Proc Natl Acad Sci U S A* **91**, 6288-6292.

Kumar, K. P., McBride, K. M., Weaver, B. K., Dingwall, C. & Reich, N. C. (2000). Regulated nuclear-cytoplasmic localization of interferon regulatory factor 3, a subunit of double-stranded RNA-activated factor 1. *Mol Cell Biol* **20**, 4159-4168.

Kuperman, D., Schofield, B., Wills-Karp, M. & Grusby, M. J. (1998). Signal transducer and activator of transcription factor 6 (Stat6)-deficient mice are protected from antigen-induced airway hyperresponsiveness and mucus production. *J Exp Med* **187**, 939-948.

Kurt-Jones, E. A., Popova, L., Kwinn, L., Haynes, L. M., Jones, L. P., Tripp, R. A., Walsh, E. E., Freeman, M. W., Golenbock, D. T., Anderson, L. J. & Finberg, R. W. (2000). Pattern recognition receptors TLR4 and CD14 mediate response to respiratory syncytial virus. *Nat Immunol* **1**, 398-401.

Kyei, G. B., Dinkins, C., Davis, A. S., Roberts, E., Singh, S. B., Dong, C., Wu, L., Kominami, E., Ueno, T., Yamamoto, A., Federico, M., Panganiban, A., Vergne, I. & Deretic, V. (2009). Autophagy pathway intersects with HIV-1 biosynthesis and regulates viral yields in macrophages. *J Cell Biol* **186**, 255-268.

La, B. C., Martinat-Botte, F., Terqui, M., Lefevre, F., Zouari, K., Martal, J. & Bazer, F. W. (1991). Production of two species of interferon by Large White and Meishan pig conceptuses during the peri-attachment period. *J Reprod Fertil* **91**, 469-478.

Laakkonen, P., Ahola, T. & Kaariainen, L. (1996). The effects of palmitoylation on membrane association of Semliki forest virus RNA capping enzyme. *J Biol Chem* **271**, 28567-28571.

LaFleur, D. W., Nardelli, B., Tsareva, T., Mather, D., Feng, P., Semenuk, M., Taylor, K., Buergin, M., Chinchilla, D., Roshke, V., Chen, G., Ruben, S. M., Pitha, P. M., Coleman, T. A. & Moore, P. A. (2001). Interferon-kappa, a novel type I interferon expressed in human keratinocytes. *J Biol Chem* **276**, 39765-39771.

Lasfar, A., Lewis-Antes, A., Smirnov, S. V., Anantha, S., Abushahba, W., Tian, B., Reuhl, K., Dickensheets, H., Sheikh, F., Donnelly, R. P., Raveche, E. & Kotenko, S. V. (2006). Characterization of the mouse IFN-lambda ligand-receptor system: IFN-lambdas exhibit antitumor activity against B16 melanoma. *Cancer Res* **66**, 4468-4477.

LaStarza, M. W., Grakoui, A. & Rice, C. M. (1994a). Deletion and duplication mutations in the C-terminal nonconserved region of Sindbis virus nsP3: effects on phosphorylation and on virus replication in vertebrate and invertebrate cells. *Virology* **202**, 224-232.

LaStarza, M. W., Lemm, J. A. & Rice, C. M. (1994b). Genetic analysis of the nsP3 region of Sindbis virus: evidence for roles in minus-strand and subgenomic RNA synthesis. *J Virol* **68**, 5781-5791.

Lawrence, B. P. & Brown, W. J. (1992). Autophagic vacuoles rapidly fuse with pre-existing lysosomes in cultured hepatocytes. *J Cell Sci* **102 (Pt 3)**, 515-526.

Le, B. A. & Tough, D. F. (2002). Links between innate and adaptive immunity via type I interferon. *Curr Opin Immunol* **14**, 432-436.

Le, M. N., Dubaele, S., Proietti De, S. L., Billecocq, A., Bouloy, M. & Egly, J. M. (2004).TFIIH transcription factor, a target for the Rift Valley hemorrhagic fever virus. *Cell* **116**, 541-550.

Lee, H. K., Lund, J. M., Ramanathan, B., Mizushima, N. & Iwasaki, A. (2007). Autophagy-dependent viral recognition by plasmacytoid dendritic cells. *Science* **315**, 1398-1401.

Lee, H. K., Myers, R. A. & Marzella, L. (1989). Stimulation of autophagic protein degradation by nutrient deprivation in a differentiated murine teratocarcinoma (F9 12-1a) cell line. *Exp Mol Pathol* **50**, 139-146.

Lee, S. B. & Esteban, M. (1994). The interferon-induced double-stranded RNA-activated protein kinase induces apoptosis. *Virology* **199**, 491-496.

Lee, Y. R., Lei, H. Y., Liu, M. T., Wang, J. R., Chen, S. H., Jiang-Shieh, Y. F., Lin, Y. S., Yeh, T. M., Liu, C. C. & Liu, H. S. (2008). Autophagic machinery activated by dengue virus enhances virus replication. *Virology* **374**, 240-248.

Lefevre, F., Guillomot, M., D'Andrea, S., Battegay, S. & La, B. C. (1998). Interferon-delta: the first member of a novel type I interferon family. *Biochimie* **80**, 779-788.

Leib, D. A., Alexander, D. E., Cox, D., Yin, J. & Ferguson, T. A. (2009). Interaction of ICP34.5 with Beclin 1 modulates herpes simplex virus type 1 pathogenesis through control of CD4+ T-cell responses. *J Virol* **83**, 12164-12171.

Lemm, J. A. & Rice, C. M. (1993). Roles of nonstructural polyproteins and cleavage products in regulating Sindbis virus RNA replication and transcription. *J Virol* **67**, 1916-1926.

Lemm, J. A., Rumenapf, T., Strauss, E. G., Strauss, J. H. & Rice, C. M. (1994). Polypeptide requirements for assembly of functional Sindbis virus replication complexes: a model for the temporal regulation of minus- and plus-strand RNA synthesis. *EMBO J* **13**, 2925-2934.

Lenardo, M. J. & Baltimore, D. (1989).NF-kappa B: a pleiotropic mediator of inducible and tissue-specific gene control. *Cell* **58**, 227-229.

Lennert, K. & Remmele, W. (1958).[Karyometric research on lymph node cells in man. I. Germinoblasts, lymphoblasts & lymphocytes]. *Acta Haematol* **19**, 99-113.

Leung, S., Qureshi, S. A., Kerr, I. M., Darnell, J. E., Jr. & Stark, G. R. (1995). Role of STAT2 in the alpha interferon signaling pathway. *Mol Cell Biol* **15**, 1312-1317.

Li, C., Ni, C. Z., Havert, M. L., Cabezas, E., He, J., Kaiser, D., Reed, J. C., Satterthwait, A. C., Cheng, G. & Ely, K. R. (2002). Downstream regulator TANK binds to the CD40 recognition site on TRAF3. *Structure* **10**, 403-411.

Li, H., Kobayashi, M., Blonska, M., You, Y. & Lin, X. (2006). Ubiquitination of RIP is required for tumor necrosis factor alpha-induced NF-kappaB activation. *J Biol Chem* **281**, 13636-13643.

Li, J. K., Liang, J. J., Liao, C. L. & Lin, Y. L. (2012a). Autophagy is involved in the early step of Japanese encephalitis virus infection. *Microbes Infect* **14**, 159-168.

Li, W., Ross-Smith, N., Proud, C. G. & Belsham, G. J. (2001). Cleavage of translation initiation factor 4AI (eIF4AI) but not eIF4AII by foot-and-mouth disease virus 3C protease: identification of the eIF4AI cleavage site. *FEBS Lett* **507**, 1-5.

Li, W. W., Li, J. & Bao, J. K. (2012b). Microautophagy: lesser-known self-eating. *Cell Mol Life Sci* **69**, 1125-1136.

Li, X., Leung, S., Qureshi, S., Darnell, J. E., Jr. & Stark, G. R. (1996). Formation of STAT1-STAT2 heterodimers and their role in the activation of IRF-1 gene transcription by interferon-alpha. *J Biol Chem* **271**, 5790-5794.

Li, X. D., Sun, L., Seth, R. B., Pineda, G. & Chen, Z. J. (2005). Hepatitis C virus protease NS3/4A cleaves mitochondrial antiviral signaling protein off the mitochondria to evade innate immunity. *Proc Natl Acad Sci U S A* **102**, 17717-17722.

Liang, C., Feng, P., Ku, B., Oh, B. H. & Jung, J. U. (2007).UVRAG: a new player in autophagy and tumor cell growth. *Autophagy* **3**, 69-71.

Liang, X. H., Jackson, S., Seaman, M., Brown, K., Kempkes, B., Hibshoosh, H. & Levine, B. (1999). Induction of autophagy and inhibition of tumorigenesis by beclin 1. *Nature* **402**, 672-676.

Liang, X. H., Kleeman, L. K., Jiang, H. H., Gordon, G., Goldman, J. E., Berry, G., Herman, B. & Levine, B. (1998). Protection against fatal Sindbis virus encephalitis by beclin, a novel Bcl-2-interacting protein. *J Virol* **72**, 8586-8596.

Liljestrom, P. & Garoff, H. (1991).A new generation of animal cell expression vectors based on the Semliki Forest virus replicon. *Biotechnology (N Y)* **9**, 1356-1361.

Liljestrom, P., Lusa, S., Huylebroeck, D. & Garoff, H. (1991). In vitro mutagenesis of a full-length cDNA clone of Semliki Forest virus: the small 6,000-molecular-weight membrane protein modulates virus release. *J Virol* **65**, 4107-4113.

Lin, R., Heylbroeck, C., Pitha, P. M. & Hiscott, J. (1998). Virus-dependent phosphorylation of the IRF-3 transcription factor regulates nuclear translocation, transactivation potential, and proteasome-mediated degradation. *Mol Cell Biol* **18**, 2986-2996.

Lin, R. J., Liao, C. L., Lin, E. & Lin, Y. L. (2004). Blocking of the alpha interferon-induced Jak-Stat signaling pathway by Japanese encephalitis virus infection. *J Virol* **78**, 9285-9294.

Lin, W., Kim, S. S., Yeung, E., Kamegaya, Y., Blackard, J. T., Kim, K. A., Holtzman, M. J. & Chung, R. T. (2006). Hepatitis C virus core protein blocks interferon signaling by interaction with the STAT1 SH2 domain. *J Virol* **80**, 9226-9235.

Lindquist, S. & Craig, E. A. (1988). The heat-shock proteins. *Annu Rev Genet* **22**, 631-677.

Lipinski, M. M., Zheng, B., Lu, T., Yan, Z., Py, B. F., Ng, A., Xavier, R. J., Li, C., Yankner, B. A., Scherzer, C. R. & Yuan, J. (2010). Genome-wide analysis reveals mechanisms modulating autophagy in normal brain aging and in Alzheimer's disease. *Proc Natl Acad Sci U S A* **107**, 14164-14169.

Liu, B., Gross, M., ten, H. J. & Shuai, K. (2001).A transcriptional corepressor of Stat1 with an essential LXXLL signature motif. *Proc Natl Acad Sci U S A* **98**, 3203-3207.

Liu, B., Liao, J., Rao, X., Kushner, S. A., Chung, C. D., Chang, D. D. & Shuai, K. (1998). Inhibition of Stat1-mediated gene activation by PIAS1. *Proc Natl Acad Sci U S A* **95**, 10626-10631.

Liu, X., Robinson, G. W., Wagner, K. U., Garrett, L., Wynshaw-Boris, A. & Hennighausen, L. (1997). Stat5a is mandatory for adult mammary gland development and lactogenesis. *Genes Dev* **11**, 179-186.

Liu, Y., Schiff, M., Czymmek, K., Talloczy, Z., Levine, B. & Dinesh-Kumar, S. P. (2005). Autophagy regulates programmed cell death during the plant innate immune response. *Cell* **121**, 567-577.

Logue, C. H., Sheahan, B. J. & Atkins, G. J. (2008). The 5' untranslated region as a pathogenicity determinant of Semliki Forest virus in mice. *Virus Genes* **36**, 313-321.

Loo, Y. M., Fornek, J., Crochet, N., Bajwa, G., Perwitasari, O., Martinez-Sobrido, L., Akira, S., Gill, M. A., Garcia-Sastre, A., Katze, M. G. &

Gale, M., Jr. (2008). Distinct RIG-I and MDA5 signaling by RNA viruses in innate immunity. *J Virol* **82**, 335-345.

Loo, Y. M. & Gale, M., Jr. (2011). Immune signaling by RIG-I-like receptors. *Immunity* **34**, 680-692.

Lopez, S., Yao, J. S., Kuhn, R. J., Strauss, E. G. & Strauss, J. H. (1994). Nucleocapsid-glycoprotein interactions required for assembly of alphaviruses. *J Virol* **68**, 1316-1323.

Lu, Y., Wambach, M., Katze, M. G. & Krug, R. M. (1995). Binding of the influenza virus NS1 protein to double-stranded RNA inhibits the activation of the protein kinase that phosphorylates the elF-2 translation initiation factor. *Virology* **214**, 222-228.

Lulla, A., Lulla, V. & Merits, A. (2012). Macromolecular assembly-driven processing of the 2/3 cleavage site in the alphavirus replicase polyprotein. *J Virol* **86**, 553-565.

Lund, J. M., Alexopoulou, L., Sato, A., Karow, M., Adams, N. C., Gale, N. W., Iwasaki, A. & Flavell, R. A. (2004). Recognition of single-stranded RNA viruses by Toll-like receptor 7. *Proc Natl Acad Sci U S A* **101**, 5598-5603.

Lundstrom, K., Ziltener, P., Hermann, D., Schweitzer, C., Richards, J. G. & Jenck, F. (2001). Improved Semliki Forest virus vectors for receptor research and gene therapy. *J Recept Signal Transduct Res* **21**, 55-70.

MacDonald, G. H. & Johnston, R. E. (2000). Role of dendritic cell targeting in Venezuelan equine encephalitis virus pathogenesis. *J Virol* **74**, 914-922.

Mach, B., Steimle, V., Martinez-Soria, E. & Reith, W. (1996). Regulation of MHC class II genes: lessons from a disease. *Annu Rev Immunol* **14**, 301-331.

Maher, S. G., Sheikh, F., Scarzello, A. J., Romero-Weaver, A. L., Baker, D. P., Donnelly, R. P. & Gamero, A. M. (2008).IFNalpha and IFNlambda differ in their antiproliferative effects and duration of JAK/STAT signaling activity. *Cancer Biol Ther* **7**, 1109-1115.

Malet, H., Coutard, B., Jamal, S., Dutartre, H., Papageorgiou, N., Neuvonen, M., Ahola, T., Forrester, N., Gould, E. A., Lafitte, D., Ferron, F., Lescar, J., Gorbalenya, A. E., de, L., X & Canard, B. (2009). The crystal structures of Chikungunya and Venezuelan equine encephalitis virus nsP3 macro domains define a conserved adenosine binding pocket. *J Virol* **83**, 6534-6545.

Mallilankaraman, K., Shedlock, D. J., Bao, H., Kawalekar, O. U., Fagone, P., Ramanathan, A. A., Ferraro, B., Stabenow, J., Vijayachari, P., Sundaram, S. G., Muruganandam, N., Sarangan, G., Srikanth, P., Khan, A. S., Lewis, M. G., Kim, J. J., Sardesai, N. Y., Muthumani, K. & Weiner, D. B. (2011).A DNA vaccine against chikungunya virus is protective in mice and induces neutralizing antibodies in mice and nonhuman primates. *PLoS Negl Trop Dis* **5**, e928.

Maniatis, T., Falvo, J. V., Kim, T. H., Kim, T. K., Lin, C. H., Parekh, B. S. & Wathelet, M. G. (1998). Structure and function of the interferon-beta enhanceosome. *Cold Spring Harb Symp Quant Biol* **63**, 609-620.

Marcello, T., Grakoui, A., Barba-Spaeth, G., Machlin, E. S., Kotenko, S. V., MacDonald, M. R. & Rice, C. M. (2006). Interferons alpha and lambda inhibit hepatitis C virus replication with distinct signal transduction and gene regulation kinetics. *Gastroenterology* **131**, 1887-1898.

Marie, I., Durbin, J. E. & Levy, D. E. (1998). Differential viral induction of distinct interferon-alpha genes by positive feedback through interferon regulatory factor-7. *EMBO J* **17**, 6660-6669.

Marsh, M., Bolzau, E., White, J. & Helenius, A. (1983). Interactions of Semliki Forest virus spike glycoprotein rosettes and vesicles with cultured-cells. *J Cell Biol* **96**, 455-461.

Martal, J. L., Chene, N. M., Huynh, L. P., L'Haridon, R. M., Reinaud, P. B., Guillomot, M. W., Charlier, M. A. & Charpigny, S. Y. (1998).IFN-tau: a novel subtype I IFN1. Structural characteristics, non-ubiquitous expression, structure-function relationships, a pregnancy hormonal embryonic signal and cross-species therapeutic potentialities. *Biochimie* **80**, 755-777.

Martinand, C., Montavon, C., Salehzada, T., Silhol, M., Lebleu, B. & Bisbal, C. (1999).RNase L inhibitor is induced during human immunodeficiency virus type 1 infection and down regulates the 2-5A/RNase L pathway in human T cells. *J Virol* **73**, 290-296.

Martinand, C., Salehzada, T., Silhol, M., Lebleu, B. & Bisbal, C. (1998).RNase L inhibitor (RLI) antisense constructions block partially the down regulation of the 2-5A/RNase L pathway in encephalomyocarditis-virus-(EMCV)-infected cells. *Eur J Biochem* **254**, 248-255.

Mathiot, C. C., Grimaud, G., Garry, P., Bouquety, J. C., Mada, A., Daguisy, A. M. & Georges, A. J. (1990). An outbreak of human Semliki Forest virus infections in Central African Republic. *Am J Trop Med Hyg* **42**, 386-393.

Matsunaga, K., Saitoh, T., Tabata, K., Omori, H., Satoh, T., Kurotori, N., Maejima, I., Shirahama-Noda, K., Ichimura, T., Isobe, T., Akira, S., Noda, T. & Yoshimori, T. (2009). Two Beclin 1-binding proteins, Atg14L and Rubicon, reciprocally regulate autophagy at different stages. *Nat Cell Biol* **11**, 385-396.

Matsuura, A., Tsukada, M., Wada, Y. & Ohsumi, Y. (1997). Apg1p, a novel protein kinase required for the autophagic process in Saccharomyces cerevisiae. *Gene* **192**, 245-250.

McInerney, G. M., Smit, J. M., Liljestrom, P. & Wilschut, J. (2004). Semliki Forest virus produced in the absence of the 6K protein has an altered spike structure as revealed by decreased membrane fusion capacity. *Virology* **325**, 200-206.

McIntosh, B. M., Worth, C. B. & kokernot, R. H. (1961). Isolation of Semliki Forest virus from Aedes (Aedimorphus) argenteopunctatus (Theobald) collected in Portuguese East Africa. *Trans R Soc Trop Med Hyg* **55**, 192-198.

McMillan, N. A., Chun, R. F., Siderovski, D. P., Galabru, J., Toone, W. M., Samuel, C. E., Mak, T. W., Hovanessian, A. G., Jeang, K. T. & Williams, B. R. (1995).HIV-1 Tat directly interacts with the interferon-induced, double-stranded RNA-dependent kinase, PKR. *Virology* **213**, 413-424.

Melancon, P. & Garoff, H. (1986). Reinitiation of translocation in the Semliki Forest virus structural polyprotein: identification of the signal for the E1 glycoprotein. *EMBO J* **5**, 1551-1560.

Meraz, M. A., White, J. M., Sheehan, K. C., Bach, E. A., Rodig, S. J., Dighe, A. S., Kaplan, D. H., Riley, J. K., Greenlund, A. C., Campbell, D., Carver-Moore, K., DuBois, R. N., Clark, R., Aguet, M. & Schreiber, R. D. (1996). Targeted disruption of the Stat1 gene in mice reveals unexpected physiologic specificity in the JAK-STAT signaling pathway. *Cell* **84**, 431-442.

Merits, A., Vasiljeva, L., Ahola, T., Kaariainen, L. & Auvinen, P. (2001). Proteolytic processing of Semliki Forest virus-specific non-structural polyprotein by nsP2 protease. *J Gen Virol* **82**, 765-773.

Meurs, E. F., Watanabe, Y., Kadereit, S., Barber, G. N., Katze, M. G., Chong, K., Williams, B. R. & Hovanessian, A. G. (1992). Constitutive expression of human double-stranded RNA-activated p68 kinase in murine cells mediates phosphorylation of eukaryotic initiation factor 2 and partial resistance to encephalomyocarditis virus growth. *J Virol* **66**, 5805-5814.

Meylan, E., Burns, K., Hofmann, K., Blancheteau, V., Martinon, F., Kelliher, M. & Tschopp, J. (2004).RIP1 is an essential mediator of Toll-like receptor 3-induced NF-kappa B activation. *Nat Immunol* **5**, 503-507.

Meylan, E., Curran, J., Hofmann, K., Moradpour, D., Binder, M., Bartenschlager, R. & Tschopp, J. (2005). Cardif is an adaptor protein in the RIG-I antiviral pathway and is targeted by hepatitis C virus. *Nature* **437**, 1167-1172.

Mibayashi, M., Martinez-Sobrido, L., Loo, Y. M., Cardenas, W. B., Gale, M., Jr. & Garcia-Sastre, A. (2007). Inhibition of retinoic acid-inducible gene I-mediated induction of beta interferon by the NS1 protein of influenza A virus. *J Virol* **81**, 514-524.

Miller, B. C., Zhao, Z., Stephenson, L. M., Cadwell, K., Pua, H. H., Lee, H. K., Mizushima, N. N., Iwasaki, A., He, Y. W., Swat, W. & Virgin, H. W. (2008). The autophagy gene ATG5 plays an essential role in B lymphocyte development. *Autophagy* **4**, 309-314.

Mizushima, N. (2004). Methods for monitoring autophagy. *Int J Biochem Cell Biol* **36**, 2491-2502.

Mizushima, N. & Levine, B. (2010). Autophagy in mammalian development and differentiation. *Nat Cell Biol* **12**, 823-830.

Mizushima, N., Noda, T., Yoshimori, T., Tanaka, Y., Ishii, T., George, M. D., Klionsky, D. J., Ohsumi, M. & Ohsumi, Y. (1998a).A protein conjugation system essential for autophagy. *Nature* **395**, 395-398.

Mizushima, N., Sugita, H., Yoshimori, T. & Ohsumi, Y. (1998b).A new protein conjugation system in human. The counterpart of the yeast Apg12p conjugation system essential for autophagy. *J Biol Chem* **273**, 33889-33892.

Mizushima, N., Yamamoto, A., Hatano, M., Kobayashi, Y., Kabeya, Y., Suzuki, K., Tokuhisa, T., Ohsumi, Y. & Yoshimori, T. (2001). Dissection of autophagosome formation using Apg5-deficient mouse embryonic stem cells. *J Cell Biol* **152**, 657-668.

Mizushima, N., Yoshimori, T. & Levine, B. (2010). Methods in mammalian autophagy research. *Cell* **140**, 313-326.

Moran, T. P., Collier, M., McKinnon, K. P., Davis, N. L., Johnston, R. E. & Serody, J. S. (2005).A novel viral system for generating antigen-specific T cells. *J Immunol* **175**, 3431-3438.

Mortimore, G. E., Lardeux, B. R. & Adams, C. E. (1988). Regulation of microautophagy and basal protein turnover in rat liver. Effects of short-term starvation. *J Biol Chem* **263**, 2506-2512.

Moynagh, P. N. (2005).TLR signalling and activation of IRFs: revisiting old friends from the NF-kappaB pathway. *Trends Immunol* **26**, 469-476.

Muller, M., Briscoe, J., Laxton, C., Guschin, D., Ziemiecki, A., Silvennoinen, O., Harpur, A. G., Barbieri, G., Witthuhn, B. A., Schindler, C. & . (1993). The protein tyrosine kinase JAK1 complements defects in interferon-alpha/beta and -gamma signal transduction. *Nature* **366**, 129-135.

Muller, U., Steinhoff, U., Reis, L. F., Hemmi, S., Pavlovic, J., Zinkernagel, R. M. & Aguet, M. (1994). Functional role of type I and type II interferons in antiviral defense. *Science* **264**, 1918-1921.

Muller-Hermelink, H. K., Stein, H., Steinmann, G. & Lennert, K. (1983). Malignant lymphoma of plasmacytoid T-cells. Morphologic and immunologic studies characterizing a special type of T-cell. *Am J Surg Pathol* **7**, 849-862.

Munder, M., Mallo, M., Eichmann, K. & Modolell, M. (2001). Direct stimulation of macrophages by IL-12 and IL-18 - a bridge built on solid ground. *Immunol Lett* **75**, 159-160.

Mundschau, L. J. & Faller, D. V. (1995). Platelet-derived growth factor signal transduction through the interferon-inducible kinase PKR. Immediate early gene induction. *J Biol Chem* **270**, 3100-3106.

Munoz-Jordan, J. L., Sanchez-Burgos, G. G., Laurent-Rolle, M. & Garcia-Sastre, A. (2003). Inhibition of interferon signaling by dengue virus. *Proc Natl Acad Sci U S A* **100**, 14333-14338.

Mutyambizi, K., Berger, C. L. & Edelson, R. L. (2009). The balance between immunity and tolerance: the role of Langerhans cells. *Cell Mol Life Sci* **66**, 831-840.

Nagata, S., Mantei, N. & Weissmann, C. (1980). The structure of one of the eight or more distinct chromosomal genes for human interferon-alpha. *Nature* **287**, 401-408.

Najjar, I. & Fagard, R. (2010).STAT1 and pathogens, not a friendly relationship. *Biochimie* **92**, 425-444.

Naka, T., Narazaki, M., Hirata, M., Matsumoto, T., Minamoto, S., Aono, A., Nishimoto, N., Kajita, T., Taga, T., Yoshizaki, K., Akira, S. & Kishimoto, T. (1997). Structure and function of a new STAT-induced STAT inhibitor. *Nature* **387**, 924-929.

Nakagawa, I., Amano, A., Mizushima, N., Yamamoto, A., Yamaguchi, H., Kamimoto, T., Nara, A., Funao, J., Nakata, M., Tsuda, K., Hamada, S. & Yoshimori, T. (2004). Autophagy defends cells against invading group A Streptococcus. *Science* **306**, 1037-1040.

Nakano, H., Yanagita, M. & Gunn, M. D. (2001).CD11c(+)B220(+)Gr-1(+) cells in mouse lymph nodes and spleen display characteristics of plasmacytoid dendritic cells. *J Exp Med* **194**, 1171-1178.

Naylor, S. L., Sakaguchi, A. Y., Shows, T. B., Law, M. L., Goeddel, D. V. & Gray, P. W. (1983). Human immune interferon gene is located on chromosome 12. *J Exp Med* **157**, 1020-1027.

Nedjic, J., Aichinger, M., Emmerich, J., Mizushima, N. & Klein, L. (2008). Autophagy in thymic epithelium shapes the T-cell repertoire and is essential for tolerance. *Nature* **455**, 396-400.

Neuvonen, M. & Ahola, T. (2009). Differential activities of cellular and viral macro domain proteins in binding of ADP-ribose metabolites. *J Mol Biol* **385**, 212-225.

Neuvonen, M., Kazlauskas, A., Martikainen, M., Hinkkanen, A., Ahola, T. & Saksela, K. (2011).SH3 domain-mediated recruitment of host cell amphiphysins by alphavirus nsP3 promotes viral RNA replication. *PLoS Pathog* **7**, e1002383.

Noguchi, T., Satoh, S., Noshi, T., Hatada, E., Fukuda, R., Kawai, A., Ikeda, S., Hijikata, M. & Shimotohno, K. (2001). Effects of mutation in hepatitis C virus nonstructural protein 5A on interferon resistance mediated by inhibition of PKR kinase activity in mammalian cells. *Microbiol Immunol* **45**, 829-840.

Novick, D., Cohen, B. & Rubinstein, M. (1994). The human interferon alpha/beta receptor: characterization and molecular cloning. *Cell* **77**, 391-400.

Novikoff, A. B. (1959). Cell heterogeneity within the hepatic lobule of the rat: staining reactions. *J Histochem Cytochem* **7**, 240-244.

Numasaki, M., Tagawa, M., Iwata, F., Suzuki, T., Nakamura, A., Okada, M., Iwakura, Y., Aiba, S. & Yamaya, M. (2007).IL-28 elicits antitumor responses against murine fibrosarcoma. *J Immunol* **178**, 5086-5098.

O'Donnell, V., Pacheco, J. M., LaRocco, M., Burrage, T., Jackson, W., Rodriguez, L. L., Borca, M. V. & Baxt, B. (2011). Foot-and-mouth disease virus utilizes an autophagic pathway during viral replication. *Virology* **410**, 142-150.

Oaten, S. W., Jagelman, S. & Webb, H. E. (1980). Further studies of macrophages in relationship to avirulent Semliki Forest virus infections. *Br J Exp Pathol* **61**, 150-155.

Oganesyan, G., Saha, S. K., Guo, B., He, J. Q., Shahangian, A., Zarnegar, B., Perry, A. & Cheng, G. (2006). Critical role of TRAF3 in the Toll-like receptor-dependent and -independent antiviral response. *Nature* **439**, 208-211.

Oliver, K. R. & Fazakerley, J. K. (1998). Transneuronal spread of Semliki Forest virus in the developing mouse olfactory system is determined by neuronal maturity. *Neuroscience* **82**, 867-877.

Oliver, K. R., Scallan, M. F., Dyson, H. & Fazakerley, J. K. (1997). Susceptibility to a neurotropic virus and its changing distribution in the developing brain is a function of CNS maturity. *J Neurovirol* **3**, 38-48.

Opitz, B., Rejaibi, A., Dauber, B., Eckhard, J., Vinzing, M., Schmeck, B., Hippenstiel, S., Suttorp, N. & Wolff, T. (2007).IFNbeta induction by influenza A virus is mediated by RIG-I which is regulated by the viral NS1 protein. *Cell Microbiol* **9**, 930-938.

Oritani, K., Kincade, P. W. & Tomiyama, Y. (2001). Limitin: an interferon-like cytokine without myeloerythroid suppressive properties. *J Mol Med (Berl)* **79**, 168-174.

Oritani, K., Medina, K. L., Tomiyama, Y., Ishikawa, J., Okajima, Y., Ogawa, M., Yokota, T., Aoyama, K., Takahashi, I., Kincade, P. W. & Matsuzawa, Y. (2000). Limitin: An interferon-like cytokine that preferentially influences B-lymphocyte precursors. *Nat Med* **6**, 659-666.

Orvedahl, A., Alexander, D., Talloczy, Z., Sun, Q., Wei, Y., Zhang, W., Burns, D., Leib, D. A. & Levine, B. (2007).HSV-1 ICP34.5 confers neurovirulence by targeting the Beclin 1 autophagy protein. *Cell Host Microbe* **1**, 23-35.

Orvedahl, A., MacPherson, S., Sumpter, R., Jr., Talloczy, Z., Zou, Z. & Levine, B. (2010). Autophagy protects against Sindbis virus infection of the central nervous system. *Cell Host Microbe* **7**, 115-127.

Osterlund, P., Veckman, V., Siren, J., Klucher, K. M., Hiscott, J., Matikainen, S. & Julkunen, I. (2005). Gene expression and antiviral activity of alpha/beta

interferons and interleukin-29 in virus-infected human myeloid dendritic cells. *J Virol* **79**, 9608-9617.

Otani, T., Nakamura, S., Toki, M., Motoda, R., Kurimoto, M. & Orita, K. (1999). Identification of IFN-gamma-producing cells in IL-12/IL-18-treated mice. *Cell Immunol* **198**, 111-119.

Pagliaccetti, N. E. & Robek, M. D. (2010). Interferon-lambda in HCV Infection and Therapy. *Viruses* **2**, 1589-1602.

Palosaari, H., Parisien, J. P., Rodriguez, J. J., Ulane, C. M. & Horvath, C. M. (2003).STAT protein interference and suppression of cytokine signal transduction by measles virus V protein. *J Virol* **77**, 7635-7644.

Pankiv, S., Clausen, T. H., Lamark, T., Brech, A., Bruun, J. A., Outzen, H., Overvatn, A., Bjorkoy, G. & Johansen, T. (2007).p62/SQSTM1 binds directly to Atg8/LC3 to facilitate degradation of ubiquitinated protein aggregates by autophagy. *J Biol Chem* **282**, 24131-24145.

Panne, D., Maniatis, T. & Harrison, S. C. (2004). Crystal structure of ATF-2/c-Jun and IRF-3 bound to the interferon-beta enhancer. *EMBO J* **23**, 4384-4393.

Panne, D., McWhirter, S. M., Maniatis, T. & Harrison, S. C. (2007). Interferon regulatory factor 3 is regulated by a dual phosphorylation-dependent switch. *J Biol Chem* **282**, 22816-22822.

Parisien, J. P., Lau, J. F., Rodriguez, J. J., Ulane, C. M. & Horvath, C. M. (2002). Selective STAT protein degradation induced by paramyxoviruses requires both STAT1 and STAT2 but is independent of alpha/beta interferon signal transduction. *J Virol* **76**, 4190-4198.

Park, C., Li, S., Cha, E. & Schindler, C. (2000). Immune response in Stat2 knockout mice. *Immunity* **13**, 795-804.

Pathak, S. & Webb, H. E. (1974). Possible mechanisms for the transport of Semliki forest virus into and within mouse brain. An electron-microscopic study. *J Neurol Sci* **23**, 175-184.

Pathak, S. & Webb, H. E. (1983). Effect of myocrisin (sodium auro-thio-malate) on the morphogenesis of avirulent Semliki Forest virus in mouse brain: an electron microscopical study. *Neuropathol Appl Neurobiol* **9**, 313-327.

Pathak, S., Webb, H. E., Oaten, S. W. & Bateman, S. (1976). An electron-microscopic study of the development of virulent and avirulent strains of Semliki forest virus in mouse brain. *J Neurol Sci* **28**, 289-300.

Pattingre, S., Tassa, A., Qu, X., Garuti, R., Liang, X. H., Mizushima, N., Packer, M., Schneider, M. D. & Levine, B. (2005). Bcl-2 antiapoptotic proteins inhibit Beclin 1-dependent autophagy. *Cell* **122**, 927-939.

Pehrson, J. R. & Fuji, R. N. (1998). Evolutionary conservation of histone macroH2A subtypes and domains. *Nucleic Acids Res* **26**, 2837-2842.

Peranen, J. (1991). Localization and phosphorylation of Semliki Forest virus non-structural protein nsP3 expressed in COS cells from a cloned cDNA. *J Gen Virol* **72 (Pt 1)**, 195-199.

Peranen, J. & Kaariainen, L. (1991). Biogenesis of type I cytopathic vacuoles in Semliki Forest virus-infected BHK cells. *J Virol* **65**, 1623-1627.

Peranen, J., Laakkonen, P., Hyvonen, M. & Kaariainen, L. (1995). The alphavirus replicase protein nsP1 is membrane-associated and has affinity to endocytic organelles. *Virology* **208**, 610-620.

Peranen, J., Takkinen, K., Kalkkinen, N. & Kaariainen, L. (1988). Semliki Forest virus-specific non-structural protein nsP3 is a phosphoprotein. *J Gen Virol* **69 (Pt 9)**, 2165-2178.

Pestka, S., Krause, C. D. & Walter, M. R. (2004). Interferons, interferon-like cytokines, and their receptors. *Immunol Rev* **202**, 8-32.

Peters, K. L., Smith, H. L., Stark, G. R. & Sen, G. C. (2002).IRF-3-dependent, NFkappa B- and JNK-independent activation of the 561 and IFN-beta genes in response to double-stranded RNA. *Proc Natl Acad Sci U S A* **99**, 6322-6327.

Pfeffer, L. M., Mullersman, J. E., Pfeffer, S. R., Murti, A., Shi, W. & Yang, C. H. (1997).STAT3 as an adapter to couple phosphatidylinositol 3-kinase to the IFNAR1 chain of the type I interferon receptor. *Science* **276**, 1418-1420.

Pialoux, G., Gauzere, B. A., Jaureguiberry, S. & Strobel, M. (2007). Chikungunya, an epidemic arbovirosis. *Lancet Infect Dis* **7**, 319-327.

Pichlmair, A., Schulz, O., Tan, C. P., Naslund, T. I., Liljestrom, P., Weber, F. & Reis e Sousa (2006).RIG-I-mediated antiviral responses to single-stranded RNA bearing 5'-phosphates. *Science* **314**, 997-1001.

Polson, H. E., de, L. J., Rigden, D. J., Reedijk, M., Urbe, S., Clague, M. J. & Tooze, S. A. (2010). Mammalian Atg18 (WIPI2) localizes to omegasome-anchored phagophores and positively regulates LC3 lipidation. *Autophagy* **6**.

Pomerantz, J. L. & Baltimore, D. (1999).NF-kappaB activation by a signaling complex containing TRAF2, TANK and TBK1, a novel IKK-related kinase. *EMBO J* **18**, 6694-6704.

Porter, F. W., Bochkov, Y. A., Albee, A. J., Wiese, C. & Palmenberg, A. C. (2006).A picornavirus protein interacts with Ran-GTPase and disrupts nucleocytoplasmic transport. *Proc Natl Acad Sci U S A* **103**, 12417-12422.

Powers, A. M., Brault, A. C., Shirako, Y., Strauss, E. G., Kang, W., Strauss, J. H. & Weaver, S. C. (2001). Evolutionary relationships and systematics of the alphaviruses. *J Virol* **75**, 10118-10131.

Prasthofer, E. F., Prchal, J. T., Grizzle, W. E. & Grossi, C. E. (1985). Plasmacytoid T-cell lymphoma associated with chronic myeloproliferative disorder. *Am J Surg Pathol* **9**, 380-387.

Precious, B., Childs, K., Fitzpatrick-Swallow, V., Goodbourn, S. & Randall, R. E. (2005). Simian virus 5 V protein acts as an adaptor, linking DDB1 to STAT2, to facilitate the ubiquitination of STAT1. *J Virol* **79**, 13434-13441.

Prentice, E., McAuliffe, J., Lu, X., Subbarao, K. & Denison, M. R. (2004). Identification and characterization of severe acute respiratory syndrome coronavirus replicase proteins. *J Virol* **78**, 9977-9986.

Pua, H. H. & He, Y. W. (2009). Autophagy and lymphocyte homeostasis. *Curr Top Microbiol Immunol* **335**, 85-105.

Punnonen, E. L., Marjomaki, V. S. & Reunanen, H. (1994).3-Methyladenine inhibits transport from late endosomes to lysosomes in cultured rat and mouse fibroblasts. *Eur J Cell Biol* **65**, 14-25.

Pusztai, R., Gould, E. A. & Smith, H. (1971). Infection patterns in mice of an avirulent and virulent strain of Semliki Forest virus. *Br J Exp Pathol* **52**, 669-677.

Qu, X., Yu, J., Bhagat, G., Furuya, N., Hibshoosh, H., Troxel, A., Rosen, J., Eskelinen, E. L., Mizushima, N., Ohsumi, Y., Cattoretti, G. & Levine, B. (2003). Promotion of tumorigenesis by heterozygous disruption of the beclin 1 autophagy gene. *J Clin Invest* **112**, 1809-1820.

Qu, X. X., Hao, P., Song, X. J., Jiang, S. M., Liu, Y. X., Wang, P. G., Rao, X., Song, H. D., Wang, S. Y., Zuo, Y., Zheng, A. H., Luo, M., Wang, H. L., Deng, F., Wang, H. Z., Hu, Z. H., Ding, M. X., Zhao, G. P. & Deng, H. K. (2005). Identification of two critical amino acid residues of the severe acute respiratory syndrome coronavirus spike protein for its variation in zoonotic

tropism transition via a double substitution strategy. *J Biol Chem* **280**, 29588-29595.

Qureshi, S. A., Salditt-Georgieff, M. & Darnell, J. E., Jr. (1995). Tyrosine-phosphorylated Stat1 and Stat2 plus a 48-kDa protein all contact DNA in forming interferon-stimulated-gene factor 3. *Proc Natl Acad Sci U S A* **92**, 3829-3833.

Randall, R. E. & Goodbourn, S. (2008). Interferons and viruses: an interplay between induction, signalling, antiviral responses and virus countermeasures. *J Gen Virol* **89**, 1-47.

Rani, M. R., Leaman, D. W., Han, Y., Leung, S., Croze, E., Fish, E. N., Wolfman, A. & Ransohoff, R. M. (1999). Catalytically active TYK2 is essential for interferon-beta-mediated phosphorylation of STAT3 and interferon-alpha receptor-1 (IFNAR-1) but not for activation of phosphoinositol 3-kinase. *J Biol Chem* **274**, 32507-32511.

Ravikumar, B., Moreau, K., Jahreiss, L., Puri, C. & Rubinsztein, D. C. (2010). Plasma membrane contributes to the formation of pre-autophagosomal structures. *Nat Cell Biol* **12**, 747-757.

Rezza, G., Nicoletti, L., Angelini, R., Romi, R., Finarelli, A. C., Panning, M., Cordioli, P., Fortuna, C., Boros, S., Magurano, F., Silvi, G., Angelini, P., Dottori, M., Ciufolini, M. G., Majori, G. C. & Cassone, A. (2007). Infection with chikungunya virus in Italy: an outbreak in a temperate region. *Lancet* **370**, 1840-1846.

Rikkonen, M. (1996). Functional significance of the nuclear-targeting and NTP-binding motifs of Semliki Forest virus nonstructural protein nsP2. *Virology* **218**, 352-361.

Rikkonen, M., Peranen, J. & Kaariainen, L. (1992). Nuclear and nucleolar targeting signals of Semliki Forest virus nonstructural protein nsP2. *Virology* **189**, 462-473.

Rikkonen, M., Peranen, J. & Kaariainen, L. (1994).ATPase and GTPase activities associated with Semliki Forest virus nonstructural protein nsP2. *J Virol* **68**, 5804-5810.

Ritossa, F. (1962).A new puffing pattern induced by temperature shock and DNP in drosophila. *Cellular and Molecular Life Sciences* **18**, 571-573.

Roberts, R. M., Liu, L., Guo, Q., Leaman, D. & Bixby, J. (1998). The evolution of the type I interferons. *J Interferon Cytokine Res* **18**, 805-816.

Rodriguez, J. J., Parisien, J. P. & Horvath, C. M. (2002). Nipah virus V protein evades alpha and gamma interferons by preventing STAT1 and STAT2 activation and nuclear accumulation. *J Virol* **76**, 11476-11483.

Rodriguez, J. J., Wang, L. F. & Horvath, C. M. (2003). Hendra virus V protein inhibits interferon signaling by preventing STAT1 and STAT2 nuclear accumulation. *J Virol* **77**, 11842-11845.

Rothenfusser, S., Goutagny, N., DiPerna, G., Gong, M., Monks, B. G., Schoenemeyer, A., Yamamoto, M., Akira, S. & Fitzgerald, K. A. (2005). The RNA helicase Lgp2 inhibits TLR-independent sensing of viral replication by retinoic acid-inducible gene-I. *J Immunol* **175**, 5260-5268.

Ruiz-Jarabo, C. M., Arias, A., Baranowski, E., Escarmis, C. & Domingo, E. (2000). Memory in viral quasispecies. *J Virol* **74**, 3543-3547.

Russo, A. T., Malmstrom, R. D., White, M. A. & Watowich, S. J. (2010). Structural basis for substrate specificity of alphavirus nsP2 proteases. *J Mol Graph Model* **29**, 46-53.

Russo, A. T., White, M. A. & Watowich, S. J. (2006). The crystal structure of the Venezuelan equine encephalitis alphavirus nsP2 protease. *Structure* **14**, 1449-1458.

Ryman, K. D., Klimstra, W. B., Nguyen, K. B., Biron, C. A. & Johnston, R. E. (2000). Alpha/beta interferon protects adult mice from fatal Sindbis virus infection and is an important determinant of cell and tissue tropism. *J Virol* **74**, 3366-3378.

Ryman, K. D., Meier, K. C., Nangle, E. M., Ragsdale, S. L., Korneeva, N. L., Rhoads, R. E., MacDonald, M. R. & Klimstra, W. B. (2005). Sindbis virus translation is inhibited by a PKR/RNase L-independent effector induced by alpha/beta interferon priming of dendritic cells. *J Virol* **79**, 1487-1499.

Ryman, K. D., White, L. J., Johnston, R. E. & Klimstra, W. B. (2002). Effects of PKR/RNase L-dependent and alternative antiviral pathways on alphavirus replication and pathogenesis. *Viral Immunol* **15**, 53-76.

Sabatini, D. M., Erdjument-Bromage, H., Lui, M., Tempst, P. & Snyder, S. H. (1994).RAFT1: a mammalian protein that binds to FKBP12 in a rapamycin-dependent fashion and is homologous to yeast TORs. *Cell* **78**, 35-43.

Saitoh, T., Fujita, N., Hayashi, T., Takahara, K., Satoh, T., Lee, H., Matsunaga, K., Kageyama, S., Omori, H., Noda, T., Yamamoto, N., Kawai, T., Ishii, K., Takeuchi, O., Yoshimori, T. & Akira, S. (2009). Atg9a controls dsDNA-

driven dynamic translocation of STING and the innate immune response. *Proc Natl Acad Sci U S A* **106**, 20842-20846.

Saitoh, T., Fujita, N., Jang, M. H., Uematsu, S., Yang, B. G., Satoh, T., Omori, H., Noda, T., Yamamoto, N., Komatsu, M., Tanaka, K., Kawai, T., Tsujimura, T., Takeuchi, O., Yoshimori, T. & Akira, S. (2008). Loss of the autophagy protein Atg16L1 enhances endotoxin-induced IL-1beta production. *Nature* **456**, 264-268.

Salonen, A., Vasiljeva, L., Merits, A., Magden, J., Jokitalo, E. & Kaariainen, L. (2003). Properly folded nonstructural polyprotein directs the semliki forest virus replication complex to the endosomal compartment. *J Virol* **77**, 1691-1702.

Santagati, M. G., Itaranta, P. V., Koskimies, P. R., Maatta, J. A., Salmi, A. A. & Hinkkanen, A. E. (1994). Multiple repeating motifs are found in the 3'-terminal non-translated region of Semliki Forest virus A7 variant genome. *J Gen Virol* **75 (Pt 6)**, 1499-1504.

Santagati, M. G., Maatta, J. A., Itaranta, P. V., Salmi, A. A. & Hinkkanen, A. E. (1995). The Semliki Forest virus E2 gene as a virulence determinant. *J Gen Virol* **76 (Pt 1)**, 47-52.

Santagati, M. G., Maatta, J. A., Roytta, M., Salmi, A. A. & Hinkkanen, A. E. (1998). The significance of the 3'-nontranslated region and E2 amino acid mutations in the virulence of Semliki Forest virus in mice. *Virology* **243**, 66-77.

Sarkar, S. N., Smith, H. L., Rowe, T. M. & Sen, G. C. (2003). Double-stranded RNA signaling by Toll-like receptor 3 requires specific tyrosine residues in its cytoplasmic domain. *J Biol Chem* **278**, 4393-4396.

Sasaki, A., Yasukawa, H., Suzuki, A., Kamizono, S., Syoda, T., Kinjyo, I., Sasaki, M., Johnston, J. A. & Yoshimura, A. (1999). Cytokine-inducible SH2 protein-3 (CIS3/SOCS3) inhibits Janus tyrosine kinase by binding through the N-terminal kinase inhibitory region as well as SH2 domain. *Genes Cells* **4**, 339-351.

Sato, A., Ohtsuki, M., Hata, M., Kobayashi, E. & Murakami, T. (2006). Antitumor activity of IFN-lambda in murine tumor models. *J Immunol* **176**, 7686-7694.

Sato, S., Sugiyama, M., Yamamoto, M., Watanabe, Y., Kawai, T., Takeda, K. & Akira, S. (2003). Toll/IL-1 receptor domain-containing adaptor inducing IFN-beta (TRIF) associates with TNF receptor-associated factor 6 and TANK-binding kinase 1, and activates two distinct transcription factors, NF-kappa B

and IFN-regulatory factor-3, in the Toll-like receptor signaling. *J Immunol* **171**, 4304-4310.

Scallan, M. F., Allsopp, T. E. & Fazakerley, J. K. (1997).bcl-2 acts early to restrict Semliki Forest virus replication and delays virus-induced programmed cell death. *J Virol* **71**, 1583-1590.

Schafer, S. L., Lin, R., Moore, P. A., Hiscott, J. & Pitha, P. M. (1998). Regulation of type I interferon gene expression by interferon regulatory factor-3. *J Biol Chem* **273**, 2714-2720.

Schindler, C., Fu, X. Y., Improta, T., Aebersold, R. & Darnell, J. E., Jr. (1992). Proteins of transcription factor ISGF-3: one gene encodes the 91-and 84-kDa ISGF-3 proteins that are activated by interferon alpha. *Proc Natl Acad Sci U S A* **89**, 7836-7839.

Schlesinger, M. J. (1990). Heat shock proteins. *J Biol Chem* **265**, 12111-12114.

Schmid, D. & Munz, C. (2007). Immune surveillance via self digestion. *Autophagy* **3**, 133-135.

Schmidt, A., Schwerd, T., Hamm, W., Hellmuth, J. C., Cui, S., Wenzel, M., Hoffmann, F. S., Michallet, M. C., Besch, R., Hopfner, K. P., Endres, S. & Rothenfusser, S. (2009).5'-triphosphate RNA requires base-paired structures to activate antiviral signaling via RIG-I. *Proc Natl Acad Sci U S A* **106**, 12067-12072.

Schroder, K., Hertzog, P. J., Ravasi, T. & Hume, D. A. (2004). Interferon-gamma: an overview of signals, mechanisms and functions. *J Leukoc Biol* **75**, 163-189.

Seglen, P. O. & Gordon, P. B. (1982).3-Methyladenine: specific inhibitor of autophagic/lysosomal protein degradation in isolated rat hepatocytes. *Proc Natl Acad Sci U S A* **79**, 1889-1892.

Seki, Y., Inoue, H., Nagata, N., Hayashi, K., Fukuyama, S., Matsumoto, K., Komine, O., Hamano, S., Himeno, K., Inagaki-Ohara, K., Cacalano, N., O'Garra, A., Oshida, T., Saito, H., Johnston, J. A., Yoshimura, A. & Kubo, M. (2003).SOCS-3 regulates onset and maintenance of T(H)2-mediated allergic responses. *Nat Med* **9**, 1047-1054.

Sen, G. C. (2000). Novel functions of interferon-induced proteins. *Semin Cancer Biol* **10**, 93-101.

Servant, M. J., Grandvaux, N. & Hiscott, J. (2002). Multiple signaling pathways leading to the activation of interferon regulatory factor 3. *Biochem Pharmacol* **64**, 985-992.

Seth, R. B., Sun, L., Ea, C. K. & Chen, Z. J. (2005). Identification and characterization of MAVS, a mitochondrial antiviral signaling protein that activates NF-kappaB and IRF 3. *Cell* **122**, 669-682.

Sharma, S., tenOever, B. R., Grandvaux, N., Zhou, G. P., Lin, R. & Hiscott, J. (2003). Triggering the interferon antiviral response through an IKK-related pathway. *Science* **300**, 1148-1151.

Shelly, S., Lukinova, N., Bambina, S., Berman, A. & Cherry, S. (2009). Autophagy is an essential component of Drosophila immunity against vesicular stomatitis virus. *Immunity* **30**, 588-598.

Sheppard, P., Kindsvogel, W., Xu, W., Henderson, K., Schlutsmeyer, S., Whitmore, T. E., Kuestner, R., Garrigues, U., Birks, C., Roraback, J., Ostrander, C., Dong, D., Shin, J., Presnell, S., Fox, B., Haldeman, B., Cooper, E., Taft, D., Gilbert, T., Grant, F. J., Tackett, M., Krivan, W., McKnight, G., Clegg, C., Foster, D. & Klucher, K. M. (2003).IL-28, IL-29 and their class II cytokine receptor IL-28R. *Nat Immunol* **4**, 63-68.

Shi, C. S. & Kehrl, J. H. (2008). MyD88 and Trif target Beclin 1 to trigger autophagy in macrophages. *J Biol Chem* **283**, 33175-33182.

Shi, C. S. & Kehrl, J. H. (2010).TRAF6 and A20 regulate lysine 63-linked ubiquitination of Beclin-1 to control TLR4-induced autophagy. *Sci Signal* **3**, ra42.

Shibata, M., Lu, T., Furuya, T., Degterev, A., Mizushima, N., Yoshimori, T., MacDonald, M., Yankner, B. & Yuan, J. (2006). Regulation of intracellular accumulation of mutant Huntingtin by Beclin 1. *J Biol Chem* **281**, 14474-14485.

Shimoda, K., Feng, J., Murakami, H., Nagata, S., Watling, D., Rogers, N. C., Stark, G. R., Kerr, I. M. & Ihle, J. N. (1997). Jak1 plays an essential role for receptor phosphorylation and Stat activation in response to granulocyte colony-stimulating factor. *Blood* **90**, 597-604.

Shirako, Y., Strauss, E. G. & Strauss, J. H. (2000). Suppressor mutations that allow sindbis virus RNA polymerase to function with nonaromatic amino acids at the N-terminus: evidence for interaction between nsP1 and nsP4 in minus-strand RNA synthesis. *Virology* **276**, 148-160.

Shirako, Y. & Strauss, J. H. (1994). Regulation of Sindbis virus RNA replication: uncleaved P123 and nsP4 function in minus-strand RNA synthesis, whereas cleaved products from P123 are required for efficient plus-strand RNA synthesis. *J Virol* **68**, 1874-1885.

Shvets, E., Fass, E. & Elazar, Z. (2008). Utilizing flow cytometry to monitor autophagy in living mammalian cells. *Autophagy* **4**, 621-628.

Siegal, F. P., Kadowaki, N., Shodell, M., Fitzgerald-Bocarsly, P. A., Shah, K., Ho, S., Antonenko, S. & Liu, Y. J. (1999). The nature of the principal type 1 interferon-producing cells in human blood. *Science* **284**, 1835-1837.

Simmons, J. D., Wollish, A. C. & Heise, M. T. (2010).A determinant of Sindbis virus neurovirulence enables efficient disruption of Jak/STAT signaling. *J Virol* **84**, 11429-11439.

Singh, R. (2010). Autophagy and regulation of lipid metabolism. *Results Probl Cell Differ* **52**, 35-46.

Sinha, S., Colbert, C. L., Becker, N., Wei, Y. & Levine, B. (2008). Molecular basis of the regulation of Beclin 1-dependent autophagy by the gamma-herpesvirus 68 Bcl-2 homolog M11. *Autophagy* **4**, 989-997.

Siren, J., Pirhonen, J., Julkunen, I. & Matikainen, S. (2005).IFN-alpha regulates TLR-dependent gene expression of IFN-alpha, IFN-beta, IL-28, and IL-29. *J Immunol* **174**, 1932-1937.

Sjoberg, E. M., Suomalainen, M. & Garoff, H. (1994).A significantly improved Semliki Forest virus expression system based on translation enhancer segments from the viral capsid gene. *Biotechnology (N Y)* **12**, 1127-1131.

Smerdou, C. & Liljestrom, P. (1999). Two-helper RNA system for production of recombinant Semliki forest virus particles. *J Virol* **73**, 1092-1098.

Smillie, J., Pusztai, R. & Smith, H. (1973). Studies of the influence of host deference mechanisms on infection of mice with an avirulent or virulent strain of Semliki Forest virus. *Br J Exp Pathol* **54**, 260-266.

Smith, T. J., Cheng, R. H., Olson, N. H., Peterson, P., Chase, E., Kuhn, R. J. & Baker, T. S. (1995). Putative receptor binding sites on alphaviruses as visualized by cryoelectron microscopy. *Proc Natl Acad Sci U S A* **92**, 10648-10652.

Smithburn, K. C. & Haddow, W. J. (1944). Semliki Forest virus I. Isolation and pathogenic properties. *J Immunol* **49**, 141-145.

SMITHBURN, K. C. & Harrow, W. J. (1944). Semliki Forest virus I. Isolation and pathogenic properties. 49 edn, pp. 141-145: J Immunol.

Soh, J., Mariano, T. M., Lim, J. K., Izotova, L., Mirochnitchenko, O., Schwartz, B., Langer, J. A. & Pestka, S. (1994). Expression of a functional human type I interferon receptor in hamster cells: application of functional yeast artificial chromosome (YAC) screening. *J Biol Chem* **269**, 18102-18110.

Sommereyns, C., Paul, S., Staeheli, P. & Michiels, T. (2008).IFN-lambda (IFN-lambda) is expressed in a tissue-dependent fashion and primarily acts on epithelial cells in vivo. *PLoS Pathog* **4**, e1000017.

Sou, Y. S., Waguri, S., Iwata, J., Ueno, T., Fujimura, T., Hara, T., Sawada, N., Yamada, A., Mizushima, N., Uchiyama, Y., Kominami, E., Tanaka, K. & Komatsu, M. (2008). The Atg8 conjugation system is indispensable for proper development of autophagic isolation membranes in mice. *Mol Biol Cell* **19**, 4762-4775.

Spuul, P., Salonen, A., Merits, A., Jokitalo, E., Kaariainen, L. & Ahola, T. (2007). Role of the amphipathic peptide of Semliki forest virus replicase protein nsP1 in membrane association and virus replication. *J Virol* **81**, 872-883.

Stancato, L. F., David, M., Carter-Su, C., Larner, A. C. & Pratt, W. B. (1996). Preassociation of STAT1 with STAT2 and STAT3 in separate signalling complexes prior to cytokine stimulation. *J Biol Chem* **271**, 4134-4137.

Stark, G. R., Kerr, I. M., Williams, B. R., Silverman, R. H. & Schreiber, R. D. (1998). How cells respond to interferons. *Annu Rev Biochem* **67**, 227-264.

Strauss, E. G., Rice, C. M. & Strauss, J. H. (1983). Sequence coding for the alphavirus nonstructural proteins is interrupted by an opal termination codon. *Proc Natl Acad Sci U S A* **80**, 5271-5275.

Strauss, J. H. & Strauss, E. G. (1994). The alphaviruses: gene expression, replication, and evolution. *Microbiol Rev* **58**, 491-562.

Strous, G. J. & Govers, R. (1999). The ubiquitin-proteasome system and endocytosis. *J Cell Sci* **112 (Pt 10)**, 1417-1423.

Subauste, C. S., Andrade, R. M. & Wessendarp, M. (2007).CD40-TRAF6 and autophagy-dependent anti-microbial activity in macrophages. *Autophagy* **3**, 245-248.

Sumpter, R., Jr., Wang, C., Foy, E., Loo, Y. M. & Gale, M., Jr. (2004). Viral evolution and interferon resistance of hepatitis C virus RNA replication in a cell culture model. *J Virol* **78**, 11591-11604.

Suomalainen, M., Liljestrom, P. & Garoff, H. (1992). Spike protein-nucleocapsid interactions drive the budding of alphaviruses. *J Virol* **66**, 4737-4747.

Suopanki, J., Sawicki, D. L., Sawicki, S. G. & Kaariainen, L. (1998). Regulation of alphavirus 26S mRNA transcription by replicase component nsP2. *J Gen Virol* **79 (Pt 2)**, 309-319.

Tabeta, K., Georgel, P., Janssen, E., Du, X., Hoebe, K., Crozat, K., Mudd, S., Shamel, L., Sovath, S., Goode, J., Alexopoulou, L., Flavell, R. A. & Beutler, B. (2004). Toll-like receptors 9 and 3 as essential components of innate immune defense against mouse cytomegalovirus infection. *Proc Natl Acad Sci U S A* **101**, 3516-3521.

Taguchi, T., Nagano-Fujii, M., Akutsu, M., Kadoya, H., Ohgimoto, S., Ishido, S. & Hotta, H. (2004). Hepatitis C virus NS5A protein interacts with 2',5'-oligoadenylate synthetase and inhibits antiviral activity of IFN in an IFN sensitivity-determining region-independent manner. *J Gen Virol* **85**, 959-969.

Takaoka, A., Yanai, H., Kondo, S., Duncan, G., Negishi, H., Mizutani, T., Kano, S., Honda, K., Ohba, Y., Mak, T. W. & Taniguchi, T. (2005). Integral role of IRF-5 in the gene induction programme activated by Toll-like receptors. *Nature* **434**, 243-249.

Takeda, K., Kaisho, T., Yoshida, N., Takeda, J., Kishimoto, T. & Akira, S. (1998). Stat3 activation is responsible for IL-6-dependent T cell proliferation through preventing apoptosis: generation and characterization of T cell-specific Stat3-deficient mice. *J Immunol* **161**, 4652-4660.

Takeda, K., Kishimoto, T. & Akira, S. (1997).STAT6: its role in interleukin 4-mediated biological functions. *J Mol Med (Berl)* **75**, 317-326.

Takeshige, K., Baba, M., Tsuboi, S., Noda, T. & Ohsumi, Y. (1992). Autophagy in yeast demonstrated with proteinase-deficient mutants and conditions for its induction. *J Cell Biol* **119**, 301-311.

Takkinen, K. (1986). Complete nucleotide sequence of the nonstructural protein genes of Semliki Forest virus. *Nucleic Acids Res* **14**, 5667-5682.

Takkinen, K., Peranen, J., Keranen, S., Soderlund, H. & Kaariainen, L. (1990). The Semliki-Forest-virus-specific nonstructural protein nsP4 is an autoproteinase. *Eur J Biochem* **189**, 33-38.

Tal, M. C. & Iwasaki, A. (2009). Autophagic control of RLR signaling. *Autophagy* **5**, 749-750.

Talloczy, Z., Virgin, H. W. & Levine, B. (2006).PKR-dependent autophagic degradation of herpes simplex virus type 1. *Autophagy* **2**, 24-29.

Talon, J., Horvath, C. M., Polley, R., Basler, C. F., Muster, T., Palese, P. & Garcia-Sastre, A. (2000). Activation of interferon regulatory factor 3 is inhibited by the influenza A virus NS1 protein. *J Virol* **74**, 7989-7996.

Tamberg, N., Lulla, V., Fragkoudis, R., Lulla, A., Fazakerley, J. K. & Merits, A. (2007). Insertion of EGFP into the replicase gene of Semliki Forest virus results in a novel, genetically stable marker virus. *J Gen Virol* **88**, 1225-1230.

Tang, X., Gao, J. S., Guan, Y. J., McLane, K. E., Yuan, Z. L., Ramratnam, B. & Chin, Y. E. (2007). Acetylation-dependent signal transduction for type I interferon receptor. *Cell* **131**, 93-105.

Tarbatt, C. J., Glasgow, G. M., Mooney, D. A., Sheahan, B. J. & Atkins, G. J. (1997). Sequence analysis of the avirulent, demyelinating A7 strain of Semliki Forest virus. *J Gen Virol* **78 (Pt 7)**, 1551-1557.

Taylor, D. R., Shi, S. T., Romano, P. R., Barber, G. N. & Lai, M. M. (1999). Inhibition of the interferon-inducible protein kinase PKR by HCV E2 protein. *Science* **285**, 107-110.

Teglund, S., McKay, C., Schuetz, E., van Deursen, J. M., Stravopodis, D., Wang, D., Brown, M., Bodner, S., Grosveld, G. & Ihle, J. N. (1998). Stat5a and Stat5b proteins have essential and nonessential, or redundant, roles in cytokine responses. *Cell* **93**, 841-850.

ten, H. J., de, J., I, Fu, Y., Zhu, W., Tremblay, M., David, M. & Shuai, K. (2002). Identification of a nuclear Stat1 protein tyrosine phosphatase. *Mol Cell Biol* **22**, 5662-5668.

Thanos, D. & Maniatis, T. (1995). Virus induction of human IFN beta gene expression requires the assembly of an enhanceosome. *Cell* **83**, 1091-1100.

Thierfelder, W. E., van Deursen, J. M., Yamamoto, K., Tripp, R. A., Sarawar, S. R., Carson, R. T., Sangster, M. Y., Vignali, D. A., Doherty, P. C., Grosveld, G. C. & Ihle, J. N. (1996). Requirement for Stat4 in interleukin-12-mediated responses of natural killer and T cells. *Nature* **382**, 171-174.

Thomas, D., Blakqori, G., Wagner, V., Banholzer, M., Kessler, N., Elliott, R. M., Haller, O. & Weber, F. (2004). Inhibition of RNA polymerase II

phosphorylation by a viral interferon antagonist. *J Biol Chem* **279**, 31471-31477.

Thurston, T. L., Ryzhakov, G., Bloor, S., von, M. N. & Randow, F. (2009). The TBK1 adaptor and autophagy receptor NDP52 restricts the proliferation of ubiquitin-coated bacteria. *Nat Immunol* **10**, 1215-1221.

Tonkin, D. R., Whitmore, A., Johnston, R. E. & Barro, M. (2012). Infected dendritic cells are sufficient to mediate the adjuvant activity generated by Venezuelan equine encephalitis virus replicon particles. *Vaccine*.

Tormo, D., Checinska, A., Alonso-Curbelo, D., Perez-Guijarro, E., Canon, E., Riveiro-Falkenbach, E., Calvo, T. G., Larribere, L., Megias, D., Mulero, F., Piris, M. A., Dash, R., Barral, P. M., Rodriguez-Peralto, J. L., Ortiz-Romero, P., Tuting, T., Fisher, P. B. & Soengas, M. S. (2009). Targeted activation of innate immunity for therapeutic induction of autophagy and apoptosis in melanoma cells. *Cancer Cell* **16**, 103-114.

Travassos, L. H., Carneiro, L. A., Ramjeet, M., Hussey, S., Kim, Y. G., Magalhaes, J. G., Yuan, L., Soares, F., Chea, E., Le, B. L., Boneca, I. G., Allaoui, A., Jones, N. L., Nunez, G., Girardin, S. E. & Philpott, D. J. (2010). Nod1 and Nod2 direct autophagy by recruiting ATG16L1 to the plasma membrane at the site of bacterial entry. *Nat Immunol* **11**, 55-62.

Trinchieri, G., Santoli, D., Dee, R. R. & Knowles, B. B. (1978). Anti-viral activity induced by culturing lymphocytes with tumor-derived or virus-transformed cells. Identification of the anti-viral activity as interferon and characterization of the human effector lymphocyte subpopulation. *J Exp Med* **147**, 1299-1313.

Tsai, T. F., Weaver, S. & Monath, T. P. (2002). Alphaviruses. In *Clinical Virology, DD Rickman, RF Whitley and FG Hayden eds.* Washington DC: ASM press.

Tsetsarkin, K. A., Vanlandingham, D. L., McGee, C. E. & Higgs, S. (2007).A single mutation in chikungunya virus affects vector specificity and epidemic potential. *PLoS Pathog* **3**, e201.

Tsukada, M. & Ohsumi, Y. (1993). Isolation and characterization of autophagy-defective mutants of Saccharomyces cerevisiae. *FEBS Lett* **333**, 169-174.

Tuittila, M. & Hinkkanen, A. E. (2003). Amino acid mutations in the replicase protein nsP3 of Semliki Forest virus cumulatively affect neurovirulence. *J Gen Virol* **84**, 1525-1533.

Tuittila, M. T., Santagati, M. G., Roytta, M., Maatta, J. A. & Hinkkanen, A. E. (2000). Replicase complex genes of Semliki Forest virus confer lethal neurovirulence. *J Virol* **74**, 4579-4589.

Udy, G. B., Towers, R. P., Snell, R. G., Wilkins, R. J., Park, S. H., Ram, P. A., Waxman, D. J. & Davey, H. W. (1997). Requirement of STAT5b for sexual dimorphism of body growth rates and liver gene expression. *Proc Natl Acad Sci U S A* **94**, 7239-7244.

Ulane, C. M. & Horvath, C. M. (2002). Paramyxoviruses SV5 and HPIV2 assemble STAT protein ubiquitin ligase complexes from cellular components. *Virology* **304**, 160-166.

van, d., V & Reggiori, F. (2010). The Golgi complex as a source for yeast autophagosomal membranes. *Autophagy* **6**, 800-801.

Vasiljeva, L., Merits, A., Auvinen, P. & Kaariainen, L. (2000). Identification of a novel function of the alphavirus capping apparatus. *J Biol Chem* **275**, 17281-17287.

Vasiljeva, L., Merits, A., Golubtsov, A., Sizemskaja, V., Kaariainen, L. & Ahola, T. (2003). Regulation of the sequential processing of Semliki Forest virus replicase polyprotein. *J Biol Chem* **278**, 41636-41645.

Veals, S. A., Santa, M. T. & Levy, D. E. (1993). Two domains of ISGF3 gamma that mediate protein-DNA and protein-protein interactions during transcription factor assembly contribute to DNA-binding specificity. *Mol Cell Biol* **13**, 196-206.

Veals, S. A., Schindler, C., Leonard, D., Fu, X. Y., Aebersold, R., Darnell, J. E., Jr. & Levy, D. E. (1992). Subunit of an alpha-interferon-responsive transcription factor is related to interferon regulatory factor and Myb families of DNA-binding proteins. *Mol Cell Biol* **12**, 3315-3324.

Velazquez, L., Fellous, M., Stark, G. R. & Pellegrini, S. (1992).A protein tyrosine kinase in the interferon alpha/beta signaling pathway. *Cell* **70**, 313-322.

Venkataraman, T., Valdes, M., Elsby, R., Kakuta, S., Caceres, G., Saijo, S., Iwakura, Y. & Barber, G. N. (2007). Loss of DExD/H box RNA helicase LGP2 manifests disparate antiviral responses. *J Immunol* **178**, 6444-6455.

Ventoso, I., Sanz, M. A., Molina, S., Berlanga, J. J., Carrasco, L. & Esteban, M. (2006). Translational resistance of late alphavirus mRNA to eIF2alpha phosphorylation: a strategy to overcome the antiviral effect of protein kinase PKR. *Genes Dev* **20**, 87-100.

Verbinnen, T., Van, M. H., Vandenbroucke, I., Vijgen, L., Claes, M., Lin, T. I., Simmen, K., Neyts, J., Fanning, G. & Lenz, O. (2010). Tracking the evolution of multiple in vitro hepatitis C virus replicon variants under protease inhibitor selection pressure by 454 deep sequencing. *J Virol* **84**, 11124-11133.

Vihinen, H., Ahola, T., Tuittila, M., Merits, A. & Kaariainen, L. (2001). Elimination of phosphorylation sites of Semliki Forest virus replicase protein nsP3. *J Biol Chem* **276**, 5745-5752.

Vyas, J., Elia, A. & Clemens, M. J. (2003). Inhibition of the protein kinase PKR by the internal ribosome entry site of hepatitis C virus genomic RNA. *RNA* **9**, 858-870.

Wahlberg, J. M. & Garoff, H. (1992). Membrane fusion process of Semliki Forest virus. I: Low pH-induced rearrangement in spike protein quaternary structure precedes virus penetration into cells. *J Cell Biol* **116**, 339-348.

Wang, C., Deng, L., Hong, M., Akkaraju, G. R., Inoue, J. & Chen, Z. J. (2001).TAK1 is a ubiquitin-dependent kinase of MKK and IKK. *Nature* **412**, 346-351.

Wang, X., Li, M., Zheng, H., Muster, T., Palese, P., Beg, A. A. & Garcia-Sastre, A. (2000). Influenza A virus NS1 protein prevents activation of NF-kappaB and induction of alpha/beta interferon. *J Virol* **74**, 11566-11573.

Wang, Y. F., Sawicki, S. G. & Sawicki, D. L. (1991). Sindbis virus nsP1 functions in negative-strand RNA synthesis. *J Virol* **65**, 985-988.

Wang, Y. F., Sawicki, S. G. & Sawicki, D. L. (1994). Alphavirus nsP3 functions to form replication complexes transcribing negative-strand RNA. *J Virol* **68**, 6466-6475.

Waterhouse, A. M., Procter, J. B., Martin, D. M., Clamp, M. & Barton, G. J. (2009). Jalview Version 2--a multiple sequence alignment editor and analysis workbench. *Bioinformatics* **25**, 1189-1191.

Weaver, S. C., Lorenz, L. H. & Scott, T. W. (1992). Pathologic changes in the midgut of Culex tarsalis following infection with Western equine encephalomyelitis virus. *Am J Trop Med Hyg* **47**, 691-701.

Weaver, S. C., Scott, T. W., Lorenz, L. H., Lerdthusnee, K. & Romoser, W. S. (1988). Togavirus-associated pathologic changes in the midgut of a natural mosquito vector. *J Virol* **62**, 2083-2090.

Weiss, B., Nitschko, H., Ghattas, I., Wright, R. & Schlesinger, S. (1989). Evidence for specificity in the encapsidation of Sindbis virus RNAs. *J Virol* **63**, 5310-5318.

White, L. J., Wang, J. G., Davis, N. L. & Johnston, R. E. (2001). Role of alpha/beta interferon in Venezuelan equine encephalitis virus pathogenesis: effect of an attenuating mutation in the 5' untranslated region. *J Virol* **75**, 3706-3718.

Wild, P., Farhan, H., McEwan, D. G., Wagner, S., Rogov, V. V., Brady, N. R., Richter, B., Korac, J., Waidmann, O., Choudhary, C., Dotsch, V., Bumann, D. & Dikic, I. (2011). Phosphorylation of the autophagy receptor optineurin restricts Salmonella growth. *Science* **333**, 228-233.

Williams, B. R. (1999).PKR; a sentinel kinase for cellular stress. *Oncogene* **18**, 6112-6120.

Witte, K., Gruetz, G., Volk, H. D., Looman, A. C., Asadullah, K., Sterry, W., Sabat, R. & Wolk, K. (2009). Despite IFN-lambda receptor expression, blood immune cells, but not keratinocytes or melanocytes, have an impaired response to type III interferons: implications for therapeutic applications of these cytokines. *Genes Immun* **10**, 702-714.

Wong, J., Zhang, J., Si, X., Gao, G., Mao, I., McManus, B. M. & Luo, H. (2008). Autophagosome supports coxsackievirus B3 replication in host cells. *J Virol* **82**, 9143-9153.

Wu, C. J., Conze, D. B., Li, T., Srinivasula, S. M. & Ashwell, J. D. (2006). Sensing of Lys 63-linked polyubiquitination by NEMO is a key event in NF-kappaB activation [corrected]. *Nat Cell Biol* **8**, 398-406.

Xie, Z., Nair, U., Geng, J., Szefler, M. B., Rothman, E. D. & Klionsky, D. J. (2009). Indirect estimation of the area density of Atg8 on the phagophore. *Autophagy* **5**, 217-220.

Xie, Z., Nair, U. & Klionsky, D. J. (2008). Atg8 controls phagophore expansion during autophagosome formation. *Mol Biol Cell* **19**, 3290-3298.

Xu, L. G., Wang, Y. Y., Han, K. J., Li, L. Y., Zhai, Z. & Shu, H. B. (2005).VISA is an adapter protein required for virus-triggered IFN-beta signaling. *Mol Cell* **19**, 727-740.

Xue, L., Borutaite, V. & Tolkovsky, A. M. (2002). Inhibition of mitochondrial permeability transition and release of cytochrome c by anti-apoptotic nucleoside analogues. *Biochem Pharmacol* **64**, 441-449.

Yamamoto, M., Sato, S., Hemmi, H., Hoshino, K., Kaisho, T., Sanjo, H., Takeuchi, O., Sugiyama, M., Okabe, M., Takeda, K. & Akira, S. (2003). Role of adaptor TRIF in the MyD88-independent toll-like receptor signaling pathway. *Science* **301**, 640-643.

Yan, H., Krishnan, K., Greenlund, A. C., Gupta, S., Lim, J. T., Schreiber, R. D., Schindler, C. W. & Krolewski, J. J. (1996). Phosphorylated interferon-alpha receptor 1 subunit (IFNaR1) acts as a docking site for the latent form of the 113 kDa STAT2 protein. *EMBO J* **15**, 1064-1074.

Yang, C. H., Shi, W., Basu, L., Murti, A., Constantinescu, S. N., Blatt, L., Croze, E., Mullersman, J. E. & Pfeffer, L. M. (1996). Direct association of STAT3 with the IFNAR-1 chain of the human type I interferon receptor. *J Biol Chem* **271**, 8057-8061.

Yasukawa, H., Misawa, H., Sakamoto, H., Masuhara, M., Sasaki, A., Wakioka, T., Ohtsuka, S., Imaizumi, T., Matsuda, T., Ihle, J. N. & Yoshimura, A. (1999). The JAK-binding protein JAB inhibits Janus tyrosine kinase activity through binding in the activation loop. *EMBO J* **18**, 1309-1320.

Yen, W. L., Shintani, T., Nair, U., Cao, Y., Richardson, B. C., Li, Z., Hughson, F. M., Baba, M. & Klionsky, D. J. (2010). The conserved oligomeric Golgi complex is involved in double-membrane vesicle formation during autophagy. *J Cell Biol* **188**, 101-114.

Yie, J., Merika, M., Munshi, N., Chen, G. & Thanos, D. (1999). The role of HMG I(Y) in the assembly and function of the IFN-beta enhanceosome. *EMBO J* **18**, 3074-3089.

Yla-Anttila, P., Vihinen, H., Jokitalo, E. & Eskelinen, E. L. (2009).3D tomography reveals connections between the phagophore and endoplasmic reticulum. *Autophagy* **5**, 1180-1185.

Yoneyama, M., Kikuchi, M., Natsukawa, T., Shinobu, N., Imaizumi, T., Miyagishi, M., Taira, K., Akira, S. & Fujita, T. (2004). The RNA helicase RIG-I has an essential function in double-stranded RNA-induced innate antiviral responses. *Nat Immunol* **5**, 730-737.

Yoneyama, M., Suhara, W. & Fujita, T. (2002). Control of IRF-3 activation by phosphorylation. *J Interferon Cytokine Res* **22**, 73-76.

Yoshikawa, Y., Ogawa, M., Hain, T., Yoshida, M., Fukumatsu, M., Kim, M., Mimuro, H., Nakagawa, I., Yanagawa, T., Ishii, T., Kakizuka, A., Sztul, E., Chakraborty, T. & Sasakawa, C. (2009). Listeria monocytogenes ActA-mediated escape from autophagic recognition. *Nat Cell Biol* **11**, 1233-1240.

Young, D. F., Didcock, L., Goodbourn, S. & Randall, R. E. (2000). Paramyxoviridae use distinct virus-specific mechanisms to circumvent the interferon response. *Virology* **269**, 383-390.

Yu, L., McPhee, C. K., Zheng, L., Mardones, G. A., Rong, Y., Peng, J., Mi, N., Zhao, Y., Liu, Z., Wan, F., Hailey, D. W., Oorschot, V., Klumperman, J., Baehrecke, E. H. & Lenardo, M. J. (2010). Termination of autophagy and reformation of lysosomes regulated by mTOR. *Nature* **465**, 942-946.

Yuan, S., Huang, S., Zhang, W., Wu, T., Dong, M., Yu, Y., Liu, T., Wu, K., Liu, H., Yang, M., Zhang, H. & Xu, A. (2009). An amphioxus TLR with dynamic embryonic expression pattern responses to pathogens and activates NF-kappaB pathway via MyD88. *Mol Immunol* **46**, 2348-2356.

Zhang, X., Blenis, J., Li, H. C., Schindler, C. & Chen-Kiang, S. (1995). Requirement of serine phosphorylation for formation of STAT-promoter complexes. *Science* **267**, 1990-1994.

Zhao, T., Yang, L., Sun, Q., Arguello, M., Ballard, D. W., Hiscott, J. & Lin, R. (2007a). The NEMO adaptor bridges the nuclear factor-kappaB and interferon regulatory factor signaling pathways. *Nat Immunol* **8**, 592-600.

Zhao, Z., Fux, B., Goodwin, M., Dunay, I. R., Strong, D., Miller, B. C., Cadwell, K., Delgado, M. A., Ponpuak, M., Green, K. G., Schmidt, R. E., Mizushima, N., Deretic, V., Sibley, L. D. & Virgin, H. W. (2008). Autophagosome-independent essential function for the autophagy protein Atg5 in cellular immunity to intracellular pathogens. *Cell Host Microbe* **4**, 458-469.

Zhao, Z., Thackray, L. B., Miller, B. C., Lynn, T. M., Becker, M. M., Ward, E., Mizushima, N. N., Denison, M. R. & Virgin, H. W. (2007b). Coronavirus replication does not require the autophagy gene ATG5. *Autophagy* **3**, 581-585.

Zheng, Y. T., Shahnazari, S., Brech, A., Lamark, T., Johansen, T. & Brumell, J. H. (2009). The adaptor protein p62/SQSTM1 targets invading bacteria to the autophagy pathway. *J Immunol* **183**, 5909-5916.

Zhong, H., Voll, R. E. & Ghosh, S. (1998). Phosphorylation of NF-kappa B p65 by PKA stimulates transcriptional activity by promoting a novel bivalent interaction with the coactivator CBP/p300. *Mol Cell* **1**, 661-671.

Zhong, Y., Wang, Q. J., Li, X., Yan, Y., Backer, J. M., Chait, B. T., Heintz, N. & Yue, Z. (2009). Distinct regulation of autophagic activity by Atg14L and Rubicon associated with Beclin 1-phosphatidylinositol-3-kinase complex. *Nat Cell Biol* **11**, 468-476.